Université d'Ottawa • University of Ottawa

EVALUATION OF RESPIROMETRY-BASED CONTROL STRATEGIES FOR THE ACTIVATED SLUDGE PROCESS BY COMPUTER SIMULATION

by
© Khanh Nguyen

A thesis
submitted under the supervision of
Dr. Gilles Patry and
Dr. Henri Spanjers

In partial fulfillment
of the requirements of the degree of
Master of Applied Science
in
Civil Engineering

Department of Civil Engineering
University of Ottawa
Ottawa, Canada
K1N 6N5

April 1999

0-612-46599-3

EVALUATION OF RESPIROMETRY-BASED CONTROL STRATEGIES FOR THE ACTIVATED SLUDGE PROCESS BY COMPUTER SIMULATION

By

Khanh Nguyen
B. A. Sc.

To my family and friends,

for their dedication and love.

ACKNOWLEDGEMENTS

I would like to especially thank my advisors, Dr. Gilles Patry (University of Ottawa) and Dr. Henri Spanjers (Wageningen Agricultural University), for their assistance and guidance throughout the development of this study.

I am also grateful for the advice and contribution given by Dr. Peter Vanrolleghem (University of Ghent) and Henk Vanhooren (University of Ghent).

I would also like to express appreciation for the assistance provided by the consultants at Hydromatis Inc. on simulation and modelling, as well as on process control. Notable gratitude is extended to Dr. Imre Takács, Éric Giroux, and Jasmin Patry.

ABSTRACT

The respiration rate has generated much interest as a means of monitoring and controlling the activated sludge process because it is directly associated with both biomass growth and substrate removal. Respirometry has long been recognized as a valuable tool for controlling the activated sludge process, and as a result, many respirometry-based control strategies have been proposed in the literature. However, few respirometry-based control strategies have ever been implemented in practice or even tested rigorously through simulation. Proposed strategies are often theoretical and do not describe realistic process implementations. This study has therefore developed a benchmark and methodology for conducting simulation studies to test the proposed control strategies within a complete and consistent set of process conditions.

The benchmark consists of a complete set of influent conditions, a standard activated sludge plant configuration, models for the activated sludge process and the secondary clarification process, as well as values for the model parameters and initial values for the state variables. The benchmark provided the framework for the development of the simulation-based methodology. The methodology uses the benchmark, and includes a set of guidelines for implementing a control strategy in the benchmark plant and a set of tests for evaluating the performance and benefits of a proposed control system.

The benchmark and methodology were then applied to test selected control strategies from the literature. In examining the strategies, it was found that controller performance is greatly affected by the high-frequency variations in the influent flow and pollutant concentrations, as well as the multi-variable interactions occurring in an activated sludge plant.

The important recommendations of this study are to extend the methodology to include: 1) the use of other activated sludge systems, such as a carbon and nutrient removal plant, for testing the control strategies; 2) more quantitative measures of performance to enable comparisons of different control strategies; and 3) the use of the benchmark and methodology as a tool for distinguishing the potentially feasible strategies from the strategies that will potentially fail.

TABLE OF CONTENTS

LIST OF TABLES

Table | Page

LIST OF FIGURES

Figure Page

Figure Page

Figure | Page

GLOSSARY

b_a	Yield for autotrophic biomass	
b_H	Yield for heterotrophic biomass	
f_P	Fraction of biomass leading to particulate products	
$f_{Q_{ww}}$	Influent flow distribution	
i_{XB}	Mass of nitrogen per mass of COD in biomass	
i_{XP}	Mass of nitrogen per mass of COD in products from biomass	
k_a	Ammonification rate	
k_h	Maximum specific hydrolysis rate	
K_c	Proportional gain of a P, PI or PID controller	
K_La	Oxygen mass transfer coefficient	$[d^{-1}]$
K_{NH}	Autotrophic saturation coefficient for S_{NH}	$[g\ NH_3\text{-}N\ m^{-3}]$
K_{NO}	Nitrate half-saturation coefficient for denitrifying heterotrophic biomass	
K_{OA}	Oxygen half-saturation coefficient for autotrophic biomass	
K_{OH}	Oxygen half-saturation coefficient for heterotrophic biomass	
K_p	Steady-state or process gain $= \dfrac{\Delta Output}{\Delta Input}$	
K_S	Heterotrophic saturation coefficient for S_S	$[g\ COD\ m^{-3}]$
K_X	Half-saturation coefficient for hydrolysis of slowly biodegradable substrate	
η_g	Correction factor for μ_H under anoxic conditions	
η_h	Correction factor for hydrolysis under anoxic conditions	
Q_{waste}	Flow rate of waste sludge	$[m^3\ d^{-1}]$
Q_{ww}	Flow rate of influent	$[m^3\ d^{-1}]$
r_h	Settling parameter associated with the hindered settling component of the settling velocity equation (Takács *et al.*, 1991)	$[m^3\ g^{-1}]$
r_p	Settling parameter associated with the low concentration and slowly settling component of the suspension (Takács *et al.*, 1991)	$[m^3\ g^{-1}]$
rr	Respiration rate	$[g\ O_2\ m^{-3}\ h^{-1}]$
rr_{act}	Actual respiration rate	$[g\ O_2\ m^{-3}\ h^{-1}]$

rr_{end}	Endogenous respiration rate	[g O_2 m^{-3} h^{-1}]
rr_{max}	Maximum respiration rate	[g O_2 m^{-3} h^{-1}]
rr_{sp}	Specific respiration rate	[mg O_2 g^{-1} MLSS h^{-1}]
rr_{ti}	Respiration rate in tank i	[g O_2 m^{-3} h^{-1}]
S_I	Soluble inert organic matter	[g COD m^{-3}]
S_{ND}	Soluble biodegradable organic nitrogen	[g N m^{-3}]
S_{NO}	Nitrate and nitrite nitrogen	[g N m^{-3}]
S_{NH}	NH^+_4 + NH_3 nitrogen	[g N m^{-3}]
S_O	DO in the liquid phase	[g (-COD) m^{-3}]
S_S	Readily biodegradable substrate	[g COD m^{-3}]
SS	Total suspended solids	[g COD m^{-3}]
T_I	Integral time constant or reset time	[days]
T_D	Derivative time constant	[days]
v_o	Maximum theoretical settling velocity	[m d^{-1}]
v_s	Settling velocity	[m d^{-1}]
$XCOD$	COD of effluent suspended solids	[g COD m^{-3}]
X_I	Particulate inert organic matter	[g COD m^{-3}]
X_{BA}	Active autotrophic biomass	[g COD m^{-3}]
X_{BH}	Active heterotrophic biomass	[g COD m^{-3}]
X_P	Particulate products arising from biomass decay	[g COD m^{-3}]
X_{ND}	Particulate biodegradable organic nitrogen	[g N m^{-3}]
X_s	Slowly biodegradable substrate	[g COD m^{-3}]
Y_A	Yield for autotrophic biomass	
Y_H	Yield for heterotrophic biomass	
τ	Time constant (characterises the speed of the response of the output variable to a change in the input variable)	[days]
θ	Dead time of a process (time interval for which there is no response in the input variable to a change in the output variable)	[days]
μ_A	Maximum specific growth rate for autotrophic biomass	
μ_H	Maximum specific growth rate for heterotrophic biomass	

Abbreviations

ASP	Activated sludge plant	
ASM	Activated sludge model	
bCOD	biodegradable chemical oxygen demand	[g m^{-3}]
C-removal	Carbon removal	
COD	Chemical oxygen demand	[g m^{-3}]
CSTR	Continuous stirred tank reactor	
DO	Dissolved oxygen concentration	[g m^{-3}]
FB	Feedback control configuration	
FF	Feedforward control configuration	
F/M	Food-to-microorganism ratio	
ISE	Integral squared error (a measure of the cumulative deviation of the controlled variable from its set point)	
MLSS	Mixed liquor suspended solids	[g m^{-3}]
N-removal	Nitrogen removal	
P controller	Proportional controller	
PI controller	Proportional-integral controller	
PID controller	Proportional-integral-derivative controller	
WWTP	Wastewater treatment plant	

1 Introduction

Wastewater treatment plants (WWTP) are generally subject to large fluctuations in hydraulic and organic loadings resulting from diurnal and seasonal variations in flows. The activated sludge process is particularly sensitive to the variations in influent conditions. Consequently, control of the activated sludge process is necessary to meet effluent quality standards and maintain low operating costs.

Respirometry is the measurement and interpretation of the biological oxygen consumption rate under well-defined experimental conditions (Spanjers *et al.*, 1998a). The respiration rate or oxygen uptake rate is the amount of oxygen consumed by the biomass per unit volume and time to remove and degrade biodegradable waste. Respiration rate is usually measured with respirometers. All respirometers are based on some technique for measuring the rate at which the biomass takes up dissolved oxygen from the liquid. Present-day respirometers can provide respiration rate measurements automatically and in real-time.

Since the respiration rate is directly associated with both biomass growth and substrate removal, respirometry has generated much interest as a means of monitoring and controlling the activated sludge process. Many respirometry-based control strategies have been proposed in literature but few have been rigorously tested or verified, or let alone have been implemented in a large-scale activated sludge plant. This is due to inadequate measurement techniques and lack of understanding of the information content of respirometric data (Spanjers *et al.*, 1998a). Furthermore, many of the control strategies are theoretical and do not provide adequate details on process implementation. As a result, the feasibility and potential benefits of these strategies are unknown.

Therefore, the first purpose of this study was to develop a simulation-based benchmark (Spanjers *et al.*, 1998a) and methodology for testing respirometry-based control strategies within a complete set of process conditions. The second purpose of this study was to apply the benchmark and methodology to evaluate some control strategies from the literature.

The benchmark is a simulation-based framework that provides a consistent set of conditions for testing control strategies. It consists of a complete set of influent conditions, a standard activated sludge plant configuration, models for the activated sludge process and the secondary clarification process, as well as values for the model parameters and initial values for the state variables.

The benchmark provided the framework for the development of the simulation-based methodology proposed in this study. The methodology employs the benchmark and provides a set of steps for implementing a control strategy in a simulation-based setting and a set of tests for examining the performance of a control strategy.

To provide some background information on respirometry-based control of the activated sludge process, the discussion will begin with the fundamentals of respiration and modelling of the respiration rate.

Following this, a literature review of the application of dynamic modelling and simulation to real-world wastewater treatment plants will be presented. The review provides the rationale for the use of well-accepted dynamic models to evaluate respirometry-based control strategies. Several examples of control strategies proposed from literature are presented to show how the respiration rate is employed as a control parameter in the activated sludge process.

A discussion of the benchmark will then be presented. This will follow with a description of the simulation-based methodology for evaluating respirometry-based control strategies. Then, the simulation of four respirometry-based control strategies from the literature will be described. These strategies were selected for the following reasons:

- Each of the proposals is interesting and seems potentially valid.
- Each strategy shows variations on how the respiration rate can be used as a control parameter.
- Each strategy uses a different manipulated variable.
- The description of the control strategy is clear and understandable.

The methodology was applied to examine three of the four control strategies: Stephenson *et al.* (1981), Stephenson *et al.* (1983) and Sekine *et al.* (1988). A fourth strategy proposed by

Fujumoto et al. (1981) was also evaluated but application of the methodology was not necessary as conclusions on the feasibility of the strategy were made from preliminary simulations.

2 Fundamentals of Respiration in the Activated Sludge Process

2.1 Biochemistry of Respiration

In biological wastewater treatment a variety of micro-organisms, principally bacteria, are used to remove biodegradable substrate. A portion of the substrate is oxidised to provide energy, which is subsequently used in cellular growth and reproduction. The remaining portion of the substrate is converted into new cell mass.

Oxidation of the biodegradable substrate into energy by biomass is referred to as respiration. More specifically, respiration is a metabolic process in which either organic or inorganic compounds serve as electron donors and inorganic compounds such as O_2, NO_2^-, NO_3^-, SO_4^{2-} serve as the ultimate electron acceptors. If oxygen is the ultimate electron acceptor, the process is known as aerobic respiration. The biomass convert energy of intermolecular bonds in the organic substrate to the high-energy phosphate bonds of adenosine triphosphate (ATP). This energy is then used to synthesize the various molecular components required for cell growth and reproduction. ATP is generated as electrons removed from the substrate are transferred along the electron transport chain from one metabolic carrier to the next, and ultimately to the terminal electron acceptor - oxygen in the aerobic activated sludge process (Spanjers *et al.*, 1998b).

Different types of bacteria use oxygen to consume various components of the wastewater. Heterotrophic biomass oxidize carbonaceous substrate, nitrifying biomass oxidize ammonia substrate, sulphur biomass oxidize hydrogen sulphide (or other reduced sulphur compounds), and iron biomass oxidize inorganic ferrous iron. These oxidation processes all typically contribute to the total respiration rate of the bacteria in the activated sludge process.

2.2 Modelling Respiration

The IAWQ Activated Sludge Model No.1 (ASM1) was employed in this study to perform simulations. This model uses the death-regeneration approach (Henze *et al.*, 1987) to model respiration. In this approach, respiration is associated only with the aerobic growth of heterotrophic biomass (X_H) and nitrifying biomass (X_A).

The main processes of heterotrophic growth and biodegradation described by the death-regeneration model are shown in Figure 2.1. In this model, decaying biomass is split into two fractions: inert matter (X_P) and slowly biodegradable matter (X_S). The latter is subsequently hydrolysed into readily biodegradable substrate (S_S). This model implies that even when all the substrate originating from the wastewater have been oxidized, oxygen consumption associated with growth from substrate released from decay and hydrolysis still occur. The amount of new biomass formed from the released substrate is always less than the amount of biomass lost.

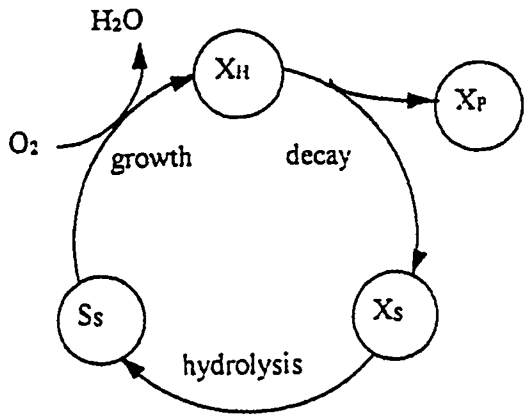

Figure 2.1: Death-regeneration model of biomass respiration (Spanjers *et al.*, 1998b)

The death-regeneration model also implies that in the absence of biodegradable matter from external resources (e.g. wastewater), respiration will decrease until all the biomass have decayed. In this situation, the respiration rate is referred to as endogenous respiration. The endogenous respiration rate (rr_{end}) is defined as the oxygen consumption rate in the absence of substrate from external sources. By this definition, endogenous respiration includes not only the decay and growth of bacteria but also oxygen consumption by protozoa. This means that substrate is oxidized only for energy generation to maintain the biomass in its current state. In other words, no new net biomass is produced. Since the endogenous respiration rate is practically independent of substrate concentration, it is indicative of the active biomass concentration (Spanjers *et al.*, 1998b).

When there is a continuous supply of biodegradable substrate, the result is a net growth of biomass and an associated increase in respiration rate, which is higher than the endogenous respiration rate. The respiration rate in this case is the actual respiration rate (rr_{act}) and is a function of the concentration of biodegradable matter in the aeration tank.

When the concentration of biodegradable matter is very high, biomass will grow at its maximum rate and the respiration rate will be close to the maximum value. The respiration rate in this case is referred to as the maximum respiration rate (rr_{max}). As with the endogenous respiration, the maximum respiration rate is practically independent of substrate concentration and is therefore indicative of the active biomass concentration.

The death-regeneration model of respiration rate, depicted in Figure 2.1, can be expressed mathematically in terms of growth and decay:

$$rr = \left(\frac{1-Y_H}{Y_H}\right)\left(\frac{\mu_{mH} S_S X_H}{K_S + S_S}\right) + \left(\frac{4.57-Y_A}{Y_A}\right)\left(\frac{\mu_{mA} S_{NH} X_A}{K_{NH} + S_{NH}}\right)$$

Eq. 2.1

where K_{NH} autotrophic saturation coefficient for S_{NH}

K_S heterotrophic saturation coefficient for S_S

S_{NH} ammonium

S_S readily biodegradable substrate

X_A autotrophic biomass

X_H heterotrophic biomass

Y_A yield autotrophic biomass

Y_H yield heterotrophic biomass

μ_{mA} maximum specific growth rate autotrophic biomass

μ_{mH} maximum specific growth rate heterotrophic biomass

The relationship in Equation 2.1 indicates that respiration rate is governed by the growth and decay of both heterotrophs and nitrifiers. When substrate concentrations, comprising of readily biodegradable substrate and ammonia nitrogen, are high the first and second terms of Eq. 2.1 approach saturation and the respiration rate accordingly approaches the maximum rate. Conversely, when most of the substrate is oxidized, so that S_s and S_{NH} concentrations are very low, a quasi steady-state situation occurs. In this situation, the respiration rate is endogenous and is governed by the biomass concentration. According to the death-regeneration model, the substrate concentration will never be zero, even when external substrate is absent. because substrate is regenerated from decay and subsequent hydrolysis (see Figure 2.1). It should be noted that during endogenous respiration ammonium released from decay will only be partly oxidized because the other part of it will be used for growth of biomass (Spanjers *et al.*, 1998b). Also note that the description given in Eq. 2.1. heterotrophic growth is only associated with only one substrate. S_S.

3 Review of the Applications of Dynamic Modelling and Simulation to Full-Scale Wastewater Treatment Plants

The advent of powerful, inexpensive computers and software applications have enabled modelling and simulation of real-world wastewater treatment plants (WWTP) to be a valuable and practical method of analysis and design. Many dynamic models for the wastewater treatment process have been developed in recent years and have been shown to adequately represent large-scale plant operations. Practical applications of dynamic models have shown to be particularly useful for investigating plant modifications and expansions, alternate operational strategies, and control strategies for large-scale wastewater treatment systems.

A majority of the dynamic modelling and simulation studies documented in the literature have been used to examine plant modifications and expansions. This was the case when Barnett and Takács (1994) used a dynamic model of a large-scale WWTP to investigate the effects of infiltration and high inflow on the plant. The simulation study showed how clarification capacity could be increased to handle larger flows. Additional simulations showed how step feed operation could be used to minimise upsets during high influent conditions, as well as an optimum strategy for the use of step feed.

Takács *et al.* (1995) performed dynamic modelling and simulation studies to evaluate expansion scenarios for several treatment plants. Simulations were conducted to investigate the implementation of nitrification in the Main WWTP in Toronto. For the Woodward Avenue treatment plant in Hamilton, a calibrated model was used by Takács *et al.* (1995) to evaluate the expansion of primary and final settling capacities. The model was also used to show that nitrification can be greatly improved by reconfiguring the aeration tanks to achieve plug flow conditions and by installing a fine pore aeration system to deliver the required oxygen transfer.

Coen *et al.* (1996) used a dynamic model of the Hoogstraten WWTP in Belgium to evaluate several plant upgrades to increase the denitrification capacity. The upgrade scenarios that were investigated include: a) creation of anoxic zones, b) implementation of step feeding, and c) introduction of internal recirculation. By conducting dynamic simulations, they optimised denitrification by creating additional anoxic zones at the head of the biological reactor during weekend operations and bypassing the primary clarifier.

A dynamic model of the Derby Sewage treatment plant in the UK was employed by Crabtree *et al.* (1996) to upgrade the plant and sewer system to better handle wet weather loadings. The simulation study also identified key discharge points, prevalent pollutants, and areas most affected by discharges.

Görgün *et al.* (1996) developed a dynamic model of the Riva WWTP in Instanbul, Turkey to examine if a step feed system would enable the plant to meet the total nitrogen effluent standard of 10 mg N L^{-1} for increased organic concentrations in the influent.

Leeuw *et al.* (1996) used dynamic modelling and simulation to evaluate various plant modifications for the Friesland Waterboard Harlingen WWTP in The Netherlands. The plant could not meet effluent standards for total nitrogen concentration because the low F/M ratio prevented complete denitrification. Simulations with a calibrated model of the plant showed that the following process modifications would enable the plant to meet effluent standards: a) mechanical mixing in all denitrification tanks; b) automatic oxygen control in all nitrification tanks; c) rearranging the nitrification and denitrification tanks; and d) higher recirculation rate.

A calibrated model of a municipal WWTP in North-Rhine Westphalia was used by Sintic *et al.* (1998) to assess if proposed plant expansions have the capacity to meet future effluent requirements. Simulations showed that the expansions would enable the plant to meet effluent requirements for ammonia and total nitrogen.

Dynamic modelling and simulation has also been a useful tool for examining operational strategies for large-scale wastewater treatment plants. Takács *et al.* (1993) used a calibrated dynamic model of the Gold Bar WWTP to identify effective operational strategies. The simulation study found that the following strategies would improve plant performance: a) decrease the SRT of the plant to prevent settler overloading and delay plant expansion; b) take off service two aeration tanks and one clarifier to achieve energy savings without jeopardizing process performance; and c) a bypass scheme to prevent operational upset during heavy storm flow conditions.

Barnett and Takács (1994) used a calibrated model of a large-scale WWTP to show that considerable aeration costs could be realised with tighter control of the dissolved oxygen levels in the plant. Takács *et al.* (1995) reported how the GPS-X simulator was installed in the Main WWTP to determine the best operational strategies to use during emergency pump shutdowns and construction periods.

Kurata *et al.* (1996) applied dynamic models of the Shinnanyo WWTP in Tokuyama Bay, Japan, to improve biological phosphorous removal (BPR) at the plant. Low organic substrate concentrations caused the plant to inefficiently remove phosphorous. Simulation studies demonstrated that the efficiency of BPR could be improved by 90% by injecting primary sludge into the activated sludge tanks and by decreasing the SRT of the plant. Full-scale experiments verified that these relatively easy modifications improved BPR at the plant by 95%.

Funamizu and Takauwa (1994) investigated the effect of using the sewage system to transport and melt snow on a municipal WWTP. Simulation studies showed that if a sewage system is to be used for such purposes, the sludge treatment system must be enlarged, or a nitrifying-bacteria-holding apparatus must be added to the aeration basins to maintain present treatment levels.

Jones *et al.* (1994) used dynamic modelling and simulation to assess the effect of various operating configurations on such plant performance as overall plant VOC emissions, and the ability of the system to attenuate sudden increases in substrate concentrations in the influent. Simulations were also used to examine factors impacting the final settling tank performance and options for improving performance.

Large-scale applications of dynamic modelling and simulation have also been used for designing, evaluating and improving the operational control of treatment plants. One interesting study was conducted by Takács *et al.* (1995) for the Coleshill WWTP in Birmingham, UK. A calibrated model of the plant was linked with an on-line monitoring system available at the plant to improve operational control of the plant.

Schilling *et al.* (1996) integrated calibrated models of the sewer system and the Klagshamn WWTP in Malmö, Sweden to develop a real-time flow control system. The objective of the control system was to reduce pollutant discharges from both plant and combined sewer overflows. The simulation study lead to a full-scale implementation of the flow control system for the plant. The control system consisted of three control actions, which are sequentially invoked depending on the flow rate: 1) use in-line storage capacity until storage capacity has exceeded; 2) switch to a step feed operation; and 3) use by-pass operation as a last resort.

Coen *et al.* (1997) conducted simulations with a calibrated model of a municipal WWTP in Belgium to design a proportional controller to regulate the methanol dosage rate. The plant treated nitrogen-rich wastewater by an intensive nitrification-denitrification process. The control of methanol dosing resulted in a 30 per cent reduction in methanol usage, which represented a saving of about 50, 000 ECU per year. Simulations were also employed to evaluate an alternative carbon source for enhancing denitrification.

Other practical large-scale applications of dynamic modelling and simulation include the works of Lin (1996), Luonsi and Halttunen (1997), and Schwarz *et al.* (1997). Lin (1996) developed a heat transfer model to predict the water temperature of aeration tanks in biological wastewater treatment plants. The various heat transfer mechanisms modelled include heat gained from solar radiation and biochemical reactions, and heat lost from evaporation, aeration, wind blowing and conduction through walls. Predicted and measured temperatures matched very well at a chemical fiber WWTP.

Luonsi and Halttunen (1997) calibrated a model of a full-scale Kraft pulp and paper mill to predict the fate of dissolved organic matter (DOM). Prediction of the fate of DOM in the mill is important in determining appropriate treatment methods. Simulations predicted that the fate of DOM starts from the oxygen delignification process and ends at the chlorine dioxide bleaching process. Results were within 10% of the DOM values measured in the mill.

Schwarz *et al.* (1997) developed a calibrated model of a fluidised bed reactor (FBR). Simulations were conducted with the model to investigate the effects of scaling-up the FBR to an industrial-sized reactor on the performance of anaerobic wastewater treatment. More specifically, the effects of increased pressure, increased feed to recirculation ratio, and increased chemical oxygen demand (COD) loading rate on pH-gradients were investigated.

This review demonstrates that dynamic models can be a useful and valid tool for improving and optimizing the performance of full-scale wastewater treatment plants. Dynamic modelling and simulation have been used for a) evaluating plant designs, expansions and modifications; b) assessing various operational strategies, and c) developing control strategies for wastewater treatment plants.

The above practical applications of dynamic modelling and simulation are summarized in Table 3.1.

Table 3.1: Applications of modelling and simulation to full-scale wastewater treatment plants

Reference	WWTP	Plant Objective of Modelling and Simulations	Models Used	Simulator
Takács *et al.* (1993)	Gold Bar WWTP, Edmonton, Alberta, Canada	Assess plant capacity Identify effective operational strategies	Modified ASM-1 (Henze et al., 1987) Double exponential settler model (Takács et al., 1991)	GPS-X (Hydromantis Inc.)
Barnett and Takács (1994)	Unspecified large-scale WWTP	Evaluate expansion alternatives and operational strategies	ASM-1 Double exponential settler model	GPS-X (Hydromantis Inc.)
Funamizu and Takakuwa (1994)	Full-scale municipal WWTP, Sapporo	Investigate effect of using sewage system to transport and melt snow on WWTP	ASM-1 Dupont and Henze (1992)	Unspecified
Jones *et al.* (1994)	WWTP at a petrochemical plant, Ontario	Evaluate different operating strategies to optimize system performance	ASM-1 Double exponential settler model	GPS-X (Hydromantis Inc.)
Takács *et al.* (1995)	Coleshill WWTP, Birmingham, U.K	Improve operational control	ASM-1 Double exponential settler model	GPS-X (Hydromantis Inc.)
Takács *et al.* (1995)	Hamilton-Woodward WWTP, Hamilton	Evaluating various plant upgrade scenarios	ASM-1 Double exponential settler model	GPS-X (Hydromantis Inc.)
Takács *et al.* (1995)	Main treatment plant, Toronto	Improve daily operation of the plant	ASM-1 Dynamic fluid model	GPS-X (Hydromantis Inc.)

Reference	WWTP	Plant Objective of Modelling and Simulations	Models Used	Simulator
Coen *et al.* (1996)	Hoogstraten WWTP, Belgium	Upgrade and optimize the plant for biological nitrogen removal	ASM-1	West (Hemmis NV)
Crabtree *et al.* (1996)	Derby sewage treatment works, Derby, UK	Upgrade plant to better handle wet weather loading	FWR (1994)	Unspecified
Görgün *et al.* (1996)	Riva WWTP, Instanbul	Determine if proposed modification to a two-stage step feed system will enable plant to meet effluent standards	Orhon and Artan (1994)	Unspecified
Kurata *et al.* (1996)	Shinnanyo WWTP, Tokuyama Bay, Japan.	Retrofit the plant to improve biological phosphorous removal (BPR)	ASM-2	Unspecified
Leeuw *et al.* (1996)	Friesland Waterboard Harlingen WWTP, The Netherlands	Evaluate various plant modifications to enable plant to meet effluent standards for total nitrogen concentration	ASM-1	SIMBA (IFAK)
Lin (1996)	Chemical fiber WWTP	-	Heat transfer model (Lin, 1996)	Unspecified
Schilling *et al.* (1996)	Klagshamn WWTP, Malmö, Sweden.	Develop a real- time flow control system for the plant	Dupont and Henze (1992)	EFOR (Dupont and Henze, 1992) MOUSE-PILOT (Bo-Nielson et al., 1993)
Luonsi and Halttunen (1997)	Full-scale Kraft pulp and paper mill	Determine appropriate treatment methods for plant	Modified Procell model (Endat, 1994).	Unspecified
Coen *et al.* (1997)	Full-scale industrial WWTP, Belgium	Improve plant performance by controlling the methanol dosage rate	ASM-1 Double exponential settler model	West (Hemmis NV)
Schwarz *et al.* (1997)	Sugar plant, Clauen	Effects of scaling-up a fluidized bed reactor for anaerobic wastewater treatment	Schwarz et al. (1996)	ACSL
Sintic *et al.* (1998)	Unspecified WWTP, North-Rhine Westphalia	Determine if plant expansion will enable plant to meet both European and German effluent regulations	ASM-1	Unspecified

4 Examples of Respirometry-Based Control Strategies Proposed in Literature

4.1 Summary of examples from literature

In the proposed strategies, respirometry-based control usually involves deducing information about the process from respiration rate measurements in order to perform some control action. In this case, the respiration rate is referred to as a measured variable. However, the respiration rate can also be used as a controlled variable. This usually involves regulating the respiration rate at a certain value by manipulating some input variable.

In discussing the various respirometry-based control strategies, a distinction must be made between the operational objectives of a wastewater treatment plant and the control objectives of a control system. The operational objective of a plant is to comply with effluent standards while minimizing costs. To accomplish this, several operational objectives must be carried out, such as maintaining the right biomass population, maintaining adequate aeration intensity, and ensuring good settling properties. Accordingly, these operational objectives can be accomplished by specifying control objectives, such as, "keep the respiration rate at 22 g m^{-3} h^{-1}", or "keep the dissolved oxygen concentration at 2 g m^{-3}", and/or "maintain a sludge retention time of 3 days". Control strategies are implemented to accomplish some control objective. Most of the control strategies documented in literature are of this nature in that respirometric measurements are employed to accomplish some control objective. The intention of the proposed strategies was that in accomplishing the control objective, operational objectives of a plant should be met.

Of the respirometry-based control strategies compiled by Spanjers *et al.* (1998b), strategies using the oxygen mass transfer rate (K_La), return activated sludge flow rate (Q_{ras}), waste sludge flow rate (Q_{waste}), influent flow rate (Q_{ww}), and influent flow distribution ($f_{Q_{ww}}$) are the most popular. Examples of respirometry-based control strategies proposed in literature are provided in Table 4.1. These strategies are classified according to the manipulated variable that is used in the control scheme.

Table 4.1: Examples of respirometry-based control strategies that have been proposed in literature

Manipulated variable	Control configuration	Controlled variable	Respiration rate measurement	Operational objectives to be achieved with control strategy	Reference
K_La	Feedforward control	DO	rr in aeration tank	Meet effluent standards with minimum aeration costs.	Haarsma and Keesman (1995)
K_La	Feedforward control	DO	Maximum rr at inlet of aeration tank	Meet effluent standards with minimum aeration costs.	Fujimoto *et al.* (1981)
K_La DO control loop	Cascade control strategy • Two feedback loops are nested, with the secondary loop (for DO control) located inside the primary loop. • The $rr_{activity}$ controller is in the primary loop. • The DO controller is in the secondary loop.	• $rr_{activity} = rr_{sp.end} / rr_{sp}$ i.e. ratio of specific endogenous respiration rate to specific respiration in the last compartment (Primary controlled variable) • DO (secondary controlled variable)	• rr_{end} in the last compartment (measured during low loading periods) • rr in the last compartment • Mixed liquor suspended solids	Ensure enough biomass activity to obtain desired effluent quality.	Sekine *et al.* (1988)
Q_{ras}	Combination of feed-forward and feedback control	rr_{sp}	rr in the aeration tank	Maintain the desired effluent quality.	Stenstrom and Andrews (1979)

Manipulated variable	Control configuration	Controlled variable	Respiration rate measurement	Operational objectives to be achieved with control strategy	Reference
Q_{ras}	Combination of feed-forward and feedback control	F/M	• rr at inlet of aeration tank • rr of the *ras* • rr in the final pass of the aeration tank	Maintain the appropriate biomass concentration for the influent load.	Flanagan (1977)
Q_{waste}	Feedback control	rr_{end}	rr_{end}: obtained by measuring the respiration rate at the outlet of the aeration tank during low loading periods	Ensure the appropriate biomass concentration to achieve adequate treatment.	Stephenson *et al.* (1981) Related references: Brouzes (1979)
Q_{waste}	Combination of feedforward and feedback control	F/M	• rr at inlet of aeration tank • rr of the *ras* • rr in the final pass of the aeration tank	Maintain the appropriate biomass concentration for the influent load.	Flanagan (1977)
Q_{ww}	Feedforward control	Total oxygen demand (TOD) into the aeration tank (kg TOD $m^{-3} \cdot d^{-1}$)	rr_{act} in aeration tank	Balance the load into the plant.	Kim *et al.* (1995)
Q_{ww}	Feedback control	rr_{act}	• rr_{act} in tank • influent flow rate • DO concentration	Prevent overloading of the plant and minimize aeration costs.	Brouwer *et al.* (1994)
f_{Qww}	Feedback control (rule-based controller)	rr_{sp}	rr_{sp} in last compartment	Produce sludge with more consistent settling properties.	Vitasovic and Andrews (1989)

Manipulated variable	Control configuration	Controlled variable	Respiration rate measurement	Operational objectives to be achieved with control strategy	Reference
f_{Qww}	Feedback control	rr_{sp} in the last compartment ($rr_{sp} = rr/X$)	• rr in last compartment • Mixed liquor suspended solids	A constant rr_{sp} value should control the effluent substrate concentration being discharged to the settler.	Stephenson *et al.* (1983) Related references: Andrews (1977)

The respirometry-based control strategies shown in Table 4.1 demonstrate the various ways in which the respiration rate is employed for controlling the activated sludge process. The strategy proposed by Haarsma and Keesman (1995) uses the respiration rate in the aeration tank as an indicator of changes in the influent loading. This respiration rate is used in a feedforward control scheme to calculate the DO set point in the aeration tank. The new set point, along with the respiration rate in the tank and other process parameters, are used to calculate the adjustment in K_La required to maintain the DO concentration at the set point. This control scheme aims at minimizing aeration costs by adjusting the aeration intensity according to the influent load.

Stenstrom and Andrews (1979) presented a strategy in which the specific respiration rate (rr_{sp}) is used as an indicator of the effluent biodegradable substrate concentration. By controlling rr_{sp} at a set point in the aeration tank, the desired effluent quality may be maintained. The proposed strategy involves a feedforward-feedback control scheme. In the feedforward component, the desired MLVSS concentration (X_{des}) is calculated based on the respiration rate in the aeration tank (rr), the rr_{sp} set point and the volume of the aeration tank (V) as follows:

$$X_{des} = \frac{rr}{V \cdot rr_{sp,setpoint}}$$

Eq. 4.1

The feedback component involves manipulating Q_{ras} to maintain the rr_{sp} set point as follows:

$$Q_{ras} = \frac{V\frac{dX_{des}}{dt} + FX_{des}}{X_1 - X_{des}}$$

Eq. 4.2

The measurements required for calculating Q_{ras} include rr, influent flow rate (F), and the MLVSS concentration in the aeration tank (X_l).

Flanagan (1977) proposed another feedforward-feedback control scheme in which Q_{ras} is manipulated to maintain the food-to-microorganism ratio (F/M) within an acceptable range. The objective of the control strategy is to maintain the appropriate biomass concentration for the influent load. The feedforward component involves adjusting Q_{ras} to meet the F/M set point. The feedback controller adjusts the F/M set point for the feedforward controller by an amount proportional to the difference between the respiration rate at the inlet and the respiration rate at the outlet of the aeration tank.

Flanagan (1977) also proposed another feedforward-feedback control scheme in which the F/M ratio is controlled by manipulating Q_{waste}. The feedforward controller adjusts Q_{waste} to meet the F/M set point, which is calculated by the feedback controller. The F/M set point is adjusted by an amount proportional to the difference between the respiration rate at the inlet and the respiration rate at the outlet of the aeration tank.

Brouwer *et al.* (1994) proposed a strategy in which Q_{ww} is used as a manipulated variable in a feedback control scheme to maintain rr_{act} in the aeration tanks at a set point. The set points for rr_{act} are chosen according to the biodegradable loading rate into the plant. This strategy requires a plant with storage capacity.

Kim *et al.* (1995) also proposed a control strategy in which Q_{ww} is used as a manipulated variable. The strategy aims to balance the load into the plant by maintaining the total oxygen demand (TOD) into the aeration tank at a set point through adjustments in Q_{ww}. rr_{act} is used as an indicator of the TOD loading rate in this proposal.

The strategy proposed by Vitasovic and Andrews (1989) involves a rule-based feedback controller that attempts to minimize the variations of rr_{sp} by manipulating f_{QWW}. In this strategy rr_{sp} is used as an indicator of biomass growth.

The remaining control strategies proposed by Fujimoto *et al.* (1981), Stephenson *et al.* (1981), Sekine *et al.* (1988) and Stephenson *et al.* (1983) will be investigated in the following sections using a simulation-based approach.

5 Methodology for Conducting Simulation Studies of Respirometry-Based Control Strategies

5.1 Introduction

Many control strategies involving the respiration rate have been proposed in literature, but few experimental or even simulation studies have been conducted to evaluate the feasibility or benefits of these strategies. This is due to confusion arising partly from the lack of details provided to implement these strategies in an activated sludge plant and partly due to the lack of understanding of the different types of respiration rates that can be monitored. Therefore a systematic simulation-based methodology for assessing respirometry-based control strategies would support the evaluation of the control strategies by providing a consistent set of process conditions.

A benchmark for testing respirometry-based control strategies was developed by the author along with Dr. Henri Spanjers (Wageningen University), Dr. Peter Vanrolleghem and Henk Vanhooren (University of Gent) and Dr. Gilles Patry (University of Ottawa). This work was published and presented by Spanjers *et al.* (1998a). The benchmark provides the framework for conducting simulation studies of respirometry-based control strategies. It consists of well-accepted process models, a complete set of influent conditions, a standard activated sludge plant layout, values for the model parameters, and initial values for the state variables.

The simulation-based methodology developed in this study was based on the benchmark. The methodology consists of the benchmark, a set of steps for implementing a control strategy, and a set of tests to evaluate the performance of a control system.

The different components of the benchmark and the methodology will be described in this section. Discussions of the benchmark are based on the work of Spanjers *et al.* (1998a) and Vanhooren and Nguyen (1996).

The benchmark and methodology was applied to conduct simulation studies of respirometry-based control strategies proposed by Stephenson *et al.* (1981), Stephenson *et al.* (1983), and Sekine *et al.* (1988). The strategy proposed by Fujimoto *et al.* (1981) was evaluated without the need for the methodology.

5.2 The Benchmark (Spanjers *et al.*, 1998a)

The benchmark is the framework of the simulation-based methodology. It consists of process models for the activated sludge process and the secondary clarification process, a complete set of influent conditions, a standard activated sludge plant configuration, values for the model parameters and initial values for the state variables. The benchmark was developed with the intention of being independent of simulation platform. It has proven to be a useful simulation tool and is currently being used by the European Cooperation in the field of Scientific and Technical Research (COST) and the IAWQ Task Group on Respirometry in Control for testing control strategies and process models. Details of the benchmark can also be found at the website, www.ensic.u-nancy.fr/COSTWWTP.

The simulations in this work were performed with GPS-X (Hydromantis Inc.. Canada). GPS-X is a modular multipurpose modelling system for the simulation of wastewater treatment plants. Features of GPS-X (Hydromantis Inc.. Canada) that make it particularly suitable for conducting simulation studies include:

- the ability to handle various plant layouts; and
- the capability to allow user-defined models and controllers to be incorporated with plant models available in GPS-X. (Hydromantis Inc., Canada).

The following components of the benchmark will be discussed in this section:

- process models for the activated sludge process and the secondary clarification process;
- influent conditions for both dry and wet weather conditions;
- values for the kinetic and stoichiometric parameters of the activated sludge model;
- values for the settling parameters of the secondary clarification model;
- initial values for the state variables; and
- a standard activated sludge plant design based on the benchmark influent conditions.

5.2.1 Process Models

The benchmark uses well-accepted process models for both the activated sludge process and the secondary clarification process. The activated sludge process is based on the IAWQ Activated Sludge Model No. 1 (ASM1) (Henze *et al.*, 1987) and the secondary clarification process is based on the double exponential settling velocity model (Takács *et al.*, 1991). A layout of the benchmark activated sludge plant is depicted in Figure 5.1.

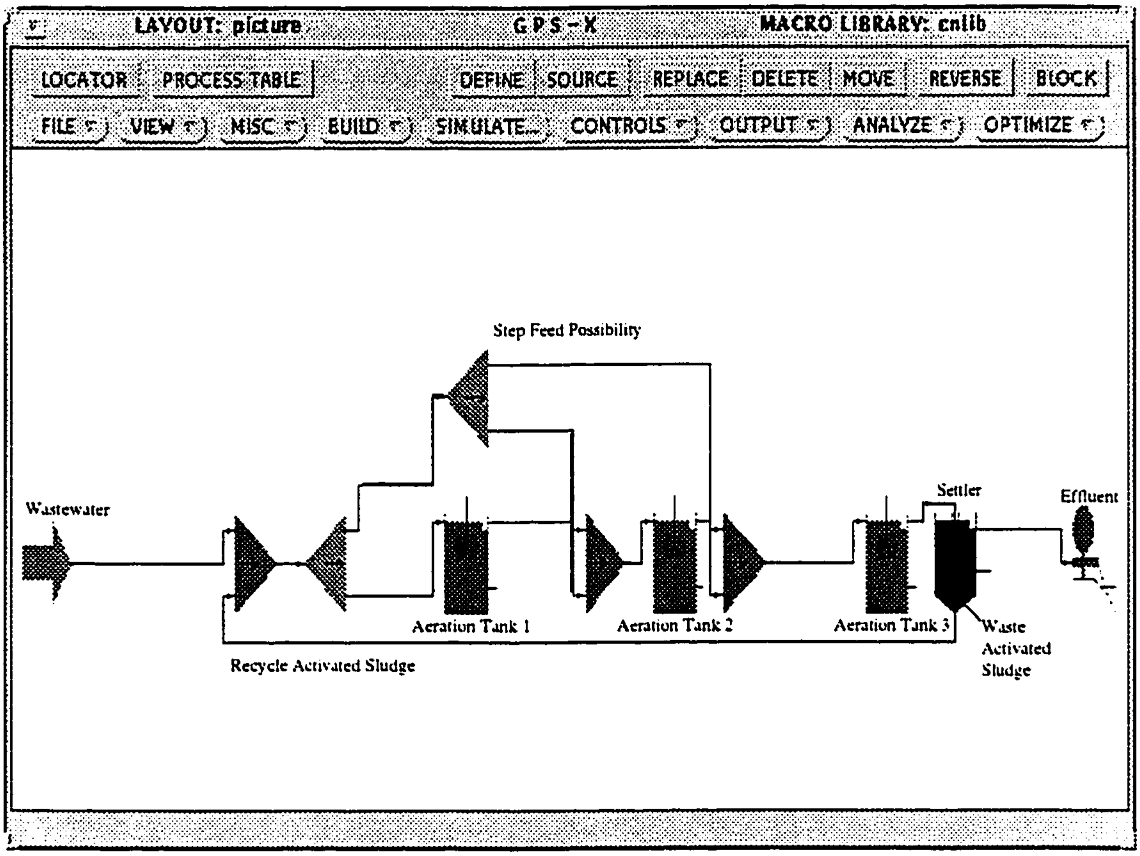

Figure 5.1: Layout of activated sludge plant

The IAWQ ASM1 (Henze *et al.*, 1987) was selected as the process model because it is widely recognized as an appropriate and well-accepted representation of the activated sludge process. Furthermore, it has been applied in numerous simulation studies and describes sufficiently the respiration process of the activated sludge generally well.

The IAWQ ASMI (Henze *et al.*, 1987) is based on a mechanistic interpretation of the behaviour of the organisms governing the process reactions. It has been shown to give a reliable description of the system response over wide ranges of system configuration (single and series reactor systems, aerated and non-aerated reactors, inter-reactor recycles), influent wastewater characteristics (COD, TKN, flow pattern) and operational parameters (sludge age, temperature, dissolved oxygen concentration) (Hydromantis, 1996). The IAWQ model can be applied directly for the simulation of any of the following systems: carbon-removal, carbon-removal with nitrification, and carbon and nitrogen removal.

The IAWQ ASM1 (Henze *et al.*, 1987) incorporates eight fundamental processes:

- aerobic growth of heterotrophic biomass;
- anoxic growth of heterotrophic biomass;
- aerobic growth of autotrophic biomass;
- decay of heterotrophic biomass;
- decay of autotrophic biomass;
- ammonification of soluble organic nitrogen;
- hydrolysis of entrapped particulate organic matter; and
- hydrolysis of entrapped organic nitrogen.

The concentration of all organic components, including biomass, are in COD units. All nitrogen species are expressed as nitrogen. The particulate components, also in COD units, must be expressed in mass units (MLSS) for the clarifier model.

In the IAWQ ASM1 (Henze *et al.*, 1987), the organic matter in a wastewater is divided into two categories: non-biodegradable and biodegradable matter. Non-biodegradable organic matter is biologically inert and passes through an activated sludge system unchanged in form. The non-biodegradable organic matter is further divided into soluble and particulate fractions. The biodegradable organic matter is also divided into two fractions: readily biodegradable and slowly biodegradable.

The nitrogenous matter in a wastewater is similarly divided into non-biodegradable and biodegradable components. The particulate portion of the non-biodegradable fraction is associated with the non-biodegradable particulate COD; the soluble portion is considered to be negligibly small and is not incorporated into the model. The biodegradable nitrogenous matter is divided into ammonia, soluble organic nitrogen and particulate organic nitrogen.

The IAWQ ASM1 (Henze *et al.*, 1987) is shown in Table 5.1. The fundamental processes of the model are listed in the leftmost column of Table 5.1, while their rate expressions are listed in the rightmost column. The components in the model are shown across the top and bottom of Table 5.1.

The parameters of the IAWQ ASM1 (Henze *et al.*, 1987) are defined as follows:

Components:

S_I	Soluble inert organic matter	[g(COD)m^{-3}]
S_S	Readily biodegradable substrate	[g(COD)m^{-3}]
X_I	Particulate inert organic matter	[g(COD)m^{-3}]
X_S	Slowly biodegradable substrate	[g(COD)m^{-3}]
X_{BH}	Active heterotrophic biomass	[g(COD)m^{-3}]
X_{BA}	Active autotrophic biomass	[g(COD)m^{-3}]
X_P	Particulate products arising from biomass decay	[g(COD)m^{-3}]
S_O	Oxygen	[g(COD)m^{-3}]
S_{NO}	Nitrate and nitrite nitrogen	[g(N)m^{-3}]
S_{NH}	NH_4^+ and NH_3 nitrogen	[g(N)m^{-3}]
S_{ND}	Soluble biodegradable organic nitrogen	[g(N)m^{-3}]
X_{ND}	Particulate biodegradable organic nitrogen	[g(N)m^{-3}]
S_{ALK}	Alkalinity	[Molar units]

Stoichiometric Parameters:

Y_H	Heterotrophic yield
Y_A	Autotrophic yield
f_P	Fraction of biomass yielding particulate products
i_{XB}	Mass N / Mass COD in biomass
i_{XP}	Mass N / Mass COD in products from biomass

Kinetic Parameters:

μ_H	Specific growth rate of heterotrophic biomass
K_S	Heterotrophic saturation coefficient for S_S
K_{OH}	Oxygen half-saturation coefficient for heterotrophic biomass

K_{NO}	Nitrate half-saturation coefficient for denitrifying heterotrophic biomass
b_H	Decay coefficient for heterotrophic biomass
μ_A	Specific growth rate of autotrophic biomass
K_{NH}	Autotrophic saturation coefficient for S_{NH}
K_{OA}	Oxygen half-saturation coefficient for autotrophic biomass
b_A	Decay coefficient for autotrophic biomass
η_g	Correction factor for anoxic growth of heterotrophs
k_a	Ammonification rate
k_h	Maximum specific hydrolysis rate
K_X	Half-saturation coefficient for hydrolysis of slowly biodegradable substrate
η_g	Correction factor for μ_H under anoxic conditions

The COD and suspended solids composite variables as well as the nitrogen composite variables involved in the IAWQ ASM1 ASM1 (Henze *et al.*, 1987) are described in Appendix A.1.

The kinetic and stoichiometric parameters of the IAWQ ASM1 (Henze *et al.*, 1987) used in this study were selected by comparing default values from the IAWQ ASM1 (Henze *et al.*, 1987) and No.2 (Henze *et al.*, 1994), as well as from the simulators, GPS-X (Hydromantis Inc., Canada) and WEST (Hemmis NV, Belgium). The parameters for the IAWQ ASM1 will be discussed further in Section 5.2.3.

Component → i / j Process ↓	1 S_I	2 S_S	3 X_I	4 X_S	5 $X_{B,H}$	6 $X_{B,A}$	7 X_P	8 S_O	9 S_{NO}	10 S_{NH}	11 S_{ND}	12 X_{ND}	13 S_{ALK}	Process Rate, ρ_j $[ML^{-3}T^{-1}]$
1 Aerobic growth of heterotrophs		$-\frac{1}{Y_H}$			1			$-\frac{1-Y_H}{Y_H}$		$-i_{XB}$			$-\frac{i_{XB}}{14}$	$\hat{\mu}_H\left(\frac{S_S}{K_S+S_S}\right)\left(\frac{S_O}{K_{O,H}+S_O}\right)X_{B,H}$
2 Anoxic growth of heterotrophs		$-\frac{1}{Y_H}$			1				$-\frac{1-Y_H}{2.86\,Y_H}$	$-i_{XB}$			$\frac{1-Y_H}{14\cdot 2.86\,Y_H}-i_{XB}/14$	$\hat{\mu}_H\left(\frac{S_S}{K_S+S_S}\right)\left(\frac{K_{O,H}}{K_{O,H}+S_O}\right)\times\left(\frac{S_{NO}}{K_{NO}+S_{NO}}\right)\eta_g X_{B,H}$
3 Aerobic growth of autotrophs						1		$-\frac{4.57-Y_A}{Y_A}$	$\frac{1}{Y_A}$	$-i_{XB}-\frac{1}{Y_A}$			$-\frac{i_{XB}}{14}-\frac{1}{7Y_A}$	$\hat{\mu}_A\left(\frac{S_{NH}}{K_{NH}+S_{NH}}\right)\left(\frac{S_O}{K_{O,A}+S_O}\right)X_{B,A}$
4 'Decay' of heterotrophs				$1-f_P$	-1		f_P					$i_{XB}-f_P i_{XP}$		$b_H X_{B,H}$
5 'Decay' of autotrophs				$1-f_P$		-1	f_P					$i_{XB}-f_P i_{XP}$		$b_A X_{B,A}$
6 Ammonification of soluble organic nitrogen										1	-1		$\frac{1}{14}$	$k_a S_{ND} X_{B,H}$
7 'Hydrolysis' of entrapped organics		1		-1										$k_h\frac{X_S/X_{B,H}}{K_X+(X_S/X_{B,H})}\left[\left(\frac{S_O}{K_{O,H}+S_O}\right)+\eta_h\left(\frac{K_{O,H}}{K_{O,H}+S_O}\right)\left(\frac{S_{NO}}{K_{NO}+S_{NO}}\right)\right]X_{B,H}$
8 'Hydrolysis' of entrapped organic nitrogen											1	-1		$\rho_7(X_{ND}/X_S)$
Observed Conversion Rates $[ML^{-3}T^{-1}]$	$r_i=\sum_j \nu_{ij}\rho_j$													
Stoichiometric Parameters: Heterotrophic yield: Y_H Autotrophic yield: Y_A Fraction of biomass yielding particulate products: f_P Mass N/Mass COD in biomass: i_{XB} Mass N/Mass COD in products from biomass: i_{XP}	Soluble inert organic matter $[M(COD)L^{-3}]$	Readily biodegradable substrate $[M(COD)L^{-3}]$	Particulate inert organic matter $[M(COD)L^{-3}]$	Slowly biodegradable substrate $[M(COD)L^{-3}]$	Active heterotrophic biomass $[M(COD)L^{-3}]$	Active autotrophic biomass $[M(COD)L^{-3}]$	Particulate products arising from biomass decay $[M(COD)L^{-3}]$	Oxygen (negative COD) $[M(-COD)L^{-3}]$	Nitrate and nitrite nitrogen $[M(N)L^{-3}]$	$NH_4^+ + NH_3$ nitrogen $[M(N)L^{-3}]$	Soluble biodegradable organic nitrogen $[M(N)L^{-3}]$	Particulate biodegradable organic nitrogen $[M(N)L^{-3}]$	Alkalinity – Molar units	Kinetic Parameters: Heterotrophic growth and decay: $\hat{\mu}_H$, K_S, $K_{O,H}$, K_{NO}, b_H Autotrophic growth and decay: $\hat{\mu}_A$, K_{NH}, $K_{O,A}$, b_A Correction factor for anoxic growth of heterotrophs: η_g Ammonification: k_a Hydrolysis: k_h, K_X Correction factor for anoxic hydrolysis: η_h

Table 5.1: IAWQ ASM1 Model (Henze *et al.*, 1987)

The secondary clarifier process was modelled using the one-dimensional clarifier based on the double exponential settling velocity (Takács *et al.*, 1991). The settler model by Takács *et al.* (1991) is divided into several layers (typically 10) and uses the traditional solids flux analysis with a mass balance around each layer. The solids flux due to settling is characterized by the double exponential function, which is able to represent both the hindered settling and flocculent settling conditions. Thus the settling velocity model is shown by equation 5.1:

$$v_{sj} = v_o e^{-r_h \cdot X_j^*} - v_o e^{-r_p X^*_j}$$

Eq. 5.1

where v_{sj} settling velocity in layer j [m d^{-1}]

v_o maximum Vesilind settling velocity [m d^{-1}]

r_h settling parameter associated with the hindered settling component of the settling velocity equation [m^3 g^{-1}]

X_j Suspended solids concentration in layer j [g m^{-3}]

X_{min} minimum attainable suspended solids concentration [g m^{-3}]

X^*_j $= X_j - X_{min}$

r_p settling parameter associated with the low concentration and slowly settling component of the suspension [m^3 g^{-1}]

Settling parameters used in this study were obtained from the literature (Takács *et al.*, 1991) and experimental studies (Vanderhasselt, 1996). These parameters will be discussed further in Section 5.2.3. A diagram of the layered settler model is depicted in Figure 5.2.

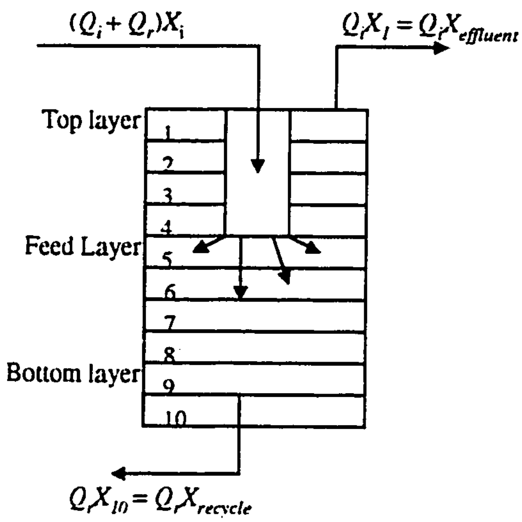

Figure 5.2: Layered Settler Model

where
Q_i = influent flow rate to the plant ($m^3\ d^{-1}$)
Q_r = recycle and wastage flow rate ($m^3\ d^{-1}$)
$X_{effluent}$ = suspended solids concentration in the effluent ($g\ m^{-3}$)
X_i = influent suspended solids concentration ($g\ m^{-3}$)
$X_{recycle}$ = suspended solids concentration in the recycle ($g\ m^{-3}$)
X_1 = suspended solids concentration in the first layer ($g\ m^{-3}$)
X_{10} = suspended solids concentration in the tenth layer ($g\ m^{-3}$)

Five different groups of layers are present in the model (Takács *et al.*. 1991). depending on their relative position to the feed point. The solids balance around each type of layer is shown in Figure 5.3.

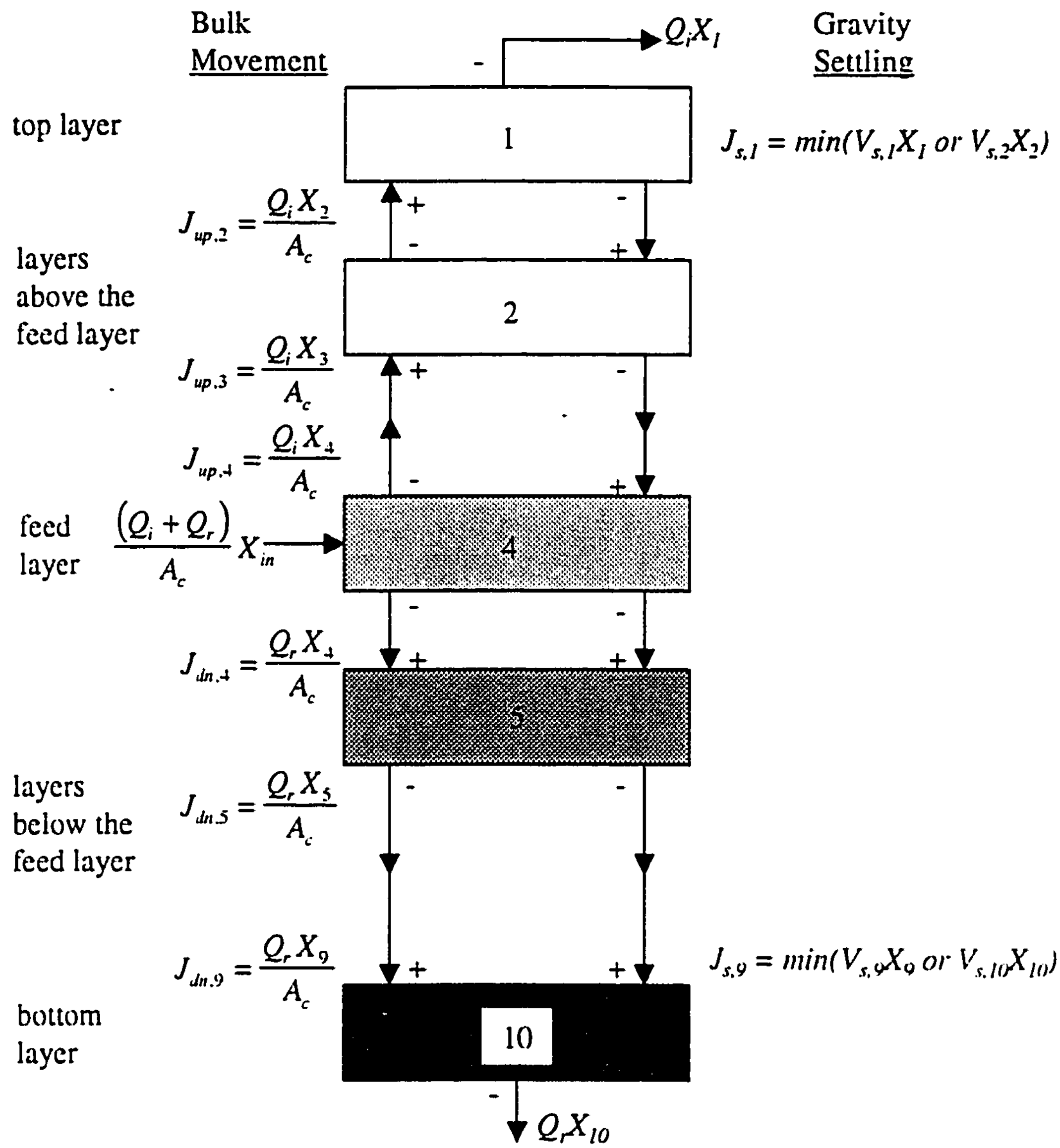

Figure 5.3: Solids balance around settler layers

where	A_c	Surface area of the clarifier [m]
	J_{dn}	Downward solids flux due to the bulk movement of the liquid [g m^{-1} d^{-1}]
	J_j	Downward solids flux in layer j [g m^{-1} d^{-1}]
	J_s	Solids flux due to gravity settling [g m^{-1} d^{-1}]
	J_{up}	Upward solids flux due to the bulk movement of the liquid [g m^{-1} d^{-1}]

5.2.2 Influent Conditions

In the development of a benchmark for evaluating respirometry-based control strategies, a realistic set of hydraulic and organic loads were generated for a standard activated sludge plant designed to treat an average flow of 20,000 m^3 d^{-1}. This set of influent data is published in the following website: www.ensic.u-nancy.fr/COSTWWTP/Benchmark/Benchmark1.htm. Influent loading conditions were developed for both dry weather and wet weather conditions.

The set of hydraulic and organic loading data were generated by modifying actual plant loading data according to available knowledge of influent loading from literature (Londong, 1994, Butler *et al.*, 1995, Verbanck, 1995, and Campos & von Sperling, 1996). The influent data is characterized by diurnal variations and were developed for a loading period of one-week at 15-minute intervals. Seasonal variations were not considered in this investigation because respirometry-based controllers act on a time scale of at most a few days (Spanjers *et al.*, 1998a).

The plant influent was designed to have an average flow of 20,000 m^3 d^{-1} and an average biodegradable chemical oxygen demand (COD) of 300 g m^{-3}. S_S and X_S concentrations are assumed to be the major components of the influent COD. The influent conditions are typical of a population equivalent of 100,000. The influent data were developed for both dry and wet weather flow conditions. Data for the two influent flow conditions include:

- hydraulic flow;
- soluble COD concentrations;
- soluble nitrogen concentrations;
- particulate COD concentrations; and
- particulate nitrogen concentrations.

5.2.2.1 Influent conditions for dry weather conditions

Hydraulic influent flow

The hydraulic influent flow generated for the simulation-based methodology was obtained by modifying actual hydraulic loading data from a large activated sludge plant. Characteristics of the influent flow were based on an analysis of the work of Campos and von Sperling (1996), Butler *et* *al.* (1995), Verbanck (1995), and Londong (1994). Hydraulic loading conditions were developed for a period of one week at 15-minute intervals.

The average flow for the large activated sludge plant was 74,619 m^3 d^{-1}, with minimum and maximum flows of 51,413 and 103,633 m^3 d^{-1}, respectively. Since the standard activated sludge plant developed for the simulation-based methodology was designed to treat an average influent flow of 20,000 m^3 d^{-1}, with minimum a flow of 10,000 m^3 d^{-1} and a maximum flow of 30,000 m^3 d^{-1}, the actual hydraulic flow data had to be scaled down. This was performed by a linear regression on the minimum and maximum flows.

The weekly fluctuations in the hydraulic loading of an activated sludge plant were based on the work of Verbanck (1995). From Monday to Friday, the hydraulic loading was decreased by 3% per day. The hydraulic loading during the weekend was reduced by 15% from the rate during the weekday. Therefore the average flow rate during the weekend was reduced to 17,000 m^3 d^{-1}, with minimum and maximum flows of 10,625 to 23375 m^3 d^{-1} respectively. The resulting influent flow used for the simulation benchmark is depicted in Figure 5.4.

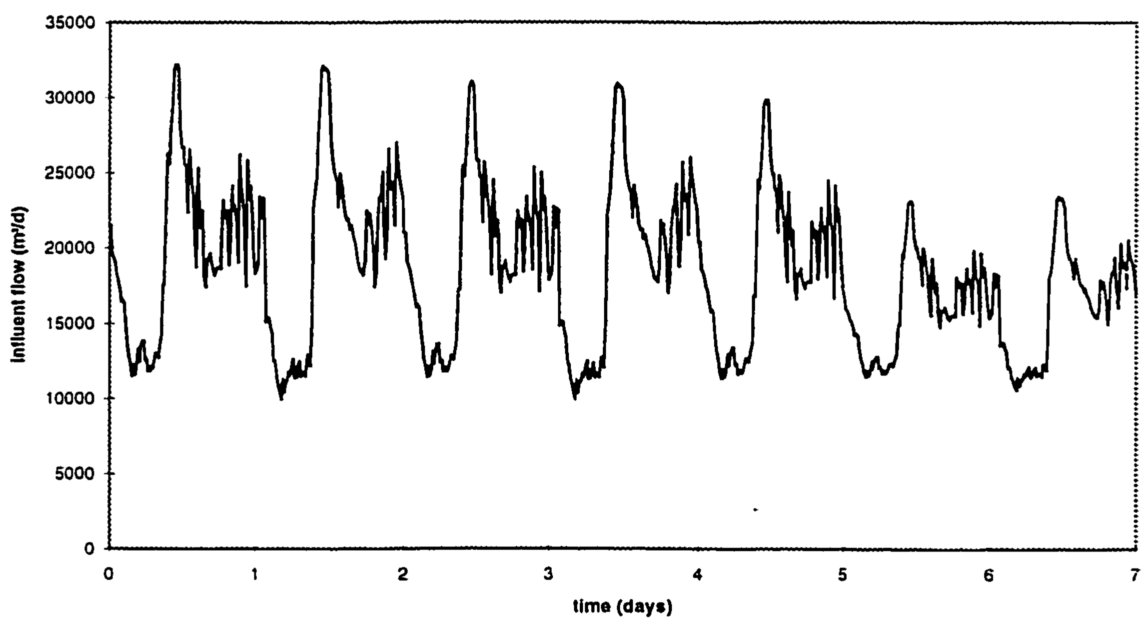

Figure 5.4: Hydraulic loading conditions during dry weather

Verbanck (1995) also reported additional loading due to infiltration. Therefore, the average hydraulic loading of 20,000 m^3 d^{-1} into the benchmark plant is assumed to consist of 40% flow from infiltration and 60% flow from domestic production.

Soluble pollutant loading (S_S, S_{NH}, S_{ND}, S_I)

The soluble components of the influent consist of S_S, S_{NH}, S_{ND} and S_I. The diurnal fluctuations in the influent soluble substrate data are shown in Figure 5.5.

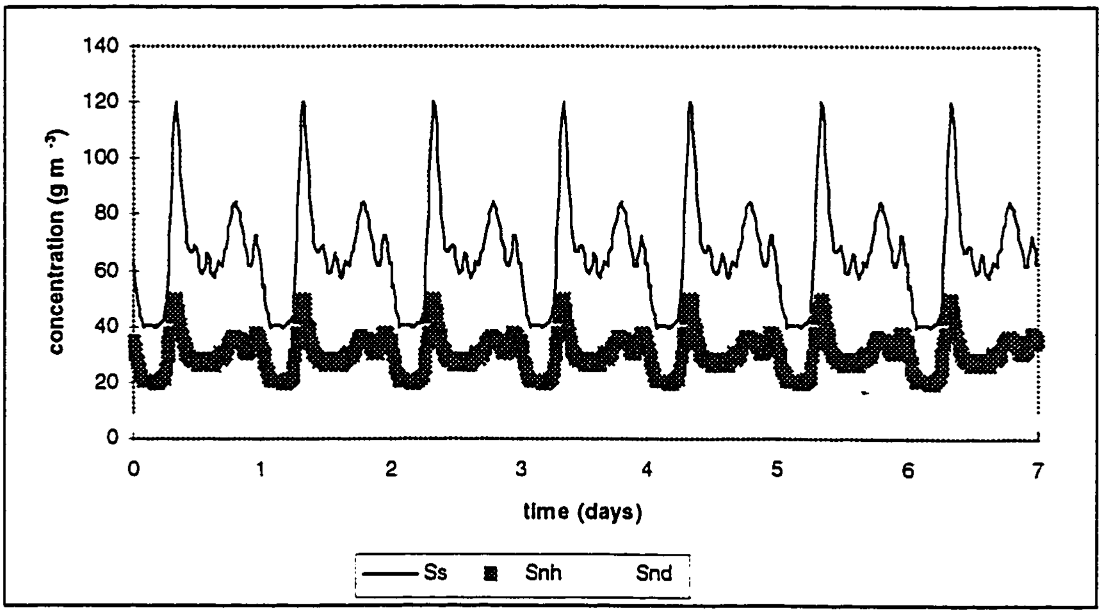

Figure 5.5: Soluble concentrations in the influent during dry weather flow

The daily concentrations of S_s and S_{NH} concentrations in the influent were derived from the work of Butler *et al.* (1995). A dilution factor had to be applied to these influent concentrations because the values reported by Butler *et al.* (1995) were obtained from domestic production and therefore did not reflect the dilution that results from infiltration. The dilution factor ($f_{dilution}$) that was applied is expressed as follows:

$$f_{dilution} = \frac{Q_{prod}}{Q_{prod} + Q_{\inf l}}$$

Eq. 5.2

where Q_{prod} = domestic wastewater flow rate (m^3 d^{-1})
Q_{infl} = infiltration flow rate (m^3 d^{-1})

Values for the flow rate of domestic wastewater production were obtained from Butler *et al.* (1995), while the value for the infiltration flow rate was considered to be constant for the purpose of this investigation. Again, it was assumed that 40% of the average influent flow is from infiltration (Verbanck, 1995) that is,

$$\frac{\overline{Q_{\inf l}}}{\left(\overline{Q_{prod}} + Q_{\inf l}\right)} = 0.4, \text{ or}$$

$$Q_{\inf l} = \frac{0.4}{0.6}\overline{Q_{prod}}$$

Eq. 5.3

Where $\overline{Q_{prod}}$ = average flow rate of domestic production

Furthermore, daily average influent concentrations were based on an analysis of the work of Lessard and Beck (1990), the IAWQ ASM1 (Henze *et al.*, 1987) and Stokes *et al.* (1993). The average influent S_S concentration was estimated to be 80 g COD m^{-3}, with minimum and maximum values of 40 and 120 g COD m^{-3} respectively. The average influent concentration for S_{NH} was estimated to be 30 g N m^{-3}, with minimum and maximum values of 20 and 50 g N m^{-3} respectively. Since Butler *et al.* (1995) reported higher daily average concentrations for S_S and S_{NH} from domestic sources, these concentrations had to be scaled down to average values of 80 and 30 g COD m^{-3} respectively. This was accomplished by performing a linear regression of the S_S and S_{NH} concentrations presented by Butler *et al.* (1995).

The S_{ND} concentration in the influent was calculated by assuming the following ratio:

$$\frac{S_{ND}}{S_S} = 0.10$$

Eq. 5.4

S_I in the influent was assumed to be constant at 30 g COD m^{-3}.

Particulate pollutant loading (X_S, X_I, X_{BH}, X_{ND})

The influent consists of the following particulate components: X_S, X_I, X_{BH} and X_{ND}. The daily total suspended solids (*SS*) loading obtained from a large activated sludge plant was used to calculate the influent particulate COD and nitrogen concentrations. From the work of Henze *et al.* (1987), Lessard and Beck (1990), Metcalf & Eddy, Inc. (1991), Butler *et al.* (1995), and Campos and von Sperling (1996), the design value for the average suspended solids concentration was assumed to be 200 g *SS* m^{-3}, with minimum and maximum values of 100 and 300 g SS m^{-3}, respectively. Since the average suspended solids concentration of the large plant was 125 g *SS* m^{-3}, with minimum and maximum values of 103 and 145 g *SS* m^{-3} respectively, the plant data had to be scaled down to design values. This was performed by a linear regression analysis.

It was assumed that the suspended solids concentration increases under high hydraulic loadings because re-suspension of solids occurs during high flows (Verbanck, 1995). As a result the influent suspended solids concentration follows the hydraulic loading variations that occur during the week. Specifically, it was assumed that from Monday through to Friday, there is an approximate 3% decrease per day in loading, and on the weekends the loading is reduced by 15% (Verbanck, 1995).

A diagram showing the suspended solids (i.e., X_I, X_{BH}, X_S and X_{ND}) loading for one week are shown on Figure 5.6. In this approach, the inert particulate material from cell decay (X_p), is added to X_I. There was no information available on the active autotrophic biomass (X_{BA}) concentrations in the influent. Therefore X_{BA} was not considered to be a component of the influent.

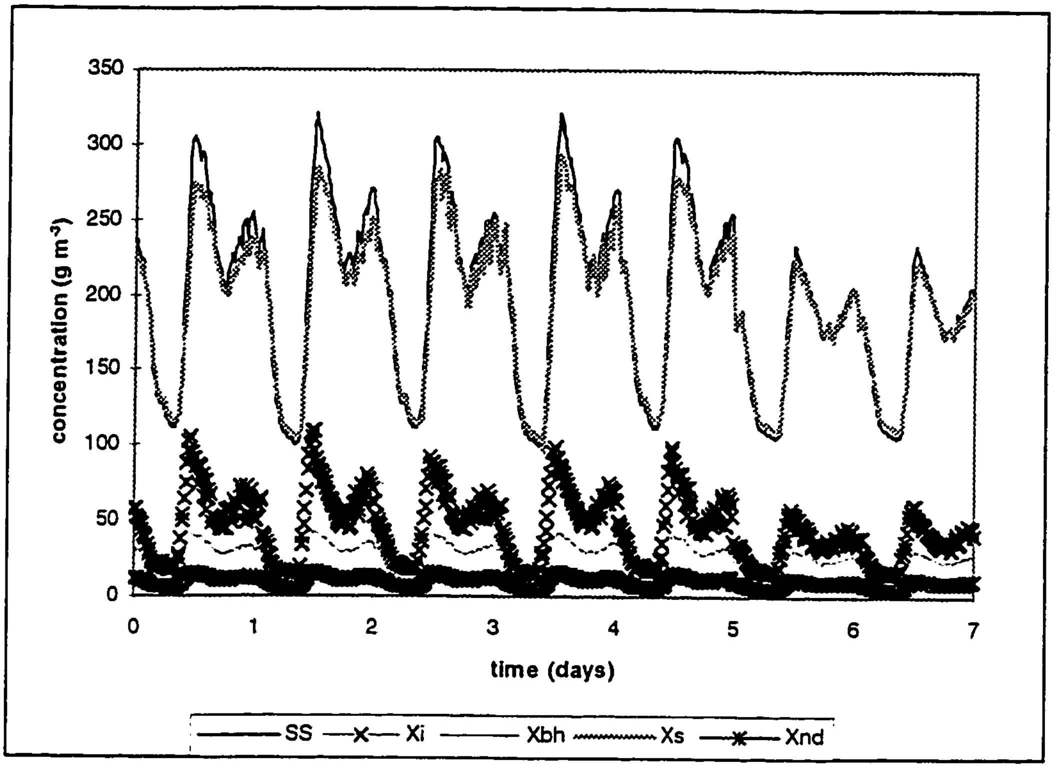

Figure 5.6: Particulate concentrations in the influent during dry weather conditions

The particulate COD (pCOD) in the influent wastewater is composed of X_S, X_{BH}, and X_I.

The following ratio of $pCOD$ to SS was used to calculate the $pCOD$ of the influent:

$$\frac{pCOD}{SS} = 1.33$$

Eq. 5.5

The $pCOD$ to volatile suspended solids (VSS) ratio has been found to be relatively consistent for domestic wastewaters and may be taken as 1.48 (Schroeter *et al.*, 1984). It was assumed that during low flow conditions, 90% of the total suspended solids are volatile. Therefore, a $pCOD/SS$ ratio of 1.33 can be used.

To take into account the variation of total suspended solids to volatile suspended solids in the influent, the non-volatile component of the influent suspended solids is assumed to be X_I, while the volatile components are X_S and X_{BH}. The X_I component, which has in reality no COD, is given a certain hypothetical COD value with this conversion. Furthermore, the X_I fraction of *pCOD* is not converted in the aeration tanks. Consequently by using the same *pCOD/SS* ratio to convert *pCOD* to *SS* in the settler, the balances for *COD* and *SS* are consistent.

The fractions of X_I, X_{BH}, and X_s making up the *pCOD* in the influent wastewater were calculated as follows:

$$f_{X_I} = 0.1 + 0.15 \cdot \frac{Q - Q_{\min}}{Q_{\max} - Q_{\min}}$$
$$f_{X_{BH}} = 0.10$$
$$f_{X_S} = 1 - f_{X_I} - f_{X_{BH}}$$

Eq. 5.6

where
- f_{XI} = fraction of X_I in the *pCOD* of the influent wastewater
- f_{XBH} = fraction of X_{BH} in the *pCOD* of the influent wastewater
- f_{XS} = fraction of X_S in the *pCOD* of the influent wastewater
- Q = influent wastewater flow rate ($m^3\ d^{-1}$)
- Q_{min} = minimum flow rate of influent wastewater ($m^3\ d^{-1}$)
- Q_{max} = maximum flow rate of influent wastewater ($m^3\ d^{-1}$)

These fractions are based on the assumption that the VSS/SS ratio drops when flow increases, which consequently increases the fraction of X_I in the influent.

Therefore, the concentration of X_S at time t is:

$$X_S = f_{XS} \cdot pCOD = f_{XS} \cdot 1.33 \cdot SS$$

Eq. 5.7

X_{ND} was calculated from the following ratio:

$$X_{ND} = 0.05 \cdot SS$$

Eq. 5.8

Please refer to Appendix A.2 for the constant influent data.

5.2.2.2 Influent conditions for wet weather conditions

The 7-day dry weather influent data discussed in the previous section were modified to include plant loading during wet weather conditions. This was accomplished by including two rain events occurring on Tuesday and Thursday. The hydraulic, suspended solids, BOD and ammonia loading characteristics during wet weather conditions were obtained from an analysis of the work of Gujer *et al.* (1986), Lessard and Beck (1990), Bertrand-Krajewski *et al.* (1995) and Rouleau and Lessard (1996).

During the first rainfall event (occurring on Tuesday), the influent loading changes as follows:

- the influent flow increases up to 3 times the average dry weather flow;
- the particulate pollutant loading increases up to 4 times the average dry weather loading and is only diluted in the second part of the rain event;
- the soluble pollutant loading is diluted to as low as 15 % of the average dry weather concentrations.

As for the second rainfall event (occurring on Thursday), the influent flow and soluble pollutant loading are similar to that of Tuesday. However, the particulate loading during this event is immediately decreased down to half the average dry weather loading because it is assumed that the sewers have been washed out as a result of the first rain event.

The influent flow, soluble and particulate loading concentrations are depicted respectively in Figures 5.7, 5.8 and 5.9.

First rain event of the week

The first rain event starts on Tuesday evening at around 7:30 p.m. and lasts for 3 hours.

Hydraulic influent flow

In the 1st hour of the rain event, the flow increases to a maximum flow of 3 times the average dry weather flow. That is, the flow increases from an average of 20000 $m^3 d^{-1}$ to 60000 $m^3 d^{-1}$. The flow into the plant continues at 60000 $m^3 d^{-1}$ for 1 hour. At the end of the second hour of the storm, the influent flow takes one hour to decrease linearly back to normal dry weather flow.

Soluble pollutant loading (S_S, S_{NH}, S_{ND}, S_I)

All soluble components of the influent are diluted during the rain event. The influent components S_S, S_{NH}, S_{ND} and S_I are diluted down to half of the average dry weather concentrations in the 1st hour of the storm event, and continue to be diluted thereafter to 15 % of the average dry weather concentrations. An exponential decrease in soluble concentrations was used in this case.

Take S_{NH} for example, which has an average value of 30 g m^{-3} in dry weather conditions, was diluted quickly (within one hour) to 15 g m^{-3}. In the following 2 hours, S_{NH} is further diluted to a concentration of 5 g m^{-3}. Thereafter, S_{NH} concentrations return to the dry weather levels. The S_S and S_I loading for Tuesday's storm event were similarly calculated (average dry weather concentrations are 80 and 30 g m^{-3} respectively). S_{ND} was then calculated from the S_S loading during the storm event as $0.1 \times S_S$.

Particulate pollutant loading (X_S, X_I, X_{BH}, X_{ND})

In the 1st hour of the storm event, the suspended solids loading to the plant increases up to 4 times the average dry weather loading. After the 1st hour of the storm event, the loading decreases to half of the average dry weather loading. The load then returns to normal dry weather levels after 3 hours of the storm event. The concentrations of the particulate components, X_I, X_{BH}, X_S and X_{ND}, were calculated from the suspended solids data using the same fractions as for dry weather conditions. This results in a relatively higher concentration of inerts due to re-suspension in the sewer.

Second rain event of the week

The second rain event of the week occurred on Thursday, starting in the evening at 10:00 p.m. and lasted for 15 hours. The rain event ended on Friday at 1:00 p.m.

Hydraulic loading

Similar to Tuesday's storm event, the flow increased up to 3 times the average dry weather loading (i.e. 60000 $m^3\ d^{-1}$) in the first hour of the storm event. Thereafter, the influent flow remains at 60000 $m^3\ d^{-1}$ for 3 hours. In the last 11 hours of the storm event, the influent flow gradually decreases to dry weather loading conditions. This gradual decrease was calculated by superimposing the variations from the average dry weather flow of 20000 $m^3\ d^{-1}$ onto the linear decrease during the remaining 11 hours of the storm event. The result is that the loading variations during these 11 hours of the storm event reflect the variations during the same time for dry weather conditions.

Soluble pollutant loading (S_S, S_{NH}, S_{ND}, S_I)

The effect of the first 4 hours of Thursday's storm event on the soluble components of the wastewater is very similar to that of Tuesday's rain event. During the first hour, the components are quickly diluted to half the average dry weather concentrations. Thereafter, the soluble components continue to be diluted exponentially down to 15% of the average dry weather concentrations for the next 3 hours. From the 5th hour to the 15th hour of the rain event (i.e. end of the rain event), the soluble component loading increases back to average dry weather concentrations. The same calculations were used for the soluble COD and nitrogen concentrations during the last 11 hours of the rain as that performed for the particulate concentrations.

Particulate pollutant loading (X_S, X_I, X_{BH}, X_{ND})

Unlike Tuesday's storm event, the particulate loading during the first hour of Thursday's storm event does not reach peak levels of 4 times the average dry weather loading. The reason is that it is assumed that solids in the sewer have already been washed out from the storm event on Tuesday. As a result the particulate loading during this storm event decreases to half of the average dry weather loading (i.e. 85 g *SS* m^{-3}) in the first hour of the storm event. Thereafter, the particulate concentration remains at this concentration for 3 hours. In the fifth hour of the storm event, the loading continually increases and reaches dry weather levels by the 15th hour of the storm. The particulate concentrations between the 5th and 15th hour of the rain event were determined by calculating a weighted average of dry weather concentrations (C_{dw}) and the storm weather concentrations (C_{storm}) as follows:

$$C_{tot} = \frac{(C_{storm} \cdot Q_{storm} + C_{dw} \cdot Q_{dw})}{Q_{tot}}$$

Eq. 5.9

where Q_{dw} = flow at time t during dry weather conditions

C_{dw} = total particulate concentration (X_S, X_I, X_{BH}, and X_{ND}) at time t during dry weather conditions

Q_{storm} = flow at time t due to rain water (storm flow)

C_{storm} = total particulate concentration at time t in the rain water

C_{tot} = total particulate concentration in the influent at time t, between the 5th and 15th hour of the storm event

Q_{tot} = total flow at time t

= $Q_{storm} + Q_{dw}$

Values for Q_{tot}, Q_{dw}, and C_{dw} were obtained from previous calculations. Q_{storm} was calculated as Q_{tot} - Q_{dw}. Values for C_{storm} were calculated by performing a linear regression of C_{storm} versus Q_{storm} data at the beginning of the 5th hour and at the end of the 15th hour of the rain event. The value of C_{storm} at the 5th hour was calculated by rearranging Eq. 5.9 as follows:

$$C_{storm} = \frac{(C_{tot} \cdot Q_{tot} - Q_{dw} \cdot C_{dw})}{Q_{storm}}$$

Eq. 5.10

where Q_{tot} $= 60000\ m^3\ d^{-1}$

C_{tot} $= 85\ g\ SS\ m^{-3}$

Q_{dw} $= 16480\ m^3\ d^{-1}$

C_{dw} $= 199.83\ g\ SS\ m^{-3}$

Q_{storm} = Q_{tot} (of 5th hour) - Q_{dw} (of 5th hour)

= 60000-16480

= $43520\ m^3\ d^{-1}$

Therefore, using Eq. (5.10),

C_{storm} = $41.63\ g\ SS\ m^{-3}$

The values for C_{storm} and Q_{storm} in the 15th hour of the rain event are 200 g SS m^{-3} (i.e. the average dry weather SS concentration) and 0 $m^3\ d^{-1}$, respectively. It is assumed that between the 5th and 15th hour of the rain event, the particulate COD concentration increases as the storm flow decreases, and that by the end of the rain event the concentration reaches 200 g SS m^{-3}, which is the same as the average dry weather concentration.

Once the linear regression was performed, particulate concentrations in the storm water may be calculated, and used in Eq. 5.9 to calculate C_{tot} values between the 5th and 15th hour of the rain event.

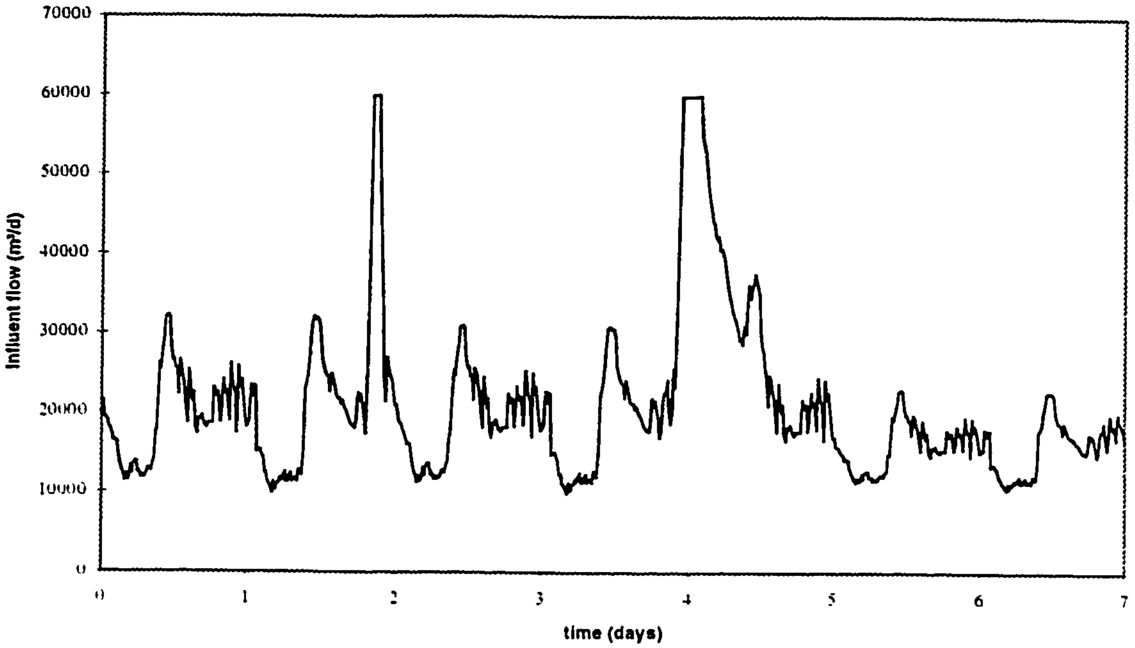

Figure 5.7: Influent flow during wet weather conditions

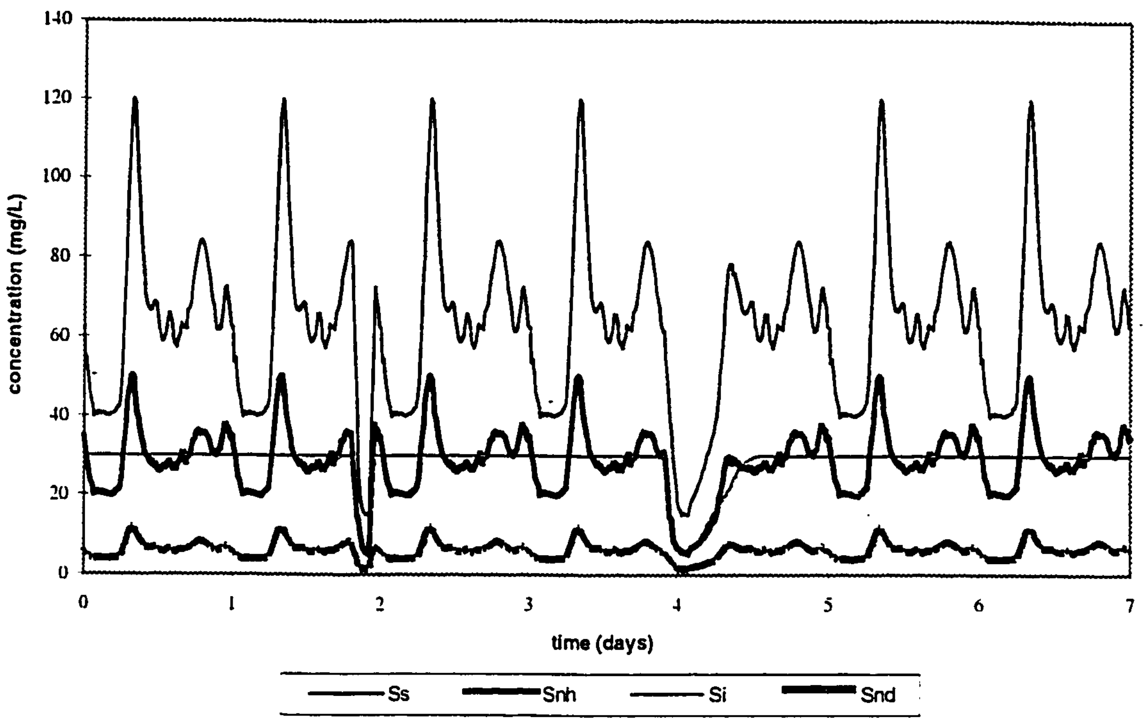

Figure 5.8: Influent soluble concentrations during wet weather conditions

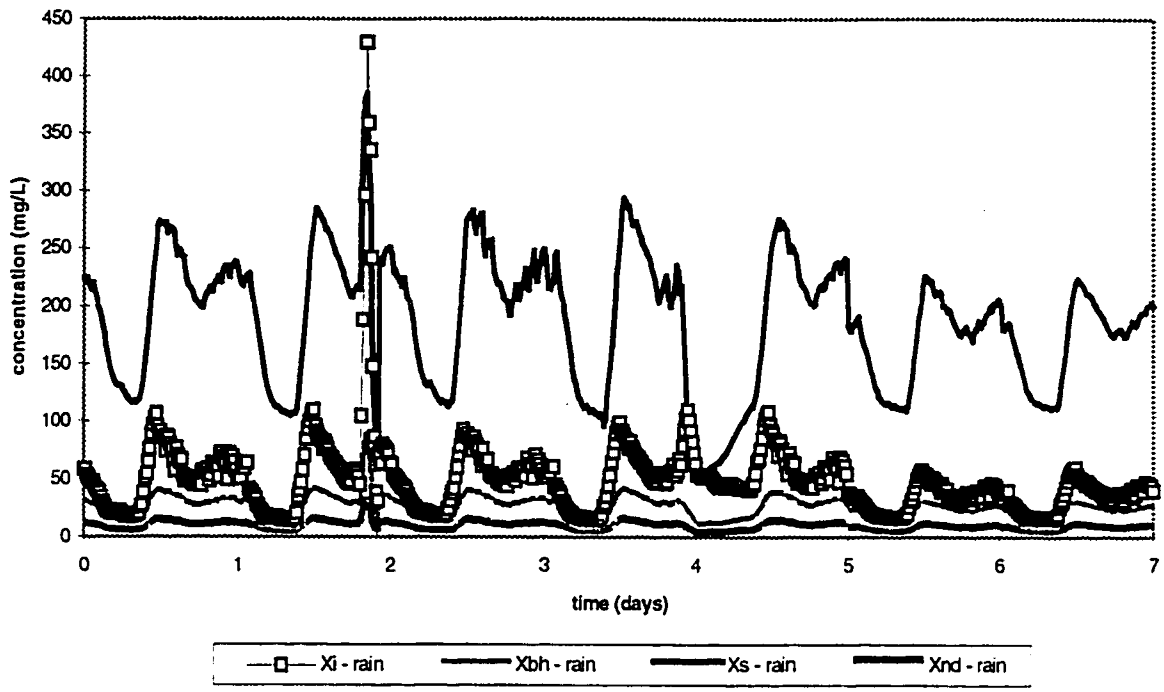

Figure 5.9: Influent Particulate Concentrations (storm weather)

5.2.3 Model Parameters

The simulation benchmark also includes a complete set of parameter values for the IAWQ ASM1 (Henze *et al.*, 1987) and the double exponential settling velocity model (Takács *et al.*, 1991).

5.2.3.1 Stoichiometric and kinetic parameters of the activated sludge model

Stoichiometric and kinetic parameter values for the benchmark were selected by comparing default values from the following sources:

- A calibrated model from GPS-X
- A calibrated model from West
- IAWQ Activated Sludge Model No.1 (ASM1)
- IAWQ Activated Sludge Model No. 2 (ASM2)

Values of the kinetic and stoichiometric parameters used in the simulations are indicated on the far right column in Table 5.2. Temperature dependent parameters were adjusted to a value corresponding to a temperature of 15 °C by using an approximated exponential relationship.

Table 5.2: Comparison of stoichiometric and kinetic parameters of the activated sludge model

	Parameter	Unit	*GPS-X*[1]	*West*[2]	*ASM1*[3]	*ASM2*[4]	**Value Used**
Heterotrophs	μ_H	d^{-1}	3.2	2.4	3-6	3-6	4
	K_s	d^{-1}	5	20	20	4-20	**10**
	b_H[5]	d^{-1}	0.62	0.24	0.20-0.62	0.2-0.4	**0.3**
	η_h	-	0.37	0.4	0.4	0.6	**0.5**
	η_g	-	0.10	0.8	0.8	0.8	
Hydrolysis	k_h[6]	d^{-1}	2.81	1.2	1-3	2-3	**3.0**
	K_x[6]	-	0.15	0.1	0.01-0.03	0.3-0.1	**0.1**
Ammonification	k_a	-	0.016	0.048	0.04-0.08	-	**0.05**
Autotrophs	μ_A	d^{-1}	0.75	0.24	0.3-0.8	0.35-1	**0.5**
	K_{NH}	$g\ m^{-3}$	1.0	0.5	1.0	1.0	**1.0**
	b_A	d^{-1}	0.04	0.024	-	0.05-0.15	**0.05**
Switching Functions	K_{OH}	$g\ m^{-3}$	0.2	0.2	0.2	0.2	**0.2**

	Parameter	Unit	*GPS-X*[1]	*West*[2]	*ASM1*[3]	*ASM2*[4]	***Value Used***
	K_{OA}	g m^{-3}	0.2	0.4	0.4	0.5	**0.4**
	K_{NO}	g m^{-3}	1.0	0.5	0.5	0.5	**0.5**
Stoichiometry[7]	gCOD/gVSS	-	1.48	-	-	-	**1.48**
	gVSS/gSS	-	0.75	-	-	-	**0.9**
	gCOD/gSS	-	-	1.33	-	-	**1.33**
	Y_H	gCOD/gCOD	0.67	0.66	0.67	0.63	**0.67**
	Y_A	gCOD/gN	0.15	0.24	0.24	0.24	**0.24**
	i_{XB}	gN/gCOD	0.068	0.086	0.088	0.07	**0.08**
	i_{XP}	gN/gCOD	0.068	0.06	0.06	0.04	**0.06**
	f_P	-	0.08	0.08	0.08	0.10	**0.08**

[1] Hydromantis Inc., Canada

[2] Hemmis NV, Belgium

[3] Henze *et al.* (1987)

[4] Henze *et al.* (1994)

Some modifications in the parameter values were made after the first few simulations:

5 The value of b_H was changed from 0.4 to 0.3 d^{-1}, and η_h was changed from 0.4 to 0.5. These changes were made to ensure a sufficiently high biomass concentration in both the anoxic and aerobic tanks in the N-removal system.

6 k_h was changed from 2.0 to 3.0 d^{-1} and K_x was changed from 0.2 to 0.1. These changes were made to increase the rate of hydrolysis in the anoxic zone, which consequently increases the availability of readily biodegradable substrate to the heterotrophs.

7 Note that 1.48 g COD/g VSS × 0.9 g VSS/g SS = 1.33 g COD/g SS

5.2.3.2 Settling parameters

Settling parameters obtained for the benchmark were from Takács *et al.* (1991) for medium loading and experimental evidence (Vanderhasselt, 1996). The values of the parameters used in the simulations are presented in Table 5.3.

Table 5.3: Settling parameters used for the secondary clarifier model

Settling Parameter	Definition	Value Used
v_o' (m d^{-1})	maximum settling velocity	250.0
v_o (m d^{-1})	maximum Vesilind settling velocity	474.4008
r_h (m^3 g^{-1} *SS*)	hindered zone settling parameter	0.000576
r_p (m^3 g^{-1} *SS*)	flocculent zone settling parameter	0.00286
f_{ns}	non-settable fraction	0.00228

5.2.4 Initial Values for State Variables

The benchmark also provides a set of initial values for the state variables belonging to the process models. Steady state values are used as the initial values for the state variables.

The built-in steady state solver in GPS-X was used in this study to calculate the steady state values for the state variables. The respirometry-based controllers were not turned on automatic during the steady state analysis. The DO controllers were however turned on during this time. Steady state values may also be obtained by conducting simulations with constant influent over time until the plant reaches steady state.

Three activated sludge systems were designed (to be discussed in Section 5.3) for the benchmark: carbon (C) removal, carbon removal and nitrification, and carbon and nitrogen (N) removal. The benchmark provides three activated sludge designs to allow the flexibility to conduct simulation studies with different plant configurations. This discussion will only present the initial state values for the C-removal system. Initial state values for the other two systems are presented in Appendix A2.

5.2.4.1 Carbon removal system

Steady state initial conditions

Initial conditions for the operation of the aeration tanks are presented in Table 5.4. Initial conditions for the settler are presented in Table 5.5.

Table 5.4: Initial values for the state variables in the three aeration tanks

		Tank 1	*Tank 2*	*Tank 3*
S_I	(g COD m^{-3})	30	30	30
S_S	(g COD m^{-3})	3.57182	1.61771	1.25408
X_I	(g COD m^{-3})	804.535	804.532	804.537
X_S	(g COD m^{-3})	130.149	99.3409	77.191
X_{BH}	(g COD m^{-3})	2717.55	2731.63	2738.82
X_{BA}	(g COD m^{-3})	$1*10^{-6}$	$1*10^{-6}$	$1*10^{-6}$
X_U	(g COD m^{-3})	166.479	168.119	169.76
S_{NO}	(g COD m^{-3})	$1*10^{-6}$	$1*10^{-6}$	$1*10^{-6}$
S_{NH}	(g COD m^{-3})	38.8715	39.9461	40.6953
S_{ND}	(g COD m^{-3})	1.83261	1.12487	0.8672
X_{ND}	(g COD m^{-3})	7.92373	6.33122	5.1647
K_La	(d^{-1})	197.748	99.9867	79.4245

Table 5.5: Initial values for the settler state variables

State Variable	Concentration (g COD m^{-3})
S_I	30
S_s	1.25408
S_{NO}	$1*10^{-6}$
S_{NH}	40.6953
S_{ND}	0.8672
Suspended solids:	
Layer 1	27.0092
Layer 2	50.7963
Layer 3	119.765
Layer 4	524.818
Layer 5	524.818
Layer 6	524.818
Layer 7	524.818
Layer 8	524.818
Layer 9	1269.98
Layer 10	5526.57

5.2.5 Activated Sludge Plant Design

In the development of the simulation benchmark, a standard activated sludge plant (ASP) was designed for the benchmark influent conditions. The plant is designed for carbon and nitrogen removal and treats a mean flow of 20,000 m^3 d^{-1} and a total biodegradable COD (S_S and X_S) of 300 g m^{-3} for a population equivalent of 100,000. The plant consists of three continuous stirred-tank reactors (CSTRs) in series followed by a secondary circular settler. The standard plant design allows influent to be distributed solely to the first compartment or by step feeding to each of the three compartments. A diagram of the activated sludge plant is shown in Figure 5.10. The dissolved oxygen (DO) concentration is automatically controlled in each tank. Once tuned, these DO controllers are considered to be part of the plant layout. The settler has a surface area of 800 m^2 and a depth of 3 m. Wastage occurs from the bottom of the settler. The design operating temperature is 15 °C.

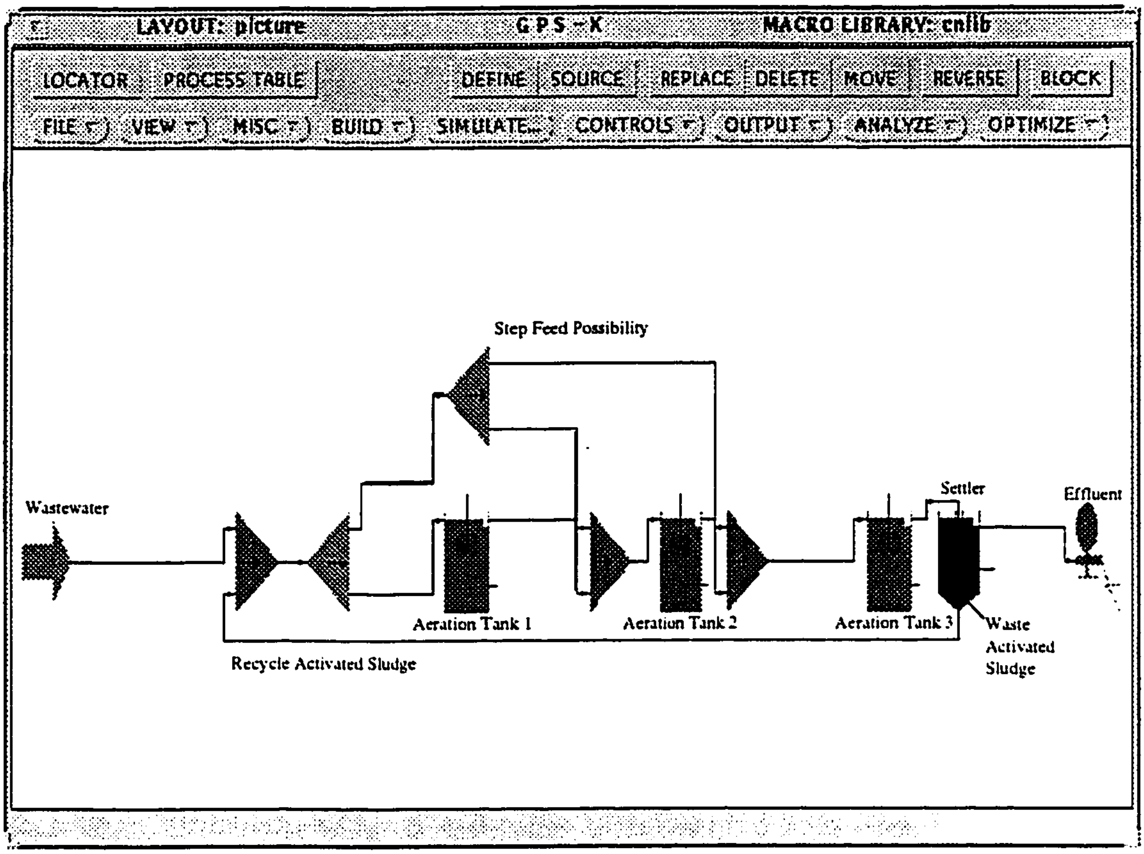

Figure 5.10: Layout of simulated activated sludge plant

The plant configuration was chosen because it is commonly used in practice, it provides flexibility for plant modifications or expansions, and it enables fast calculations during simulations. For example, an anoxic zone and step feed can be easily integrated into the model.

The three CSTRs allow the flexibility to implement the following process configurations: C-removal, C-removal and nitrification, and C- and N-removal. Design of the three systems initially involved the use of biomass and volumetric loading rates from literature. Details of the initial designs of the three activated sludge processes are provided in Appendix A.4. The design was then refined through simulations to reflect more realistic operating conditions. The final dimensions of the aeration tanks and settlers for the activated sludge systems are summarized in Tables 5.6 and 5.7.

Table 5.6: Design parameters for the aeration tanks

Activated Sludge Systems	Influent:		Aeration tanks						
	Qavg (m^3/d)	Influent bCOD (mg/L)	DO conc. in aeration tanks (mg/L)			Total volume of 3 tanks (m^3)	hyraulic retention (d)	sludge age (d)	MLSS (kg/m^3)
			1st tank	2nd tank	3rd tank				
Carbon Removal System without Nitrification	20000	300	2	2	2	3000	4	4	4
Carbon Removal System with Nitrification	20000	300	2	2	2	6500	8	15	4
Carbon and Nitrogen Removal	20000	300	0	2	2	8000	12	15	4

Influent: 20,000 $m^3 d^{-1}$, 300 gCOD m^{-3}

Activated sludge: 4 kgMLSS m^{-3}

Table 5.7: Design parameters for the secondary clarifier

Activated Sludge Systems	Settler design:						
	sludge recycle ratio	nitrate-rich recycle ratio	Qw (m^3/d)	overflow rate (m/h)	surface area, A (m^2)	depth (m)	hyraulic retention (h)
Carbon Removal System without Nitrification	1	0	500	1	800	3	1,4
Carbon Removal System with Nitrification	1	0	250	1	800	3	1,4
Carbon and Nitrogen Removal	1	5	270	1	800	3	1,4

In the carbon and nitrogen removal plant, the nitrate-rich mixed liquor is recycled from the third tank to the first tank.

5.2.5.1 Final Designs of the Activated Sludge Systems

After performing simulations with both constant and dynamic influent, the original designs of the C-removal, C-removal and nitrification, and C- and N-removal systems were modified to reflect more realistic operating conditions. The final designs for the C-removal and nitrification, and C- and N-removal systems are presented in Appendix A.5. It must be noted that the benchmark values, shown in Tables 5.6 and 5.7, can be used as initial values and only provide a framework for starting the simulations. These values may be used when none are specified in the proposals, and may be adjusted to obtain the appropriate operating conditions.

5.2.5.2 Carbon removal system

In the original design, the wastage rate was too high to maintain MLSS at a reasonable concentration. Consequently, Q_{waste} had to be limited to 500 $m^3\,d^{-1}$. To maintain the sludge age at 4 days, the total volume of the three aeration tanks had to be reduced to 3000 m^3.

An overview of the first approximation of the values of the state variables in the aeration tanks and the secondary settler are given in Tables 5.8 and 5.9, respectively. These initial values were used to obtain precise initial values for the state variables in the benchmark.

Table 5.8: Approximate initial values for the state variables in the aeration tanks

State Variable		*Tank 1*	*Tank 2*	*Tank 3*
S_I	(g COD m^{-3})	30	30	30
S_s	(g COD m^{-3})	10	5	2
X_I	(g COD m^{-3})	900	900	900
X_s	(g COD m^{-3})	120	90	70
X_{BH}	(g COD m^{-3})	2500	2500	2500
X_{BA}	(g COD m^{-3})	30	30	30
S_{NO}	(g COD m^{-3})	0	0	0
S_{NH}	(g COD m^{-3})	30	30	30
S_{ND}	(g COD m^{-3})	0	0	0

State Variable		*Tank 1*	*Tank 2*	*Tank 3*
X_{ND}	(g COD m^{-3})	0	0	0
K_La	(d^{-1})	160	90	90

Table 5.9: Approximate initial values of the state variables in the settler

State Variable	Concentration (g COD m^{-3})
S_I	30
S_s	1
S_{NO}	0
S_{NH}	30
S_{ND}	0
Suspended solids:	
Layer 1	20
Layer 2	100
Layer 3	200
Layer 4	900
Layer 5	900
Layer 6	900
Layer 7	900
Layer 8	900
Layer 9	2000
Layer 10	5500

The value of the mean cell residence time of 4 days was a good choice. A value slightly higher than 4 days caused significant nitrification to occur after 7 days.

The dissolved oxygen (DO) controllers maintained the DO concentration in each of the three compartments at 2 g m^{-3} with the following values for the proportional-integral (PI) control parameters:

Compartments 1 and 2:

K_c = 30

T_I = 0.05 d

Compartment 3:

K_c	=	20
T_I	=	0.05 d

where	K_c	Proportional gain
	T_I	Integral time constant

5.3 Implementation of a Respirometry-Based Control Strategy

Many of the control strategies documented in the literature are theoretical and lack details on controller design and implementation in a large-scale activated sludge plant. Therefore, to ensure that the control strategies are tested on an equal basis, there has to be a consistent set of procedures to implement a control strategy. The following 6-step strategy was used to implement a control strategy in the benchmark plant:

1. Identify the objective of the respirometry-based control strategy.
2. Identify the input and output variables of the control system.
3. Identify the implied control configuration.
4. Determine the appropriate control algorithm.
5. Design / tune the controller.
6. Determine the appropriate range of variation for the manipulated variable.

5.3.1 Identify the Objectives of the Respirometry-Based Control Strategy

In implementing the proposed control strategy for simulation, the objectives of the control strategy must first be identified qualitatively. There are usually two levels to the control objective. The first is the operational objective and the second is the controller objective. The controller objective can be view as one approach to achieving the operational objective. Application of respirometry-based control is often apparent in the controller objective.

An example of an operational objective is to maintain the effluent BOD below 25 mg/L. The associated controller objective would be for example to maintain the respiration rate at a set point of 22 mg/L·h in the aeration tank. In maintaining the respiration rate at a set point, the contuoller objective helps to ensure the operational objective by guaranteeing an active biomass activity in the aeration tank for adequate degradation of the biodegradable waste.

5.3.2 Identify Input and Output Variables of the Control System

Determining the output and input variables of the control system will facilitate identification of the proposed control system. The control system involves the controller, process, and instrumentation.

Output Variables

Output variables denote the effect of the process on the surroundings. Output variables are further classified into *measured* output variables and *unmeasured* output variables. Measured variables are known by directly measuring them, whereas unmeasured variables are not or cannot be measured directly. A diagram of the output and input variables around a process is shown in Figure 5.11.

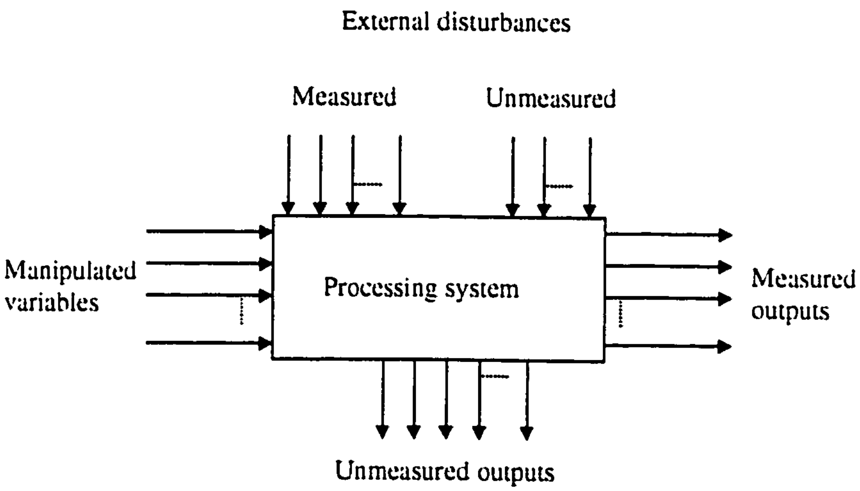

Figure 5.11: Input and output variables around a process

Controlled variables are measured output variables and should have a substantial effect on the process performance.

The ability to deduce useful process data from respiration rate measurements makes the use of respirometers in controlling wastewater treatment plants potentially beneficial. Spanjers *et al.* (1998b) have documented the various parameters that may be deduced from respiration rate measurements. These deduced parameters are shown in Table 5.10.

Table 5.10: Process Parameters Deduced from Respiration Rate Measurements (Spanjers *et al.*, 1998b)

Symbol	Description
BOD_{st}	Short-term BOD
$\%I$	Percentage inhibition
$\%I_H$	$\%I$ of heterotrophs
$\%I_A$	$\%I$ of autotrophs
K_{NH}	Nitrogen saturation coefficient
rr_{act}	Actual respiration rate
R_{COD}	Specific carbonaceous respiration rate
rr_{end}	Endogenous respiration rate
$R_{NH,max}$	Maximum nitrification rate
S_A	Concentration of volatile fatty acids (VFAs)
S_{NH}	Concentration of NH_4^+
S_S	Concentration of readily biodegradable substrate
Tte	Time to endogenous
X	Biomass concentrations
μ_A	Maximum autotrophic growth rate

It is sometimes difficult to identify what the actual controlled variable is in many of the respirometry-based control proposals. Spanjers *et al.* (1998b) have compiled a list of variables that have been proposed as controlled variables in the control of wastewater treatment plants. The list is provided in Table 5.11.

Table 5.11: Proposed Controlled Variables (Spanjers *et al.*, 1998b)

Symbol	Description
B_I	Inhibitor loading rate
B_V	Volumetric loading rate
B_X	Sludge loading rate
$\%I$	Percentage inhibition
r_{act}	Actual respiration rate

Symbol	Description
R_{COD}	Specific carbonaceous respiration rate
r_{end}	Endogenous respiration rate
$R_{NH,max}$	Maximum nitrification rate
S_A	Concentration of volatile fatty acids (VFAs)
S_{NH}	Concentration of NH_4^+
S_{NO2}	NO_2^- concentration
S_{NO}	NO_3^- concentration
S_O	Dissolved oxygen concentration
S_S	Concentration of readily biodegradable substrate
SBH	Sludge blanket height
tte	Time to endogenous
X	Biomass concentrations
θ_X	Sludge age

Input Variables

Input variables denote the effect of the surroundings on the process. Input variables may be further classified into *manipulated* (or *adjustable*) variables and *disturbances*. Manipulated variables must be external variables that can be adjusted independently by the human operator or a control mechanism. Disturbances are inputs that change due to external conditions and affect the controlled variable. An example of a disturbance on a respiration-based controller in the activated sludge plant could be the large fluctuations on the incoming biodegradable waste concentration.

The various manipulated variables used in the proposed control strategies have been documented from literature by Spanjers *et al.* (1998b) and are listed in Table 5.12.

Table 5.12: Manipulated Variables Used in Proposed Respirometry-Based Control Strategies for ASPs (Spanjers *et al.*, 1998b)

Symbol	Description
K_La	Mass transfer efficiency
Q_{chem}	Chemical dosage rate
Q_{dis}	Influent flow rate distribution
Q_{in}	Influent flow rate
Q_{ras}	Return sludge flow rate
Q_{rec}	Nitrate recycle flow rate
Q_{rl}	Sludge treatment return liquor flow rate
Q_{store}	Sludge storage rate
Q_{waste}	Sludge wastage flow rate
$T_{recycle}$	Cycle length in periodic process

5.3.3 Identify the Implied Control Configuration

A control configuration is the information structure that is used to connect the available measurements to the available manipulated variables (Stephanopoulos. 1984). The objective of this discussion is to provide a qualitative description of the different process control configurations. In this way the reader will be able to identify the configuration of the proposed respirometry-based control strategy and refer to the appropriate literature to implement a practical design of the strategy into the benchmark activated sludge plant.

Feedback Control

The most widely used control configuration is the feedback control loop. The feedback control configuration uses direct measurements of the controlled variables to adjust the values of the manipulated variables. The objective is to keep the controlled variables at desired levels (i.e. set points). A schematic of a general feedback system is provided in Figure 5.12.

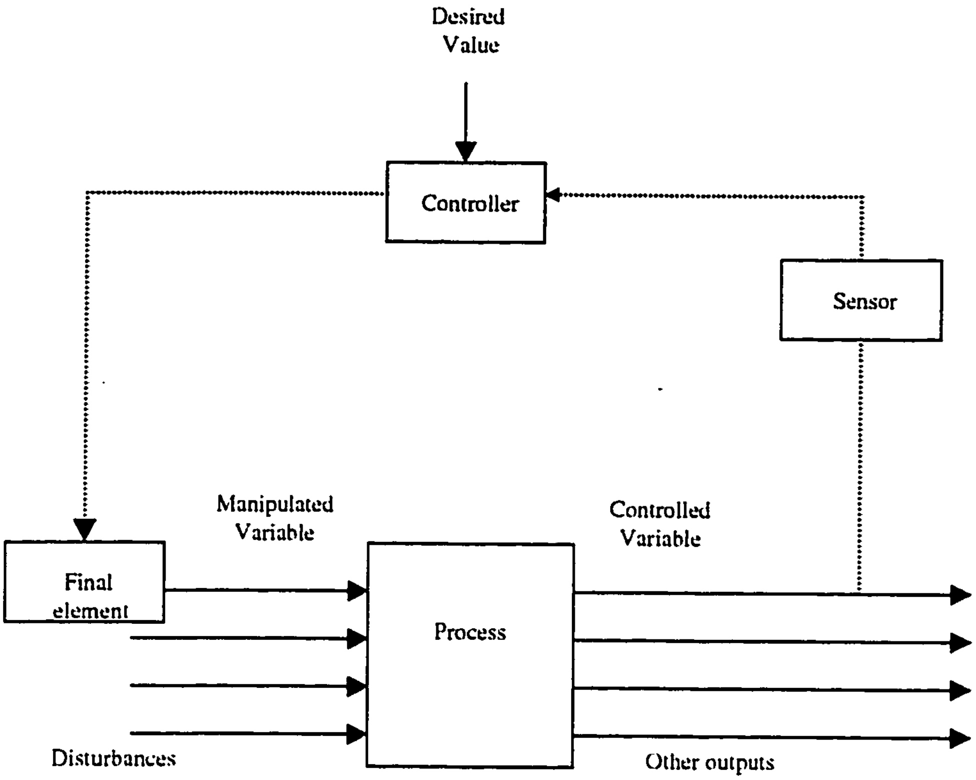

Figure 5.12: Schematic of feedback system (Marlin, 1995)

The feedback control loop cannot address all control requirements. Changing the process design is the best approach for improving control performance. However, this approach may not be possible or may not be the best economic decision. In this case, feedback control can be enhanced through one or more of the following steps (Marlin, 1995):

1. Use additional measures of process outputs.
2. Use additional measurements of the process inputs.
3. Use explicit modelling in the control calculation.
4. Modify the PID algorithm and tuning to match the control objective.

The control enhancements include cascade, feedforward, nonlinear process, inferential, and predictive control. Regardless of the complexity of the enhancements, feedback control should always be retained (when the sensor exists) so that negligible offset is achieved at steady state (Marlin, 1995). Therefore in identifying the control configuration for the proposed strategy, the reader should be aware that the feedback configuration is usually a fundamental component of most control strategies. A summary of single-loop control enhancements is provided in Table

5.13 that may helpful to refer to when deciding on the control configuration of a respirometry-based control strategy.

Table 5.13: Summary of single-loop control enhancements (Marlin, 1995)

Enhancement	Key issue	New input measure-ment	New output measurement	Process modeling	Standard or Modified PID	New control algorithm
Cascade control	Feedback dynamics		X		X	
Feedforward control	Feedback Dynamics	X				X

Cascade Control

Cascade control uses additional measurements of a process variable to assist in the feedback control system. The selection of this extra measurement, which is based on information about the most common disturbances and about the process dynamic responses, is critical to the success of the cascade controller (Marlin, 1995). The configuration of a cascade control system is two feedback loops in which the primary controller's output serves as the secondary controller's set point. A schematic representation of a cascade system is illustrated in Figure 5.13.

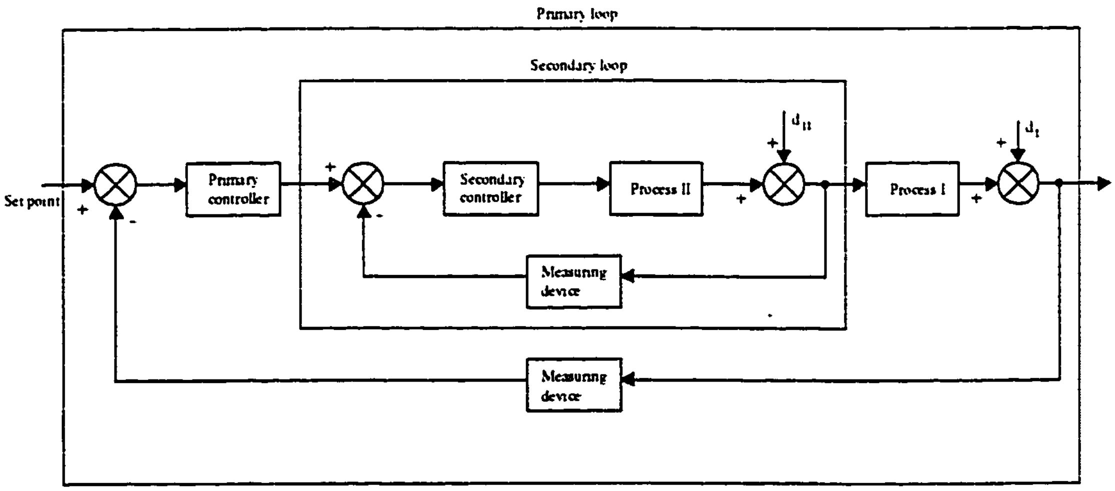

Figure 5.13: Schematic representation of cascade control (Stephanopoulos, 1984)

Useful design criteria for cascade control are shown in Table 5.14.

Table 5.14: Cascade control design criteria (Marlin, 1995)

Cascade control is desired when:
1. Single-loop control does not provide satisfactory control performance. 2. A measured secondary variable is available.
A secondary variable must satisfy the following criteria:
1. The secondary variable must indicate the occurrence of an important disturbance. 2. There must be a causal relationship between the manipulated and secondary variables. 3. The secondary variable dynamics must be faster than the primary variable dynamics.

The cascade control design criteria outlined in Table 5.14 will assist the reader in determining if the proposed control strategy involves a cascade configuration. The criteria for the secondary variable specified in Table 5.14 will also assist the reader in evaluating the performance of a cascade control system. Once the strategy has been identified as having a cascade configuration. the reader may then refer to Marlin (1995) or Stephanopoulos (1984) on controller algorithm. tuning. and implementation issues.

Feedforward Control

A feedforward control configuration uses measurements of an input disturbance to adjust the values of the manipulated variables. The disturbance measurements are used as additional information for enhancing single-loop feedback control performance. Feedforward is usually combined with feedback so that the important features of feedback are retained in the overall strategy. The structure of a feedforward control scheme is depicted in Figure 5.14.

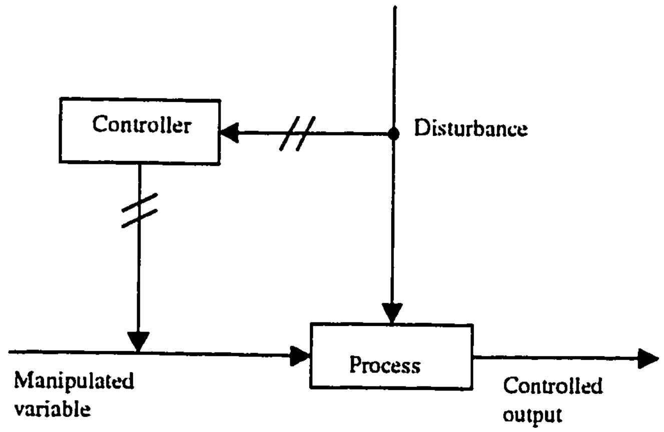

Figure 5.14: Schematic representation of feedforward control (Stephanopoulos, 1984)

A summary of design criteria for feedforward control is provided by Marlin (1995) and is presented in Table 5.15. The design criteria will be useful in determining if the proposed control strategy has a feedforward control configuration.

Table 5.15: Feedforward control design criteria (Marlin, 1995)

Feedforward control is desired when:
1. Feedback control does not provide satisfactory control performance. 2. A measured feedforward variable is available.
A feedforward variable must satisfy the following criteria:
1. The variable must indicate the occurrence of an important disturbance. 2. There must not be a causal relationship between the manipulated variable and the feedforward variable. 3. The disturbance dynamics must not be significantly faster than the manipulated-output variable dynamics (when feedback control is also present).

The third and fourth criteria are especially important because they provide clear distinctions between variables used for feedforward and feedback control configurations.

The feedforward controller attains perfect control if (1) the models used are perfect. (2) the measured disturbance is the only disturbance experienced by the process, and (3) the control calculation is realisable. However, conditions 1 and 2 are rarely satisfied. Therefore, feedforward control is usually combined with feedback control, when possible, to ensure zero steady state offset. A summary is provided in Table 5.16 on how the advantages of one controller compensate for deficiencies of the other.

Table 5.16: Comparison of feedforward and feedback principles (Marlin, 1995)

	Feedforward	Feedback
Advantages	Compensates for a disturbance before the process output is affected	Provides zero steady-state offset
	Does not affect the stability of the control system	Effective for all disturbances
Disadvantages	Cannot eliminate steady-state offset	Does not take control action until the process output variable has deviated from its set point
	Requires a sensor and model for each disturbance	Affects the stability of the closed-loop control system

5.3.4 Determine the Control Algorithm

Once the control configuration of the respirometry-based control strategy has been identified. the control algorithm can be determined since it depends on the configuration. Many of the proposals qualitatively describe the control strategy. This makes it difficult to model the controller and implement in the benchmark ASP. Therefore it is recommended that control algorithms from process control theory be used as a starting point for the dynamic simulations.

The aim of this discussion is to provide an introduction to the various process control algorithms available. The reader is referred to Marlin (1995) for a complete description on the application of the various algorithms that may be used. Control algorithms for the feedback and feedforward controllers described in this section can be applied to most systems. The feedback PID control algorithm may be applied for cascade controllers. Digital forms of the control algorithms will be emphasized in this discussion.

The Feedback PID Algorithm

The proportional-integral-derivative (PID) algorithm provides a formula for automatically performing feedback control calculations. Each element of the algorithm is termed a mode and uses the time-dependent behaviour of the feedback information in a different manner. as indicated by the name proportional-integral-derivative. The PID controller provides the best control performance for most process situations out of all the feedback control approaches.

Proportional mode

The first mode enables the control action (i.e. the adjustment to the manipulated variable) to be proportional to the error signal. As the error increases, adjustment to the manipulated variable also increases. The proportional mode of the PID controller is expressed as follows:

$$MV_p(t) = K_c E(t) + I_p$$

Eq. 5.11

where

MV(t)	=	Manipulated variable
K_c	=	Controller gain, units of [manipulated]/[controlled] variables
E(t)	=	Error
	=	CV(t) - SP(t)
CV(t)	=	*Controlled variable*
SP(t)	=	Set point for the controlled variable
I_p	=	Initialization constant

The controller gain, K_c, is the first of three adjustable parameters that enables one to adapt the PID controller to various applications. The proportional mode provides a rapid adjustment of the manipulated variable and speeds the dynamic response of the controller. However, it does not provide zero-offset although it does reduce the error. The proportional mode can cause instability if it is tuned improperly (i.e. if the value of K_c is too large).

Integral Mode

The integral mode adjusts the manipulated variable until the magnitude of the error is reduced to zero for a step-like input. This mode is important because the proportional mode does not completely eliminate the effects of disturbances. The integral mode of a PID controller is expressed as:

$$MV_I(t) = \frac{K_c}{T_I}\int_0^t E(t')dt' + I_I$$

Eq. 5.12

The integral time, T_I, is the second adjustable parameter of the PID controller and has units of time. The integral mode enables the controller to achieve zero-offset for step-like disturbances. However, this mode adjusts the manipulated variable in a slower manner than the proportional mode and as a result gives poor dynamic performance. The integral mode can also cause instability if tuned improperly (i.e. if the value of T_I is too small).

Derivative Mode

The derivative mode anticipates what the error will be in the immediate future and adjusts the manipulated variable in a manner proportional to the rate of change of the controlled variable. The derivative control action uses the following equation:

$$MV_d(t) = K_c T_d \frac{dCV(t)}{dt} + I_d$$

Eq. 5.13

The third adjustable parameter of the PID controller is the derivative time. T_d. The derivative mode provides rapid correction of the controlled variable based on the rate of change of the controlled variable. It does not influence the final steady-state value of the error because when the controlled variable is constant, the derivative mode makes no change in the manipulated variable. In many control applications the derivative mode is not employed. This is the case when high-frequency measurements of the controlled variable causes excessive variation in the manipulated variable.

PID feedback control can be implemented by using continuous (analog) or digital computing equipment. In this simulation study, only digital implementations of the PID control algorithm were employed. Digital controllers are executed periodically using sampled values of the controlled variable to determine the value of the controller output. There are two digital forms of the PID algorithm: the full-position form and the velocity form.

The full-position PID control algorithm calculates the value to be output to the manipulated variable at each execution and is expressed as follows:

$$MV_N = K_c\left(E_N + \frac{\Delta t}{T_I}\sum_{i=1}^{N} E_i + \frac{T_d}{\Delta t}(CV_N - CV_{N-1}) \right) + I$$

Eq. 5.14

The velocity algorithm calculates the change in the controller output at each execution. This means that the controller calculates the amount by which the manipulated variable must be adjusted in order to meet the set point. The velocity form algorithm is expressed as follows:

$$\Delta MV_N = K_c\left(E_N - E_{N-1} + \frac{\Delta t}{T_I} E_N + \frac{T_d}{\Delta t}(CV_N - 2CV_{N-1} + CV_{N-2}) \right)$$

Eq. 5.15

$$MV_N = MV_{N-1} + \Delta MV_N$$

Eq. 5.16

where ΔMV = Magnitude of change in manipulated variable

Δt = Controller execution time

In this study, only the velocity form of the digital PI controller was used because it provides protection against reset windup. Reset windup occurs when an error persists for a long time and the controller becomes saturated. In physical terms, this means that the valve cannot be adjusted because it is fully opened or closed before the control action has been completed (i.e. before the error has been driven to zero). This situation is not a deficiency of the control algorithm. it represents a shortcoming of the process and control equipment. The condition arises because the equipment capacity is not sufficient to compensate for large disturbances (Marlin, 1995).

Feedforward Control Algorithm

A digital form of the feedforward controller was developed in Marlin (1995) and is expressed as follows:

$$MV_n = \left(\frac{\frac{T_{lg}}{\Delta t}}{\frac{T_{lg}}{\Delta t}+1} \right) MV_{n-1} + K_{ff} \left(\frac{\frac{T_{ld}}{\Delta t}+1}{\frac{T_{lg}}{\Delta t}+1} \right) (D_m)_{n-\Gamma} - K_{ff} \left(\frac{\frac{T_{ld}}{\Delta t}}{\frac{T_{lg}}{\Delta t}+1} \right) (D_m)_{n-\Gamma-1}$$

Eq. 5.17

where

feedforward controller lead time	=	T_{ld}	=	τ
process time constant	=	τ		
feedforward controller lag time	=	T_{lg}	=	τ_d
disturbance time constant	=	τ_d		
feedforward controller gain	=	K_{ff}	=	$-K_d/K_p$
process gain	=	K_p		
disturbance gain	=	K_d		
disturbance model in the time domain	=	D_m		
Γ	=	θ / Δt. an integer value		
process dead time	=	θ		

This form of the feedforward controller provides sufficient accuracy for most cases. Adjustable parameters for this algorithm are K_{ff}, T_{ld}, and T_{lg}. The parameters K_p, τ, τ_d, and θ belong to the process model, which is assumed to have first-order-with-dead-time dynamics. The disturbance model used in this algorithm is assumed to have first-order dynamics with the parameters, K_d and τ_d. The general definition of a gain is the ratio of the change in output variable to the change input variable. The time constant characterizes the "speed" of the dynamic response. The dead time is the time interval during which no effect is observed on the outputs of the system. The first-order dynamic model of a system will be discussed in the next section.

The feedforward algorithm in Eq. 5.17 is also characterized by the lead and lag times. When the lead time is less than the lag time, the process time constant is shorter than the disturbance time constant. When this occurs, the control action needs to be slowed so that the effects of the disturbance and the feedforward controller cancel. The resulting control action is that the manipulated variable approaches the steady state as a first-order response but never reaches the final steady state value. When the lead and lag times are equal, the process has an equal time constant with the disturbance. In this case, the manipulated variable immediately attains its steady state value. Finally, when the lead time is longer than the lag time, the process has a slower time constant than the disturbance. The response of the manipulated variable in this case is that it initially exceeds and then slowly returns to its steady-state value.

5.3.5 Design / Tune the Controller

Once the controller algorithm is defined, appropriate values for the adjustable tuning constants must be determined to achieve good control performance. Many tuning methods can be used to calculate values for the tuning constants. A good summary of the tuning methods is provided in Marlin (1995).

There are several key factors that must be considered in tuning a controller. First, most tuning methods require a simplified dynamic model of the open-loop process. As a result, good control performance from the tuning depends on reasonably accurate model identification. Second, calculated values for the tuning constants should enable the control system to achieve the desired performance objectives relevant to the process. Different tuning methods have different objectives and consequently, each provides somewhat different dynamic performance, which should be matched to the process requirements. Third, all methods identify only the initial values for the control parameters. The values are then modified by fine-tuning, which corrects for modelling errors and adapts the performance to that desired for the process.

The following procedures were applied to tune each of the digital controllers in this study:

1. Obtain the simplified dynamic model of the open-loop process.
2. Determine the sample period.

3. Determine the initial values of the control parameters by employing the appropriate tuning method.
4. Fine-tune the control parameters.

5.3.5.1 Obtain a simplified dynamic model of the process

The dynamic model of a process can be obtained analytically or empirically. However for digital control systems, only the empirical model can be obtained. The most widely used empirical method for identifying dynamic models is the process reaction curve method (Marlin, 1995). It is simple to perform and provides adequate models for many applications. The method involves the following four steps:

1. Allow the process to reach steady state.
2. Introduce a single step change in the input variable.
3. Collect input and output response data until the process reaches a new steady state.
4. Perform the graphical process reaction curve calculations, which are explained in detail in Marlin (1995).

The process reaction curve method only calculates the parameters for a first-order-with-dead-time model. This model approximates the dynamics of processes with monotonic responses to step inputs. The general for a step change in the input with $t \geq 0$ is:

$$Y(t) = K_p \delta (1 - e^{-(t-\theta)/\tau})$$

Eq. 5.18

where Δ = Steady state change in the output

δ = Magnitude of t he input change

K_p = Process or steady-state gain = Δ/δ

= $\Delta CV/\Delta MV$

τ = Time constant

θ = Dead time

The process parameters, K_p, τ, and θ, characterize the dynamic response of the output variable to a change in the input variable. For a control system, the output variable refers to the controlled variable and the input variable refers to the manipulated variable. The process gain, K_p, is the ratio of the magnitude of the steady-state gain of the controlled variable to the magnitude of change in the manipulated variable. The process time constant, τ, characterizes the "speed" of the dynamic response. The dead time, θ, is the time interval for which no effect is observed in the controlled variable.

5.3.5.2 Determine the sample period

In digital control, the measured controlled variables are obtained by sampling from the continuous signal and converting this signal to digital form via A/D conversion. Sampling introduces an additional delay in the feedback loop and can be approximated as a dead time of $\Delta t/2$. Thus in tuning digital controllers, the dead time used in the calculations is the process dead time plus one-half of the sample period (i.e., $\theta' = \theta + \Delta t/2$).

In this study, the controller sample period was taken to be equal to the sample period of the influent wastewater data, which was every 15 minutes.

It must be noted that selecting the appropriate sample period is not trivial. Sampling must be frequent enough so that the continuous signal can be reconstructed from the sampled signal without loss of essential information. Too long a sample period can reduce the controller's effectiveness, especially its ability to cope with disturbances. Therefore it is important to consider both the process dynamics and the disturbance characteristics in selecting the sampling period.

5.3.5.3 Initial tuning of the controller

Tuning methods are used to calculate the initial values for the adjustable parameters of the control algorithm. For a PID controller, the adjustable control parameters are K_C, T_I, and T_d.

The appropriate tuning method is selected based on the control performance goals. Tuning methods involve optimization, correlations, or stability analysis. Marlin (1995) recommends the following tuning methods, with the first being the preferred method:

(i) Ciancone tuning correlations if the open-loop process can be estimated by first-order-with-dead-time dynamics.

(ii) Bode/(closed loop) Ziegler-Nichols if the process cannot be satisfactorily fitted by a first-order-with-dead-time model.

(iii) Nyquist/gain margin method when the process does not satisfy the Bode criteria.

(iv) Any other correlations described in Marlin (1995) as appropriate for the application scenario.

(v) Detailed analysis of the robustness of the system, through either optimization methods described in Marlin (1995) or the robust performance applied to the IMC as described in Morari and Zafiriou (1989). Marlin (1995) notes that this is the best method but requires more effort than is usually justified for initial tuning. This method may be required for systems with complex dynamics and large model errors.

In this study, the Ciancone correlations were used to determine the initial values for K_c, T_I, and T_d of the PID algorithm. The correlations are based on the values of K_P, τ, and θ, parameters of the dynamic process model. The tuning goals of the Ciancone correlations are as follows:

1. The integral of the absolute value of the error (IAE) of the controlled variable is minimized. The IAE is calculated as follows:

$$IAE = \int_0^{\infty} |SP(t) - CV(t)| dt$$

Eq. 5.19

2. ±25% change in the process model parameters are accounted for by the correlations. This factor is important because the well-tuned controller must provide acceptable control performance as the process dynamics change.
3. Limits on the variation of the manipulated variable are specified. This is to prevent excessive variation in the manipulated variable.

The Ciancone correlations apply to processes that can be represented by a first-order-with-dead-time model. Stability is not explicitly considered in the Ciancone method, tuning that makes the system unstable or oscillatory would have a large IAE and thus would not have been selected as optimum. The Ciancone correlations give lower controller gain values, partly because of the objectives of robust performance with model errors and partly because of the limitation on the manipulated variable variation with a noisy measured controlled variable. The Ciancone correlations yield controllers that are more robust than those developed with Ziegler-Nichols tuning and thus perform better when realistic model errors occur (Marlin, 1995, p.356).

5.3.5.4 Fine-tune the controller

Fine-tuning involves implementing the initial values of the control parameters in the control algorithm and modifying them until acceptable closed-loop control performance is achieved. This step is necessary because of errors in the base-case process model and simplifications in the tuning method. To determine whether the tuning is satisfactory, Marlin (1995) recommends examining the performance of the controller to changes in the set point. The integral of the squared error (ISE) and settling time of the controlled variable were used in this study to measure the performance of the controller.

The ISE is one measure of the cumulative deviation of the controlled variable from its set point during the transient response (Marlin, 1995). It is expressed as follows:

$$ISE = \int_{0}^{\infty} \left[SP(t) - CV(t) \right]^2 dt$$

Eq. 5.20

The settling time is defined as the time the controller takes to attain a "nearly constant" value, usually ±5 percent of its final value (Marlin, 1995), after a disturbance has been introduced into the system.

To fine-tune a controller, enter the initial values of the tuning parameters into the algorithm and switch the controller's status in the automatic position to allow the controller to perform its calculation and adjust the manipulated variable accordingly. Then, the response to a set point change is diagnosed to determine whether the tuning is satisfactory. The easiest type of disturbance to implement to test the controller's response is a step change in the set point. The magnitude of the step change is selected such that the effects on the controlled variable are apparent. It is important to mention that no controller can reduce the delay, between when the set point is changed and when the controlled variable initially responds, to be less than the dead time.

5.3.6 Determine the Range of Variation for the Manipulated Variable

An appropriate range of variation, or the maximum and minimum rates, must be specified for the manipulated variable when implementing the controller in the benchmark activated sludge plant. The variation in the manipulated variable is of concern because it influences plant performance.

The manipulated variable must have sufficient "range" in that allowable adjustments must be large enough to achieve desired set points and compensate for expected disturbances. Large-magnitude and high-frequency variations in the manipulated variable must be avoided so that undesired oscillations do not occur in the process. However, if the range is too small the control action will be inadequate and the set point will not be reached.

5.4 Evaluation of the Control Performance of the Respirometry-Based Controller

With so many proposed control strategies, there is a need for a systematic and objective technique to test the potential and benefits of these strategies. Therefore, five different types of evaluations have been developed for the simulation-based methodology to examine various aspects of the control system. The five types of tests are:

1. Evaluation of the response of the controlled variable to changes in the manipulated variable with the automatic controller disabled. The response of the controlled variable with the controller disabled is often referred to as an *open-loop* response.
2. Stability analysis of the control system. The purpose of stability analysis is to determine the ability of a control system to dampen out any oscillations that result from a disturbance on the plant. There are many methods available to evaluate the stability, including the Bode and Nyquist analyses. The Bode method is the easiest to implement while the Nyquist method has the most general applicability
3. Evaluation of the dynamic performance of the controller to changes in the set point under constant influent conditions.
4. Evaluation of the dynamic performance of the controller under diurnal influent loading conditions.
5. Evaluation of the effect of the controller on plant performance under stress loading conditions.

5.4.1 Open-Loop Dynamic Behaviour of the Control System

A key factor of a good control system is a causal relationship between the manipulated variable and controlled variable. When the controller is disabled and a change in the manipulated is introduced, the response of the controlled variable is referred to as an open-loop response. The dynamic behaviour between the manipulated variable and the controlled variable is referred to as open-loop dynamics.

The purpose of obtaining the open-loop dynamics of the control system is to examine the dynamic relationship between the manipulated variable and the controlled variable. The performance of a controller depends on the causal relationship between the manipulated variable and the controlled. The open-loop dynamic behaviour is obtained by introducing a step change in the manipulated variable and measuring the response of the controlled output variable. The process reaction curve method, described in Marlin (1995), can be used to calculate the parameters characterising the relationship between the two variables. In this analysis, simulations are conducted with constant average influent loading.

The open-loop response of the controlled variable to changes in the manipulated variable usually exhibits first-order-plus-dead-time dynamics. The following parameters characterize a first-order-plus-dead-time system:

- Kp (process gain) – ratio of the change in the controlled variable to the change in the manipulated variable,
- τ_p (process time constant) – characterizes the speed of the response of the controlled variable to the change in the manipulated variable,
- θ (dead time) – the time interval for which no effect is observed in the controlled variable once a change in the manipulated variable has been introduced.
- $\theta/\theta+\tau$ (fraction dead time)

5.4.2 Stability Evaluation of the Control System with Frequency Response Analysis

The purpose of the stability analysis is to determine the ability of the control system to dampen out any oscillations that can result from a disturbance on the plant. In other words, a stability analysis is a method of verifying that the design or tuning of the controller provides stable performance over a wide range of input frequencies.

In process control theory, the bounded input, bounded output stability is often employed for defining stability:

> A system is stable if all output variables are bounded when all input variables are bounded. A system that is not stable is unstable (Marlin, 1995).

"Bounded" is an input that always remains between an upper and a lower limit. Sinusoidal and step inputs are examples of bounded inputs, whereas a ramp input is unbounded. Unbounded output exists only in theory and not in practice because all physical quantities are limited. Therefore, the term "unbounded" means very large in this context (Stephanopoulos, 1984).

Stability is required for good control system performance. However, a control system can be stable and perform poorly (Marlin, 1995). The action of a controller can potentially cause instability in a process by introducing oscillations in an originally overdamped system. A thorough understanding of the stability of dynamic systems is essential because it provides important relationships among process dynamics, controller tuning, and achievable performance (Marlin, 1995).

In the feedback control system shown in Figure 5.15, all elements of the feedback loop affect the stability of the process. These elements include the process, sensors, transmission, final elements, and controller.

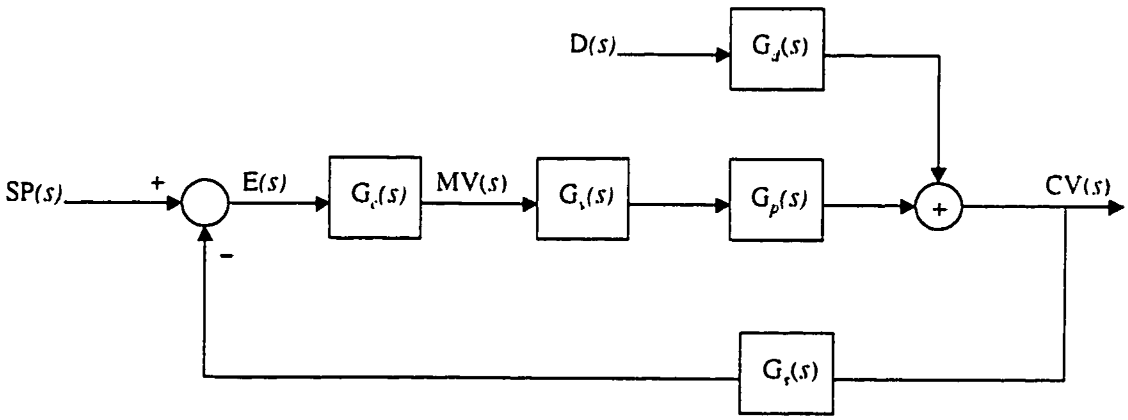

Figure 5.15: Block diagram of a feedback control system

where CV(s) = Process output variable, referred to as the controlled variable

MV(s) = Process input variable, referred to as the manipulated variable

SP(s) = Set point value of the controlled variable

E(s) = Error, difference between the set point and the measured controlled variable

D(s) = Disturbance input that changes due to external conditions and affects the controlled variable

$G_c(s)$ = Controller transfer function

$G_v(s)$	=	Transmission, transducer, and valve transfer function
$G_p(s)$	=	Process transfer function
$G_s(s)$	=	Sensor, transducer, and transmission transfer function
$G_d(s)$	=	Disturbance transfer function

A quick way to demonstrate how these elements affect stability is to examine the denominator of the closed-loop transfer functions of the feedback control system. The denominator of the closed-loop transfer function is referred to as the characteristic polynomial. When the characteristic polynomial is set to equal zero, it is referred to as a characteristic equation. Stability analysis methods that require polynomial transfer functions include the root locus and the Routh methods.

The solutions of the characteristic equation determine whether the system is stable or unstable. If all roots of the characteristic equation have negative real parts, the control system is stable because it is able to dampen input disturbances. However, if any root has a real part greater than or equal to zero the system is considered to be unstable. This means that the controlled variable increases without limit upon a disturbance on the system.

The closed-loop transfer function relating the response of the controlled variable to a disturbance for the system shown in Figure 5.14 is expressed as follows:

$$\frac{CV(s)}{D(s)} = \frac{G_d(s)}{1 + G_p(s)G_v(s)G_c(s)G_s(s)}$$

Eq. 5.21

The closed-loop transfer function relating the controlled variable to the set point for the system in Figure 5.14 is:

$$\frac{CV(s)}{SP(s)} = \frac{G_d(s)}{1 + G_p(s)G_v(s)G_c(s)G_s(s)}$$

Eq. 5.22

Since the characteristic polynomial of the transfer functions, shown in Eq. 5.21 and Eq. 5.22, both contain the process, sensors, transmission, final elements, and controller, all these elements affect stability. The disturbance and set point changes are not in the characteristic polynomial because they affect the input forcing and therefore do not affect stability. Furthermore, since both the disturbance and set point transfer functions have the same characteristic polynomial, stability analyses for set point changes and disturbances yield the same results.

Since the dynamic models of many plants have dead time, determining the stability of a control system with polynomial transfer functions may be difficult. The reason is that the characteristic equations are usually complicated so the roots may not be easily calculated. An alternative for evaluating the stability characteristics is frequency response analysis. This analysis involves calculating the ultimate response of a system to a sinusoidal input.

The frequency response of a system with the transfer function $G(s)$, to a sinusoidal input is characterized by two key parameters: amplitude ratio and phase angle. The amplitude ratio is defined as the ratio of the output amplitude to the input amplitude, and is a function of the frequency, ω, of the input disturbance:

$$\begin{aligned} Amplitude\ ratio = \mathrm{AR} &= \frac{Output\ magnitude}{Input\ magnitude} \\ &= |G(j\omega)| \\ &= \sqrt{\mathrm{Re}[G(j\omega)]^2 + \mathrm{Im}[G(j\omega)]^2} \end{aligned}$$

Eq. 5.23

The amplitude ratio gives the magnitude of the variation in the controlled variable for a unit sine input. Therefore, the smaller the amplitude ratio for a disturbance response, the better the control performance.

The phase angle or phase shift is the angle by which the output wave lags behind the input wave. The phase angle is also a function of the frequency, ω:

$$
\begin{aligned}
\textit{Phase angle} &= \text{Phase difference between input and output} = \phi \\
&= \angle G(j\omega) \\
&= tan^{-1}\left(\frac{\mathrm{Im}[G(j\omega)]}{\mathrm{Re}[G(j\omega)]}\right)
\end{aligned}
$$

Eq. 5.24

There are several methods that apply frequency response analysis to determine the stability of a control system. Two commonly used methods include the Nyquist method and the Bode method. The Nyquist method is the most general, while the Bode method is the easiest to implement. These methods provide information on the relative stability of the system (i.e. how much a parameter must change to change the stability of the system). In this study, only Nyquist plots were employed to evaluate the stability characteristics of the control systems since it has the most general applicability.

The Nyquist method graphically determines if the characteristic equation, $[1 + G_p(s)G_v(s)G_c(s)G_s(s)]$, of the closed-loop transfer functions given by equations 5.20 and 5.21 has any positive roots. The Nyquist diagram is a plot in a complex plane of the amplitude ratio and phase angle as the frequency is varied from zero to infinity. It uses the Im $[G(jw)]$ as ordinate and Re $[G(jw)]$ as abscissa. An example of a Nyquist plot is shown in Figure 5.16.

A specific value of the frequency ω defines a point on this plot. Thus the following characteristics are observed at point A in Figure 5.16:

1. The frequency has a value ω_l.
2. The distance from point A to the origin (0,0) is the amplitude ratio at the frequency ω_l.
3. The angle ϕ with the real axis is the phase shift at the frequency ω_l.

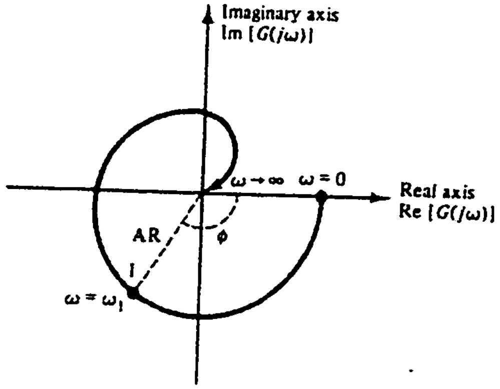

Figure 5.16: Form of a Nyquist plot (Stephanopoulos, 1984)

The *Nyquist stability criterion* states that a closed-loop control system is stable if the open-loop system is stable and the Nyquist plot does not enclose the point $-1+j0$. In other words, $[1 + G_p(s)G_v(s)G_c(s)G_s(s)]$ has only negative roots and the control system is stable.

The Nyquist plots for the control systems evaluated in this study were obtained by first converting the dynamic process models (describe in Section 5.2.1) from the time domain to the state space form in GPS-X. The process models were converted into the state space form because they were much too complex to be converted into the laplace transform. Hence, equations 5.21 and 5.22 were not applied in this study and were described for the purpose of providing theory on the Nyquist plots. The state space form was then transferred to Matlab whereupon the Nyquist plots were calculated. The following steps were performed to obtain the state space form of the time domain model of the activated sludge process:

1. Use constant influent loading.
2. Run the simulations, with all controllers turned off except for the DO controllers, until both the DO concentrations and K_La values in all three CSTRs reach steady state. The DO concentrations should be constant at 2 g m^{-3}. Once steady state has been reached, turn the DO controllers off.
3. To ensure that the system is in steady state and stable, the eigen values were computed in GPS-X. Negative eigen values indicated that the system was stable.
4. The Jacobian was then calculated about the current point in state space by numerical perturbation.

5. The state space form of the activated sludge process was then imported into Matlab to plot the Nyquist diagrams.

5.4.3 Dynamic Performance of the Controller to Changes in the Set Point

Useful information can be determined by assessing the controller's response to step changes in the set point under constant influent conditions. In this way, the speed of the control action and the ability of the controller is meeting the set point can be determined. Additionally, this analysis allows one to examine the variation in the manipulated variable. Therefore, by analysing the responses of the controlled and manipulated variables to a step change in the set point the diagnostic information on the causes of good and poor control performance are revealed. Two measures of control performance were examined: (1) deviation of the controlled variable from its set point and (2) the variation of the manipulated variable. The following parameters were calculated to determine the dynamic response of the controller:

- Standard deviation from the set point (σ_{sp})
- Settling time (which is the amount of time the controlled variable takes to meet the new set point value)
- Offset between set point and steady-state value of controlled variable

5.4.4 Dynamic Performance of the Controller Under Diurnal Influent Conditions

The next test of the methodology involves examining the performance of the controller under diurnal influent loading conditions. The purpose of this evaluation is to test the controller under realistic influent conditions and its impact on plant performance in terms of effluent quality. The influent flow has a maximum to average ratio of approximately 1.5 per day and is illustrated in Figure 5.17. In this assessment, the ability of the controller in maintaining the set point and the variation of the manipulated variable were investigated. The effect of employing different set points on effluent quality was also examined. The following performance measures were calculated to support the assessment:

- Standard deviation from the set point (σ_{sp})
- Standard deviation of the manipulated variable (σ_{mv}),
- Comparison of the effluent quality for the uncontrolled and controlled cases.

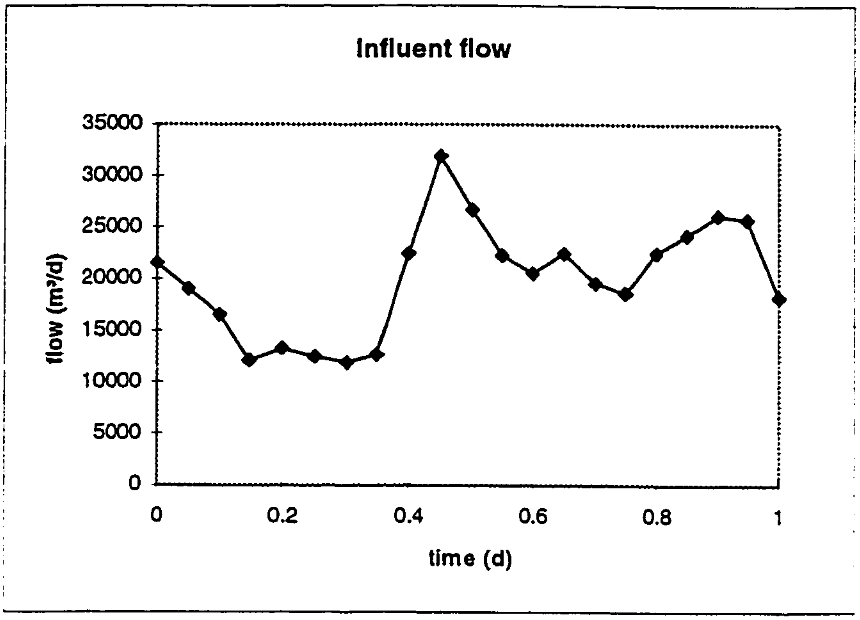

Figure 5.17: Daily hydraulic loading experienced by the plant (maximum to average flow ratio = 1.5)

5.4.5 Effect of the Controller on Plant Performance Under Stress Loading Conditions

The last evaluation of the methodology involves testing the performance of a controller under five loading conditions over a 35-day period. The purpose of this assessment is to determine the benefits of control and when control is necessary. This test reveals if respirometry-based control enables the plant to maintain effluent quality compliance longer during stress loading conditions and the impact of control on energy costs.

Each loading scenario was 7-days long. Of the five scenarios, two were stress-loading conditions. One stress scenario involved subjecting the plant to a 50 per cent increase in both the hydraulic and pollutant loading. The other scenario consisted of two storm events. Influent loading scenarios for the 35-day simulation period are described in Table 5.17.

Table 5.17: Influent Loading Scenarios

Week	Influent Loading Period	Influent Loading Condition
1	day 0 to day 7	Normal diurnal influent loading
2	day 7 to day 14	50 per cent increase in the hydraulic and pollutant loading
3	day 14 to day 21	Normal diurnal influent loading
4	day 21 to day 28	Two storm events
5	day 28 to day 35	Normal diurnal influent loading

The flow rate, biodegradable concentration, and particulate concentration of the 35-day influent loading are depicted in Figures 5.18, 5.19 and 5.20 respectively.

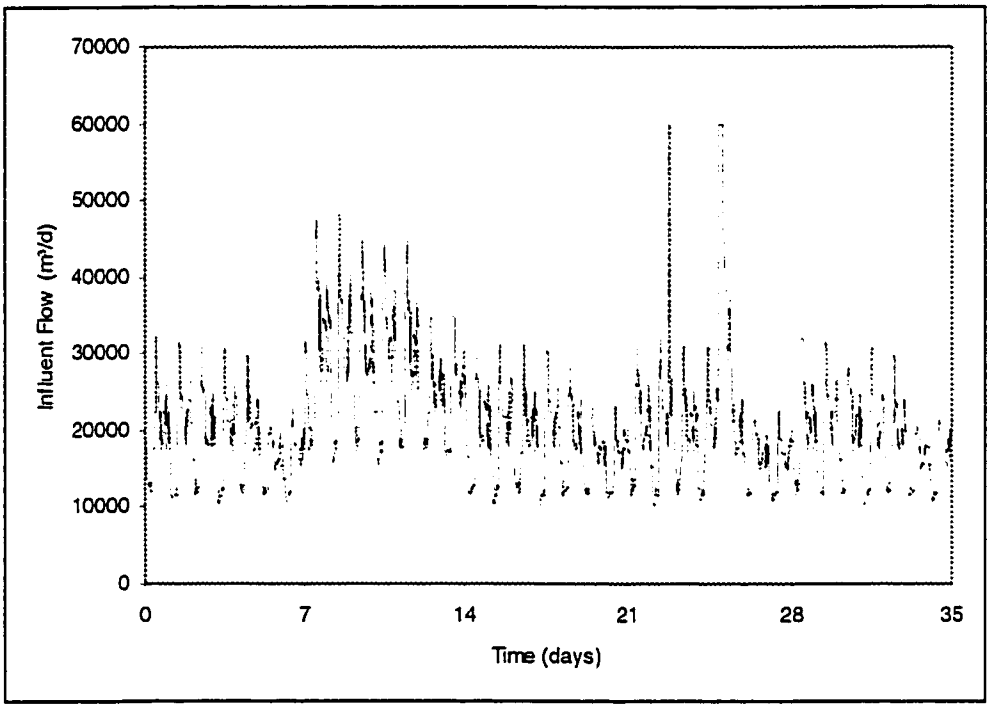

Figure 5.18: Influent flow rate of 35-day loading scenarios

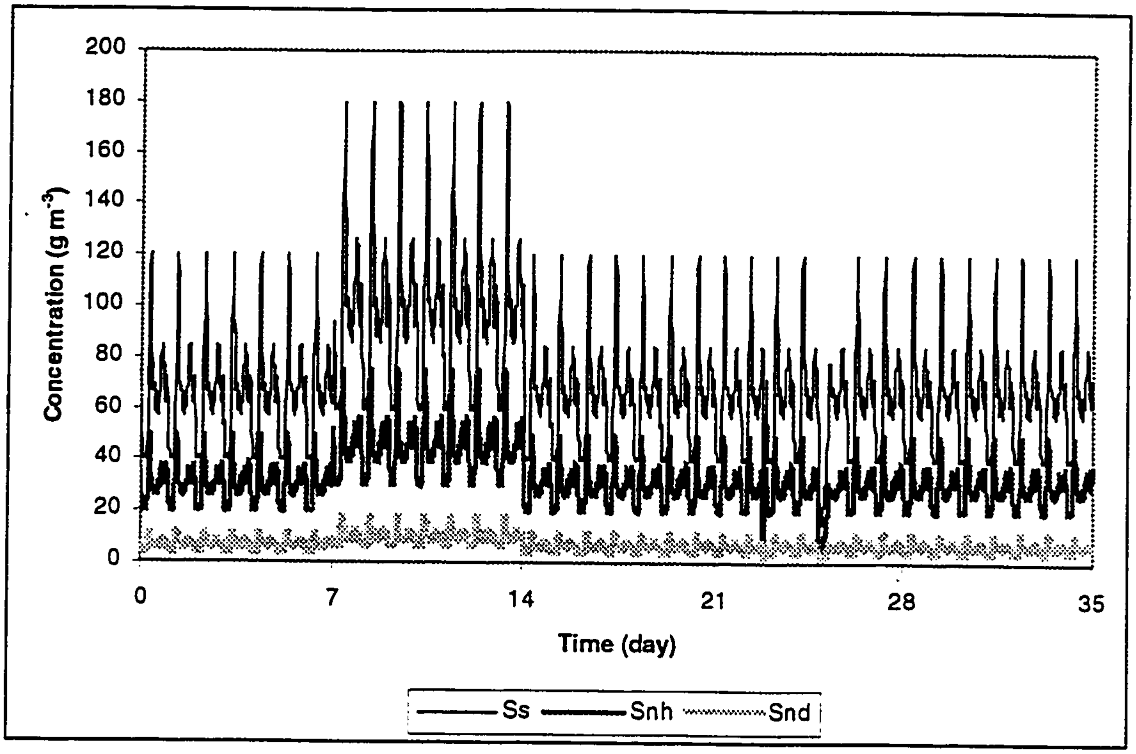

Figure 5.19: Influent readily biodegradable substrate, ammonia and slowly biodegradable nitrogen of 35-day loading scenarios

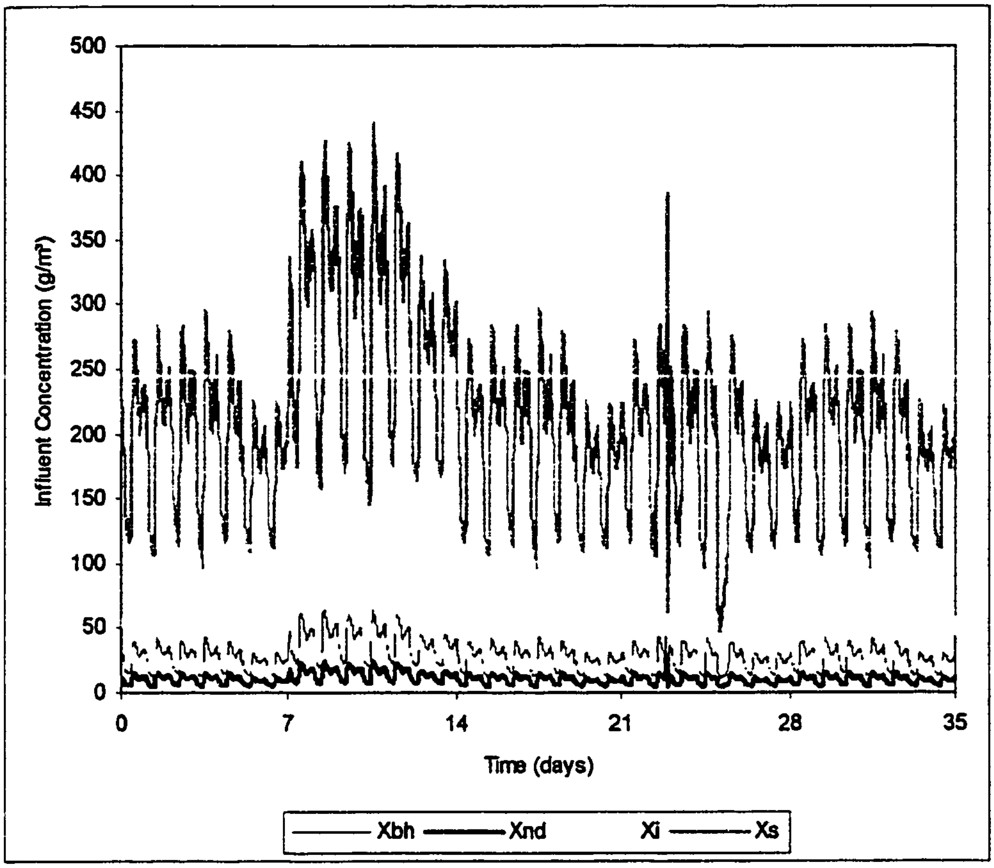

Figure 5.20: Influent particulate concentration of 35-day loading scenarios

6 Evaluation of a Respiration Rate Control Strategy that Uses the Sludge Wastage Rate

6.1 Introduction

This section will discuss a respirometry-based control strategy proposed by Stephenson *et al.* (1981) in which the active biomass concentration is controlled by manipulating the sludge wastage rate (Q_{waste}) according to measurements of the respiration rate (rr). Flanagan (1977), Arthur (1984), and Klapwijk *et al.* (1993) are additional examples of proposals in which Q_{waste} is used as a manipulated variable in the respirometry-based control strategy. The strategy proposed by Stephenson *et al.* (1981) was selected for evaluation for several reasons: 1) experimental data were reported from pilot plant studies; 2) plant operating conditions were reported; 3) the control strategy was easy to understand; and 4) the strategy was a good starting point for developing the simulation-based methodology.

The objective of the control strategy proposed by Stephenson *et al.* (1981) was to manipulate the sludge wastage rate (Q_{waste}) to maintain the endogenous respiration rate (rr_{end}) in the aeration tank at a set point. The underlying concept of the strategy is that rr_{end} is a measure of the active biomass concentration. The set point rr_{end} is selected to provide the degree of biomass activity and substrate oxidation required.

The pilot plant study conducted by Stephenson *et al.* (1981) will first be reviewed. Then the evaluation of the control strategy will be discussed based on the simulation-based methodology described in Section 5. The simulation model and the activated sludge plant employed in the evaluation will be described. Following this, a discussion on the implementation of the control strategy will be provided. Lastly, the performance of the controller and its potential benefits on plant performance will be discussed.

6.2 Review of the Pilot Plant Study Conducted by Stephenson *et al.* (1981) on Respiration Rate Control

6.2.1 Summary of the Pilot Plant Study Conducted by Stephenson *et al.* (1981)

The pilot-scale activated sludge plant used by Stephenson *et al.* (1981) was a carbon removal plant. The plant consisted of a primary clarifier, followed by an aeration tank and a secondary clarifier. A diagram of the plant layout used in the simulations is shown in Figure 6.1. The dissolved oxygen concentration in the aeration tank was automatically controlled. The hydraulic loading resembled a sinusoidal function with a peak/mean/minimum ratio of 2/1/0.5. The mean hydraulic flow to the reactor was 7.2 $m^3\ d^{-1}$.

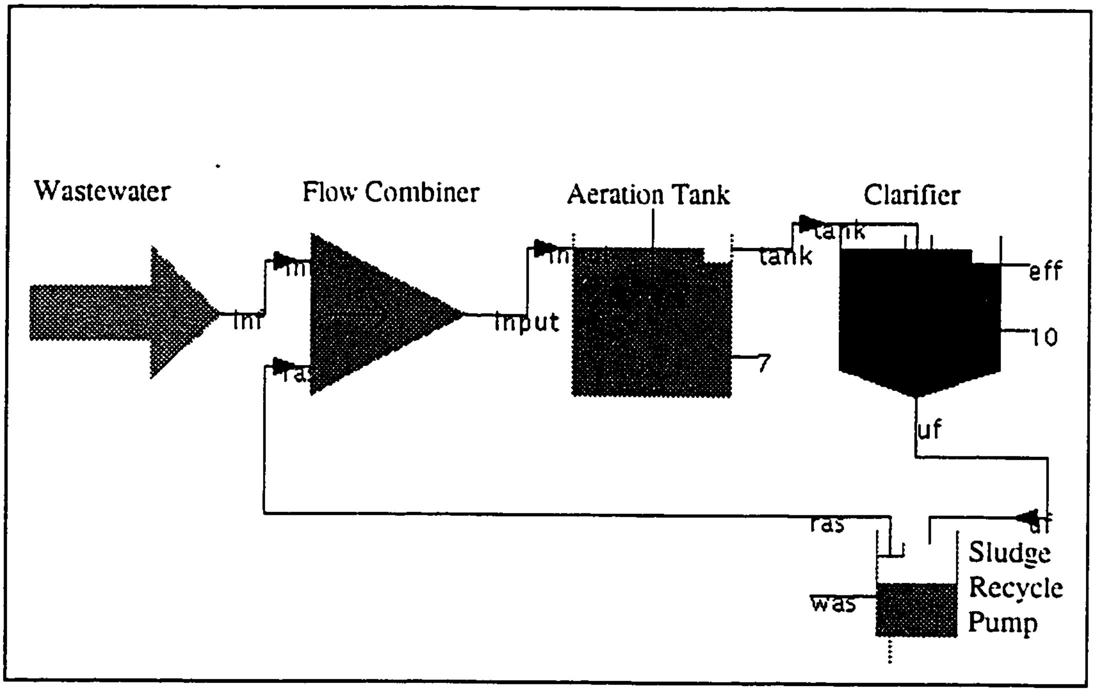

Figure 6.1: Layout of pilot plant used by Stephenson *et al.* (1981)

The type of controller used by the authors to maintain the respiration rate set point was an on-off controller. The controller regulated the respiration in the aeration tank for the expected load of the subsequent day by automatically wasting the sludge at 30-minute intervals between 3 and 8 A.M. During this time, rr_{end} could be measured because the plant hydraulic and organic loadings were low. A rr_{end} set point of 22 g m^{-3} h^{-1} was used in the study and was selected because previous plant records showed adequate treatment at this value.

Stephenson *et al.* (1981) observed that the respiration rate in the aeration tank coincided with the influent loading. The respiration rate increased when the loading increased and decreased when the loading was low. The rr_{end} set point of 22 g m^{-3} h^{-1} was not met in the time or wasting constraints allocated for the particular loading conditions of the plant (Stephenson *et al.*, 1981). However, the authors observed that control of the respiration rate slightly improved the mean effluent suspended solids over the 24-hour testing period.

6.2.2 Simulation of the Pilot Plant Study Conducted by Stephenson *et al.* (1981)

Simulations were performed to replicate the pilot plant and on-off *rr* controller used by Stephenson *et al.* (1981). The on-off controller employed in the simulations wasted sludge between 3 and 8 a.m. as was done in the study. But wasting only occurred when the respiration rate measured in the aeration tank increased above the set point value of 22 g m^{-3} h^{-1}. The GPS-X macro for the on-off controller is provided in Appendix B.1. The simulated hydraulic influent flow is depicted in Figure 6.2.

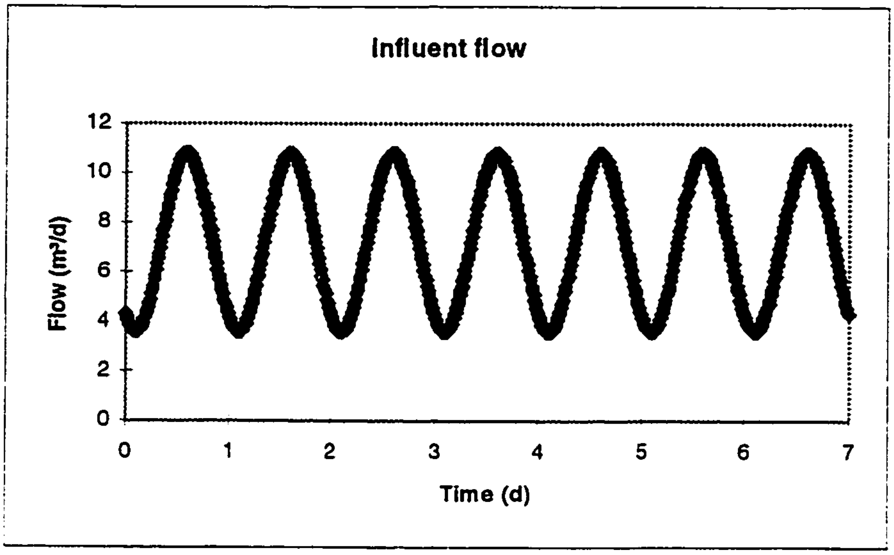

Figure 6.2: Simulated hydraulic flow into the pilot plant

The simulations indicated that the on-off controller was not able to maintain the rr_{end} at the set point when subjected to the influent flow depicted in Figure 6.2. This is shown in Figure 6.3. The *rr* in the aeration tank oscillates about the set point value of 22 g m^{-3} h^{-1} and does not show any signs of settling towards the set point. The simulations did however reveal a slight decrease in the effluent suspended solids as was observed in the pilot plant study conducted by Stephenson *et al.* (1981).

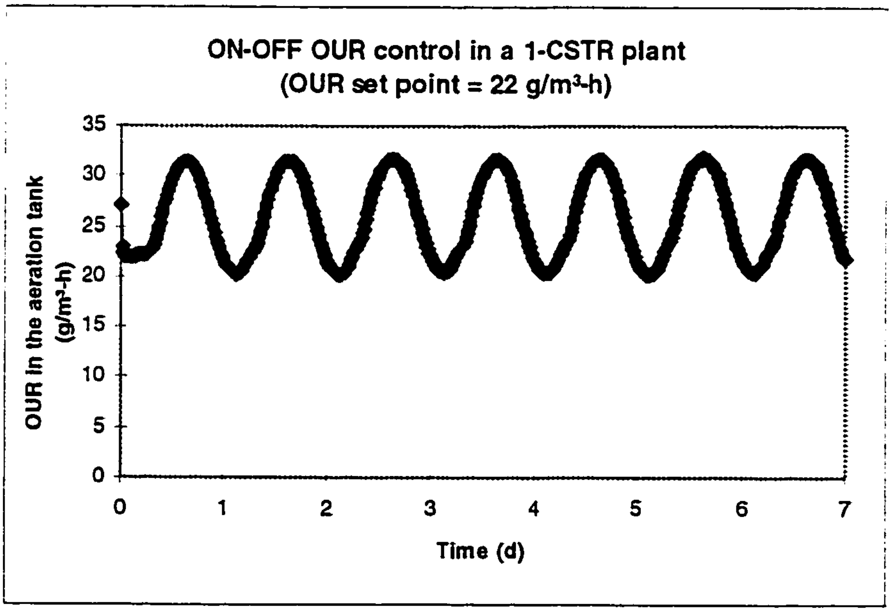

Figure 6.3: Control of *rr* with an ON-OFF controller

6.3 Application of the Benchmark (Spanjers *et al.*, 1998a)

The benchmark (Spanjers *et al.*, 1998a) was used to conduct simulation studies of the control strategy proposed by Stephenson *et al.* (1981). As described in Section 5.2, the benchmark consists of: the following components:

1) the process models for the activated sludge process (IAWQ ASM1 Henze *et al.*, 1987) and the secondary clarification process (Takács *et al.*, 1991) (Section 5.2.1);
2) the set of influent conditions for both dry and wet weather (Section 5.2.2);
3) values for the parameters of the ASM1 (Henze *et al.*, 1987) and the double exponential settler model (Takács *et al.*, 1991) (Section 5.2.3);
4) the set of initial values for the state variables (Section 5.2.4); and
5) the carbon removal activated sludge plant (Section 5.2.5).

The control strategy proposed by Stephenson *et al.* (1981) was implemented in the benchmark plant designed for carbon-removal. Control of *rr* is performed through a feedback control loop. A diagram of the control configuration is provided in Figure 6.4.

The operating conditions of the benchmark plant were slightly modified to reflect the operating conditions of the pilot plant used by Stephenson *et al.* (1981):

- A recycle ratio of 0.5 was used in this study instead of 1.0, as was specified in the benchmark. because this was specified in the proposal by Stephenson *et al.* (1981).
- Since a sludge retention time of 3 days was reported in Stephenson *et al.* (1981). a 3-day sludge retention time was used in this study instead of the 4 days in the benchmark plant.

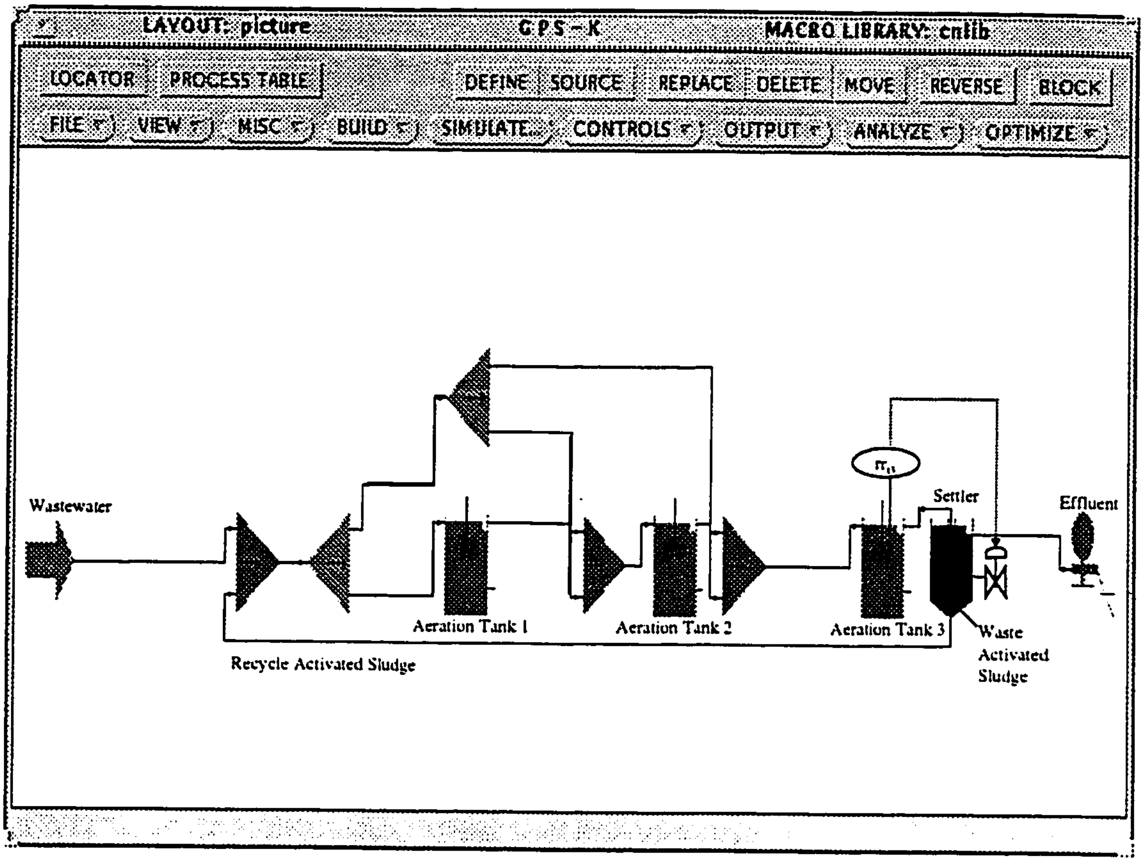

Figure 6.4: Feedback control configuration of the rr control strategy the benchmark plant

Several differences exist between this simulation study and the pilot plant study conducted by Stephenson *et al.* (1981):

1. The influent was different in the two cases. The synthetic influent used in the simulations had larger fluctuations than the influent used in the pilot plant study.
2. The activated sludge plants differed in the two cases. A 3-tank system was used for the simulations, while a 1 tank system was used the pilot plant study.
3. Measurement of rr_{end} differed. Stephenson *et al.* (1981) measured the respiration rate during low loading periods to obtain rr_{end}. In addition, rr_{end} was calculated at 5-second intervals and averaged at 15-minute intervals in the pilot plant study. However in this study, rr_{end} was measured continuously in the third tank. It was assumed that the respiration rate in the third tank (rr_{t3}) was close to endogenous because the biodegradable substrate concentration was low (between 1 – 2.5 g COD m^{-3}).
4. rr_{end} was measured every 15 minutes in the third tank for this study.

5. In this study, wasting occurred continuously throughout the entire day to meet the set point respiration rate. However in the pilot plant study, wasting occurred only at specific time intervals for 5 consecutive hours each day.
6. Different types of controllers were implemented in the two cases. The controller used in the simulations was a 'textbook' feedback controller. An on-off controller was used in the pilot plant study.

6.4 Implementation of the Respiration Rate Control Strategy

Implementation of the control strategy proposed by Stephenson *et al.* (1981) involved the following 6-step procedure that was described in Section 5.3:

1. Identify the objective of the respirometry-based control strategy (Section 5.3.1).
2. Identify the input and output variables of the control system (Section 5.3.2).
3. Identify the implied control configuration (Section 5.3.3).
4. Determine the appropriate control algorithm (Section 5.3.4).
5. Design/tune the controller (Section 5.3.5).
6. Determine the appropriate range of variation for the manipulated variable (Section 5.3.6).

6.4.1 Objective of the Respiration Rate Control Strategy

The objective of the proposed control strategy is to maintain the active biomass concentration at the set point to ensure adequate treatment of the wastewater. In other words, the operational objective of the control strategy is to ensure effluent concentrations meet standards, and the control objective is to maintain rr_{t3} at the set point.

6.4.2 Input and Output Variables of the Control System

rr_{t3} is the controlled variable and Q_{waste} is the manipulated variable. The control strategy proposed by Stephenson *et al.* (1981) uses rr_{end} as a measure of the active biomass. Stephenson *et al.* (1981) assumed that the respiration rate measured during low loading periods is endogenous. In this study, it was assumed that the respiration rate in the third aeration tank was close to endogenous.

The graph in Figure 6.5 shows the respiration rate in each of the three tanks for simulations conducted with normal diurnal influent over a 7-day period. Note how rr_{t3} was much lower than the respiration rates in the first and second tanks. The S_S concentration during the same simulation run is depicted in Figure 6.6. Also note how the S_S concentration in the third tank (S_{St3}) ranges between 1 and 2.5 g COD m^{-3}, which is sufficiently low to assume that endogenous respiration is occurring in the third tank. The death-regeneration model (Henze *et al.*, 1987) from Eq.2.1 shows how rr_{t3} directly varies with X_{BH}, and S_S:

$$rr = \left(\frac{1-Y_H}{Y_H}\right)\left(\frac{\mu_{mH} S_S X_{BH}}{K_S + S_S}\right) + \left(\frac{4.57-Y_A}{Y_A}\right)\left(\frac{\mu_{mA} S_{NH} X_{BA}}{K_{NH} + S_{NH}}\right)$$

Eq. 2.1

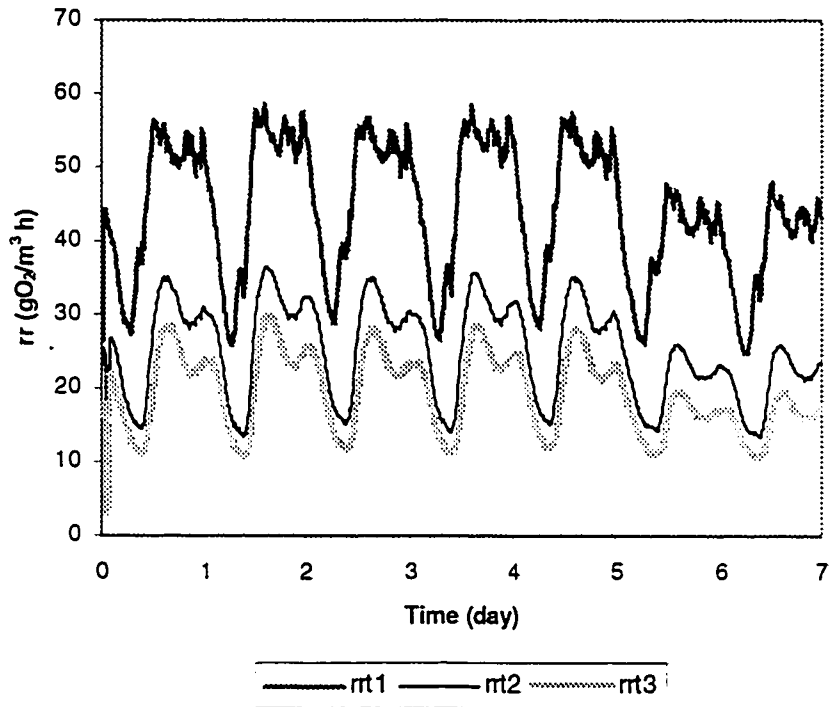

Figure 6.5: Respiration rate in each tank simulated under diurnal influent loading

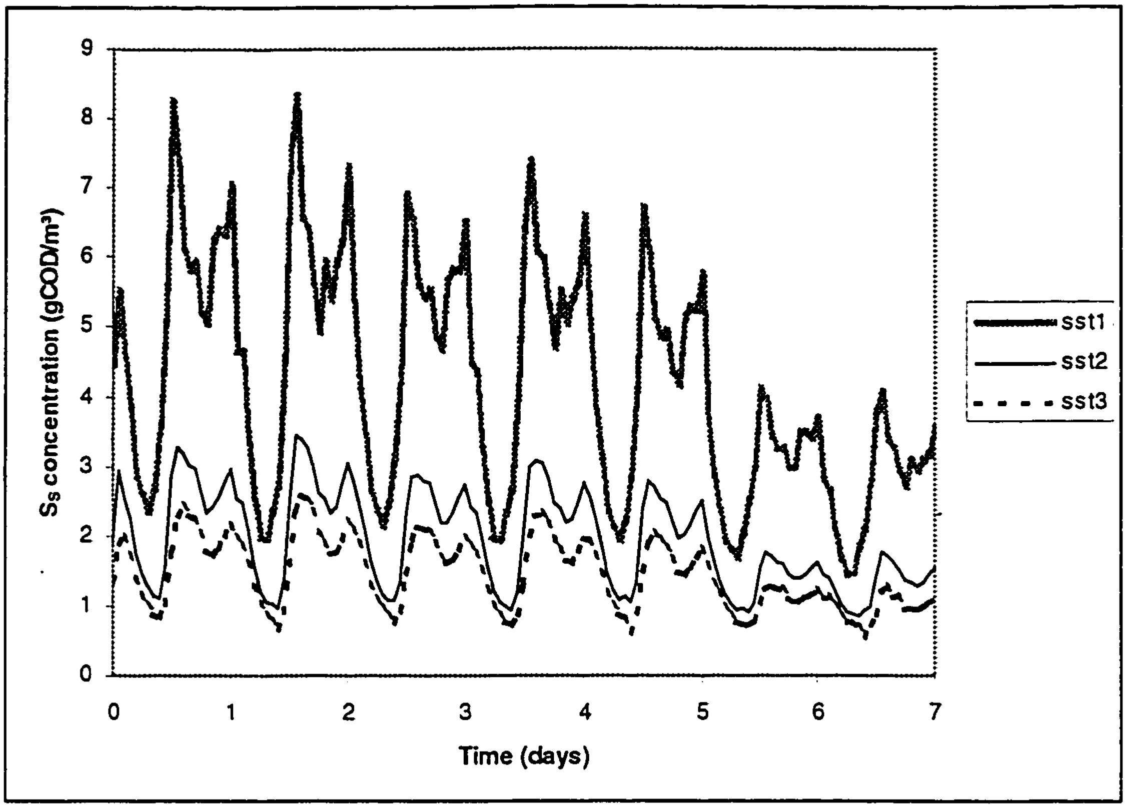

Figure 6.6: S_S concentration in each tank simulated with diurnal influent loading

6.4.3 Implied Control Configuration

Since Q_{waste} depends on the value of rr_{t3}, the control strategy proposed by Stephenson *et al.* (1981) was implemented in a feedback loop.

6.4.4 Control Algorithm

The velocity-form of the digital PI controller (described in Section 5.3.4) was chosen as the appropriate control algorithm for automatic control of rr_{t3}. As discussed earlier, the velocity PI algorithm calculates the change in the controller output at each execution. This means that the controller calculates the amount by which the manipulated variable must be adjusted in order to meet the set point.

Only the proportional and integral modes of the digital PID controller were employed for controlling rr_{t3}. The derivative mode was not used because it amplifies high-frequency variations which can cause excessive variation in the manipulate variable (and this could lead to disturbances in the settler). The macro for the respiration rate control strategy is provided in Appendix B.2.

6.4.5 Design or Tuning of the Respiration Rate Controller

The parameters for the digital PI controller, K_C and T_I, were initially tuned by evaluating the process reaction curve, fitting an approximate first-order-with-dead-time model, and using the Ciancone correlations (Marlin, 1995). The process reaction curve was obtained by first bringing the system to steady-state, then introducing a step change in Q_{waste}, and finally recording the response of rr_{t3} until a new steady-state was reached. For more details on tuning controllers, please refer to Section 5.3.5.

Fine-tuning of K_C and T_I involved measuring the performance of the controller to changes in the set point under constant influent conditions. Values of the control parameters were adjusted until the controller's response became satisfactory, with a small integral squared error (ISE) and short settling time.

After applying the Ciancone tuning correlations and fine-tuning, final values of K_c and T_I for the PI controller were determined to be:

K_c = -22.0

T_I = 0.1 days

A negative value for K_c is reasonable because Q_{waste} is inversely proportional to rr_{t3}. In other words, increases in Q_{waste} cause rr_{t3} to decrease. This is demonstrated in Figure 6.8.

The sampling time for the controller was selected to be every 15 minutes since the influent flow and pollutant concentration were measured every 15 minutes.

6.4.6 Range of Variation for the Wastage Rate

The range of variation chosen for Q_{waste} was selected to be from 0 to 1000 $m^3 d^{-1}$. A limit on Q_{waste} had to be applied to prevent the process from becoming unstable. This was especially important when the plant experienced shock or stress loadings.

6.5 Performance of the Respiration Rate Control Strategy

The dynamic performance of the velocity form of the PI respiration rate controller was examined under various input disturbances. The five different types of evaluations, described Section 5.4, were employed to test the control strategy. This involved examining both open-loop and closed-loop performances. The closed-loop dynamic performance of the controller was examined under three influent conditions: constant influent, diurnal influent, and stress loading conditions. A stability analysis of the control system was also conducted.

6.5.1 Open-Loop Dynamic Behaviour

The dynamic behaviour between Q_{waste} and rr_{t3} provides important information on the performance of the feedback control system. The following procedures were performed to obtain the process reaction curve of rr_{t3} in response to a change in Q_{waste}:

1. Under constant influent conditions, the process was brought to steady state.
2. A step change in Q_{waste} was introduced and the subsequent change in the rr_{t3} was recorded.
3. The process was allowed to reach a new steady state.

The graph in Figure 6.7 shows that once the process was brought to steady state on day 14, Q_{waste} was increased from 500 to 800 m^3 d^{-1}. rr_{t3} reached a new steady state in approximately 4 days.

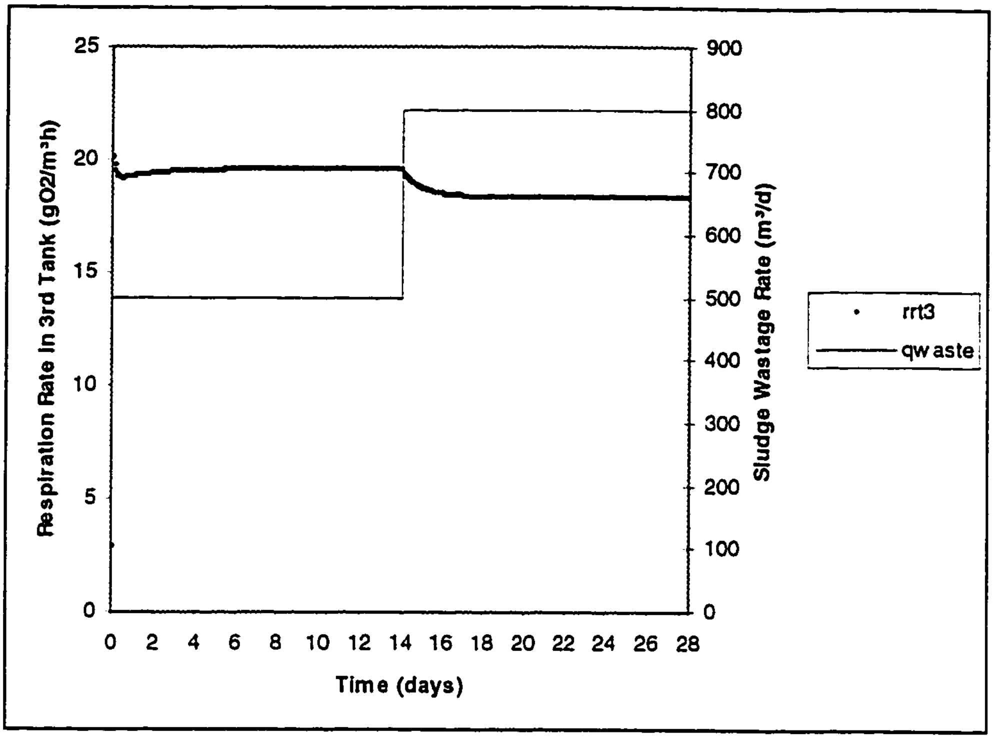

Figure 6.7: Open-loop response of rr_{t3} to a step change in the wastage rate

As shown in Figure 6.7, rr_{t3} decreased when Q_{waste} was increased. The response curve of rr_{t3} is characteristic of first-order-with-dead-time processes. Parameters of a first-order-with-dead-time model include: process or steady-state gain (K_p), time constant (τ), and dead time (θ). K_p is the ratio of the change in respiration rate to the change in the wastage rate. τ characterizes the "speed" of the dynamic response of the controller. θ is the time interval for which no effect is observed in rr_{t3}. Values for these parameters were calculated by employing the process reaction curve, method II (Marlin, 1995). They were found to be as follows:

K_p $= \Delta\, rr / \Delta\, Q_{waste}$

$= -0.234$ g

τ $= 1.465$ days

θ $= 0.153$ days $= 3.67$ hours

The diagram in Figure 6.8 shows that the first-order-plus-dead-time model closely predicts the response of rr_{t3} to changes in Q_{waste}.

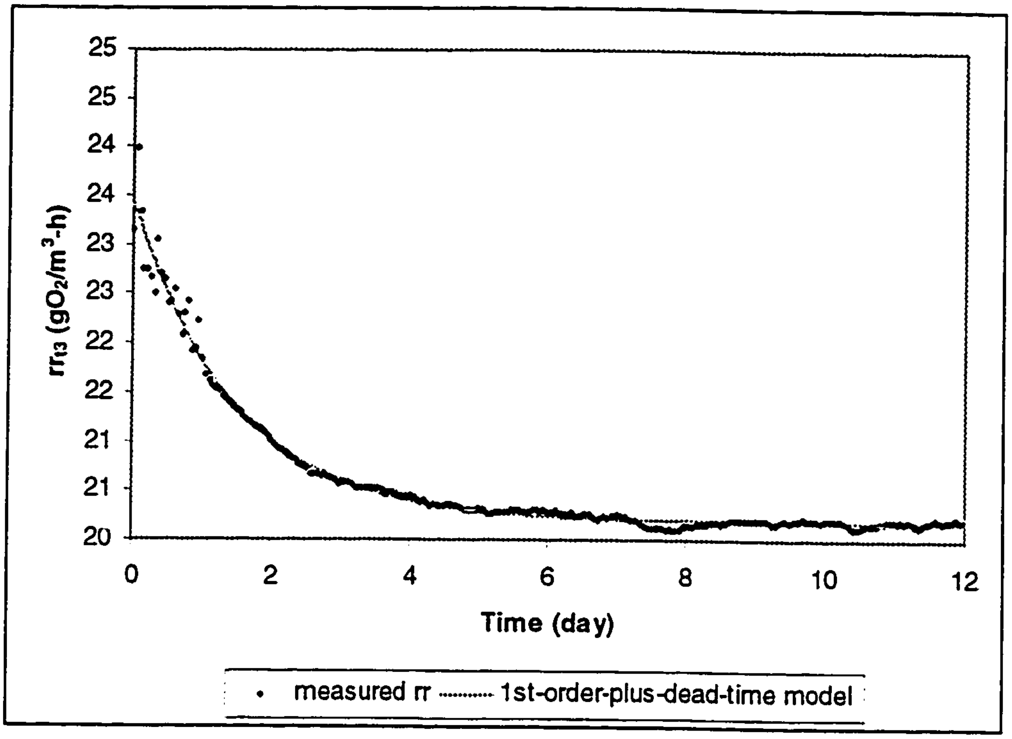

Figure 6.8: Comparison of actual and model-predicted response of rr_{t3} to changes in Q_{waste}

The feedback process speed and fraction dead time may be determined with these parameters:

Feedback process "speed" = $\theta + \tau = 0.153 + 1.465 = 1.618$ days

$$\text{Feedback fraction dead time} = \frac{\theta}{\theta+\tau} = \frac{0.153}{0.153+1.465} = 0.0946$$

The feedback process "speed" indicates that it took rr_{t3} approximately 1.6 days to respond to an increase of 500 to 800 m³ d^{-1} in Q_{waste}. The feedback fraction dead time reveals that about 9 per cent of the total response time is dead time. The feedback process speed shows that the response of rr_{t3} is quite slow to changes in Q_{waste}. Since the rr controller must respond to the diurnal fluctuations in the influent, which occurs at a frequency of 1 cycle/day (as depicted in Figure 5.4), a feedback response time of 1.6 days is too long. Furthermore, the small value of K_p indicates that the magnitude of the response of rr_{t3} is small compared to the large change introduced in Q_{waste}. The response of rr_{t3} is slow and relatively weak because the first two activated sludge tanks dampen the effects of the sludge wasting. These results indicate that the dynamics between rr_{t3} and Q_{waste} are quite sluggish. Slow dynamics between controlled and manipulated variables affect the dynamic performance of the controller, particularly when disturbances have high-frequency variations.

The response of the heterotrophic biomass concentration, X_{BH}, in the third aeration tank to a step change in Q_{waste} was examined and is illustrated in Figure 6.9. The response curve of the biomass shows that the relationship between Q_{waste} and the biomass also follows first-order dynamics. This demonstrates that rr_{t3} is an indicator of X_{BH}.

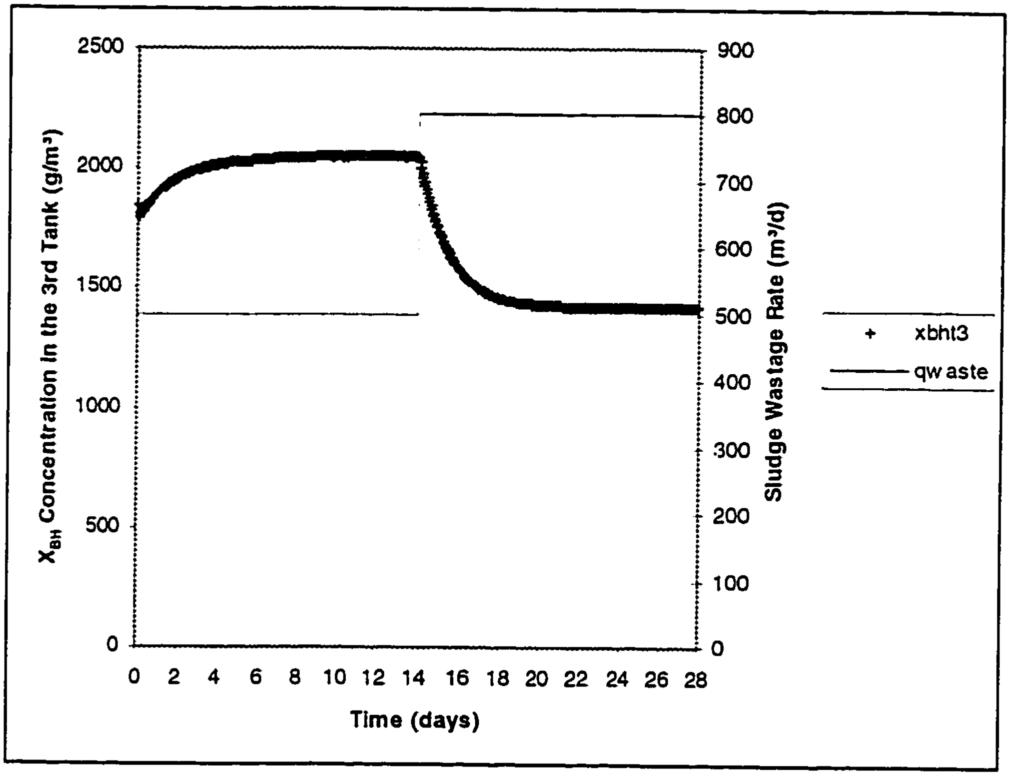

Figure 6.9: Response of heterotrophic biomass in tank 3 to a step increase in Q_{waste}

6.5.2 Stability Analysis

In this study, the Nyquist stability criterion was employed for assessing the stability of the digital PI rr_{t3} controller. The Nyquist plot for the respiration rate controller is shown in Figure 6.10. The solid line covers the frequency range $0 \leq \omega < +\infty$, and the dashed part covers the frequencies from $-\infty$ to 0. The dashed segment of the Nyquist plot is the mirror image of the solid-line segment with respect to the real axis. Please refer to Section 5.4.2 for details on frequency-response analysis.

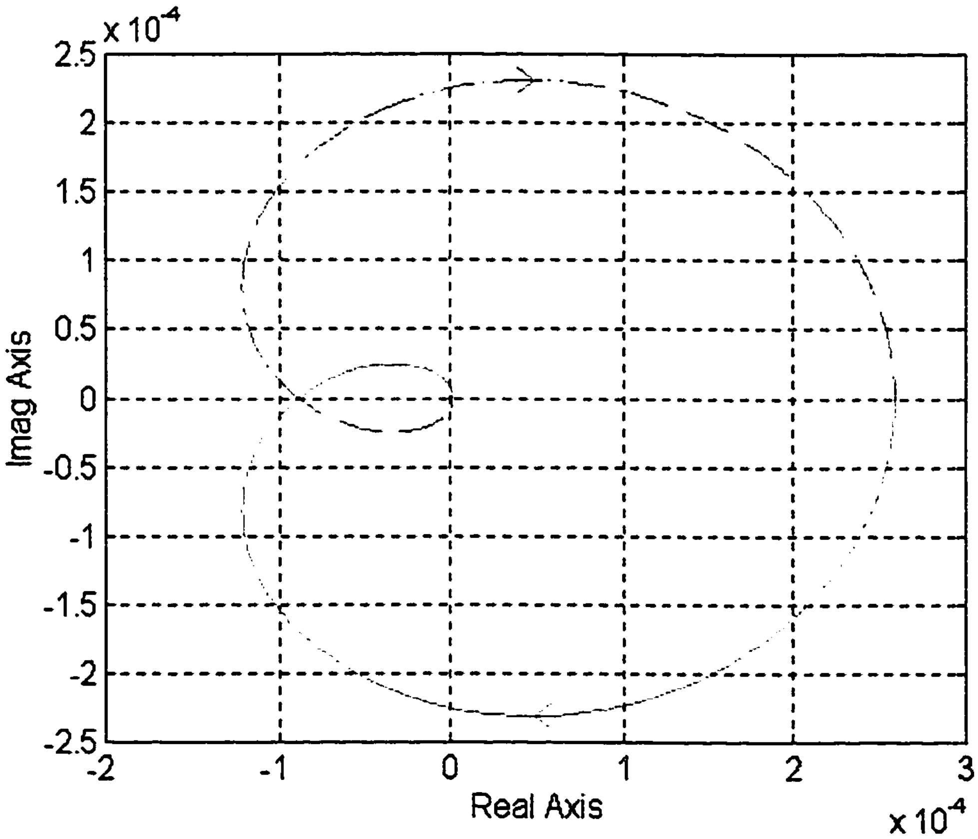

Figure 6.10: Nyquist plot of respiration rate control system

The plot in Figure 6.10 shows that the point (-1,0) is not encircled. Thus according to the Nyquist stability criterion, the closed-loop response of the rr controller to a range of input frequencies is stable. This means that the PI control algorithm and the tuning constants (K_c = -22.0, T_I = 0.1 days) selected for the rr control strategy proposed by Stephenson *et al.* (1981) give stable performance over a range of operating conditions. This implies that the response of the rr controller to fluctuations in rr_{t3} will not introduce large oscillations in the system.

6.5.3 Control Performance Under Set Point Changes

The dynamic response of the rr_{t3} controller to step changes in the set point was examined. The controller's ability to meet set point changes under constant influent conditions is depicted in Figure 6.11. After running the simulations until steady state was reached, the rr controller was turned on automatic and the set point was fixed at 22 gO_2 $m^{-3}\cdot h^{-1}$ on day 14. The set point was then changed to 23 gO_2 $m^{-3}\cdot h^{-1}$ on day 60, and subsequently to 19 gO_2 $m^{-3}\cdot h^{-1}$ on day 100.

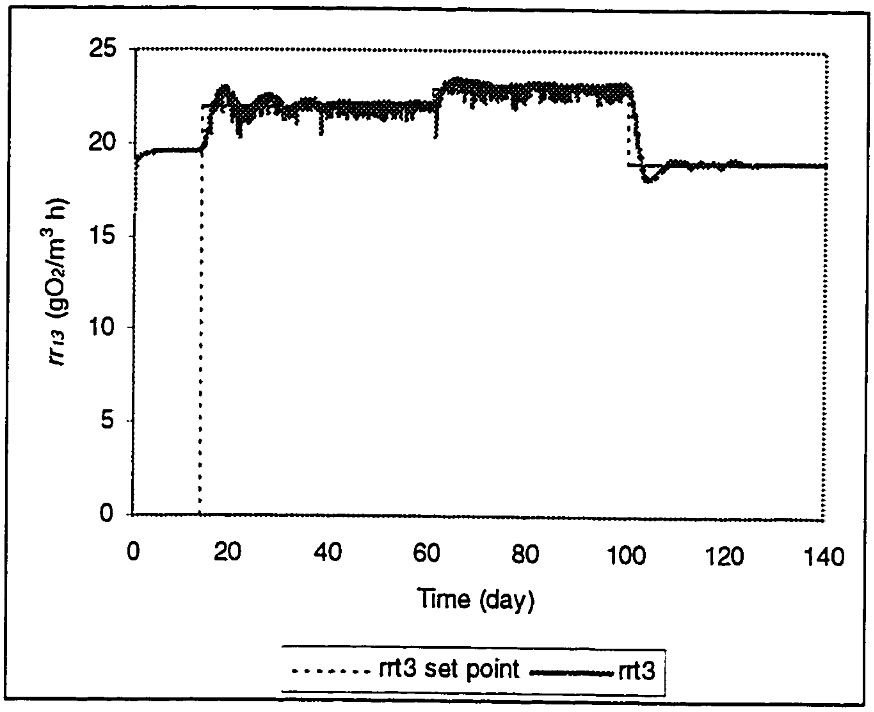

Figure 6.11: Closed-loop response of the rr controller to step changes in the set point

The control performance for the set point changes is summarised in Table 6.1.

Table 6.1: Performance of rr Controller to Step Changes in the Set Point

Time Interval (days)	rr_{t3} Set Point ($gO_2\ m^{-3}\cdot h^{-1}$)	Average rr_{t3} ($gO_2\ m^{-3}\cdot h^{-1}$)	Standard Deviation from Average rr_{t3}	Standard Deviation from Set Point	Settling Time of rr_{t3} (days)
0 to 14	No control	19.465	0.277	-	-
14 to 60	22.0	21.956	0.663	0.477	34
60 to 100	23.0	23.008	0.308	1.054	23
100 to 140	19.0	19.130	0.765	2.972	23

Average values of rr_{t3} shown in Table 6.1 demonstrate that the controller was able to meet each set point with negligible offset. This is confirmed by the low values obtained for the standard deviations from each set point. As depicted in Figure 6.11, the controller's response to the first set point change was more oscillatory and took longer to stabilise. The reason for this was that the jump from the initial or uncontrolled value of 19.5 $gO_2\ m^{-3}\cdot h^{-1}$ to the set point of 22.0 $gO_2\ m^{-3}\cdot h^{-1}$ was greater than any subsequent set point changes. The set point change from 23 to 19 $gO_2\ m^{-3}\cdot h^{-1}$ shows that the controller is able to meet the set point when it is decreased.

The controller performed poorly in terms of the settling time, which is the amount of time the controlled variable takes to meet the new set point value. It took the controller at least 23 days to stabilise after a change in the set point was introduced. As previously noted, the settling times are slow because it a takes a long time for the effects of the sludge wastage from the settler to reach the third tank.

The response of Q_{waste} to each set point change is depicted in Figure 6.12. Each time the set point was changed, there was a large, high-frequency variation in the Q_{waste}. As rr_{t3} settled towards the set point, fluctuations in Q_{waste} decreased accordingly.

The oscillatory response of the controller, shown by both the fluctuations in rr_{t3} and Q_{waste} (Figure 6.12), indicates that the controller tuning might be too aggressive. This is usually caused by the controller gain, K_c, being too large or the integral time, T_I, being too short, or a combination of both. The high-frequency variation in Q_{waste} indicates that the aggressive response was probably due to both the controller gain and the integral time. Values for these control parameters were fine-tuned when the plant was operating under diurnal influent conditions. As a result the controller's response to step changes in the set point was aggressive.

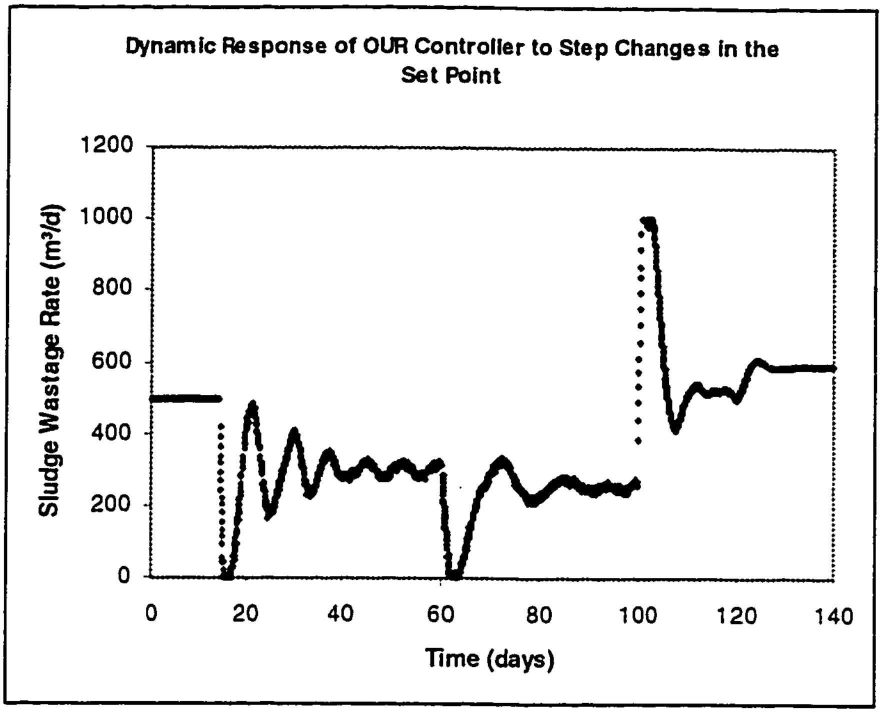

Figure 6.12: Close-loop response of the rr controller under constant influent shown by adjustments in the wastage rate

The effect of the oscillations in Q_{waste} on the effluent quality is shown in Figure 6.13. The simulations show that there was very little variation in the effluent readily biodegradable substrate concentration (S_{seff}) and effluent slowly biodegradable substrate concentration (X_{seff}). However when the set point was changed from 22 to 23 g O_2 m^{-3}·h^{-1} on day 60, the particulate inert organic concentration in the effluent (X_{ieff}) increased with the decrease in Q_{waste}.

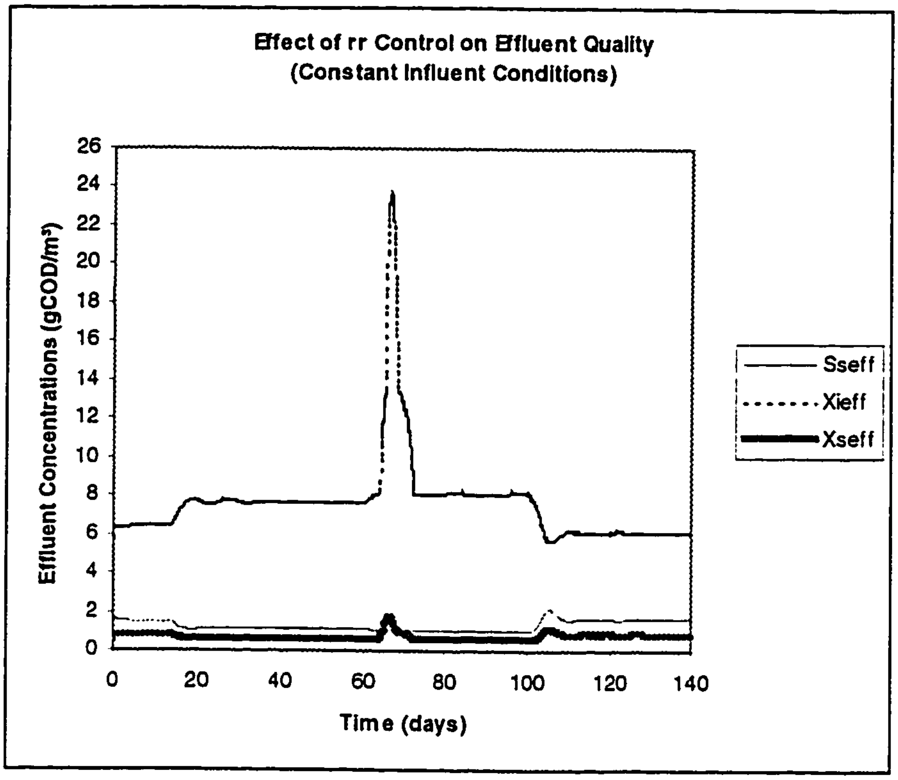

Figure 6.13: Effect of set point changes on the effluent concentration under constant influent condit ions

6.5.4 Control Performance Under Diurnal Influent Conditions

The dynamic performance of the controller was also examined under diurnal influent loading conditions. The ability of the controller to maintain rr_{t3} at set points of 18 and 22 $gO_2\ m^{-3}{\cdot}h^{-1}$ is shown in Figure 6.14. As depicted, rr_{t3} follows the fluctuations of the influent flow and oscillates around the set point. The controlled rr_{t3} will likely never decrease and settle towards the set point because the rate of change of the influent wastewater is much too fast for the controller to respond adequately. Evidence of this was shown by the slow dynamics between rr_{t3} and Q_{waste} from the open-loop analysis discussed in Section 6.5.1. The sluggish performance of the controller in meeting set point changes, discussed in Section 6.5.3 also demonstrates how the controller will not meet the set point during diurnal influent conditions.

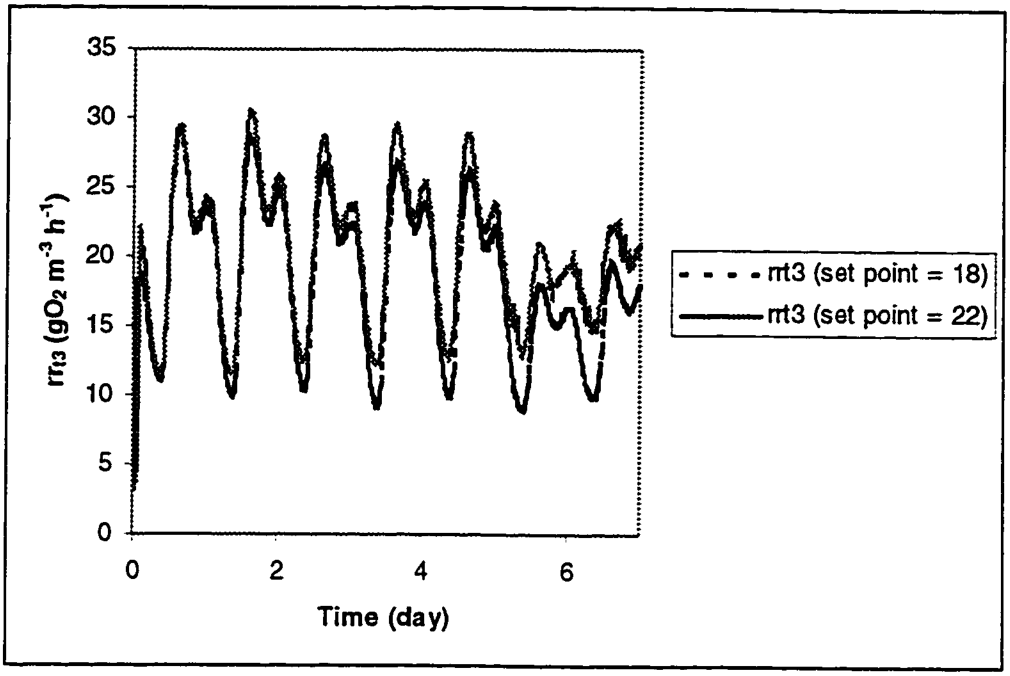

Figure 6.14: Performance of the rr controller in maintaining the set point under diurnal influent conditions

Statistics on the performance of the controller in regulating the different rr_{t3} set points under diurnal influent conditions are presented in Table 6.2.

Table 6.2: Statistics on the performance of the PI controller under diurnal influent conditions

rr_{t3} Set Point (mg O_2 g^{-1}MLSS·h^{-1})	Average rr_{t3} (mg O_2 g^{-1}MLSS·h^{-1})	Standard Deviation from the Average rr_{t3}	Standard Deviation from the Set Point	Standard Deviation of Q_{waste}
No control	19.4	5.4	-	constant flow
18.0	18.5	5.4	5.5	349
22.0	20.5	5.0	5.2	232

As shown in Table 6.2, the controller was able to meet the set point of 18 g O_2 m^{-3}·h^{-1} on average. However when the set point was changed to 22 gO_2 m^{-3}·h^{-1}, the controller was unable to bring rr_{t3} past a value of 20.5 gO_2 m^{-3}·h^{-1}. A set point of 18 gO_2 m^{-3}·h^{-1} was attainable because this value is close to the average value of rr_{t3} measured during uncontrolled operations. Furthermore, similar values obtained for the standard deviations of the average rr_{t3} during uncontrolled and controlled simulations show that the controller is unable to attenuate the effects of high-frequency influent variations on rr_{t3}.

The effect of different rr_{t3} set points on the concentration of biodegradable substrate in the effluent (Ss_{eff} and Xs_{eff}) is illustrated in Figures 6.15 and 6.16. It is shown in these figures that the concentrations of both Ss_{eff} and Xs_{eff} were lowest when rr_{t3} was controlled to a set point of 22 $gO_2\ m^{-3}{\cdot}h^{-1}$. However, Ss_{eff} and Xs_{eff} were higher when rr_{t3} was controlled when a set point of 18 $gO_2\ m^{-3}{\cdot}h^{-1}$ was used. The significance of these observations is that the substrate concentrations in the effluent can be reduced if the rr_{t3} set point is greater than the average value $\overline{rr}_{t3}$ of measured during uncontrolled operations. The reason is that with a higher set point, the controller is able maintain a higher concentration of active biomass by decreasing the sludge wastage rate. Therefore, the higher concentration of biomass means that more substrate will be decomposed.

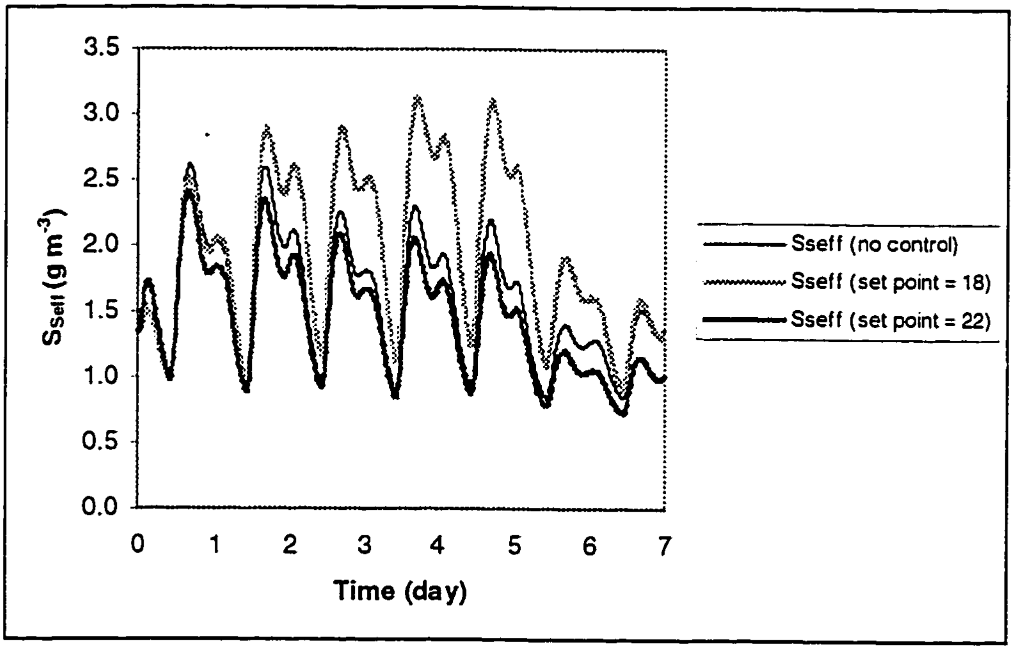

Figure 6.15: Effect of control on the concentration of readily biodegradable substrate in the effluent

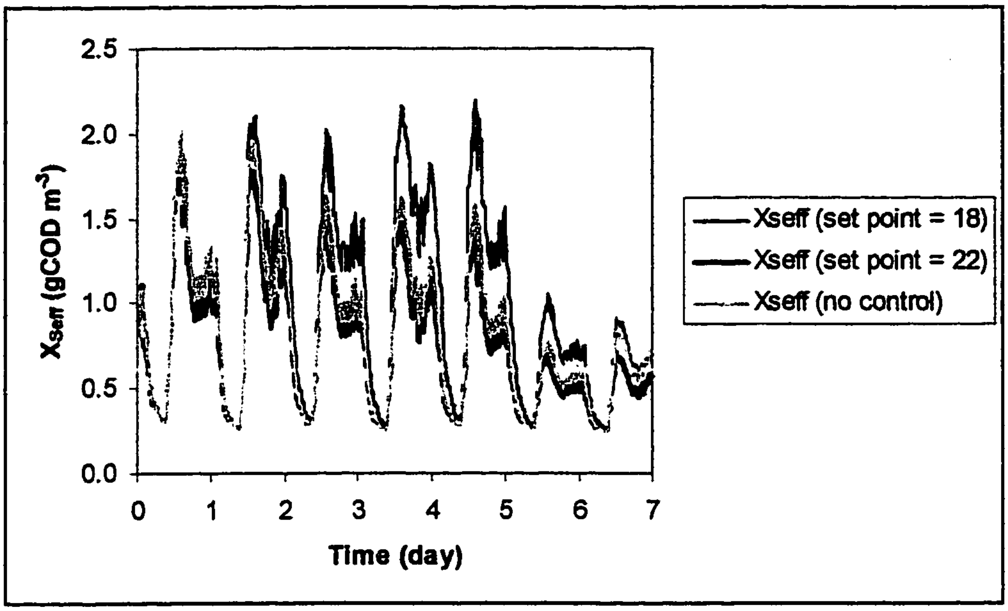

Figure 6.16: Effect of rr control on the concentration of slowly biodegradable substrate in the effluent

With the high rr_{t3} set point of 22 gO_2 $m^{-3}\cdot h^{-1}$, it was also observed that the COD of the effluent suspended solids ($XCOD_{eff}$) was greater than when a set point of 18 g O_2 $m^{-3}\cdot h^{-1}$ was used. In other words $XCOD_{eff}$ can be reduced from uncontrolled operations if a set point of 18 g O_2 $m^{-3}\cdot h^{-1}$ is used. The $XCOD_{eff}$ over a 7-day period for controlled and uncontrolled operations are shown in Figure 6.17. As depicted, $XCOD_{eff}$ is highest when the respiration rate is controlled to 22 g O_2 $m^{-3}\cdot h^{-1}$, whereas it is lowest when rr_{t3} is controlled to 18 g O_2 $m^{-3}\cdot h^{-1}$. The reason that $XCOD_{eff}$ is lower when a set point of 18 g O_2 $m^{-3}\cdot h^{-1}$ is used is that the controller must increase Q_{waste} in order to bring rr_{t3} to its set point. The increased sludge wastage rates cause $XCOD_{eff}$ to be reduced.

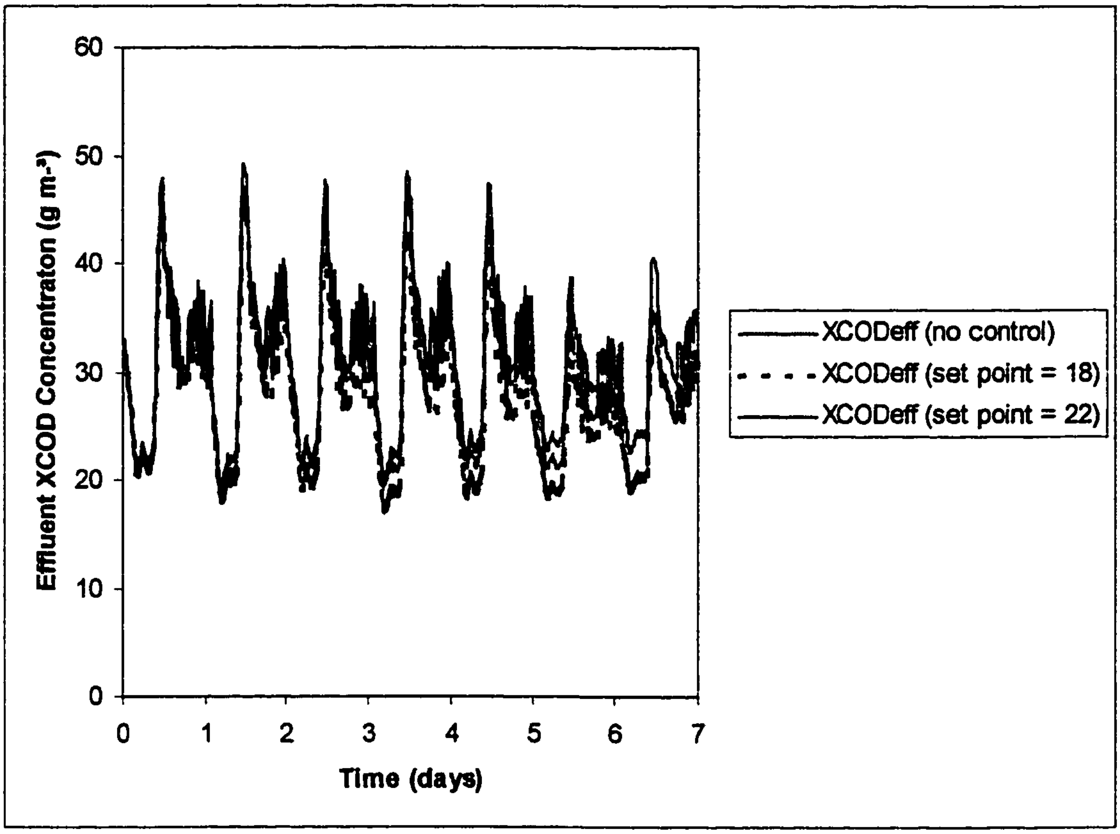

Figure 6.17: Effect of rr control on the COD of the effluent suspended solids

As demonstrated in Figure 6.18, Q_{waste} is higher throughout the 7-day period when the set point was at 18 g O_2 $m^{-3}{\cdot}h^{-1}$. The standard deviation of the average Q_{waste} at a set point of 18 g O_2 $m^{-3}{\cdot}h^{-1}$ was 349 m^3 d^{-1}, whereas the standard deviation at a set point of 22 g O_2 $m^{-3}{\cdot}h^{-1}$ was 232 m^3 d^{-1}. The variation of Q_{waste} in both cases is reasonable since it follows the diurnal variations in the influent flow rate.

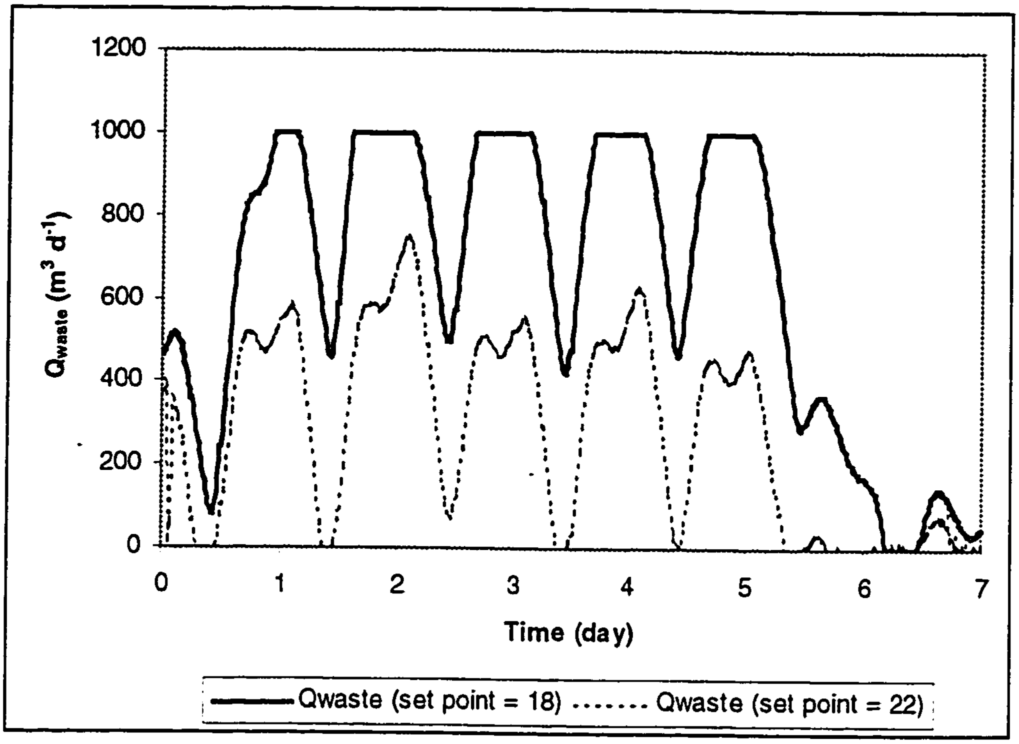

Figure 6.18: Dynamic response of the rr controller with different set points under diurnal influent loading

6.5.5 Effect of Control on Plant Performance Under Stress Loading Conditions

The benefits of the respiration rate controller were not fully apparent in the previous analyses because the ASP was already providing adequate treatment without control. As a result. simulations were conducted to test the performance of the controller under the five different loading conditions over a 35-day period. The loading scenarios were described in Section 5.4.5 and are presented again in Table 6.3.

Table 6.3: Influent Loading Scenarios

Week	Influent Loading Period	Influent Loading Condition
1	day 0 to day 7	Normal diurnal influent loading
2	day 7 to day 14	50 per cent increase in the hydraulic and pollutant loading
3	day 14 to day 21	Normal diurnal influent loading
4	day 21 to day 28	Two storm events
5	day 28 to day 35	Normal diurnal influent loading

Overall, the simulations with the 35-day influent loading showed that respiration rate control improved effluent quality and reduced energy costs over uncontrolled operations. When the respiration rate was controlled to 18 gO_2 $m^{-3} \cdot h^{-1}$, reductions in both the effluent COD and energy costs were observed. The benefit of control in terms of effluent quality is demonstrated in Figure 6.19 when the plant experienced a 50 percent increase in both hydraulic and pollutant loading during week 2. Lower effluent COD concentrations were maintained throughout this week when rr_{t3} was controlled at a set point of 18 gO_2 $m^{-3} \cdot h^{-1}$. Also notice that when the influent loading returned to normal conditions in week 3, the controller brought the effluent quality back to normal levels. However the effluent COD was slightly higher than normal during this week when no control was used. The controller was also able to lower the effluent COD concentrations during the two storm events in week 4 over uncontrolled operations.

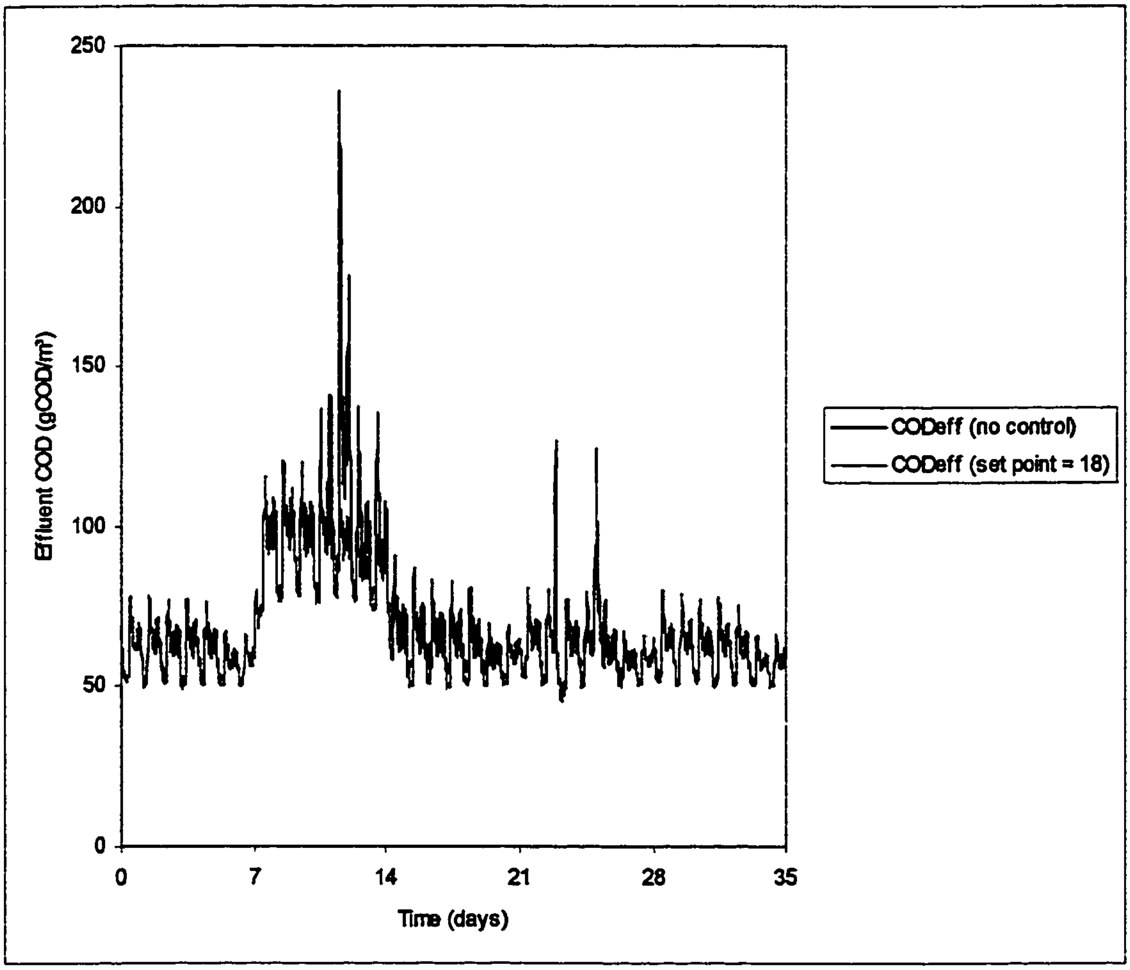

Figure 6.19: Effect of rr control on the effluent COD

$XCOD_{eff}$ was also substantially reduced when rr_{t3} was controlled during week 2 in which the influent loading increased by 50 percent. This can be seen in Figure 6.20 during days 7 to 14. The controller managed to maintain lower effluent COD concentrations during this period because it compensated for the increased loading by wasting at higher rates to bring rr_{t3} to its set point.

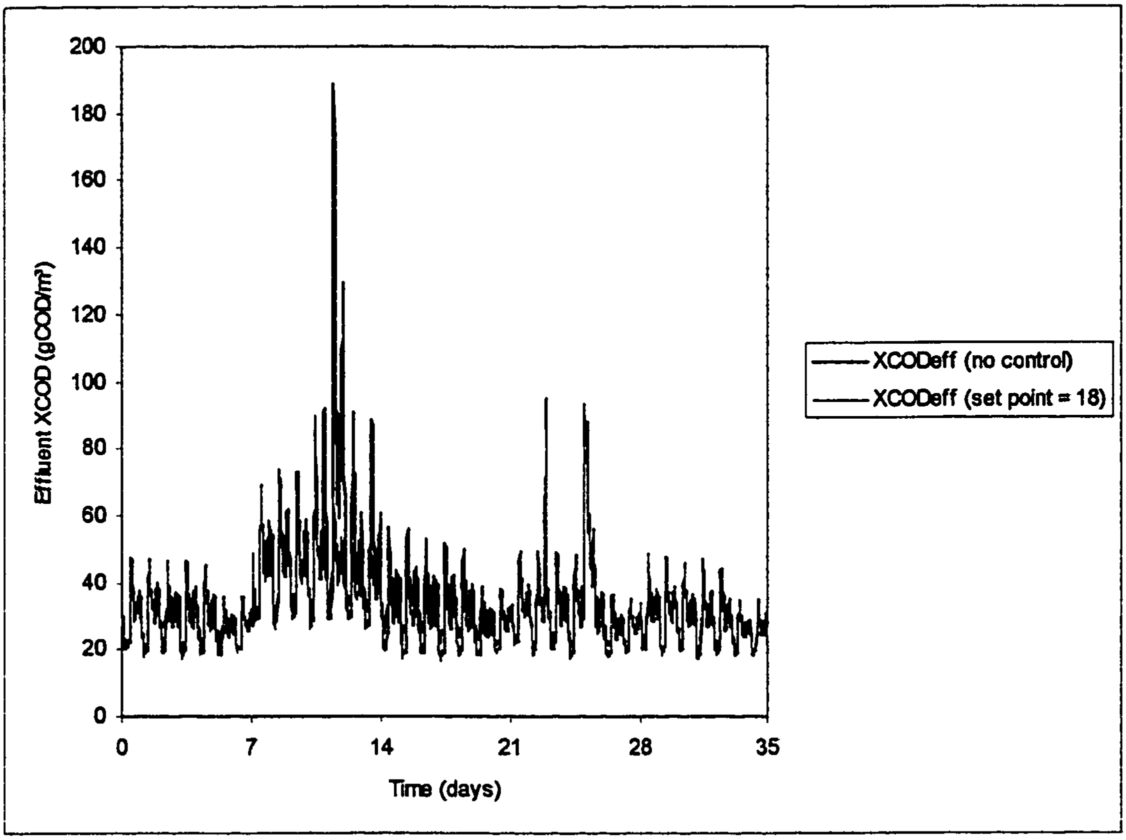

Figure 6.20: Effect of rr control to set point of 18 gO_2/m^3-h on the COD of the effluent suspended solids

The effect of control on energy costs is depicted in Figure 6.21. The energy costs are based on the power expended to aerate the three tanks to a dissolved oxygen concentration of 2 g m^{-3}. The energy costs were calculated as follows:

$$\text{Daily energy cost (\$ / day)} = Power \cdot \frac{cost}{kWh} \cdot 24$$

Eq. 6.1

$$\text{Power (kW)} = \frac{K_L a \cdot V \cdot S_{O,ST}}{\alpha \cdot \eta \cdot 24000.0}$$

Eq. 6.2

where	cost / kWh	= \$0.08 / kWh
	V	= aeration volume of the three tanks (m^3)
	$S_{O,ST}$	= saturated oxygen concentration (mg L^{-1})
	α	= wastewater / clean water coefficient
	η	= specific oxygen capacity (kg O_2 / kW h)
	24000.0	= conversion from kg to g and hours to days

As shown in Figure 6.21. lower energy costs were achieved under controlled operations because lower biomass concentrations (which was X_{BH} in this case) were maintained in the third tank by the controller. A reduced biomass concentration potentially results in a lower oxygen requirement. The reduction in the biomass concentration is illustrated in Figure 6.22.

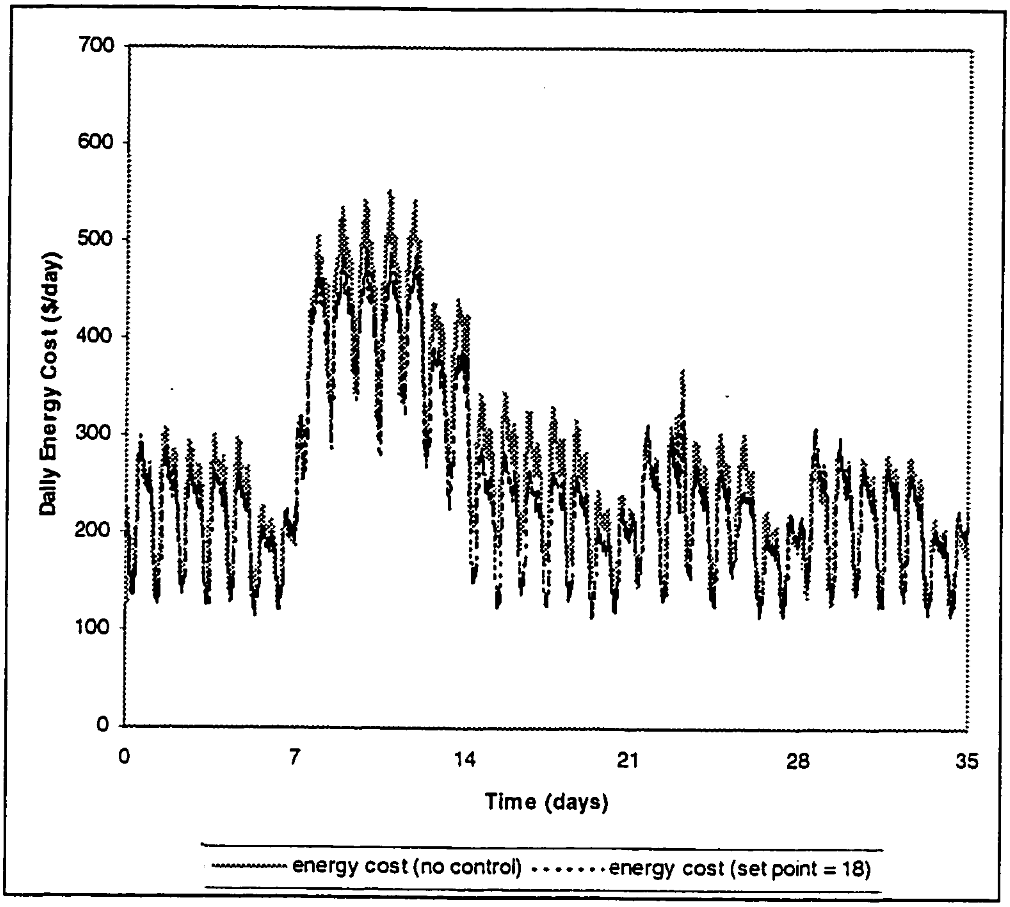

Figure 6.21: Effect of rr control on energy costs

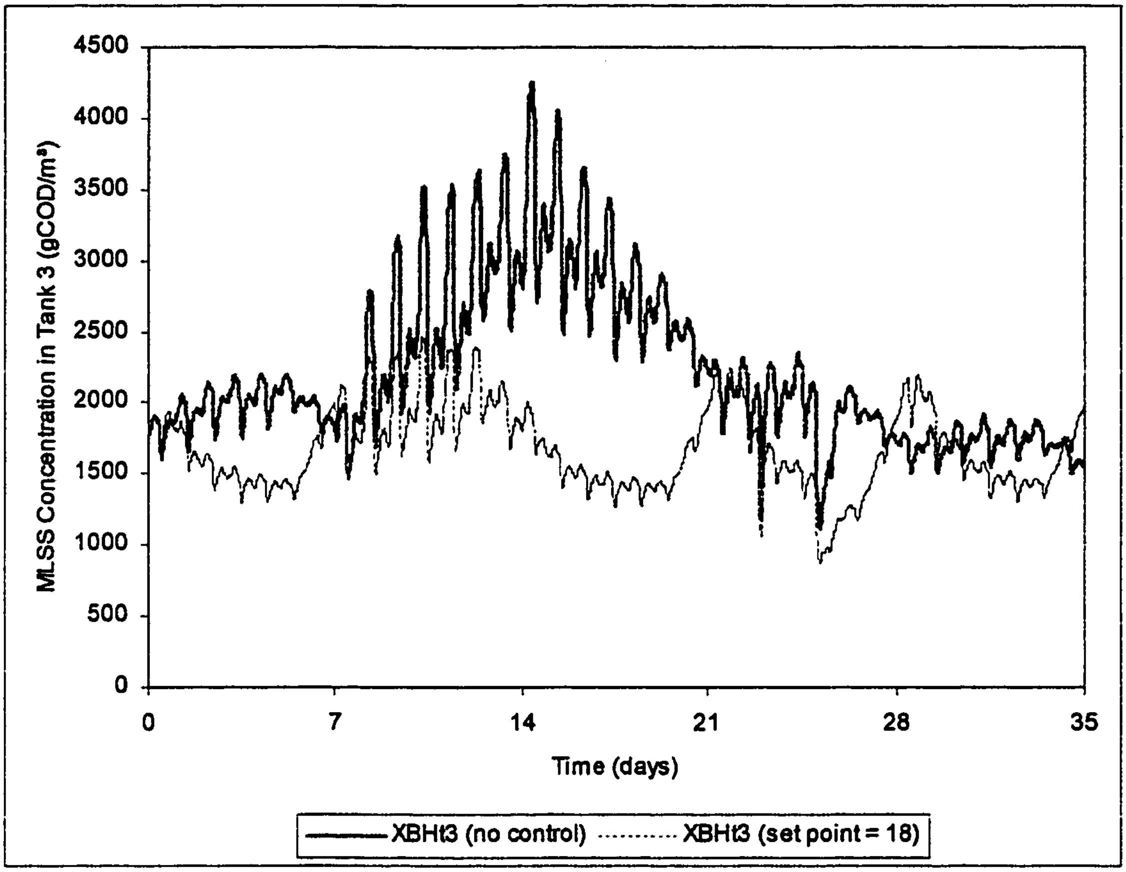

Figure 6.22: Effect of rr control on the X_{BH} concentration in the 3rd tank

When a set point of 22 $gO_2\ m^{-3} \cdot h^{-1}$ was used, the controller was able to reduce the biodegradable substrate concentrations (i.e. S_S and X_S) in the effluent during the weeks with normal diurnal influent loading and during week 3 with the two rain events. However when the plant experienced a 50 per cent loading increase in week 2, the controller was unable reduce effluent substrate concentrations over uncontrolled operations. These observations are shown in Figure 6.23. In fact, substrate concentrations in the effluent were lowest when there was no control. Higher effluent substrate concentrations were observed during controlled operations because the biomass concentration was lower than what was observed during uncontrolled operations. The biomass concentration was lower when the plant was controlled because the controller tried to meet the set point by wasting sludge at higher rates (which ranged from 800 to 1000 $m^3\ d^{-1}$) than uncontrolled operations (which had a constant wastage rate of 500 $m^3\ d^{-1}$).

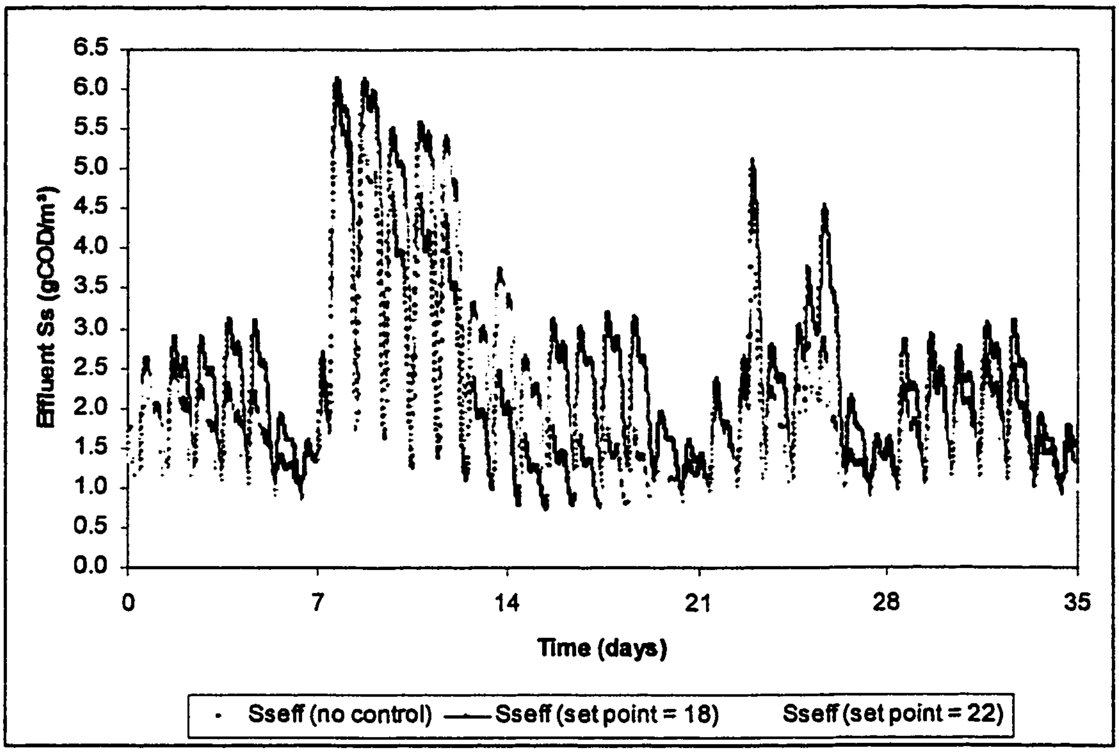

Figure 6.23: Effect of rr control on the S_S concentration in the effluent

6.6 Summary on the Evaluation of the Respiration Rate Control Strategy

The objective of the control strategy proposed by Stephenson *et al.* (1981) was to maintain the endogenous respiration rate of the sludge in the aeration tank at a set point value by manipulating the wastage flow. The strategy is based on the concept that endogenous respiration is representative of the active biomass concentration in the aeration tank. Therefore, by controlling the endogenous respiration rate, the degree of treatment may be controlled. The control algorithm used to implement the strategy was the velocity form of the digital PI controller.

The methodology used for evaluating the performance and benefits of the control strategy proposed by Stephenson *et al.* (1981) was described in Section 5.4. The results are summarized as follows:

1. By examining the open-loop response of rr_{t3} to a step change in Q_{waste}, the following observations were made:
   - The response of rr_{t3} to changes in Q_{waste} was slow because the first two aeration tanks dampened the effects of changes in Q_{waste}.
   - The relationship between rr_{t3} and Q_{waste} follow first-order-plus-dead-time dynamics.
   - The dynamics between rr_{t3} and Q_{waste} are slow compared with the frequency of the influent loading.
   - The sluggish response indicates that the controller will likely perform poorly under the high-frequency variation of the influent loading.

2. According to the Nyquist stability criterion, the PI control algorithm and the tuning constants (K_c = -22.0, T_I = 0.1 days) implemented for the rr control strategy provide stable performance over a range of operating conditions

3. Under constant influent loading, the performance of the rr controller to step changes in the set point was as follows:
   - The controller was able to meet various set points with negligible offset.
   - The response of the controller to changes in the set point was slow because the first two aeration tanks dampened the effects of changes in Q_{waste}.

4. The following observations were made with performance of the rr controller under diurnal influent loading:
   - The controller was not able to meet the set point under diurnal influent conditions because the controller was much too slow for the high-frequency fluctuations of the influent loading. Furthermore, oscillations in the respiration rate followed variations in the influent. These two facts lead to the conclusion that the high-frequency variation of the influent is the major disturbance on a control system in the activated sludge process.
   - The controller was able to reduce S_S and X_S concentrations in the effluent under normal diurnal influent loading if the set point is higher (22 $gO_2\ m^{-3}{\cdot}h^{-1}$ was used in this case) than the average rr_{t3} measured during uncontrolled operations. Biodegradable substrate concentrations in the effluent were reduced because a higher set point resulted in the controller maintaining a higher biomass concentration by wasting sludge at lower rates.
   - Conversely, rr control decreased the effluent suspended solids when the set point is lower (18 $gO_2\ m^{-3}{\cdot}h^{-1}$ in this case) than the average rr_{t3} obtained during uncontrolled operations. This occurred because a lower rr set point caused the controller to maintain a lower degree of biomass activity by wasting at higher rates.

5. The rr controller showed the greatest benefit during stress loading conditions. The simulations revealed the following results:
   - The effluent COD and suspended solids concentrations were substantially reduced when rr_{t3} was controlled at set points lower than the average rr_{t3} measured during uncontrolled conditions. The solids concentration was lower during both elevated loading and storm events for controlled operations because the rise in rr_{t3}, due to the increase in substrate, caused the controller to increase the wastage rate, thereby preventing washout of the solids in the effluent.
   - rr control resulted in reduced energy costs incurred from aeration. Under controlled operations, the oxygen requirement was less because the controller maintained lower and more constant MLSS concentrations.
   - rr control increased the S_s concentration in the effluent when the plant experienced a 50 per cent increase in both flow and pollutant concentration. This occurred because the controller increased the wastage rate to maintain the set point. The result was that more biomass left the system and less S_s was consumed.

7 Evaluation of a Specific Respiration Rate Control Strategy that Uses a Step Feed System

7.1 Introduction

This section will discuss a dynamic step feed control system for the activated sludge process proposed by Stephenson *et al.* (1983). Several respirometry-based control strategies have proposed the use of the feed distribution as a manipulated variable; they include Stenstrom (1979), Sørenson (1990), and Vitasovic (1986). The strategy proposed by Stephenson *et al.* (1983) was selected for evaluation for several reasons: 1) experimental data were reported from pilot plant studies; 2) plant operating conditions were reported; and 3) details on the implementation of the control strategy were provided.

The control strategy proposed by Stephenson *et al.* (1983) involves controlling the specific respiration rate (rr_{sp}) in the last compartment at a set point by manipulating the influent feed distribution in a multi-staged step feed system. The objectives of this control scheme are to regulate the active biomass concentration as well as to control the diurnal and stress loadings on a plant. It has been well documented (Andrews. 1977) that rr_{sp} is a dynamic indicator of sludge activity, the nature of the pollutants, and the MLSS concentration. Therefore by maintaining rr_{sp}, the MLSS concentration and sludge activity can be regulated. Furthermore, since the sludge activity is controlled, the effluent substrate concentration may be controlled. A constant low value of rr_{sp} in the last compartment indicates that the substrate concentration is low in the effluent.

The pilot plant study conducted by Stephenson *et al.* (1983) will first be summarized to provide some background information. This will be followed with a summary of results obtained from simulations of the step feed control algorithm implemented in the pilot plant study.

The dynamic step feed control strategy proposed by Stephenson *et al.* (1983) was implemented through two types of controllers. The first controller used a PI algorithm. This controller distributed influent between the first and last compartments to maintain rr_{sp} in the last tank at the set point. The fraction of influent distributed between the two tanks was automatically adjusted to minimize the difference between rr_{sp} set point and the actual rr_{sp} in the last tank.

The second controller used a split-range algorithm. This controller decides how much influent is to be distributed amongst the three tanks in order to bring the rr_{sp} in the third tank to its set point.

Implementation of the two controllers in the standard C-removal activated sludge plant will be discussed. As well, the performance of each controller in will be evaluated. The methodology for conducting simulations of respirometry-based control strategies, previously described in section 5, was employed to implement and evaluate the step feed control strategy proposed by Stephenson *et al.* (1983).

7.2 Review of the Pilot Plant Study Conducted by Stephenson *et al.* (1983) on Dynamic Step Feed Control

7.2.1 Summary of Pilot Plant Study

In the study conducted by Stephenson *et al.* (1983), the pilot plant consisted of a three-compartment step feed process with recycle to the first compartment. The plant was a carbon removal system. Wastewater flow into the plant was controlled to an approximate 24-hour sinusoidal curve with peak flow coinciding with the period of maximum influent organic. The SRT was automatically controlled at three days. The recycle ratio was maintained at 0.5. The DO was controlled in all three compartments with digital PI controllers. In the first two compartments, the DO was maintained at 2 g/m^3, while the DO in the last compartment was maintained at 3 g/m^3.

The pilot plant study demonstrated that the specific respiration rate in the third tank ($rr_{sp,3}$) can be controlled to a set point of 15 mg O_2/g MLSS·h by manipulating the influent feed distribution. $rr_{sp,3}$ was controlled by continuously calculating the optimal feed distribution to the first and third compartments of the step feed system. The optimal contacting pattern was determined by minimizing the difference between the desired MLSS concentration and the actual concentration in the third compartment. The desired MLSS concentration was based on the measured rr in the aeration tank and the rr_{sp} set point, and is calculated as follows:

$$X_{des} = \frac{rr_N}{rr_{sp(setp)}}$$

Eq. 7.1

where X_{des} = the desired MLSS concentration in the last compartment (g/m^3)

rr_N = the volumetric respiration rate in the last compartment (gO_2/m^3-h)

$rr_{sp(setp)}$ = the specific respiration rate set point in the last compartment (gO_2/gMLSS-h)

$$rr_{sp} = \frac{rr}{X}$$

Stephenson *et al.* (1983) found that the variability in $rr_{sp,3}$ was minimized when more influent flow was distributed to the first compartment during high loading periods. Conversely, when the loading was low all the influent was directed to the last compartment. The results for the step feed control of $rr_{sp,3}$ obtained by Stephenson *et al.* (1983) are summarized in Table 7.1.

Table 7.1: Dynamic Step Feed Control Results (rr_{sp} set point = 15.0 mg O_2/g MLSS-h)

Influent Loading (g BOD_5/g MLSS·d)	rr_{sp} in tank 3 (g O_2/g MLSS·h)	EFOC (mg L^{-1})	ESS (mg L^{-1})
0.6	15.0 ± 1.8	21 ± 4	30 ± 7
0.2	14.1 ± 2.1	18 ± 3	33 ± 13

EFOC = Effluent Filterable Organic Carbon

ESS = Effluent Suspended Solids

Stephenson *et al.* (1983) reported that control of $rr_{sp,3}$ minimized variations in the filterable organic concentrations in the effluent during high organic loading periods. However, no improvement in either EFOC or ESS was obtained during periods of low influent loading.

7.2.2 Simulation of the Pilot Plant Study Conducted by Stephenson *et al.* (1983)

Simulations were performed to replicate the step feed control system used in the Stephenson *et al.* (1983) pilot plant study. The controller used in the pilot plant study distributed influent between the first and third compartments of a three-compartment ASP to maintain a constant sludge activity in the third tank. A diagram in Figure 7.1 illustrates the simulation layout of the activated sludge plant. No influent was added directly to the second tank. As previously described. Stephenson *et al.* (1983) reported that variations in $rr_{sp,3}$ were minimized by distributing more influent to the first compartment during high loading periods and more to the third compartment during low loadings.

A layout of the C-removal ASP and rr_{sp} controller is depicted in Figure 7.1.

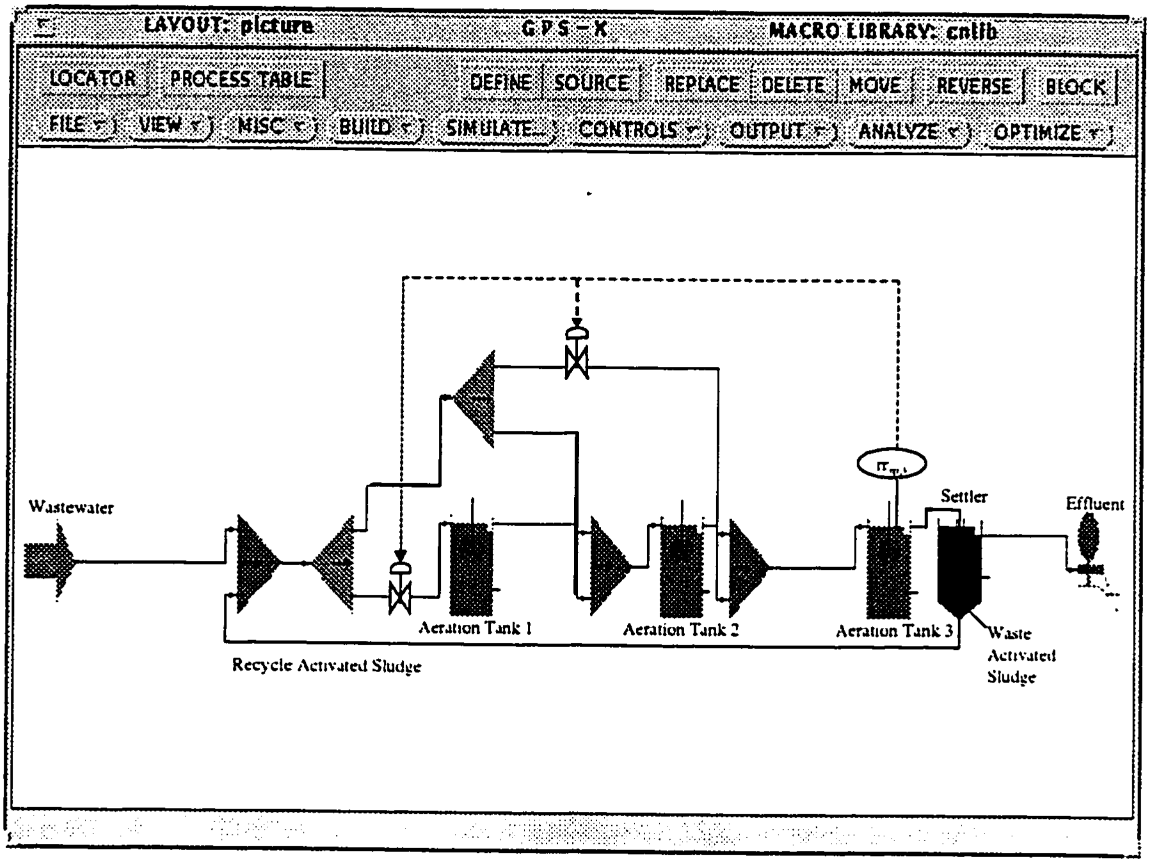

Figure 7.1: ASP layout with rr_{sp} control in the third compartment using two-compartment step feed

$rr_{sp,3}$ was calculated in the simulations as follows:

$$\frac{rr_{t3}}{X_{BHt3} + X_{BAt3}}$$

Eq. 7.2

Where rr_{t3} = respiration rate in the third tank

X_{BHt3} = heterotrophic biomass concentration in the third tank

X_{Bat3} = autotrophic biomass concentration in the third tank

Simulations showed that $rr_{sp.3}$ was closest to its set point of 15 mg O_2/g MLSS·h when all of the influent was distributed to the first tank during high loading periods and 50 per cent of the influent was distributed to each of the first and third tanks when the loading was low. The loading was considered high when the flow into the plant was greater than 20,000 m^3 d^{-1} (which is the average flow), and considered low when the influent was below this average value. Results of the simulations for controlled and uncontrolled cases are presented in Table 7.2.

Table 7.2: Simulation results ($rr_{sp.3}$ set point = 15 mg O_2/g MLSS·h)

Simulation Scenario	Average rr_{sp} measured in 3rd tank (mg O_2/g MLSS·h)	EFOC (mg L^{-1})	ESS (mg L^{-1})
No step feed control of $rr_{sp.3}$ (all of the influent is distributed to the 1st tank)	12.0 ± 2.8	16.4 ± 2.1	23.8 ± 3.1
Step feed control of $rr_{sp.3}$ (High loading: 100% of influent fed to 1st tank) (Low loading: 50% of influent fed to 1st tank and 50% fed to 3rd tank)	13.5 ± 1.7	18.4 ± 1.8	27.0 ± 2.9

Mean load = 0.6 g BOD_5/g MLSS·d

The results in Table 7.2 show that the simulation results for EFOC and ESS are similar to the results reported in Table 7.1 by Stephenson *et al.* (1983). $rr_{sp.3}$ only reached an average value of 13.5 mg O_2/g MLSS·h in the simulations, whereas an average value of 15.0 mg O_2/g MLSS·h was obtained in the pilot plant study. The reason that $rr_{sp.3}$ did not reach its set point in the simulations is that only 50 per cent of the influent was distributed to the third compartment during low loading periods (and none during high loadings). The simulations also showed that if distribution to the third tank was increased over 50 per cent during low loading periods, large variations in $rr_{sp.3}$ resulted.

In comparing controlled and uncontrolled $rr_{sp.3}$ from Table 7.2, EFOC (from 16.4 to 18.4 mg L^{-1}) and ESS (from 23.8 to 27.0 mg L^{-1}) increased when $rr_{sp.3}$ was controlled. These effluent concentrations both increased with control because the third compartment was loaded with a higher pollutant concentration. However as indicated in Table 7.2, the benefit of step-feed control is that fluctuations in both EFOC and ESS decreased as a result of controlling $rr_{sp.3}$.

The two-compartment step feed control of $rr_{sp,3}$ is demonstrated in Figure 7.2 and its affect on the effluent quality is depicted in Figure 7.3.

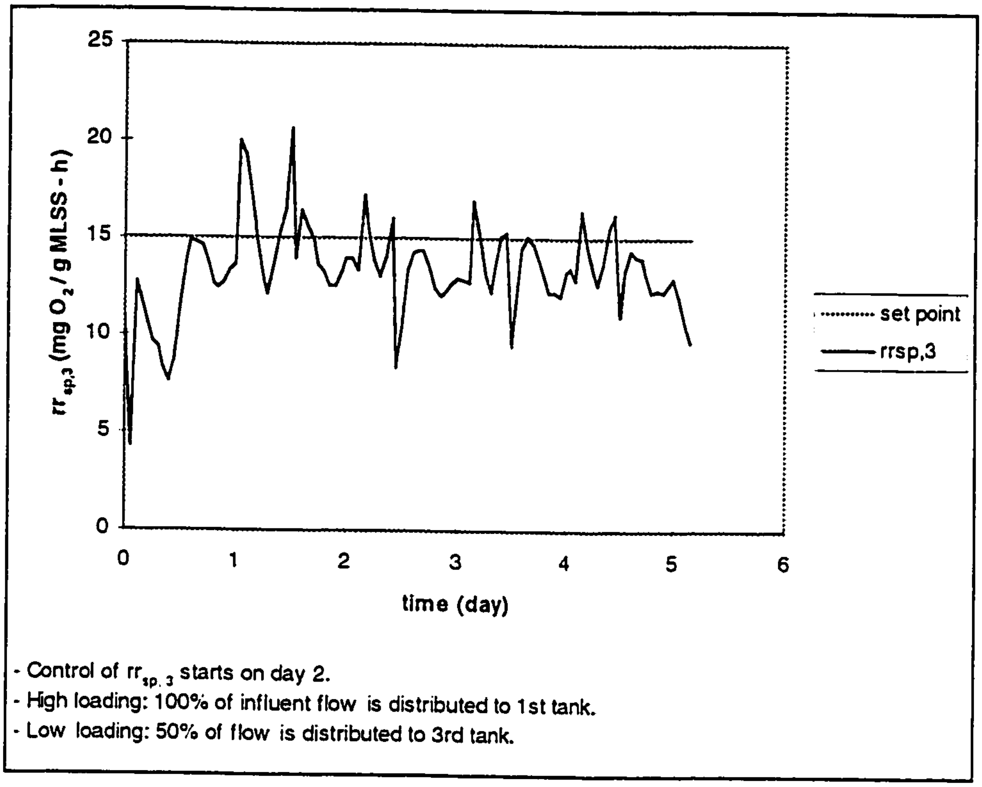

Figure 7.2: Control of $rr_{sp,3}$ to a set point of 15 mg O_2/g MLSS·h

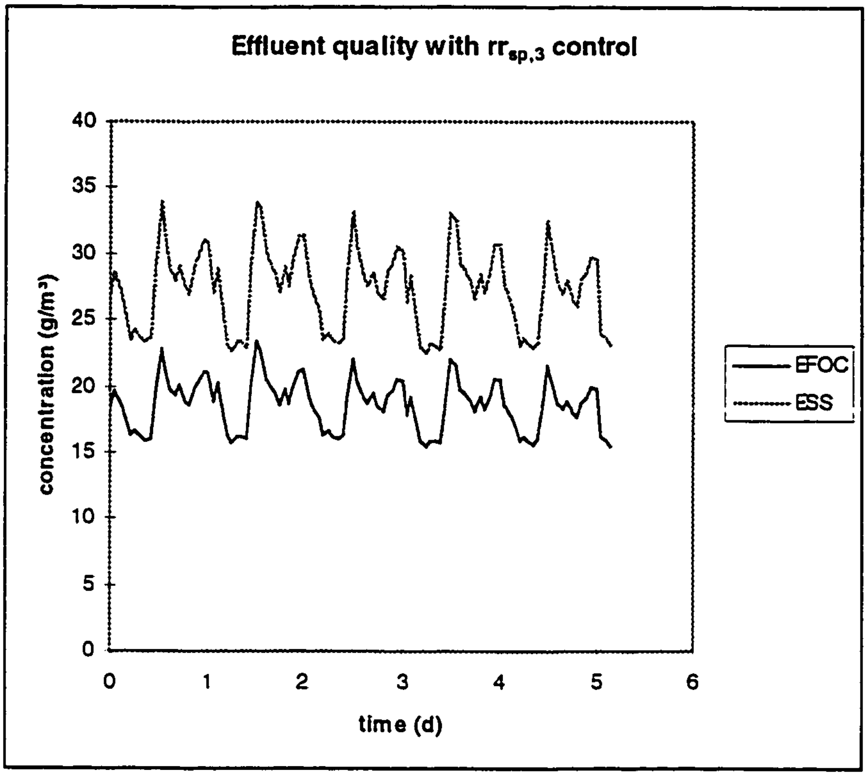

Figure 7.3: Effect of step feed control of $rr_{sp,3}$ on the effluent concentrations

7.3 Application of the Benchmark (Spanjers *et al.*, 1998a)

The benchmark, described in Section 5.2, was used to evaluate the rr_{sp} control strategy proposed by Stephenson *et al.* (1983). The components of the benchmark are:

- process models for the activated sludge process and the secondary clarification process (Section 5.2.1);
- influent conditions for both dry and wet weather conditions (Section 5.2.2);
- values for the model parameters of the IAWQ ASM1 (Henze *et al.*, 1987) and the double exponential settler model (Takács et al., 1991) (Section 5.2.3);
- set of initial values for the state variables (Section 5.2.4); and
- carbon removal activated sludge plant (Section 5.2.5).

The rr_{sp} control strategy proposed by Stephenson *et al.* (1983) was implemented in the benchmark plant. The operating conditions of the benchmark plant were adjusted as follows for this simulation study:

1. The activated sludge is recycled to the first tank at a recycle ratio of 0.5 in this study instead of 1.0 as was specified in the benchmark, because this was specified in the proposal by Stephenson *et al.* (1983).
2. Since a sludge retention time of 3 days was reported in Stephenson *et al.* (1983), a 3-day sludge retention time was used in this study instead of the 4 days in the original plant design.

Several differences in the operating conditions existed between this simulation study and the pilot plant study conducted by Stephenson *et al.* (1983):

1. The influent loading into the benchmark plant is much greater than that of the pilot plant. The influent used in the simulations has an average rate of 20,000 $m^3\ d^{-1}$, with a maximum to average flow ratio of 1.5. The influent coming into the pilot plant had an average flow of 11.52 $m^3\ d^{-1}$ and a maximum to average flow ratio of 1.3.
2. In this simulation study, the DO concentration was automatically controlled to 2 $g\ m^{-3}$ in each of the three compartments. The DO concentration in the pilot plant was also automatically controlled to 2 $g\ m^{-3}$ in the first two compartments, but in the third compartment it was controlled to 3 $g\ m^{-3}$.

3. Different types of controllers were implemented in the two cases. The control algorithm used in the pilot plant study involved controlling $rr_{sp,3}$ at a set point by optimizing the feed distribution between the first and third compartments according to the plant loading. In this study, two feedback control algorithms were used to implement the control strategy proposed by Stephenson *et al.* (1983).

7.4 Implementation of the Specific Respiration Rate Control Strategy

The control strategy proposed by Stephenson *et al.* (1983) was implemented by applying the six-step procedure described in Section 5.3:

1. Identify the objective of the respirometry-based control strategy.
2. Identify the input and output variables of the control system.
3. Identify the implied control configuration.
4. Determine the appropriate control algorithm.
5. Tune the controller.
6. Determine the appropriate range of variation for the manipulated variable.

7.4.1 Objective of the Control Strategy

The objective of the rr_{sp} control strategy proposed by Stephenson *et al.* (1983) is to maintain a constant low value of rr_{sp} in the last compartment so as to control the effluent substrate concentration. A constant low value of rr_{sp} in the last compartment ($rr_{sp,3}$) indicates that the substrate concentration is low in the effluent.

7.4.2 Input and Output Variables of the Control System

The controlled variable is $rr_{sp,3}$. The manipulated variable is the split fraction or distribution of influent to the third tank (α_3). Note that the influent flow is composed of the wastewater stream and the return activated sludge stream.

7.4.3 Implied Control configuration

The control configuration is a feedback loop since the amount of influent fed to the third compartment depends on the value of $rr_{sp,3}$.

7.4.4 Control Algorithm

Two different feedback control algorithms were used to implement the specific respiration rate control strategy proposed by Stephenson *et al.* (1983): the velocity-form of the digital PI controller and the split range controller.

The digital PI controller distributes influent between the first and third compartments to bring $rr_{sp,3}$ to its the set point. The fraction of influent distributed between the two tanks was automatically adjusted to minimize the difference between the $rr_{sp,3}$ set point and the actual $rr_{sp,3}$ measured in the third tank. The macro for the step feed system with the PI controller is provided in Appendix B.3.1. The diagram of the PI controller implemented in the benchmark plant is depicted in Figure 7.4.

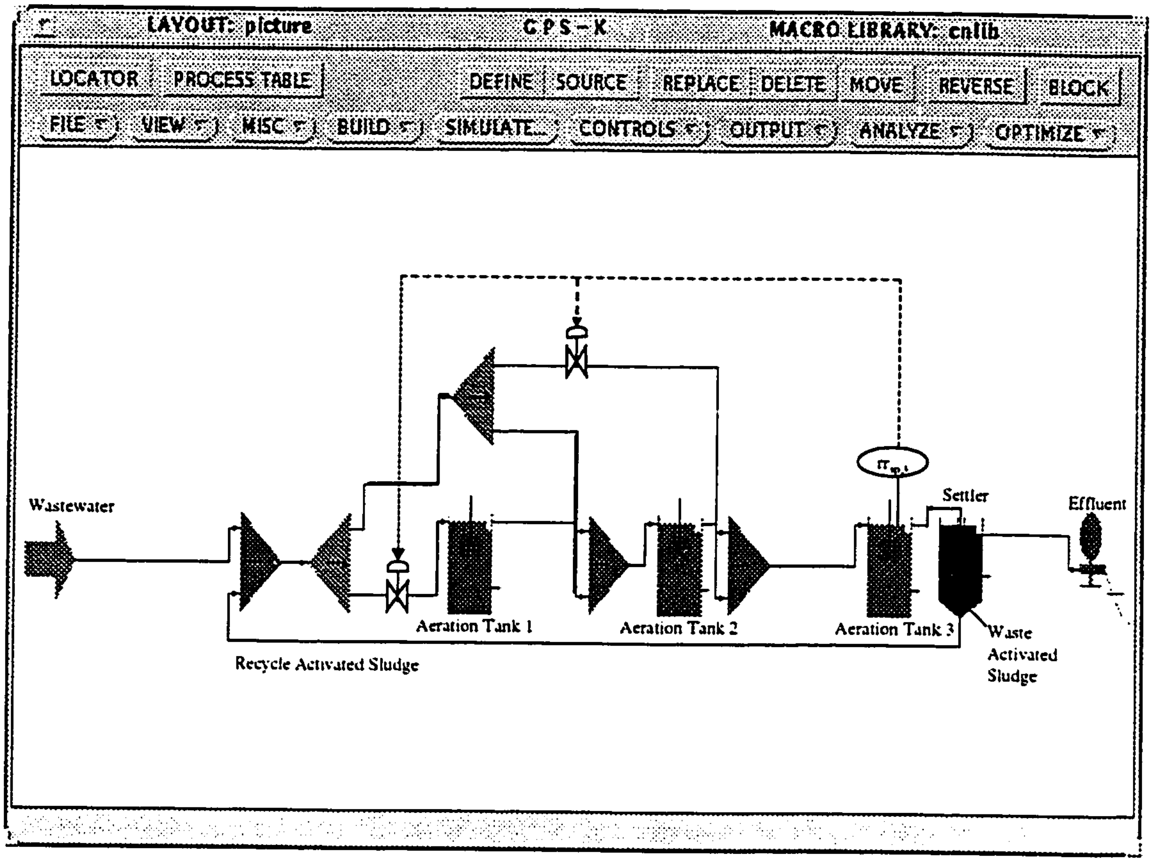

Figure 7.4: Configuration of the PI controller in the benchmark plant

The split range control scheme enables a single process output ($rr_{sp,3}$ in this case) to be controlled by coordinating the actions of several manipulated variables, all of which have the same effect on the controlled output. With split range control, each manipulated variable is assigned a "range" of the controller output.

The split range controller automatically adjusts the distribution of influent amongst the three aeration tanks to bring $rr_{sp,3}$ to its set point. This controller manipulates the influent flow distribution between the first and third compartments until the fraction of flow going to the third compartment exceeds 50 per cent. When this value is reached, the split range controller distributes the influent between the second and third compartments to bring $rr_{sp,3}$ to its set point. The third compartment receives a maximum of 50 per cent of the total influent flow because loadings greater than this amount caused large fluctuations in $rr_{sp,3}$, which could not be reduced by the controller. A diagram of the split range $rr_{sp,3}$ controller in the benchmark plant is shown in Figure 7.5.

Split range control of $rr_{sp,3}$ was implemented in the benchmark plant by designing two velocity-form digital PI controllers. One controller adjusts the feed distribution between the first and third compartments (PI_{split1}), and the other manipulates the feed distribution between the second and third compartments (PI_{split2}). As long as the feed distribution to the third compartment remains below 50 per cent of the total influent loading, PI_{split1} remains active. As soon as distribution to the third compartment exceeds 50 per cent, PI_{split2} is activated and PI_{split1} is deactivated. When PI_{split2} is activated, the flow distribution to the first compartment is fixed at 50 per cent of the total influent loading (this includes wastewater and return activated sludge), and the remaining 50 per cent is distributed between the second and third compartments to bring the $rr_{sp,3}$ to its set point. The feed distribution of the split range controller is presented in Table 7.3.

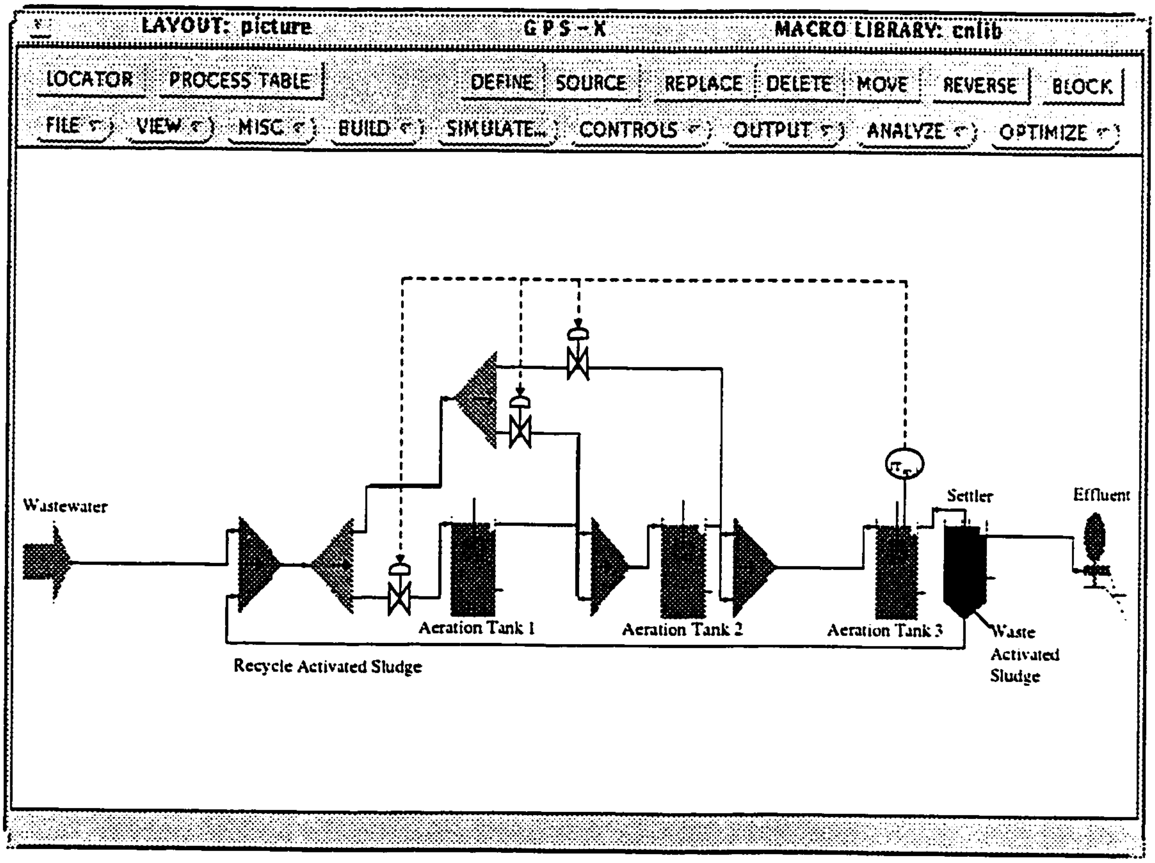

Figure 7.5: Implementation of the split range controller in the benchmark plant

Table 7.3: Feed distribution for the split range controller

PI controller	α_1	α_2	α_3
PI_{split1}	0 to 0.50	0	0 to 0.50
PI_{split2}	0.50	$1 - \alpha_3$	0 to 0.50

α_i = split fraction of total influent flow to compartment I

The macro for the split range controller is provided in Appendix B.3.2.

7.4.5 Design or Tuning of the PI Controller and the Split Range Controller

The parameters of the two digital controllers, K_C and T_I, were initially tuned by evaluating the process reaction curve, fitting an approximate first-order-with-dead-time model, and using the Ciancone tuning correlations (Marlin, 1995). The process reaction curve was obtained by first bringing the system to steady-state, then introducing a step change in α_3, and finally recording the response of the $rr_{sp,3}$ until a new steady-state is reached. A step change in α_3 was performed because it directly affects the controlled variable, $rr_{sp,3}$.

It was discovered that control of $rr_{sp,3}$ was affected by the DO controller in the third compartment. This interaction between the DO controller and the $rr_{sp,3}$ will be discussed in detail in the following section. To reduce the adverse effects on the rr_{sp} controller, the DO controller in the third compartment had to be de-tuned from its single-loop tuning. This involved reducing the value of K_c and increasing the value of T_I for the DO controller from their single-loop values. De-tuning of the DO controller in the third compartment was performed prior to fine-tuning each of both the PI controller and the split range controller.

Fine-tuning of K_C and T_I for the PI controller and the split range controller involved measuring the performance of the controller to changes in the set point under constant influent conditions. Values of the control parameters were adjusted until the controller's response became satisfactory, with a minimized ISE value and short settling time.

Therefore, optimum values of the parameters for the single velocity-form PI controller were determined to be:

$K_{c,rr}$ = 80,000

$T_{I,rr}$ = 0.005 days

Optimum parameter values for the DO controller in the third compartment were found to be:

$K_{c,DO}$ = 10.0

$T_{I,DO}$ = 0.5 days

where K_{ci} is the proportional gain for loop i.

T_{Ii} is the integral time for loop i.

Tuning of the split range controller involved the same procedures as for the single PI controller. The control parameters of the two PI controllers in the split range scheme are equal in value and remain constant throughout the simulations because the process dynamics for the two closed-loop paths are the same. As previously described, the PI_{split1} controller automatically distributes influent between the first and third tanks to bring $rr_{sp,3}$ to its set point until the fraction of the influent fed to the third tank exceeds 50 per cent. At this split fraction, PI_{split1} is deactivated and PI_{split2} is activated to distribute influent between the second and third tank. The final control parameters were calculated to be as follows:

$K_{c,split1} = K_{c,split2} = 80{,}000$

$T_{I,split1} = T_{I,split2} = 0.005$ days

where $K_{c,split1}$ and $K_{c,split2}$ are the proportional gains for PI_{split1} and PI_{split2} respectively.

$T_{I,split1}$ and $T_{I,split2}$ are the time integrals for PI_{split1} and PI_{split2} respectively.

The DO controller in the third compartment was similarly de-tuned for the split range controller as previously described. Final values for the DO control parameters are:

$K_{c,DO}$ = 10.0

$T_{I,DO}$ = 0.5 days

The sampling time interval for both the 2-tank PI controller and the split range controller was every 15 minutes.

7.4.6 Range of Variation for the Manipulated Variable

Distribution of the influent to the third compartment had to be limited to 50 per cent of the total loading. Values greater than this caused large oscillations in $rr_{sp,3}$.

7.5 Performance of the Specific Respiration Rate Control Strategy

The dynamic performance of both the single PI controller and the split range controller were examined with the five different types of tests described in Section 5.4. This involved examining both open-loop and closed-loop performances. Assessment of the open-loop dynamics involved obtaining the response of $rr_{sp,3}$ to a step change in feed rate to the third compartment. The closed-loop dynamic performance of each controller was examined under three different influent conditions: constant influent, normal diurnal influent, and stress loading conditions. A stability analysis of the control system was also conducted.

7.5.1 Open-Loop Dynamic Behaviour

The dynamic behaviour between $rr_{sp,3}$ and the feed rate to the third compartment (Q_{t3}) provides important information on the performance of the feedback control system. Since both the PI controller and the split range controller have the same manipulated and controlled variables, only one set of open-loop response analyses was conducted. The open-loop analysis involves observing the uncontrolled response of $rr_{sp,3}$ to a step change in Q_{t3}. To investigate the interaction between the DO controller and the $rr_{sp,3}$ controller, the open-loop analysis was performed both with and without DO control.

The following procedures were performed to obtain the process reaction curve of $rr_{sp,3}$ in response to changes in Q_{t3}:

1. Under constant influent conditions, allow the process to reach steady state.
2. A step change in Q_{t3} was introduced and the subsequent response of $rr_{sp,3}$ was recorded.
3. The process was allowed to reach a new steady state.

7.5.1.1 Open-loop response of rr_{sp} without interaction from the DO controller

The open-loop response of $rr_{sp,3}$ to a step change in Q_{t3} is depicted in Figure 7.6. In this simulation, the DO controller was disabled in the third compartment and Q_{t3} was increased from 10 to 5000 m³ d^{-1} on day 3.

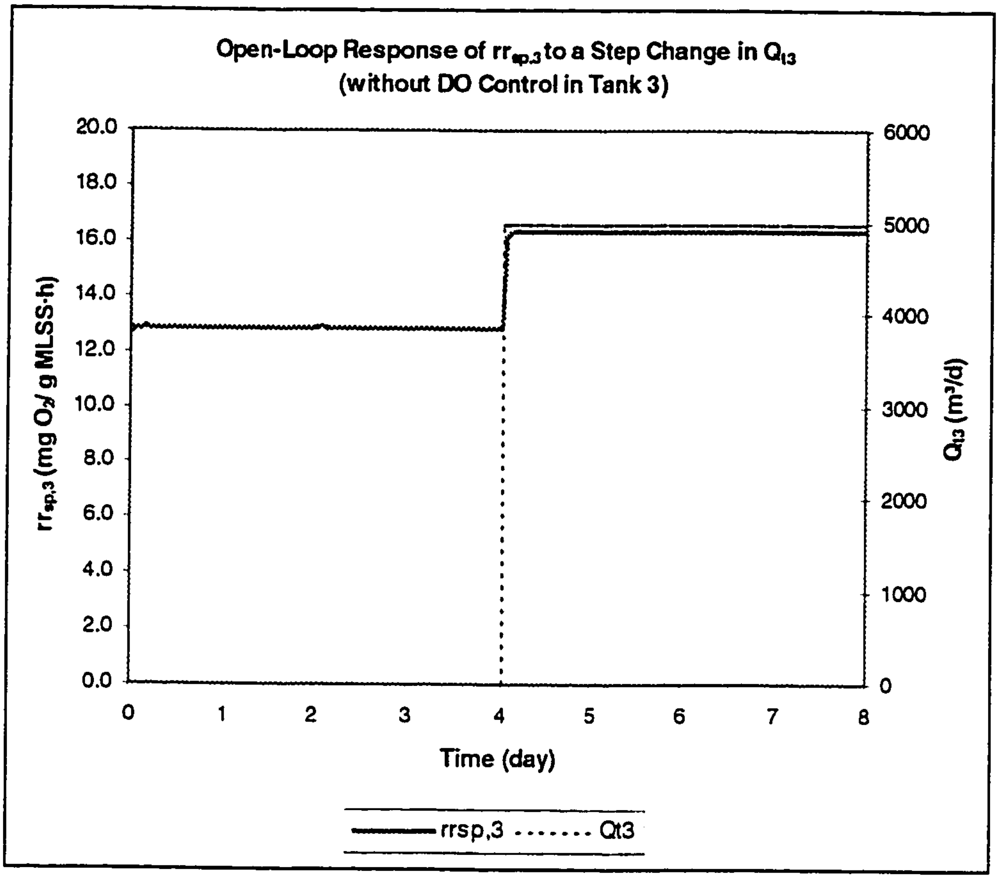

Figure 7.6: Open-loop dynamic behaviour between $rr_{sp,3}$ and Q_{t3} (with DO controller disabled)

As shown in Figure 7.6, $rr_{sp,3}$ quickly increases with an increase in Q_{t3}. This shows that there is a good causal relationship between $rr_{sp,3}$ and Q_{t3}. The shape of the response curve of $rr_{sp,3}$ indicates that the dynamic relationship between $rr_{sp,3}$ and Q_{t3} is first-order-plus-dead-time. Values characterising the first-order dynamics were found to be:

K_p = 1.04E-05 m^{-3}

τ = 2.16 minutes

θ = 0.0 minutes

These parameters were calculated by employing the process reaction curve, method II (Marlin. 1995). K_p is the ratio of the magnitude of change in $rr_{sp,3}$ to the magnitude of change in Q_{t3}. The low value of K_p reveals that the magnitude of the response of $rr_{sp,3}$ was modest compared to the large change in Q_{t3}. The low value obtained for τ and a zero dead time show that $rr_{sp,3}$ responds quickly to a change in Q_{t3}.

7.5.1.2 Effect of DO control on the open-loop response of $rr_{sp,3}$

With the DO controller in automatic, it was observed that a step change in Q_{t3} caused $rr_{sp,3}$ to overshoot from 16.4 to16.6 mg O_2 g^{-1}MLSS·h^{-1}. $rr_{sp,3}$ then settled to a new steady state value of 16.4 mg O_2 g^{-1}MLSS·h^{-1}. The overshoot in $rr_{sp,3}$ degrades the performance of the rr_{sp} controller and is caused by an interaction between the DO controller and the rr_{sp} controller in the third compartment. Processes using the multiloop approach for multivariable control, meaning multiple single-loop controllers are used in the process, often experience interaction among the individual control loops. These single-loop controllers are completely independent algorithms and do not communicate directly among themselves. Therefore, in examining the dynamics of the rr_{sp} control system, the effects of multiloop interaction with the DO controller must be considered. This was accomplished by:

1. Obtaining the open-loop response of $rr_{sp,3}$ to a step change in Q_{t3} with the DO controller in automatic.
2. Calculating the quantitative measure of interaction.
3. Examining the performance of the rr_{sp} control loop under various degrees of DO control.

By de-tuning the DO controller in the third compartment, the initial overshoot was minimized. This involved decreasing the value of K_c and increasing the value of T_I. The result of de-tuning the DO controller on the open-loop response of $rr_{sp,3}$ to a step increase Q_{t3} is depicted in Figure 7.7.

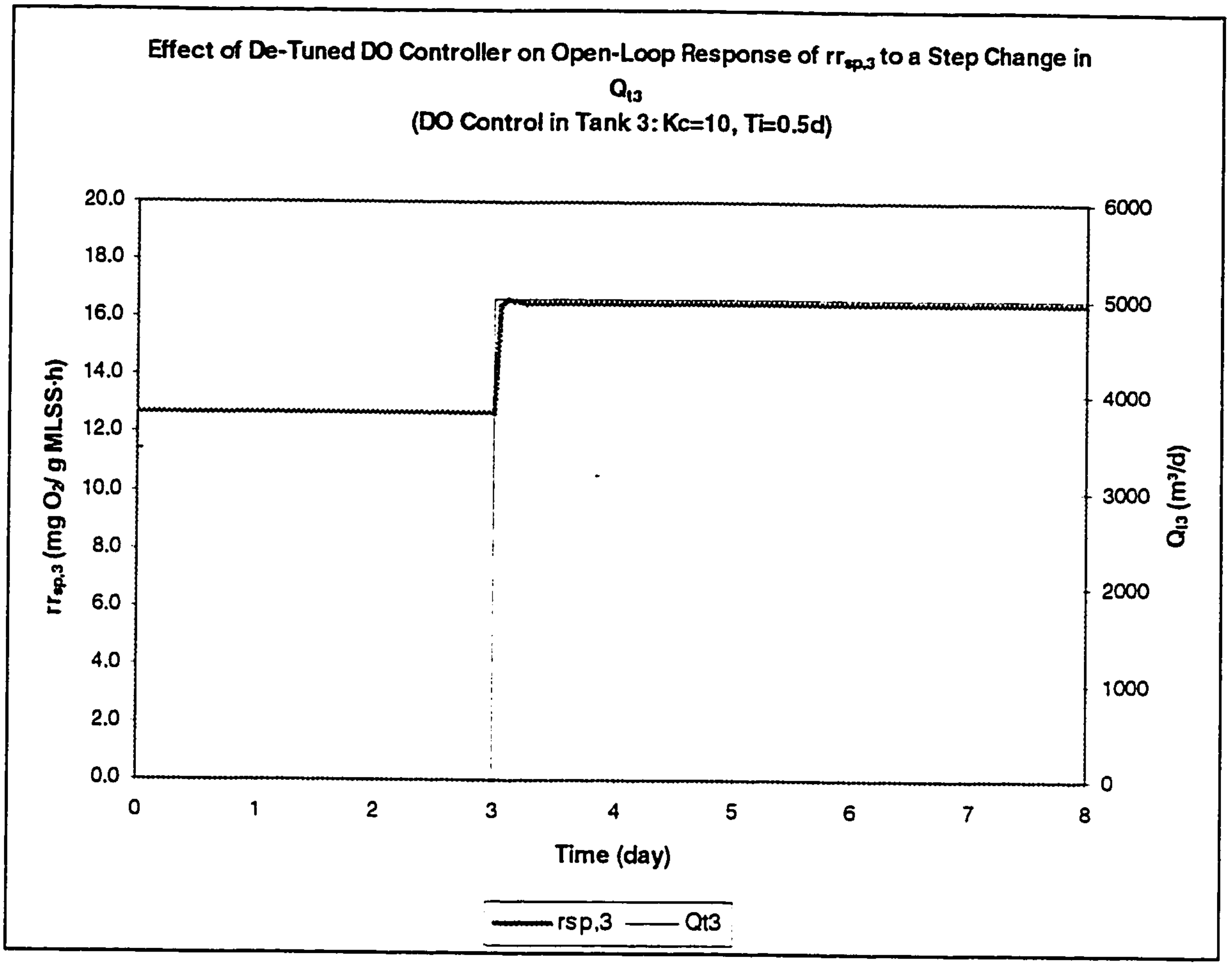

Figure 7.7: Open-loop response of $rr_{sp,3}$ to a step change in the Q_{t3} with the DO controller enabled and de-tuned in the third compartment.

As shown in Figure 7.7, the small initial overshoot of $rr_{sp,3}$ in response to a step change in Q_{t3}, illustrates that the de-tuned DO controller still exerts an influence on the rr_{sp} controller.

Further evidence that an interaction exists between the rr_{sp} controller and the DO controller in the third compartment can be seen from the open-loop responses of $rr_{sp,3}$ to a step change in K_La in the third compartment (K_La_{t3}), and of DO in the third compartment (DO_{t3}) to a step change in Q_{t3}. The responses of $rr_{sp,3}$ and DO_{t3} are depicted in Figures 7.8 and 7.9 respectively. The usual procedures were carried out to obtain the open-loop step responses of both $rr_{sp,3}$ and DO_{t3}: 1) allow the process to reach steady state, 2) introduce a step change in the input variable, and 3) collect the input and output response data until the process reaches a new steady state.

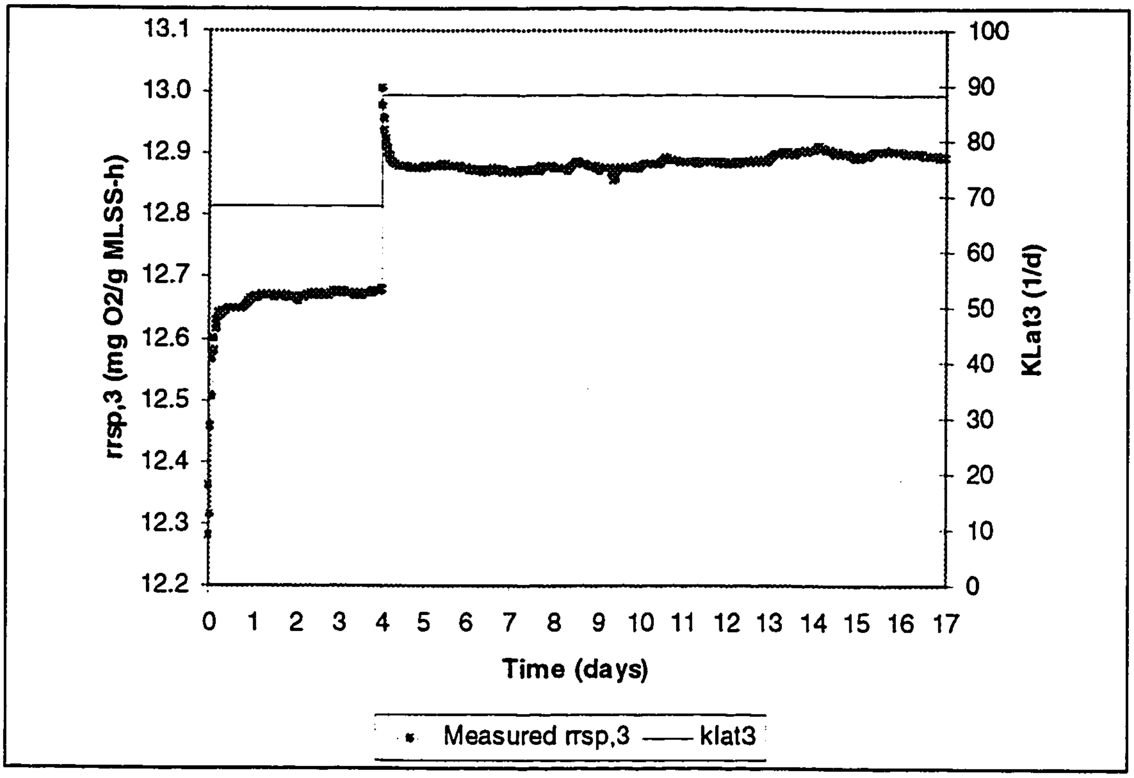

Figure 7.8: Open-loop response of $rr_{sp,3}$ to a step change in K_La_{t3} (with DO controller de-tuned)

As shown in Figure 7.8. the K_La_{t3} was increased from 68.245 to 88.245 d^{-1} on day 4. The response of $rr_{sp,3}$ is fast. and is characterized by an initial overshoot to 13.0 mg O_2/g MLSS·h and then a sharp decrease towards the new steady state value of 12.9 mg O_2/g MLSS·h. The value of τ for the open-loop response of $rr_{sp,3}$ was calculated to be about 1.44 minutes. No dead time was observed in the response of $rr_{sp,3}$.

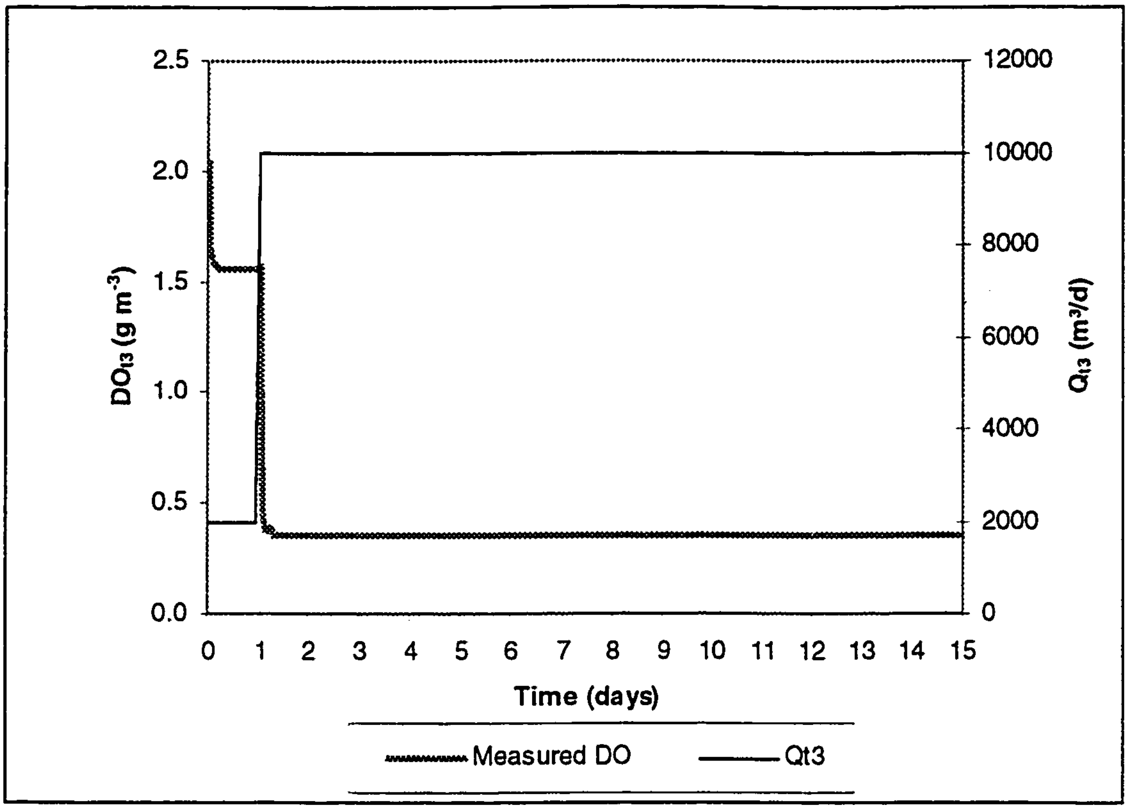

Figure 7.9: Open-Loop response of DO in 3rd compartment to a step change Q_{t3}

The response of DO_{t3} to a step increase in Q_{t3} on day 1 is characterized by quick decrease in concentration. The value of τ for the dynamic response of DO is about 21 minutes. and there was no dead time observed.

The interaction between the $rr_{sp,3}$-Q_{t3} control loop (shown in Figure 7.7) and the DO_{t3}-K_La_{t3} control loop can now be explained from Figures 7.8 and 7.9. The initial overshoot of $rr_{sp,3}$ when the DO controller was enabled, shown in Figure 7.7, is caused by an increase in the K_La_{t3}. K_La_{t3} increased when Q_{t3} increased because the DO controller was trying to compensate for the drop in the DO concentration. The decrease in the DO concentration in the third compartment was caused by the increase in Q_{t3}. The step response of $rr_{sp,3}$, shown in Figure 7.8, confirms that the initial overshoot observed in Figure 7.7 was caused by the increase in K_La_{t3}. The step response of DO_{t3}, depicted in Figure 7.9, confirms that the DO_{t3} decreases upon an increase in Q_{t3}. Thus, the open-loop responses depicted in Figures 7.8 and 7.9 indicate that a two-way interaction exists between the $rr_{sp,3}$-Q_{t3} and DO_{t3}-K_La_{t3} control loops.

The regulatory action of the $rr_{sp,3}$-Q_{t3} control loop causes the DO_{t3} to deviate from its set point. This prompts the DO controller to compensate by increasing or decreasing K_La_{t3}, which then affects the value of $rr_{sp,3}$. This two-way interaction is referred to as transmission interaction and exists when a change in the set point of one controller affects its controlled variable through a path that includes another controlled variable and controller. A diagram depicting the interaction between the rr_{sp} and DO controllers is shown in Figure 7.10.

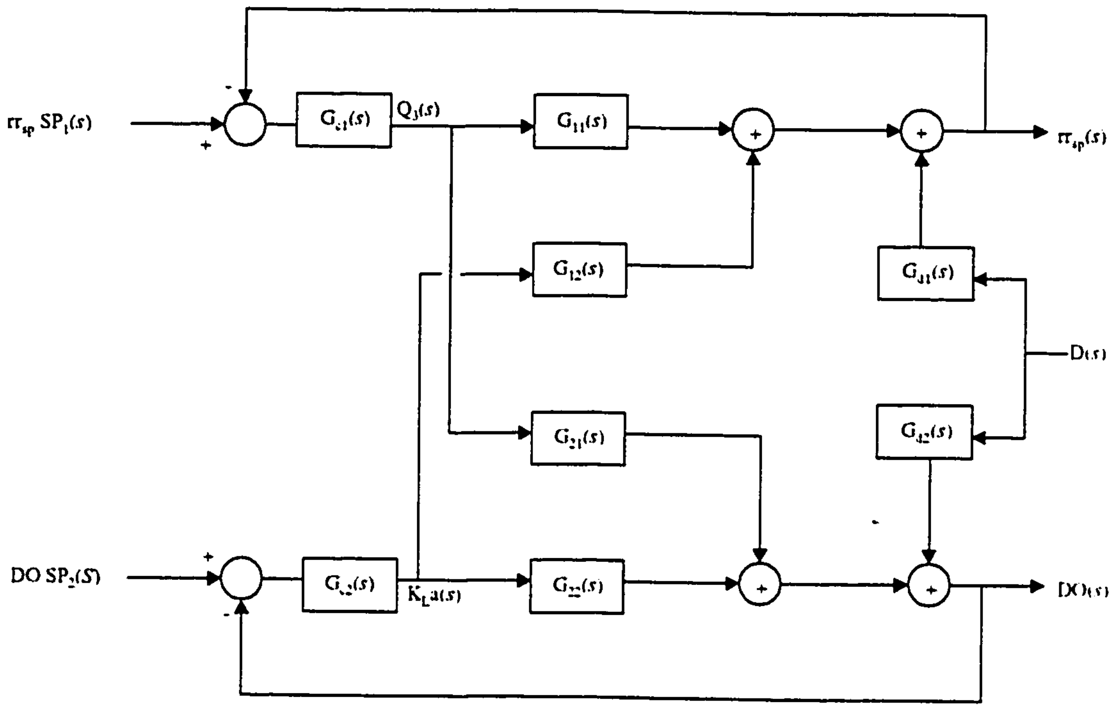

Figure 7.10: Block diagram showing the interaction between the $rr_{sp,3}$ and DO controllers

where rr_{sp} $SP_1(s)$ = rr_{sp} set point

DO $SP_2(s)$ = DO set point

$G_{c1}(s)$ = rr_{sp} controller transfer function

$G_{c2}(s)$ = DO controller transfer function

$Q_{t3}(s)$ = Influent flow rate to the third compartment

$G_{11}(s)$ = Transfer function for relationship between rr_{sp} and $Q_3(s)$

$$= \frac{rr_{sp}(s)}{Q_{t3}(s)}$$

$G_{12}(s)$ = Transfer function for relationship between rr_{sp} and K_La

$$= \frac{rr_{sp}(s)}{K_La(s)}$$

$G_{21}(s)$ = Transfer function for relationship between DO and Q_3

$$= \frac{DO(s)}{Q_{t3}(s)}$$

$G_{22}(s)$ = Transfer function for relationship between DO and K_La

$$= \frac{DO(s)}{K_La(s)}$$

7.5.1.3 A quantitative measurement of the interaction between the rr_{sp} controller and the DO Controller in the third compartment

A quantitative measure of interaction among the control loops is the relative gain array (RGA). The RGA is a matrix composed of elements defined as ratios of open-loop to closed-loop gains as expressed by the following equation. which relates the jth input and the ith output.

$$\lambda_{ij} = \frac{\left(\dfrac{\partial CV_i}{\partial MV_j}\right)_{MV_k=\text{const}, k\neq j}}{\left(\dfrac{\partial CV_i}{\partial MV_j}\right)_{CV_k=\text{const}, k\neq i}} = \frac{\left(\dfrac{\partial CV_i}{\partial MV_j}\right)_{\text{other loops open}}}{\left(\dfrac{\partial CV_i}{\partial MV_j}\right)_{\text{other loops closed}}}$$

Eq. 7.3

where λ_{ij} = relative gain of output i for a change in input j

CV_i = output i is the controlled variable

MV_j = input j is the manipulated variable

Consistent with prior terminology, the open-loop gain (K_{ij}) is the change in output i for a change in input j with all other inputs constant (for stable processes) (Marlin, 1995). Closed-loop gain refers to the steady-state relationship between MV_j and CV_i with all other control loops closed (i.e. in automatic).

The relative gain is a useful measure of interaction. A relative gain of 1.0 signifies that the process gain is unaffected by the other control loops and that no (transmission) interaction exists. Thus, the amount by which the relative gain deviates from 1.0 indicates, in some sense, the "extent" of transmission interaction in a quantitative manner.

The expression in Eq. 7.3 suggests that both open-loop and closed-loop data are required to determine the relative gain. However, the relative gain can be calculated from the open-loop data alone, which can be determined by rearranging Eq. 7.3 to give.

$$\lambda_{ij} = \left(\frac{\partial CV_i}{\partial MV_j}\right)_{MV_k = const, k \neq j} \left(\frac{\partial MV_j}{\partial CV_i}\right)_{CV_k = const, k \neq i}$$

Eq. 7.4

For a system with two inputs and two outputs, i.e. a 2 X 2 system, the (1,1) element of the relative gain array can be shown to be:

$$\lambda_{ij} = \frac{1}{1.0 - \frac{K_{12}K_{21}}{K_{11}K_{22}}}$$

Eq. 7.5

Furthermore, the rows and columns of the relative gain array sum to 1.0. This property enables 2X2 systems to be characterized by the λ_{11} element, as follows:

	MV_1	MV_2
CV_1	λ_{11}	$1-\lambda_{11}$
CV_2	$1-\lambda_{11}$	λ_{11}

Marlin (1995) warns that the relative gain calculation can be very sensitive to errors in the process gain (K_{ij}) calculation. He suggests that the best method for accurately determining the process gain is to derive an analytical model and evaluate the process gains from analytical derivatives. However, few complex industrial processes, such as the activated sludge process in this study, can be accurately modelled by sets of equations small enough to be conveniently manipulated analytically by hand. According to Marlin (1995), another accepted approach to determining the process gain is to perform a separate simulation where each input MV_j is changed by a small amount from the steady state and observing the change in the output CV_i from the steady state. In other words, the process gains are calculated using the equation below, and the relative gain array is calculated with Eq. 7.5.

$$K_{ij} \approx \frac{CV_i(MV_1, MV_2, \ldots, MV_j + \Delta MV_j, \ldots) - CV_i(MV_1, MV_2, \ldots)}{\Delta MV_j}$$

Eq. 7.6

Thus for the 2X2 system in the third compartment, let

$rr_{sp,3}$-Q_{t3} loop	=	loop #1
$rr_{sp,3}$	=	CV_1
Q_{t3}	=	MV_1
DO_{t3}-K_La_{t3}	=	loop #2
DO_{t3}	=	CV_2
K_La_{t3}	=	MV_2.

The process gains were calculated using Eq.7.6 and were found to be as follows:

$$K_{11} = \frac{\Delta rr_{sp,3}}{\Delta Q_{t3}}$$

$$= \quad 9.3\text{E-06 m}^{-3}$$

$$K_{21} = \frac{\Delta DO_{t3}}{\Delta Q_{t3}}$$

$$= \quad -1.5\text{E-04 g}\cdot\text{d m}^{-6}$$

$$K_{12} = \frac{\Delta rr_{sp.3}}{\Delta K_L a_{t3}}$$

$$= \quad 2.82\text{E-04}$$

$$K_{22} = \frac{\Delta DO_{t3}}{\Delta K_L a_{t3}}$$

$$= \quad 0.055 \text{ g}\cdot\text{d m}^{-3}$$

The above process gain values were used in Eq. 7.5 to calculate λ_{ij}. The resulting relative gain values are:

λ_{11} = Relative gain between $rr_{sp.3}$ and Q_{t3}

$$= \frac{\left(\Delta rr_{sp.3} / \Delta Q_{t3}\right)_{K_L a_{t3}}}{\left(\Delta rr_{sp.3} / \Delta Q_{t3}\right)_{DO\,t3}}$$

$$= \quad 0.924$$

λ_{12} = Relative gain between $rr_{sp.3}$ and $K_L a_{t3}$

$$= \frac{\left(\Delta rr_{sp.3} / \Delta K_L a_{t3}\right)_{Q_{t3}}}{\left(\Delta rr_{t3} / \Delta K_L a_{t3}\right)_{DO_{t3}}}$$

$$= \quad 1-\lambda_{11}$$

$$= \quad 0.0764$$

λ_{21} = Relative gain between DO_{t3} and Q_{t3}

$$= \frac{\left(\Delta DO_{t3} / \Delta Q_{t3}\right)_{K_L a_{t3}}}{\left(\Delta DO_{t3} / \Delta Q_{t3}\right)_{rr_{t3}}}$$

$$= \quad 1-\lambda_{11}$$

$= \quad 0.0764$

$\lambda_{22} \quad = \quad$ Relative gain between DO_{t3} and K_La_{t3}

$$= \frac{(\Delta DO_{t3} / \Delta K_L a_{t3})_{Q_{t3}}}{(\Delta DO_{t3} / \Delta K_L a_{t3})_{rr_{t3}}}$$

$= \quad \lambda_{11}$

$= \quad 0.924$

The smaller the value of λ_{ij}, the larger the interaction between control loops 1 and 2. Thus a value of 0.924 for λ_{11} indicates that some interaction does exist between the rr_{sp} controller and the DO controller, and that as K_La_{t3} varies it affects the steady-state value of $rr_{sp,3}$. Similarly, the value for λ_{22} indicates that as Q_{t3} varies it slightly affects the steady-state value of DO_{t3}. The values for λ_{11} and λ_{22} are close to 1.0 because the DO controller for the third compartment was de-tuned. The values of λ_{12} and λ_{21} are obviously low because of the strong interaction between $rr_{sp,3}$ and Q_{t3} and DO_{t3} and K_La_{t3}, respectively. Thus from the relative gain analysis, the interaction between the rr_{sp} controller and the DO controller is low and therefore should not significantly impede the performance of either the PI controller or the split range controller.

7.5.1.4 Effect of multiloop interaction on the performance of the rr_{sp} controller

Four separate simulations were performed under variable influent loading conditions to demonstrate the effect of the DO controller on the split range rr_{sp} controller. Each simulation shows the performance of the rr_{sp} controller under varying degrees of DO control. The integral of the squared error of $rr_{sp,3}$ from its set point is used as a measure of the performance of the rr_{sp} controller. This is presented in Table 7.4.

Table 7.4: Effect of DO Controller on the Split Range rr_{sp} Controller

Run	Degree of DO control [1]	ISE [5]
1	DO control disabled in 3rd compartment[2]	2.16E-05
2	De-tuned DO control in 3rd compartment[3]	2.66E-05
3	DO control disabled in all three compartments	2.50E-05
4	De-tuned DO control in all three compartments [4]	2.88E-05

1. Unless specified, control parameters for the DO controller in compartments 1 and 2 are:
   $K_{c1} = K_{c2} = 30.0$
   $T_{I1} = T_{I2} = 0.05$ days
2. DO control was enabled in compartments 1 and 2.
3. DO control was enabled in compartments 1 and 2. De-tuned control parameters for DO controller in compartment 3 were: $K_{c3} = 10.0$, $T_{I3} = 0.5$ days
4. Control parameters for DO controllers in all three compartments were de-tuned as follows:
   $K_{c1} = K_{c2} = K_{c3} = 10.0$
   $T_{I1} = T_{I2} = T_{I3} = 0.05$ days
5. ISE is the integral of the squared error and gives a measure of the deviation of $rr_{sp,3}$ from its set point value of 15.0 mg O_2/g MLSS·h. The ISE values are based on a 7-day simulation period.

The ISE values for runs 1 and 2 in Table 7.4 show that the $rr_{sp,3}$ deviates slightly more from its set point when DO control is enabled in the third compartment. The ISE values for runs 1, 3 and 4 also reveal that the deviation of $rr_{sp,3}$ from its set point increases as DO control in all three compartments is relaxed. The reason for this is that when DO control is relaxed, higher fluctuations occur in the DO concentration, which in turn cause greater fluctuations in the $rr_{sp,3}$. Therefore, interaction between the DO controller and the rr_{sp} controller can be minimized by maintaining full control of the DO concentration in the first and second compartments and de-tuning the DO controller in the third compartment.

7.5.2 Stability Analysis

The Nyquist stability criterion was employed for assessing the stability of both the PI rr_{sp} controller and the split range rr_{sp} controller. Since both controllers have the same controlled and manipulated variables and the same tuning, identical Nyquist plots were calculated for both controllers. The Nyquist plot is shown in Figure 7.11. The solid line covers the frequency range $0 \le \omega < +\infty$, and the dashed part covers the frequencies from $-\infty$ to 0. The dashed segment of the Nyquist plot is the mirror image of the solid-line segment with respect to the real axis.

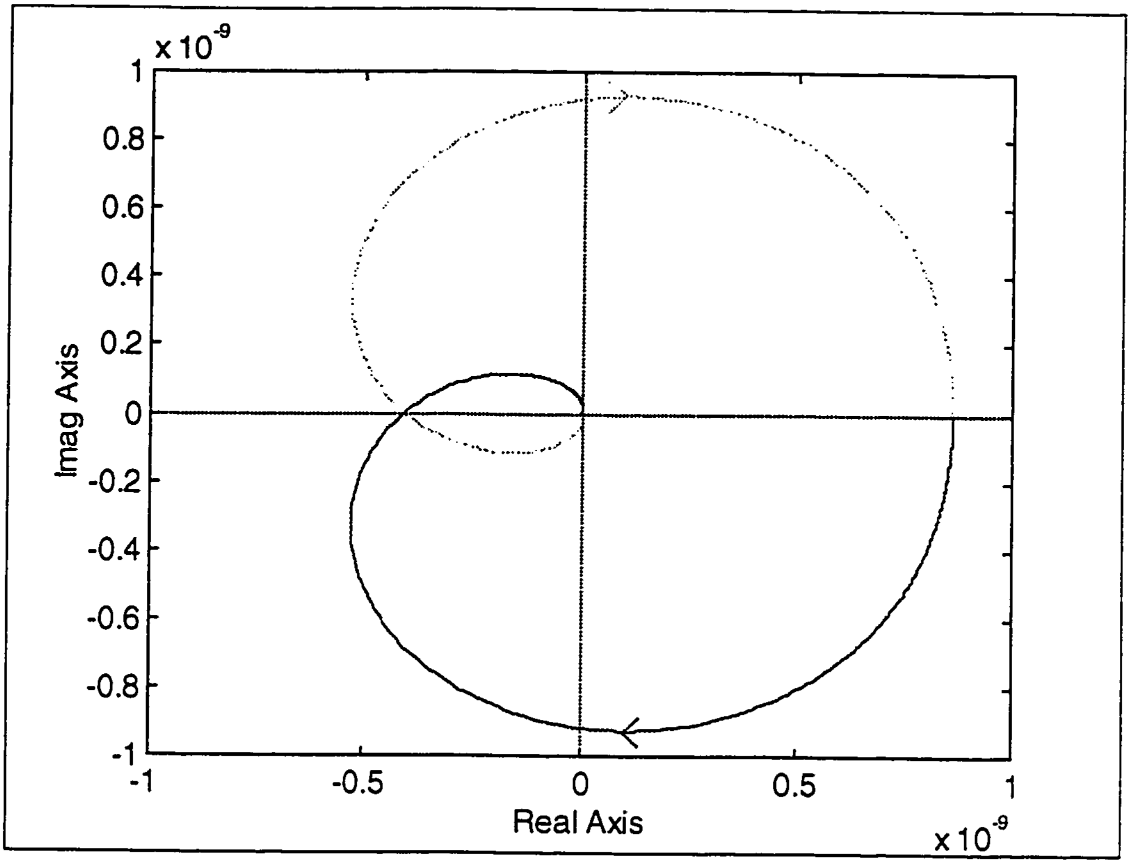

Figure 7.11: Nyquist plot for the both the PI controller and split range controller

The plot in Figure 7.11 shows that the point (-1,0) is not encircled. Thus according to the Nyquist stability criterion, the closed-loop responses of the two rr_{sp} controllers to a range of input frequencies is stable. This implies that the PI tuning constants, K_c = 80.000, T_I = 0.005 days, calculated for both controllers give stable performance over a range of operating conditions.

7.5.3 Control Performance Under Set Point Changes

The dynamic responses of both the PI and split range controllers to step changes in the set point were examined.

7.5.3.1 Performance of the 2-tank PI controller In response to set point changes

The ability of the PI $rr_{sp,3}$ controller to meet set point changes under constant influent conditions was tested and is demonstrated in Figure 7.12. The set point was first changed to 15.0 mg O_2 g^{-1}

MLSS h^{-1}, then it was changed to 20.0 mg O_2 g^{-1} MLSS h^{-1} after day 3, and finally to 12.0 mg O_2 g^{-1} MLSS h^{-1} after day 9. Statistics on the performance of the controller are presented in Table 7.5.

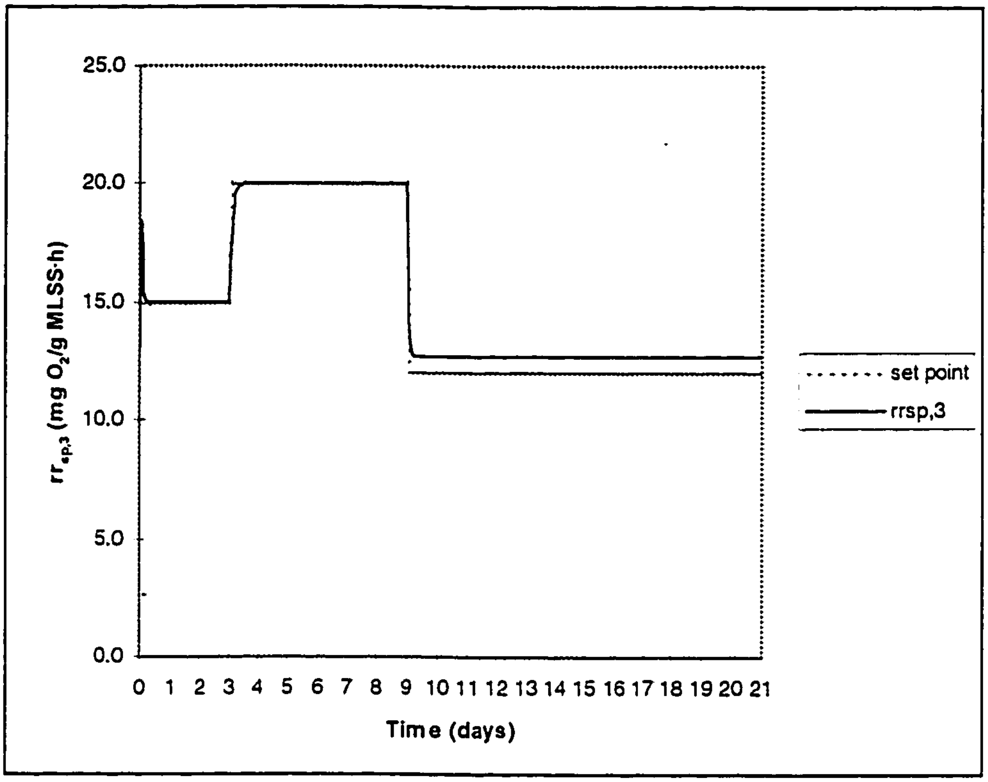

Figure 7.12: Closed-loop response of the PI $rr_{sp,3}$ controller to changes in the set point

Table 7.5: Performance of $rr_{sp,3}$ PI controller to step changes in the set point

Time Interval (days)	$rr_{sp,3}$ Set Point (mg O_2 g^{-1} MLSS·h^{-1})	Average $rr_{sp,3}$ (mg O_2 g^{-1} MLSS h^{-1})	Standard Deviation from Set Point	Settling Time of $rr_{sp,3}$ (days)
0 to 3	15.0	15.1	0.604	0.55
3 to 9	20.0	20.0	0.305	0.60
9 to 21	12.0	12.7	0.769	Does not settle to set point

The PI controller is able to meet each new set point with little or no offset. This is shown in Figure 7.12 and by the relatively low values obtained for the standard deviations of $rr_{sp,3}$ (Table

7.5) from each set point. Additionally, the controller was able to bring $rr_{sp,3}$ to set points of 15.0 and 20.0 mg O_2 g^{-1} MLSS h^{-1} relatively quickly with relatively short settling times. The PI controller was unable to meet a set point of 12.0 mg O_2 g^{-1} MLSS h^{-1}. The offset value was 0.7 mg O_2 g^{-1} MLSS h^{-1}. A likely reason why the controller did not meet the set point of 12.0 mg O_2 g^{-1} MLSS h^{-1} was that endogenous respiration (which occurs in the absence of substrate) was already occurring at 13.0 mg O_2 g^{-1} MLSS h^{-1} in the third compartment.

7.5.3.2 Performance of the split range controller in response to set point changes

Similar results were obtained when the response of the split range controller was tested for meeting set point changes under constant influent conditions. The controller's response is depicted in Figure 7.13. Statistics of the test are presented in Table 7.6.

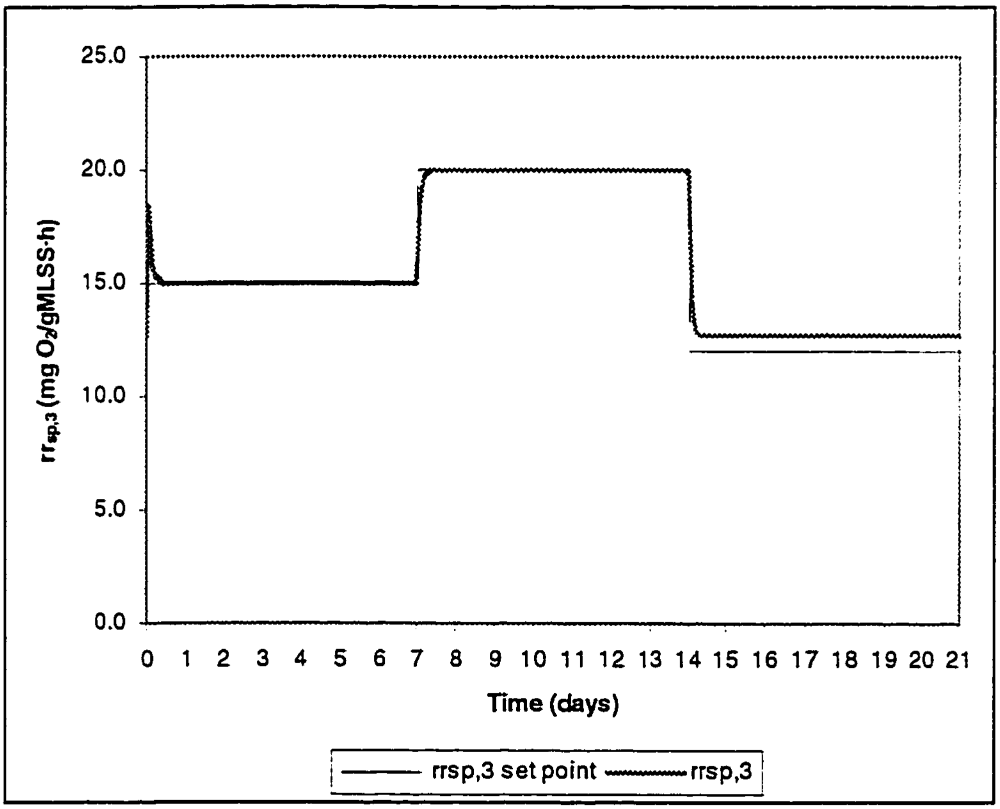

Figure 7.13: Closed-loop response of the Split Range $rr_{sp,3}$ controller to changes in the set point

Table 7.6: Performance of Split Range $rr_{sp,3}$ Controller to Step Changes in the Set Point

Time Interval (days)	$rr_{sp,3}$ Set Point (mg O_2 g^{-1} MLSS·h^{-1})	Average $rr_{sp,3}$ (mg O_2 g^{-1} MLSS h^{-1})	Standard Deviation from Set Point	Settling Time of $rr_{sp,3}$ (days)
0 to 7	15.0	15.0	0.394	0.85
3 to 9	20.0	20.0	0.299	0.65
9 to 21	12.0	12.7	0.843	Does not settle to set point

The plot in Figure 7.13 and statistics shown in Table 7.6 reveal that the split range controller performs similarly well as the PI controller in meeting new set points.

7.5.4 Control Performance Under Diurnal Influent Conditions

7.5.4.1 Dynamic performance of the 2-tank PI rr_{sp} controller under diurnal influent conditions

The dynamic performance of the PI controller was examined under diurnal influent loading conditions. Recall that this controller distributes the feed between compartments 1 and 3 only. The ability of the controller in maintaining $rr_{sp,3}$ at set points of 15.0 and 20.0 mg O_2 g^{-1}·MLSS h^{-1} is shown in Figure 7.14. The graph shows that $rr_{sp,3}$ follows the fluctuations of the influent flow and oscillates around the set point. The plots in Figure 7.14 also show that the PI controller is unable to attenuate the effects of high-frequency influent variations on $rr_{sp,3}$. Therefore, $rr_{sp,3}$ will likely never settle towards its set point.

The dynamic response of the PI controller in bringing $rr_{sp,3}$ to a set point of 15.0 mg O_2 g^{-1}MLSS·h^{-1} during diurnal loading conditions is depicted in Figure 7.15. The feed flow into the 1st and 3rd compartments (Q_{t1} and Q_{t2}) vary according to the diurnal variations observed in the influent wastewater.

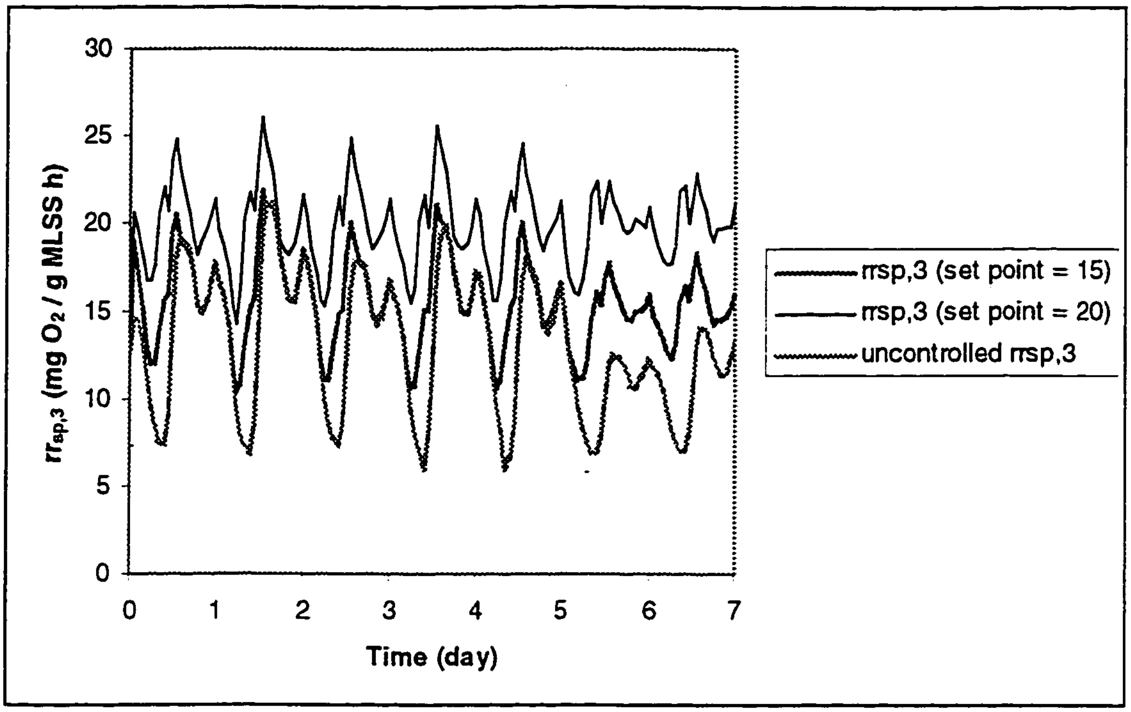

Figure 7.14: Performance of the 2-tank PI controller in maintaining the set point under diurnal influent conditions

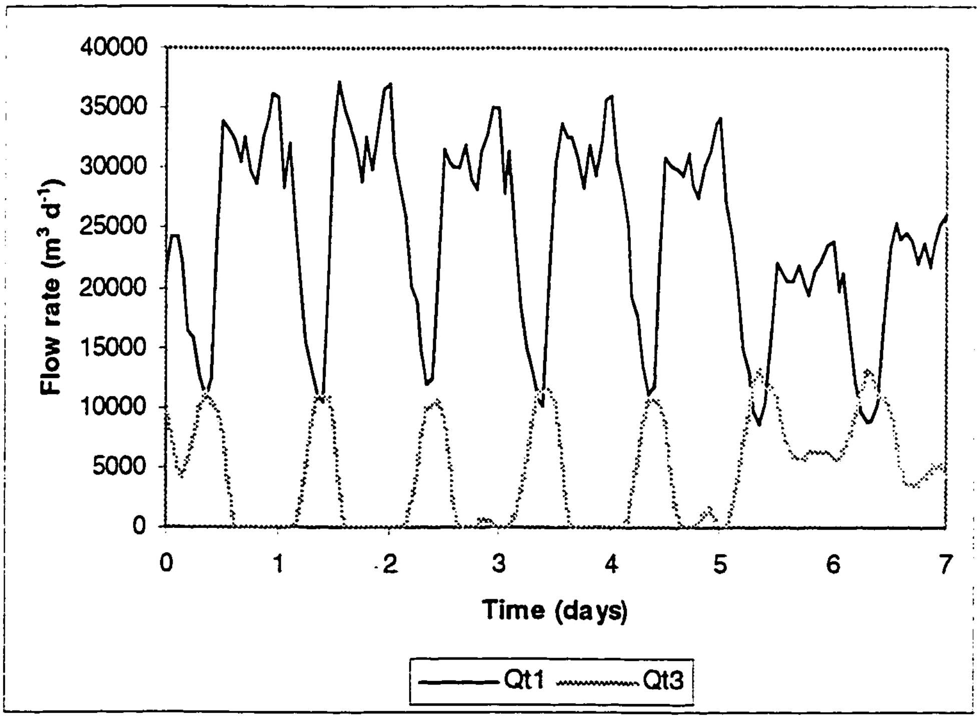

Figure 7.15: Dynamic response of the 2-tank PI controller showing adjustments in the influent flow into to the 1st and 3rd compartments ($rr_{sp,3}$ set point = 15 mg O_2/g MLSS·h)

Statistics on the performance of the PI controller in regulating the different $rr_{sp,3}$ set points under diurnal influent conditions are presented in Table 7.7.

Table 7.7: Statistics on the performance of the 2-tank PI controller under diurnal influent conditions (2-tank step feeding)

$rr_{sp,3}$ Set Point (mg O_2 g^{-1}MLSS·h^{-1})	Average $rr_{sp,3}$ (mg O_2 g^{-1}MLSS·h^{-1})	Standard Deviation from the Average $rr_{sp,3}$	Standard Deviation from the Set Point	Standard Deviation of Q_{t1}	Standard Deviation of Q_{t3}
No control	13.0	3.90	-	Flow to tank1 only	-
15.0	15.6	2.56	2.61	8010	4350
20.0	19.9	2.38	2.38	8776	4828

The average value of $rr_{sp,3}$, shown in Table 7.7, for the controlled cases reveals that the PI controller is able to meet the set point on average. Also note that the standard deviation values from the average $rr_{sp,3}$ are lower in the controlled cases than in the uncontrolled case. This shows that the PI controller is able to reduce fluctuations in $rr_{sp,3}$, which implies that the controller might reduce variations in the active biomass concentration in the third compartment.

The effect of different $rr_{sp,3}$ set points on the effluent biodegradable substrate concentrations (Ss_{eff} and Xs_{eff}) are illustrated respectively in Figures 7.16 and 7.17. As shown in Figure 7.16, Ss_{eff} increases when $rr_{sp,3}$ is controlled. The reason Ss_{eff} increases is that the PI controller must raise the feed rate to the third compartment in order to bring $rr_{sp,3}$ up to set points of 15.0 and 20.0 mg O_2 g^{-1}MLSS·h^{-1}. Furthermore, it is shown in Figure 7.16 that fluctuations in Ss_{eff} are reduced when $rr_{sp,3}$ is controlled. These results are consistent with those found by Stephenson *et al.* (1983).

Plots of X_{seff} under diurnal loading conditions in Figure 7.17 indicate that PI control of $rr_{sp,3}$ has negligible effect on X_{seff}.

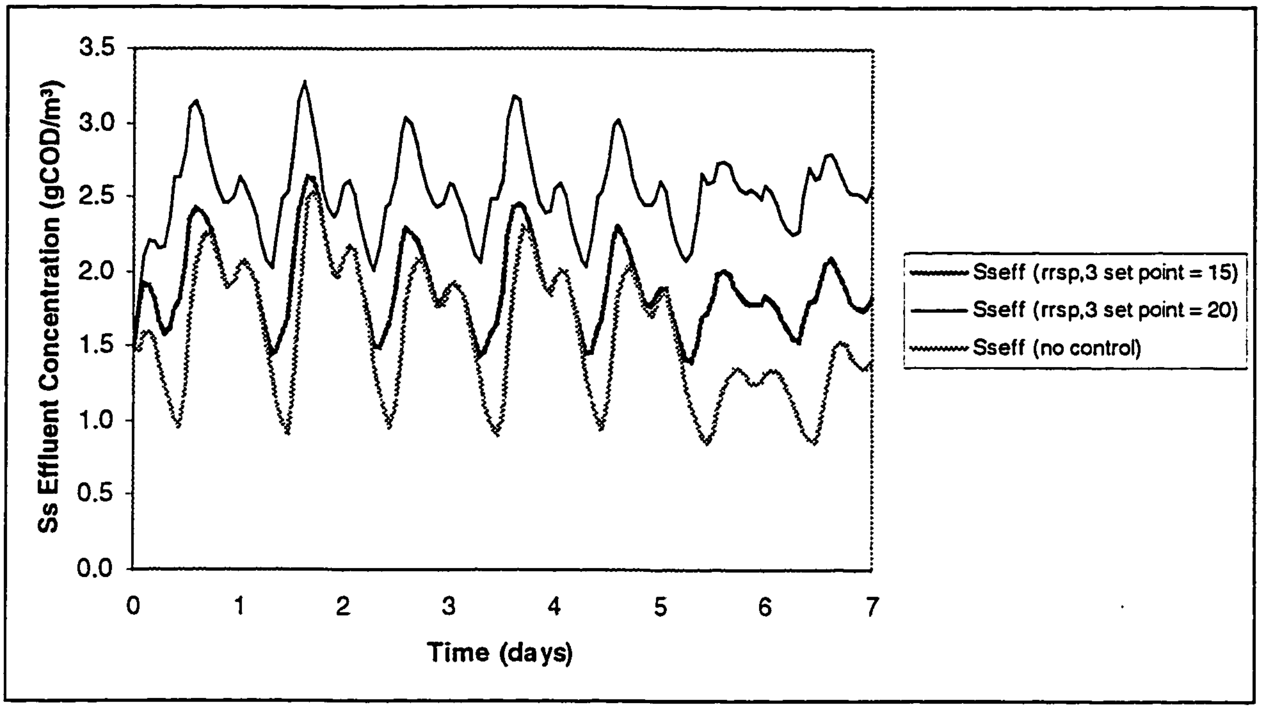

Figure 7.16: Effect of PI control under diurnal influent conditions on the soluble substrate concentration in the effluent

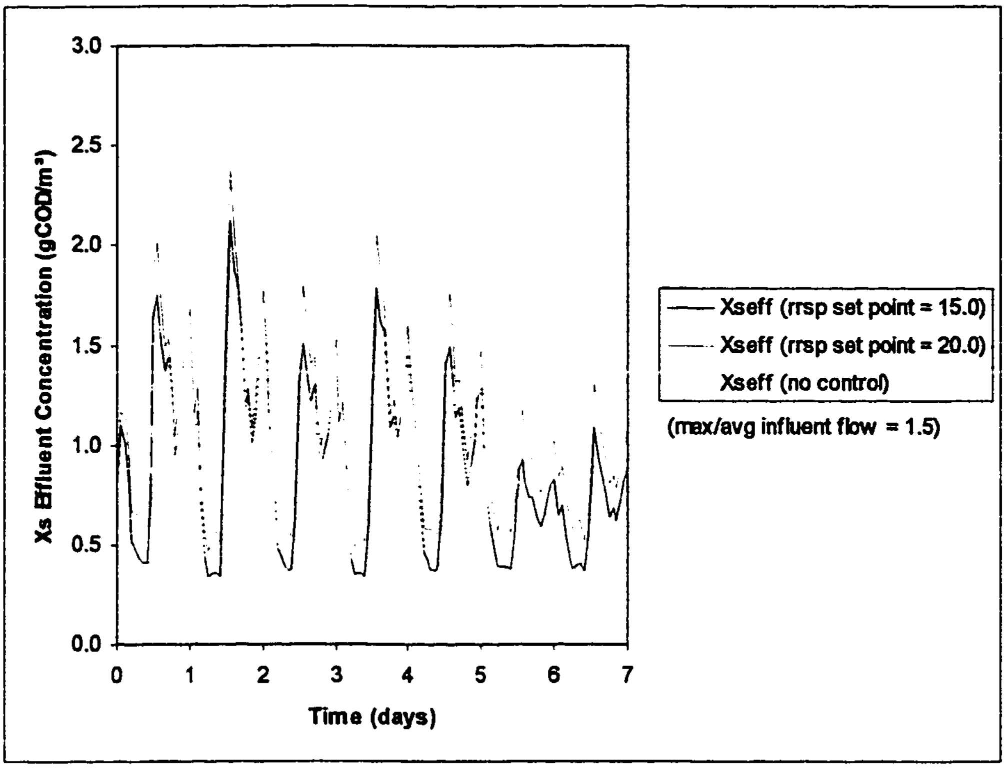

Figure 7.17: Effect of PI control under diurnal influent conditions on the slowly biodegradable substrate concentration in the effluent

7.5.4.2 Dynamic performance of the split range rr_{sp} controller under diurnal influent conditions

The dynamic performance of the split range controller was also examined under diurnal influent loading conditions. Recall that this controller distributes influent amongst all three compartments. Statistics of the controller's performance are presented in Table 7.8. The performance is also depicted in Figures 7.18 and 7.19.

The ability of the split range controller in maintaining $rr_{sp,3}$ at set points of 15.0 and 20.0 mg O_2 g^{-1}·MLSS h^{-1} is similar to that of the PI controller. The graph in Figure 7.18 shows that $rr_{sp,3}$ follows the fluctuations of the influent flow and oscillates around the set point. Furthermore, it is evident that the split range controller is unable to attenuate the high-frequency variations of the influent.

The dynamic response of the split range controller in bringing $rr_{sp,3}$ to a set point of 15.0 mg O_2 g^{-1}MLSS·h^{-1} during diurnal loading conditions is depicted in Figure 7.19. The feed flow to all three compartments vary according to the diurnal variations observed in the influent flow rates.

In comparing the performance of the PI and split range controllers under diurnal loading conditions, the PI controller meets a set point of 20 mg O_2 g^{-1}MLSS·h^{-1} slightly more often than the split range controller. However, there are smaller fluctuations in Q_{t3} with split range control.

Table 7.8: Statistics on the performance of the split range controller under diurnal influent conditions (3-tank step feeding scheme)

$rr_{sp,3}$ Set Point (mg O_2 g^{-1}MLSS·h^{-1})	Average $rr_{sp,3}$ (mg O_2 g^{-1}MLSS·h^{-1})	Standard Deviation from the Average $rr_{sp,3}$	Standard Deviation from the Set Point	Standard Deviation of Q_{t1}	Standard Deviation of Q_{t2}	Standard Deviation of Q_{t3}
No control	13.0	3.90	-	Flow to tank1 only		-
15.0	15.5	2.61	2.64	7917	4144	657
20.0	18.8	2.98	3.19	7319	3459	795

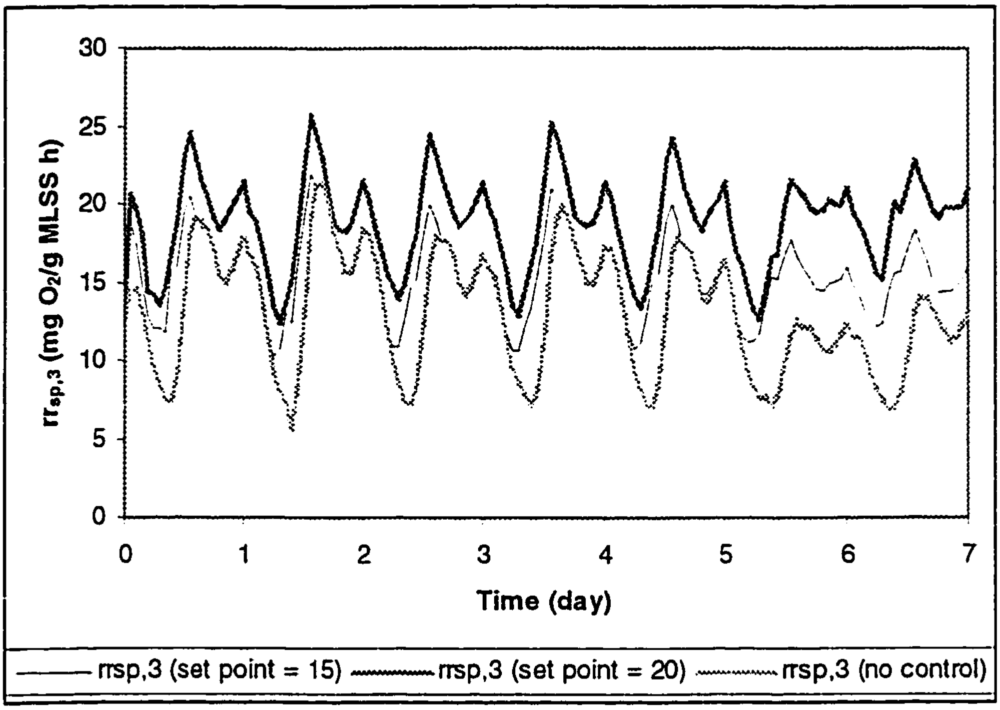

Figure 7.18: Performance of split range controller in maintaining the set point under diurnal influent conditions

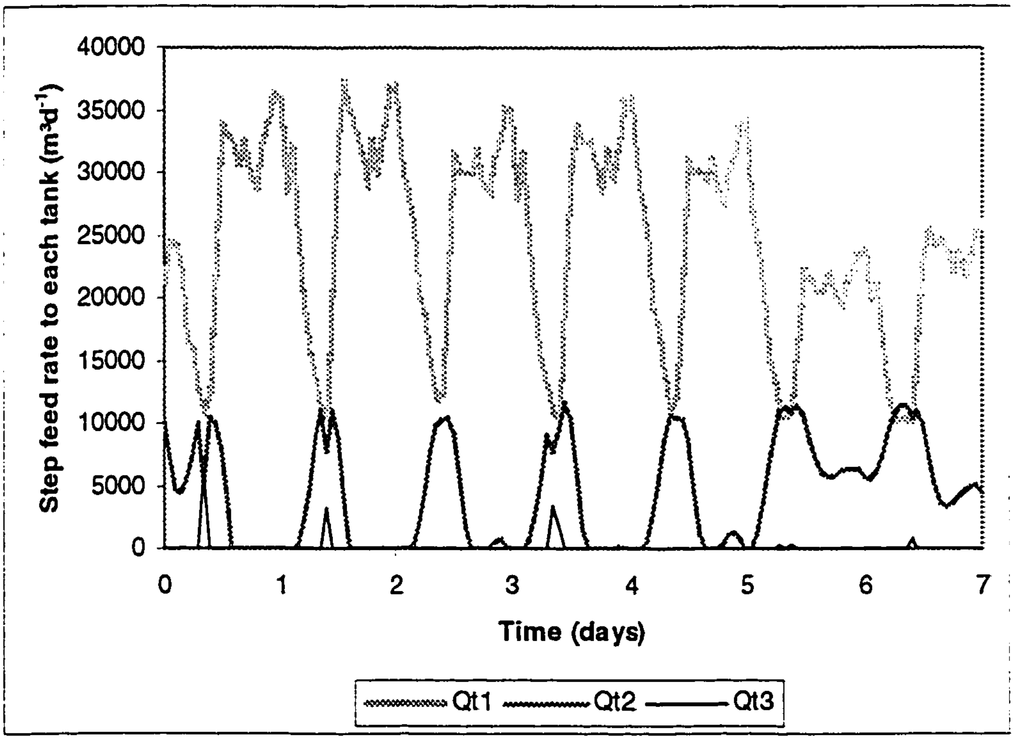

Figure 7.19: Dynamic response of the split range controller showing adjustments in the influent flow rates to each tank (with $rr_{sp,3}$ set point of 15 mg O_2/g MLSS·h)

The effects of the split range controller on the biodegradable substrate concentrations in the effluent are depicted in Figures 7.20 and 7.21. As demonstrated in Figures 7.16, 7.17, 7.20 and 7.21, it seems that both the PI controller and the split range controller did not improve the effluent biodegradable substrate concentrations over uncontrolled operations.

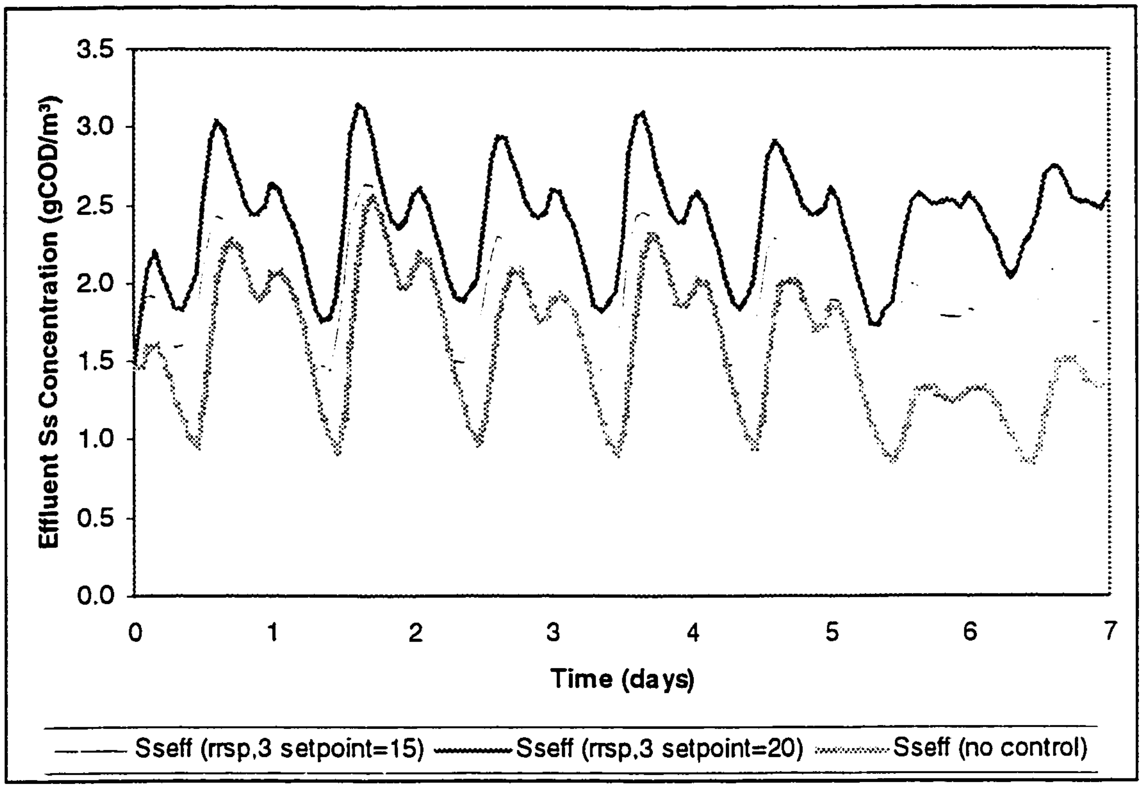

Figure 7.20: Effect of split range control on the readily biodegradable substrate concentration in the effluent

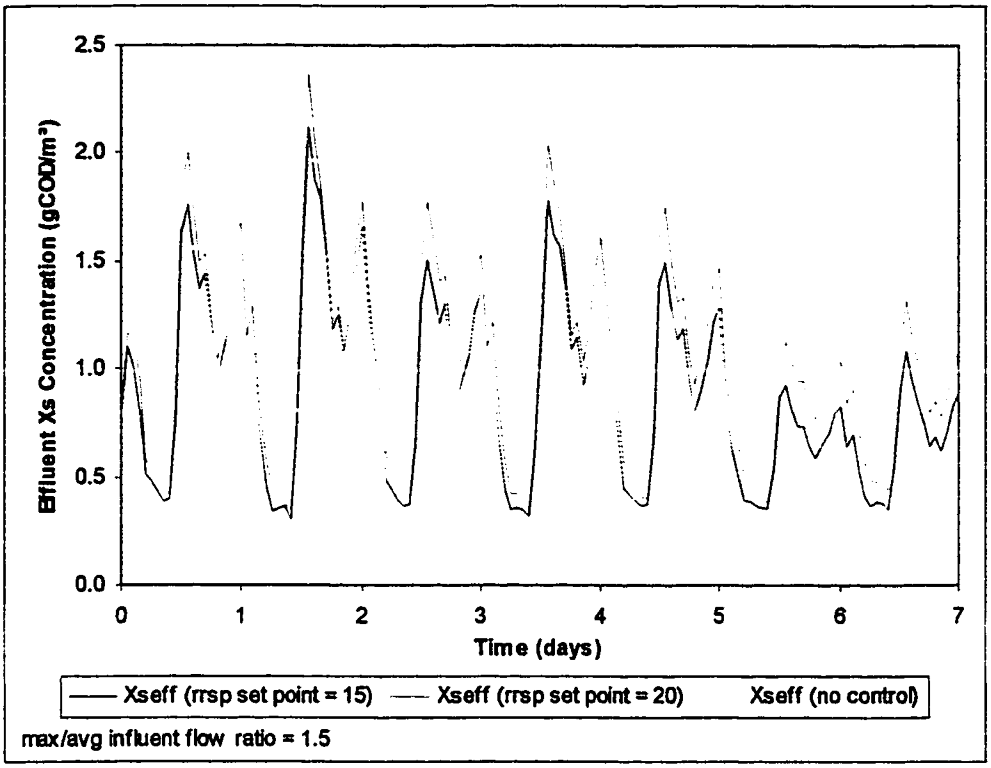

Figure 7.21: Effect of split range control on the slowly biodegradable concentration in the effluent

7.5.5 Effect of Control on Plant Performance Under Stress Loading Conditions

Simulations were conducted to test the performance of the controller under the five loading conditions over a 35-day period. The loading scenarios described in Section 5.4.5 are presented again in Table 7.9.

Table 7.9: Influent Loading Scenarios

Week	Influent Loading Period	Influent Loading Condition
1	day 0 to day 7	Normal diurnal influent loading
2	day 7 to day 14	50 per cent increase in the hydraulic and pollutant loading
3	day 14 to day 21	Normal diurnal influent loading
4	day 21 to day 28	Two storm events
5	day 28 to day 35	Normal diurnal influent loading

No observable differences were observed between the PI and split range controllers in terms of performance in maintaining the $rr_{sp,3}$ at the set point under the various loading scenarios. This can be seen from Figures 7.22 and 7.23.

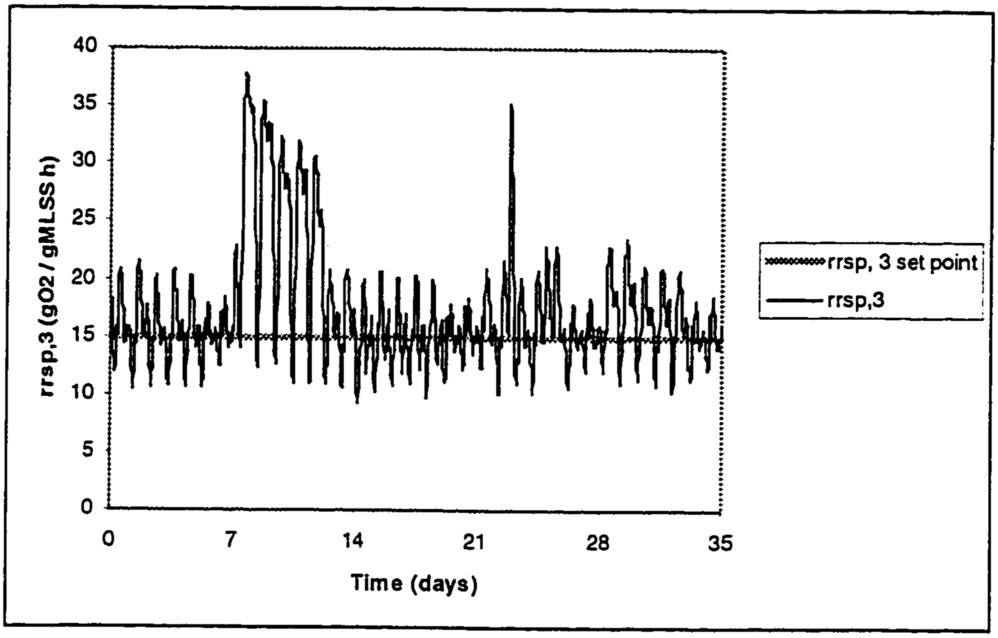

Figure 7.22: Performance of the 2-tank PI controller in maintaining the $rr_{sp,3}$ set point at 15 mg O_2 g^{-1}MLSS·h^{-1}

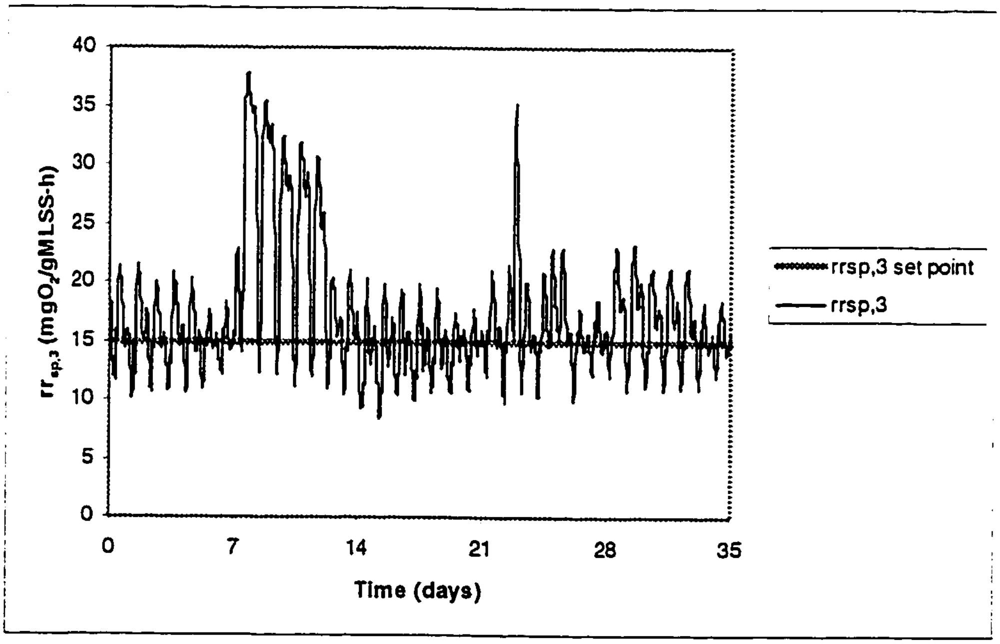

Figure 7.23: Performance of the split range controller in maintaining the $rr_{sp,3}$ set point at 15 mg O_2 g^{-1}MLSS·h^{-1}

The step feed control systems did not show any improvements in the effluent quality over uncontrolled operations. This is demonstrated by effluent COD concentration in Figure 7.24.

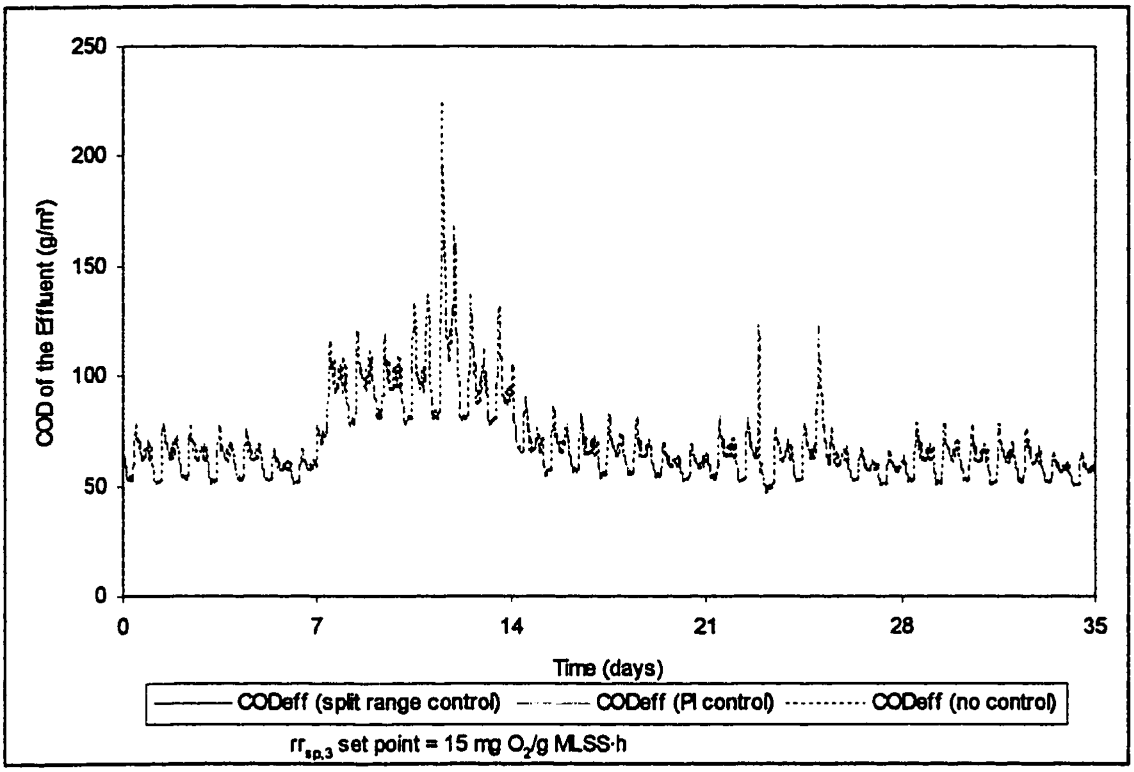

Figure 7.24: Effect of $rr_{sp,3}$ control on the effluent COD

Furthermore, the $rr_{sp,3}$ controllers did not demonstrate any impacts on energy costs. The daily energy costs were calculated using equations 6.1 and 6.2. The impact of the PI controller and the split range controller on the daily energy costs is shown by Figure 7.25.

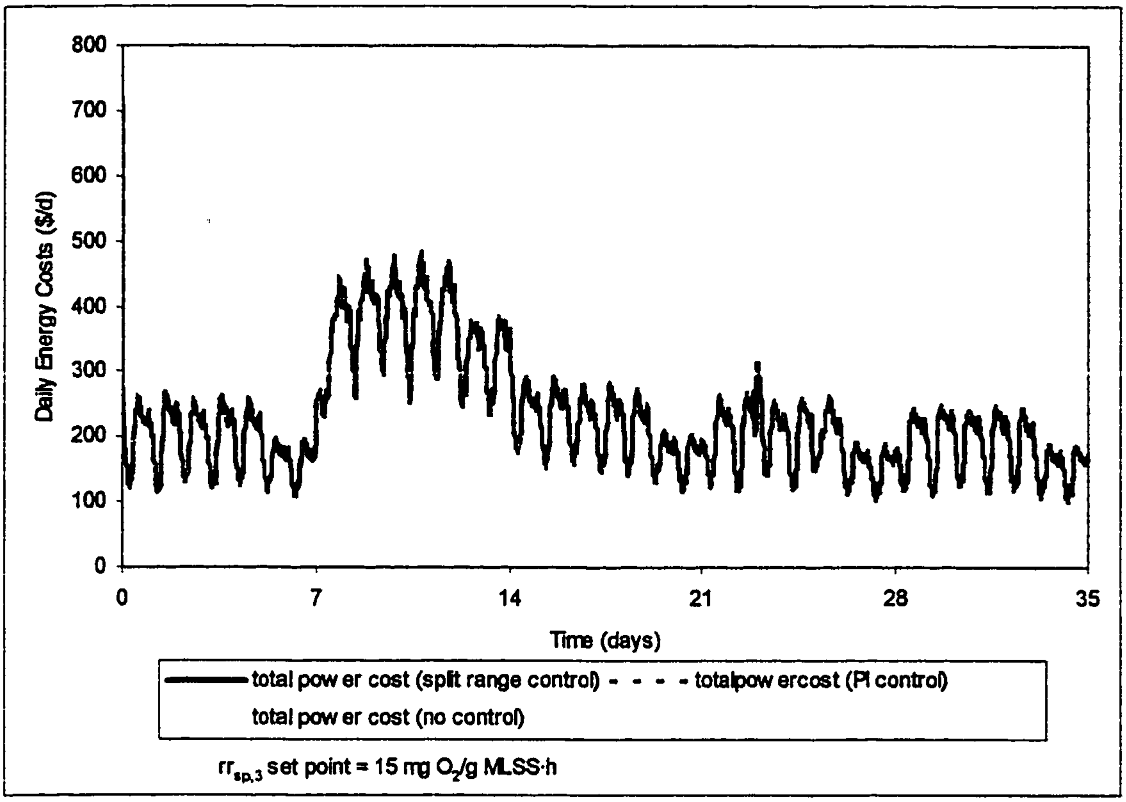

Figure 7.25: Effect of rr$_{sp,3}$ control on the daily energy costs

The only observable impact that the two controllers had over the uncontrolled case was the readily biodegradable substrate concentration in the effluent. This is demonstrated in Figures 7.26 and 7.27. It is shown in these figures that S_{seff} increases when $rr_{sp,3}$ is controlled. The reason for this is that the controller must increase Q_{t3} to bring $rr_{sp,3}$ to the set point, which is higher than uncontrolled rates. The result of increasing Q_{t3} is an increase in the S_S concentration in the 3rd compartment. The effluent consequently contains more S_s because the wastewater coming into the 3rd compartment receives less treatment time.

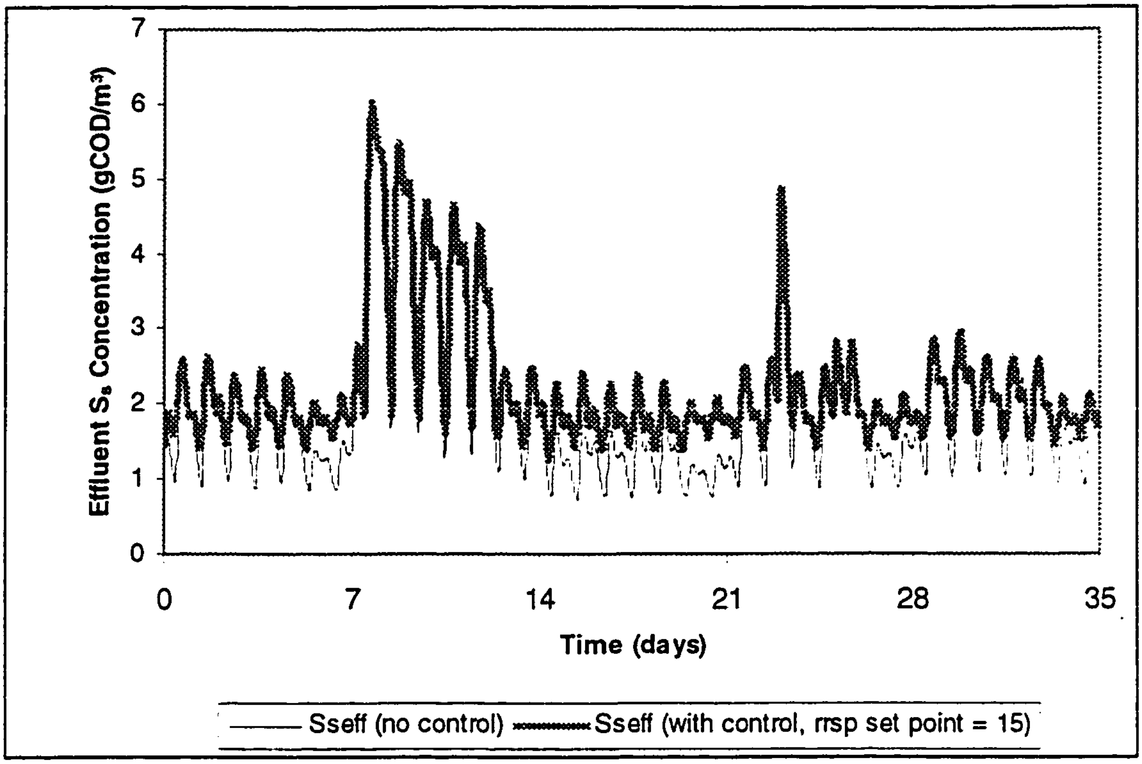

Figure 7.26: Effect of PI control on the readily biodegradable substrate concentration in the effluent

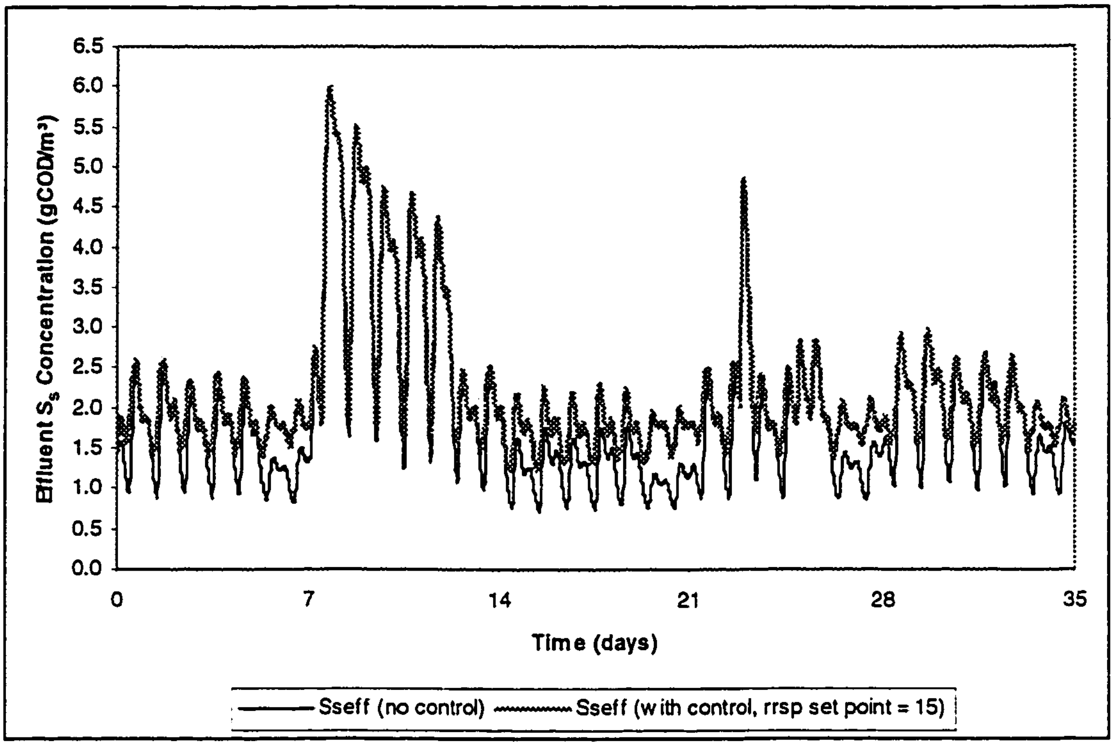

Figure 7.27: Effect of split range control on the readily biodegradable substrate concentration in the effluent

7.6 Summary on the Evaluation of the Specific Respiration Rate Control Strategy

The specific respiration rate control system proposed by Stephenson *et al.* (1983) was evaluated according to the methodology described in Section 5. This control strategy involved controlling the specific respiration rate in the last compartment at a set point by manipulating the influent feed distribution in a multi-staged step feed system. In addition to introducing a method for regulating the sludge activity, this strategy also provides a means for controlling the diurnal and stress loadings on a plant. A constant low value of $rr_{sp,3}$ in the last compartment indicates that the substrate concentration is low in the effluent.

The control strategy proposed by Stephenson *et al.* (1983) was implemented through two types of digital feedback controllers. The first controller used a PI algorithm and the second controller used a split-range algorithm.

The 2-tank digital PI controller distributes influent between the first and third compartments to bring $rr_{sp,3}$ to it's the set point. The fraction of influent distributed between the two tanks was automatically adjusted to minimize the difference between the $rr_{sp,3}$ set point and the actual measured $rr_{sp,3}$.

The split-range controller automatically adjusts the distribution of influent amongst the three aeration tanks to bring $rr_{sp,3}$ to its set point. This controller manipulates the influent flow distribution between the first and third compartments until the fraction of flow going to the third compartment exceeds 50 per cent. When this value is reached, the split range controller then distributes the influent between the second and third compartments to control $rr_{sp,3}$. Split range control of $rr_{sp,3}$ was implemented by designing two velocity-form digital PI controllers. One controller adjusts the flow distribution between the first and third compartments (PI_{split1}), and the other manipulates the flow distribution between the second and third compartments (PI_{split2}).

The results of the evaluation of the specific respiration rate controllers are summarized as follows:

1. By examining the open-loop response of $rr_{sp,3}$ to a step change in Q_{t3}, the following observations were made:
   - The response of $rr_{sp,3}$ to changes in Q_{t3} was very quick.
   - The relationship between $rr_{sp,3}$ and Q_{t3} follow first-order dynamics when the DO controller in the last compartment was disabled.
   - Interaction exists between the rr_{sp} controller and the DO controller. When the step feed rate to the third compartment increases the DO concentration drops. The DO controller responds to this drop by increasing K_La to bring the DO concentration back to the set point. The increase in K_La consequently causes the $rr_{sp,3}$ to overshoot.
   - A relative gain analysis showed that the interaction between the $rr_{sp,3}$-Q_{t3} loop and the DO_{t3}-K_La_{t3} loop was low and should not significantly impede control performance when the DO controller in the third compartment is de-tuned.
   - It was found that the $rr_{sp,3}$ controller performed best when full DO control ($K_c = 30$, $T_I = 0.05$ d) was used in the first two compartments and de-tuned DO control ($K_c = 10$, $T_I = 0.5$ d) was employed in the last compartment where $rr_{sp,3}$ was controlled.

2. According to the Nyquist stability criterion, the tuning constants ($K_c = 80{,}000$, $T_I = 0.005$ d) calculated for both the 2-tank PI and the split range controllers provide stable control performance over a range of operating conditions.

3. Under constant influent loading, the performance of the 2-tank PI and split range controllers to step changes in the set point were found to be as follows:
   - Both controllers were able to meet various set points quickly and with negligible offset.
   - Both controllers were unable to meet set points lower than the average value of $rr_{sp,3}$ measured during uncontrolled operations.

4. The following results were observed on the performance of the 2-tank PI and split range controllers under diurnal influent loading:
   - Both controllers were unable to meet the set point under diurnal influent conditions because of the high-frequency variations of the influent loading. Furthermore, oscillations in the respiration rate followed variations in the influent. These two results lead to the conclusion that the high-frequency variation of the influent is the major disturbance on control systems in the activated sludge process.

- The readily biodegradable substrate concentration in the effluent increased when both PI and split range control was employed to regulate $rr_{sp,3}$. Both controllers did however reduce fluctuations in the readily biodegradable substrate concentration in the effluent. These observations were also reported by Stephenson *et al.* (1983).

5. Simulations with the 2-tank PI controller and split range controller operating under stress loading conditions failed to show any real benefits in terms of effluent quality and energy costs over uncontrolled operations. The only impact that the rr_{sp} controllers seem to have on plant performance was an increase in the readily biodegradable substrate concentration in the effluent.

8 Respiration rate activity control strategy proposed by Sekine *et al.* (1988)

The control strategy by Sekine *et al.* (1988) proposes to control a parameter called the respiration rate activity ($rr_{activity}$) in a cascade control configuration. $rr_{activity}$ is ratio of the specific endogenous respiration rate ($rr_{sp,end}$) to the specific respiration (rr_{sp}) in the aeration tank. The objective of the strategy is to ensure that the biomass activity is sufficient to obtain the desired effluent quality. The underlying principal of the strategy is that when $rr_{activity}$ is close to 1, it is assumed that substrate removal is almost complete. In other words, $rr_{activity}$ is used as an indicator of the effluent quality. Therefore, by controlling $rr_{activity}$, the effluent quality may be controlled.

The cascade control configuration used in this strategy consists of a primary or outer loop in which $rr_{activity}$ is controlled in the aeration tank by manipulating S_O. In the secondary or inner loop, S_O is controlled by adjusting K_La. The S_O set point for the secondary loop is calculated in the primary loop. In this way, the effluent quality may be controlled by adjusting the amount of aeration. A diagram of the control configuration is shown in Figure 8.1.

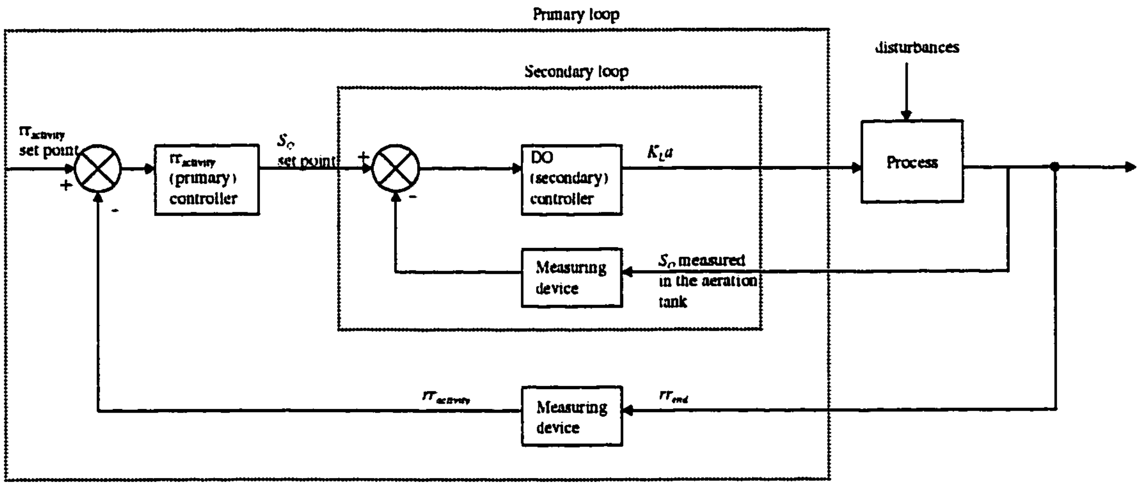

Figure 8.1: Cascade control of $rr_{activity}$

Sekine *et al.* (1988) defines $rr_{activity}$ as follows:

$$rr_{activity} = \frac{rr_{sp,end}}{rr_{sp}}$$

Eq. 8.1

where $rr_{sp,end}$ = specific endogenous respiration rate in the last compartment

rr_{sp} = specific respiration rate in the last compartment

The underlying idea of this strategy is that $rr_{activity}$ is assumed to be a good measure of the effluent quality and thus is controlled in the last compartment. $rr_{sp,end}$ occurs when the substrate concentration at the tank outlet is negligible. rr_{sp} at the tank outlet denotes the amount of substrate remaining. Therefore, when $rr_{activity}$ is close to 1, substrate removal is assumed to be almost complete.

The benchmark and methodology were used to evaluate this control strategy. The control strategy was implemented in the benchmark activated sludge plant and is depicted in Figure 8.2.

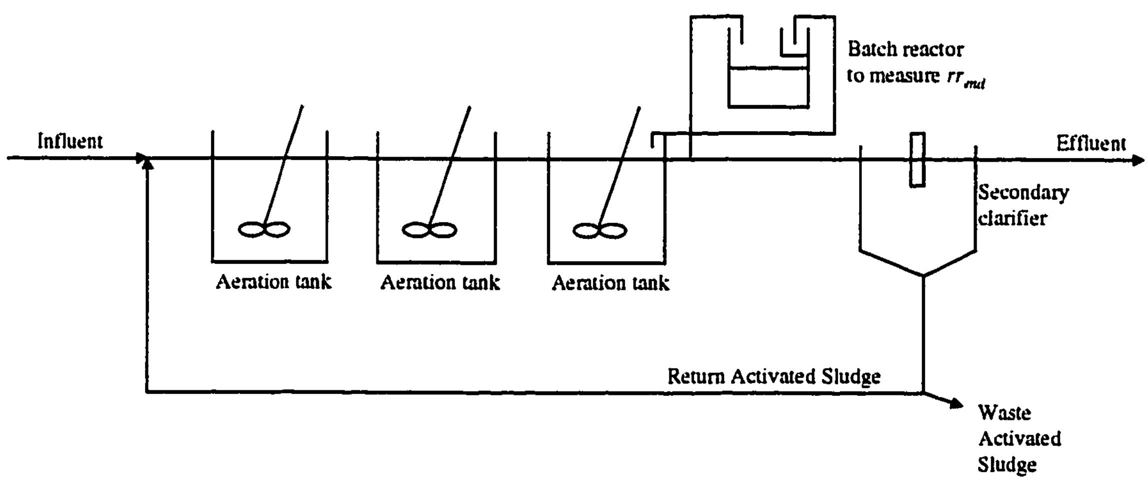

Figure 8.2: Plant layout used in simulation of $rr_{activity}$ controller

The plant was loaded with dry weather diurnal influent. Both the $rr_{activity}$ and DO controllers of the cascade configuration were implemented as digital proportional-integral (PI) controllers in the velocity form. The $rr_{activity}$ in the last compartment (i.e. the 3rd tank) was controlled.

Sekine *et al.* (1988) measured rr_{end} by running a batch test with sludge sampled from the last compartment at 5 a.m., which was the time when the influent loading was at a minimum. The batch test, ran for 4 hours, is used to generate an average rr_{end}-value. In this study, rr_{end} was measured by simulating a small bypass tank with an average retention time of 4 hours. Sludge from the last compartment is continuously re-circulated through the bypass tank. The respiration rate was continuously measured in the bypass for the $rr_{activity}$ controller. With an average retention time of 4 hours, it was assumed that the respiration rate in the bypass tank is equivalent with the rate obtained by Sekine *et al.* (1988).

Simulations indicated limitations with the controller proposed by Sekine *et al.* (1988) because of the complex relationship between $rr_{activity}$ and S_O in the aeration tank. Analysis of the open-loop response (i.e. occurs when both the $rr_{activity}$ and DO controllers are disabled) of $rr_{activity}$ to a step change in the S_O set point showed that $rr_{activity}$ and S_O are directly related. However, this was not the case for the close-loop response (i.e. when both controllers are turned on automatic) of the $rr_{activity}$ controller to changes in the set point. When the $rr_{activity}$ set point was increased from 0.5 to 0.8, the measured $rr_{activity}$ actually decreased to values lower than 0.5. The reason was that when the $rr_{activity}$ set point was increased, the $rr_{activity}$ controller responded by increasing the S_O set point. This consequently caused rr_{sp} to increase. Since $rr_{sp,end}$ was essentially constant and $rr_{activity}$ is inversely proportional to rr_{sp} (since $rr_{activity} = rr_{sp,end} / rr_{sp}$), the net effect was a decrease in $rr_{activity}$. This problem affects the stability of the process and therefore may not be a valid controller strategy. The GPS-X macro for the $rr_{activity}$ control strategy is found in Appendix B.4.

9 Dissolved Oxygen Control Strategy Proposed by Fujimoto *et al.* (1981)

Simulations were conducted to assess the feasibility of a dissolved oxygen control strategy proposed by Fujimoto *et al.* (1981). The objective of this strategy is to control the dissolved oxygen concentration (S_o) in the aeration tank by manipulating the air supply, i.e. the mass transfer coefficient (K_La), in a feedforward control configuration. The principal of the control strategy is that *rr* at the aeration tank inlet is the feedforward variable and is used as a measure of the disturbance in the influent. *rr* is used to calculate the value of K_La required to bring S_o to its set point. A diagram of the control configuration is depicted in Figure 9.1.

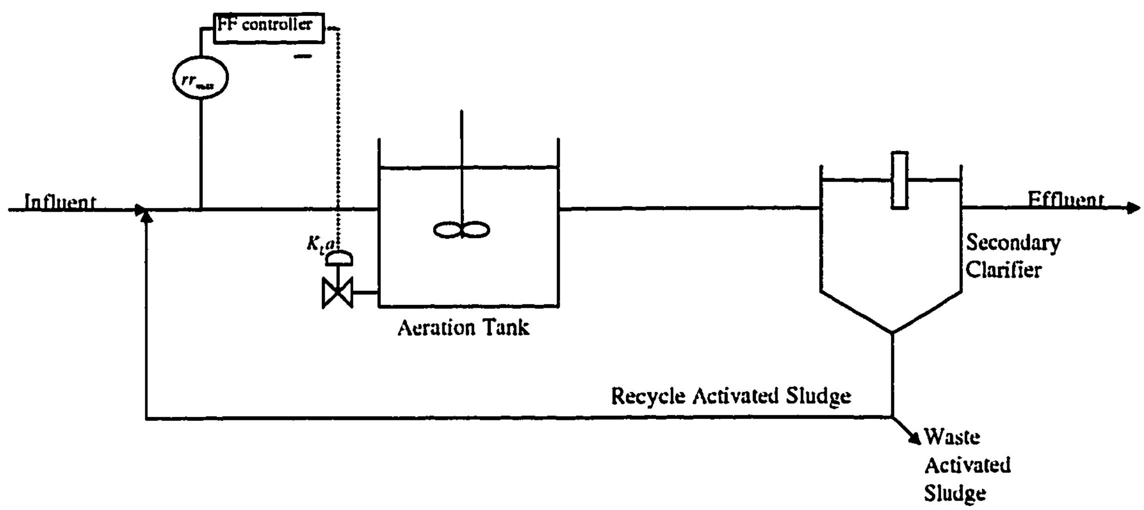

Figure 9.1: Feedforward control scheme in the activated sludge plant

The following expression was used by Fujimoto *et al.* (1981) to derive an equation for K_La:

$$\frac{dS_o}{dt} = K_La \cdot (S^*_o - S_o) - rr$$

Eq. 9.1

where S^*_o = saturation DO concentration

It was then assumed that the S_O can be controlled at a constant value, $S_{o,set}$. Therefore, $dS_o/dt = 0$. Consequently, K_La can then be expressed as a function of rr by re-writing Eq. 9.1 as follows:

$$K_La = \frac{rr}{\left(S^*_o - S_{o,set}\right)}$$

Eq. 9.2

The control strategy was implemented in the activated sludge plant described by Fujimoto *et al.* (1981) which consisted of an aeration tank and a secondary settler. The ASM No.1 (Henze *et al.*, 1987) and the double exponential settler model (Takács *et al.*, 1991) were employed in the simulations. It was not necessary to use the benchmark and methodology to evaluate the control strategy because preliminary simulations with the replicate plant were sufficient to make conclusions on the feasibility of the strategy. The influent flow and pollutant concentrations had sinusoidal variations. rr was measured continuously in the aeration tank.

The simulations pointed to a number of problems with the control strategy proposed by Fujimoto *et al.* (1981). The first problem results from the fact that an interaction existed between K_La, the manipulated variable, and rr, the measured disturbance. This makes the controller potentially unstable, depending on the initial conditions. Marlin (1995) states that for a feedforward controller, the feedforward variable, in this case rr, must *not* be influenced by the manipulated variable. The instability caused by the interaction between the manipulated and disturbance variables was evident in the simulations when an initial low value for K_La was used. The low K_La caused rr to decrease to small values. This in turn caused K_La to decrease rapidly to zero when it was subsequently computed from the new rr values. Therefore, in principle, the controller proposed by Fujimoto *et al.* (1981) is not a valid feedforward control configuration.

Another problem in simulating this strategy was that the control system essentially consists of two equations and two unknowns as follows:

Controller:	K_La	=	$f(rr)$
Process or process model:	rr	=	$g(K_La)$

Again, this system is potentially unstable because convergence depends on the equations themselves and the initial condition (i.e., the initial value of *rr*). Marlin (1995) states that feedforward control should not affect the stability of the process. These problems lead to the conclusion that the configuration proposed by Fujimoto *et al.* (1981) is not a suitable controller design.

10 Discussion and Conclusions

Many respirometry-based control strategies have been proposed in the literature but few have been rigorously tested or verified through simulation, and fewer have ever been implemented in a large-scale activated sludge plant. Furthermore, many of the control proposals are theoretical and do not provide adequate details on process implementation. Therefore, the objective of this study was to develop a simulation-based benchmark and methodology for testing control strategies.

Since many of the control strategies were proposed for completely different plant configurations, influent characteristics, process operations, etc., the benchmark and methodology developed in this study have shown to be useful testing tools because they provide a complete and consistent set of process conditions for conducting simulation studies. The benchmark and methodology include:

- well-accepted process models for the activated sludge process and secondary clarification process;
- a complete set of realistic influent data for both dry and wet weather conditions;
- values for the model parameters;
- initial values for the state variables;
- a standard activated sludge plant designed for the set of influent conditions.
- a six-step strategy for systematically implementing a control strategy in the benchmark plant; and
- a set of tests for determining the feasibility of a control strategy.

Most importantly, the methodology has shown to be useful in distinguishing the potentially good strategies from the strategies that will potentially fail.

Four respirometry-based control strategies from the literature were evaluated in this study. The first strategy was proposed by Stephenson *et al.* (1981) and involves manipulating the sludge wastage flow rate from the secondary clarifier to maintain the endogenous respiration rate of the sludge in the last compartment at a set point value. The objective of this control strategy was to maintain an adequate active biomass concentration to achieve the necessary treatment. The PI control algorithm was used to implement the control strategy. In this strategy, high organic loadings caused the respiration rate to increase, which resulted in the controller wasting more sludge. Conversely, during low loading conditions the respiration rate was low so that the controller wasted less sludge.

The respiration rate control strategy (Stephenson *et al.*, 1981) did not show any substantial benefits over uncontrolled operations during normal diurnal influent conditions. Simulations showed that the response of the respiration rate in the last compartment to changes in the wastage rate was slow. This resulted in the controller performing poorly under diurnal influent conditions in that it was not able to maintain the set point and dampen disturbances from the influent. Additionally, the controller did not show any substantial improvement over uncontrolled operations in terms of reducing soluble substrate concentrations from the effluent or daily energy costs. Another potential problem with this strategy is that large and frequent changes in the sludge wastage rate could disturb the settling process in the clarifier. The control strategy did however show real benefits when the plant experienced a 50 per cent increase in both influent flow and pollutant concentrations in that it was able to substantially reduce effluent COD and suspended solids concentrations over uncontrolled operations. The controller was also able to reduce daily energy costs during this time. Thus, this strategy seems potentially feasible and useful during stress loading conditions.

The second strategy that was evaluated was one proposed by Stephenson *et al.* (1983). This strategy involves controlling the specific respiration rate in the last compartment by adjusting the step feed rates. The objectives of the strategy are to regulate the active biomass concentration as well as to control the diurnal and stress loadings on a plant. Two control algorithms were used to implement the strategy. The 2-tank PI algorithm distributed the influent between the first and third compartments. The split range algorithm distributed the influent amongst all three compartments. Simulations showed that both controllers failed to show any benefits in terms of reduction in effluent concentrations and daily energy costs over uncontrolled operations during both diurnal influent and stress loading conditions. The control scheme caused problems with the effluent quality because the controller would increase the feed rate to the third compartment to bring the specific respiration rate to its set point. This resulted in higher substrate concentrations in the effluent over uncontrolled operations because there was less treatment time with the wastewater coming into the third compartment. Another problem with the strategy was that an interaction existed between the specific respiration rate controller and the DO controller in the third compartment. This problem was minimised by de-tuning the DO controller in the third compartment. Both controllers did however reduce variations in the effluent concentrations. Even though this control scheme did not improve the effluent quality or reduce daily energy costs over uncontrolled operations, it does show potential in reducing fluctuations in the plant. Therefore, this control strategy should be further investigated with more advanced control algorithms.

The simulations of the control strategies by Stephenson *et al.* (1981) and Stephenson *et al.* (1983) have shown that controller performance is greatly affected by the high-frequency variations in the influent flow and pollutant concentrations coming into an activated sludge plant. Due to the influent disturbances and multi-variable interactions, implementing respirometry-based control strategies with digital PI control designs provides inadequate control.

The third control strategy evaluated was by Sekine *et al.* (1988). In this strategy the respiration rate activity ($= rr_{sp,end} / rr_{sp}$) is controlled to a set point in a cascade control configuration. The primary loop is used to control $rr_{activity}$ by manipulating S_O in the aeration tank. By controlling $rr_{activity}$, the effluent quality may be maintained since $rr_{activity}$ is assumed to be a measure of the effluent quality. The secondary loop uses the S_O value calculated in the primary loop as a set point for controlling S_O in the aeration tank. K_La is manipulated in the secondary loop to maintain the S_O set point. Simulations showed that the controller proposed by Sekine *et al.* (1988) was unstable because of the complex interactions between the $rr_{activity}$ controller, S_O and rr_{sp}. The value of $rr_{activity}$ could never be stable because S_O is adjusted accordingly to bring $rr_{activity}$ to the set point. However in adjusting the value of S_O, the value of rr_{sp} is also changed. When rr_{sp}, changes, the value of $rr_{activity}$ consequently changes. These findings lead to the conclusion that the control strategy will potentially fail.

The fourth strategy was proposed by Fujimoto *et al.* (1981). This strategy involves controlling the DO in a feedforward configuration by manipulating K_La. The respiration rate at the aeration tank inlet is the feedforward variable and is used as a measure of the disturbance in the influent. The main problem found with this control strategy was that the interaction between the manipulated variable, K_La, and the feedforward variable, the respiration rate at the tank inlet, caused the controller to become unstable. This problem shows that the control strategy is not feasible.

The purpose of this study was not to compare the relative performance of the different control strategies. However, if a comparison were to be made based on the application of the methodology, the control strategy proposed by Stephenson *et al.* (1981) showed to be the most feasible because the controller was able reduce both the effluent COD concentration and the daily energy costs during stress loading conditions.

11 Recommendations

The simulation-based benchmark and methodology developed in this study was designed to test respirometry-based control strategies and be used as a tool to distinguish the potentially feasible control strategies from the ones that will potentially fail. A more comprehensive evaluation of the control strategies may be achieved by extending the methodology as follows:

- Include more quantitative measures of performance to enable comparisons of different control strategies. One example is to include the costs associated with operating a wastewater treatment plant.
- Expand the plant layout, which currently consists of three CSTRs in series followed by a circular secondary settler, to include equalization basins, combined sewer overflows, primary clarifiers, etc.
- Use other activated sludge systems, such as a carbon and nutrient removal plant, to test the control strategies.
- Incorporate noise into the measured variables to provide a more realistic control environment.
- Use the first three tests outlined in the methodology as acceptance test cases. They include:

  1) a good causal relationship between the controlled variable and the manipulated variable;
  2) the controller satisfies stability analysis criteria; and
  3) the controller is able to meet set point changes quickly and with little offset.

  During this series of testing, use a digital PID control algorithm. If the controller passes the acceptance tests, evaluate the controller's performance under diurnal influent conditions. If the controller is unable to attenuate the influent disturbances, implement the strategy with more advance control algorithms. Then perform a stability analysis of the new control design and test the controller under diurnal and stress loading conditions.

References

Andrews J.F. (1977). Specific oxygen utilization rate for control of the activated sludge process. *Prog. Wat Tech.*, **8** (6), 451-460.

Arthur R.M. (1984). Discussion: measurement and validity of oxygen uptake rate as an activated sludge control parameter. *J. Wat. Pollut. Control Fed.* **56**, 111-112.

Barnett M.W., Stenstrom M.K. and Andrews J.F. (1998). *Dynamics and Control of Wastewater Systems.* Vol.6, 2nd ed. Lancaster: Technomic Publishing Co., Inc.

Barnett M.W. and Takács I. (1994). Dynamic modelling of a large-scale wastewater treatment facility. In *Proceedings of the Chemical Engineering Chemputers Conference*, McGraw-Hill Science and Technology Group, Chemical Engineering Magazine, February 1-2, Houston, Texas.

Barnett M.W., Watson B.W. and Gall R.A.B. (1995). Dynamic modelling and simulation of wastewater treatment processes: application and state-of the art. *Water Environment and Technology.*

Bertrand-Krajewski J.-L., Lefebvre M., Lefai B. and Audic J.-M. (1995). Flow and pollutant measurements in a combined sewer system to operate a wastewater treatment plant and its storage tanks during storm events. *Wat. Sci. Tech.*, **31** (7), 1-12.

Bo-Nielsen J., Lindberg S., Harremoës P. (1993). Model based on on-line control of sewer systems. 6th *IAWQ Workshop on ICA*. June 17-25, Banff, Canada.

Brouzes P.H. (1979). Monitoring and controlling activated sludge plants in connection with aeration. *Prog. Wat. Tech.* **11** (3), 193-200.

Brouwer H., Klapwijk A. and Keesman K.J. (1994). Modelling and control of activated sludge plants on the basis of respirometry. *Wat. Sci. Technol.* **30** (4), 265-274.

Butler D., Friedler E. and Gatt K. (1995). Characterizing the quantity and quality of domestic wastewater inflows. *Wat. Sci. Tech.*, **31**(7), 13-24.

Campos H.M. and von Sperling M. (1996). Estimation of domestic wastewater characteristics in a developing country based on socio-economical variables.
Proceedings WQI '96. Singapore, June 23-28 1996. Vol. 5, 276-283.

Coen F., Vanderhaegen B., Boonen I., Vanrolleghem P.A. (1997). Improved design and control of industrial and municipal nutrient removal plants using dynamic models. *Wat. Sci. Tech.*, **35** (10), 53-61.

Coen F., Vanderhaegen B., Boonen I., Vanrolleghem P.A., Van Eyck L., and Van Meenen P. (1996). Nitrogen removal upgrade of a wastewater treatment plant within existing reactor volumes: a simulation supported scenario analysis. *Wat. Sci. Tech.*, **34** (3-4), 339-346.

Crabtree B., Earp W., Whalley P. (1996). Demonstration of the benefits of integrated wastewater planning for controlling transient pollution. *Wat. Sci. Tech.*, **33** (2), 209-218.

Dupont R. and Henze H. (1992). Modelling of the secondary clarifier combined with the activated sludge model No.1. *Wat. Sci Tech.* **25** (6), 285-300.

Endat Ltd. (1994). Procell user's guide. (Unpublished manual).

Ekster A. (1998). Automatic waste control. *Water Environment & Technology.*

Flanagan M. J. (1977). Control strategies for the activated sludge process. *Instrumentation Technology* (July), 35-43.

Fujimoto E., Iwahori K. and Sato N. (1981). Automatic measurement device of the respiration rate and experimental investigation on the constant DO control by using the device for the activated sludge process. *Wat. Sci. Tech.* 13, 193-198.

Funamizu N. and Takakuwa T. (1994). Simulations of the operating conditions of the municipal wastewater treatment plant at low temperatures using a model that includes the IAWPRC activated sludge model. *Wat. Sci. Tech.*, **30** (4), 105-113.

Fujimoto E., Iwahori K., and Sato N. (1981). Automatic measurement device of the respiration rate and experimental investigation on the constant DO control by using the device for the activated sludge process. *Wat. Sci Tech.* **13** (9), 193-198.

FWR. (1994). Urban Pollution Management Manual. *Foundation for Water Research.* **FR/CL0002.**

Giroux E., Spanjers H., Patry G.G., and Takács I. (1995). Dynamic modelling for operational design of a respirometer. *Wat. Sci. Tech.* **33** (1), 297-309.

Görgün E. (1995). Design of Step Feeding Activated Sludge Systems for Nitrogen Removal. Ph.D. Thesis, Istanbul Technical University.

Görgün E., Artan N., Orhon D., and Sözen S. (1996). Simulation of nitrogen removal by step feeding for Instanbul Wastewaters. *Wat. Sci. Tech.*, **33** (12), 259-264.

Gujer W., Krejci V., Schwarzenbach R. and Zobrist J. (1986). Storm event in the Glatt river valley: I. Documentation of results. In: Urban Storm Water Quality and Effects upon Receiving Waters. TNO committee on Hydrological Research, The Hague, The Netherlands, 235-249.

Haas C.N. (1979). Oxygen uptake rate as an activated sludge control parameter. *Journal of Water Pollution Control Federation,* 51, 938-943.

Haarma G.J. and Keesman K. (1995). Robust model predictive dissolved oxygen control. *Med. Fac. Landbouww. Univ. Gent,* **60**, 2415-2425.

Hemmis (West), Biomath, University of Gent, Belgium

Henze M., Grady C.P.L. Jr., Gujer W., Marais G.v.R. and Matsuo T. (1987). *Activated Sludge Model No. 1.* IAWPRC Scientific and Technical Reports No. 1. IAWPRC, London, England.

Henze M., Gujer W., Takahashi M., Matsuo T., Wentzel M. and Marais G.v.R. (1994). Activated sludge model no. 2. *IAWQ Scientific and Technical Reports, IAWQ Specialised Seminar: Modelling and Control of Activated Sludge Processes.* August 22-24, Copenhagen, Denmark.

Hill R.D. (1985). Dynamics and control of the solids-liquid separation in the activated sludge process. Ph.D. dissertion, Rice University, Houston, Tex.

Hydromantis Inc., 1685 Main St. West, Suite 302, Hamilton, Ontario, L85 1G5

Hydromantis, Inc. (1996). *GPS-X Technical Reference.* Hamilton, Ontario.

Hydromantis, Inc. (1996). *GPS-X User's Guide.* Hamilton, Ontario.

IAWQ. (1994). International Association on Water Quality: Specialized Seminar, Modelling and Control of Activated Sludge Processes, Kollekolle, Denmark, August 22-24.

IFAK. (1996). SIMBA 3.0 User's Guide. *Institut für Automation and Kommunikation,* Steinfeldstr.3, D-39179 Barleben, Germany.

Jones R.M., Dold P.L., Baker A.J., and Briggs T.A. (1994). Simulation for optimization of a biological wastewater treatment process at a petrochemical plant. *49th Purdue University Industrial Waste Conference Proceedings.* Lewis Publishers, Chelsea, Michigan.

Kalte P. (1990). The continuous measurement of short-time BOD. *In Proc. 5th IAWPRC Workshop.* Yokohama and Kyoto, July 25 – August 3, 59-56.

Kim C.W., Choi E.H., Kim B.G., Lee T.H. and Park T.J. (1995). Stable loading control in field-scale activated sludge plant using on-line respiration meter. *Submitted IAWQ Conference in Singapore, 1995.*

Klapwijk A., Spanjers H., and Temmink H. (1993). Control of activated sludge plants based on measurement of respiration rates. *Wat. Sci Tech.* **28** (11/12), 369-376.

Klapwijk A., Brouwer H., Vrolijk E., Kujawa K., and Kujawa K. (1998). Control of intermittently aerated nitrogen removal plants by detection endpoints of nitrification and denitrification using respirometry only. *Wat. Res.* **32** (5), 1700-1703.

Kurata G., Tsumura K., Nakamura S., Kuwahara M., Sato A., and Kanaya T. (1996). Retrofit of biological nutrient removal process assisted by numerical simulation with activated sludge model no. 2. *Wat. Sci. Tech.*, **34** (1-2), 221-228.

Leeuw E.J., Kramer J.F., Bult B.A., Wijcherson M.H. (1996). Optimization of nutrient removal with on-line monitoring and dynamic simulation. *Wat. Sci. Tech.*, **33** (1), 203-209.

Lessard P. and Beck M.B. (1988). Dynamic modeling of primary sedimentation. *J. Environ. Eng.*, **114**, 753-769.

Lessard P. and Beck M.B. (1990). Operational water quality management: control of storm sewage at a wastewater treatment plant. *J. Water Pollut. Control Fed.*, **62**, 810-819.

Lin S.H. (1996). Heat transfer model for biological wastewater treatment systems. *International Symposium on Heat Transfer 1996*. Tsinghua University, 766-771.

Londong J. (1994). Consequences of the behaviour of activated sludge plants with combined sewage inflows. *Wat. Sci. Tech.*, **30** (1), 139-146.

Luonsi A. and Halttunen S. (1997). Development of simulation system to combine production process and wastewater treatment: calibration of bleached kraft process model through dissolved oxygen organic matter in fibreline. *Wat. Sci. Tech.*, **35** (2-3), 15-23.

Marlin, T.E. (1995). Process Control – Designing Process and Control Systems for Dynamic Performance. Montreal: McGraw-Hill, Inc.

Metcalf & Eddy, Inc. (1991). Wastewater engineering – treatment, disposal and reuse. McGraw-Hill, Inc. (Revised by Tchobanoglous G. and Burton F. L.).

Mitchell & Gauthier Associates Inc. (1986). *Advanced Continuous Simulation Language*. Mitchell & Gauthier, Concord, Mass.

Orhon D. and Artan N. (1994). Modelling of Activated Sludge Systems. Technomic Publ. Co. Inc., Lancaster, USA.

Parker W.J., Bell J.P. and Melcer H. (1994). Modelling the fate of chlorinated phenols in wastewater treatment plants. *Environmental Progress*, **13** (2), 98-104.

Patry G.G. and Takács I. (1992). Dynamic modelling and simulation of large scale wastewater treatment plants using the general purpose simulator. *Dynamics and Control of the Activated Sludge Process* (Andrews J. F., Ed.). Lancaster, PA: Technomic Publishing Company, Inc., 245-275.

Rouleau S. and Lessard P. (1996). Impacts of storm flows on a small wastewater treatment plant: A case study. *Proceedings WEF Specialised Conference on Urban Wet Weather Pollution*, Quebec City, June 16-19 1996. 15/69-79.

Schroeter W.D., Dold P.L. and Marais G.V.R. (1984). The COD/VSS ratio of the volatile solids in the activated sludge process. Research Report. No. W45. Dept. of Civil Eng., Univ. of Cape Town, Cape Town, South Africa.

Schilling W.S., Andersson B., Nyberg U., Aspegren H., and Rauch W. (1996). Real time control of wastewater systems. *Journal of Hydraulic Research*, **34** (6), 785-797.

Schwarz A., Yahyavi B., Mösche M., Burkhardt C., Jördening H.-J, Buchholz K. and Reuss M. (1996). Mathematical modelling for supporting scale up of anaerobic wastewater treatment in a fluidized bed reactor. *Wat. Sci Tech.* **34** (5/6), 501-508.

Schwarz A., Mösche M., Wittenberg A., Jördening H.-J., Buchholz K. and Reuss M. (1997). Mathematical modelling and simulation of an industrial scale fluidized bed reactor for anaerobic wastewater treatment – scale-up effect on pH-gradients. *Wat. Sci. Tech.* **36** (6-7), 219-227.

Sekine T., Sato S., Furuya N. and Sunuhara H. (1988). Supervision and control of the activated sludge process utilizing the respiration rate activity. *Environmental Technology Letters* **9**, 1317-1327.

Sintic A., Rolfs T., Freund M. and Dorgeloh E. (1998). Dynamic simulation for upgrading of wastewater treatment plants – an assessment of treatment plant performance with regard to the EC-directive concerning urban wastewater treatment. *Wat. Sci. Tech.* **37** (9), 73-79.

Sørensen P.E. (1990). Evaluation of operational benefits of the activated sludge process using step feed control strategies. *Prog. Wat. Tech.* 12, Toronto, 109-125.

Spanjers H., Vanrolleghem P.A., Nguyen K., Vanhooren H., Patry G.G. (1998a). Towards a simulation benchmark for evaluating respirometry-based control strategies. *Wat. Sci. Tech.* **37**(12), 219-226.

Spanjers H., Vanrolleghem P.A., Olsson G. and Dold P.L. (1998b). Respirometry in control of the activated sludge process; Principles. Scientific and Technical Report No. 1, ISBN 1 900222043 IAWQ, London UK.

Stenstrom M.K. and Andrews J.F. (1979). Real-time control of the activated sludge process. *J. Environ. Eng.*, **105**, 245-260.

Stephanopoulos, G. (1984). *Chemical Process Control – An Introduction to Theory and Practice.* New Jersey: Prentice-Hall, Inc.

Stephenson J.P., Monaghan B. A., Laughton P. J. (1981). Automatic control of solids retention time and dissolved oxygen in the activated sludge process. *Wat. Sci. Tech.* **13** (10/11), 751-758.

Stephenson J. P., Monaghan B. A., Yust L. J. (1983). Pilot scale investigation of computerized control of the activated sludge process. Report SCAT-12, Environmental Protection Service, Environment Canada, Ottawa, K1A 1C8.

Stokes L., Takács I., Watson B., and Watts J. B. (1993). Dynamic modelling of an ASP sewage works – case study. *Wat. Sci. Tech.*, **25** (11-12), 151-161.

Takács I., Patry G.G. and Nolasco D. (1991). A dynamic model of the clarification-thickening process. *Wat. Res.*, **25** (10), 1263-1271.

Takács I., Patry G.G., Watson B., and Gall B. (1995). Case studies in dynamic modelling of large-scale wastewater treatment plants. *Mathematical Modelling of Systems*, **1** (3), 185-199.

Takács I., Patry G.G., Watson B., and Shivji M. (1993). Dynamic modeling of the Gold Bar wastewater treatment plant. *66th Annual Conference & Exposition*. October 3-7, 1993, Anaheim, California.

Vanhooren H. and Nguyen K. (1996). *Development of a simulation protocol for evaluation of respirometry-based control strategies*. Technical Report. University of Gent, Belgium and University of Ottawa, Canada.

Vanrolleghem P.A., Jeppsson U., Carstensen J., Carlsson B. and Olsson G. (1996)

Integration of WWT plant design and operation – A systematic approach using cost functions. *Wat. Sci. Tech.*, **34** (3-4), 159-171.

Verbanck M. (1995). Variabilité des charges solides en suspension à l'exutoire des réseaux de collecte. Journée d'étude CB-IAWQ, Liège, 31 May 1995.

Vitasovic Z.Z. (1986). An integrated control strategy for the activated sludge process. Ph.D. thesis, Rice University.

Vitasovic Z.Z. (1989). Continuous settler operation: a dynamic model. In *Dynamic Modelling and Expert Systems in Wastewater Engineering* (Edited by Patry G. G. and Chapman D.). Lewis, Chelsea, Mich. 59-81.

Vitasovic Z.Z. and Andrews J.F. (1989). An integrated dynamic model and control system for activated sludge wastewater treatment plants. Part II – control systems. *Wat. Pollut. Res. J. Can.* **24**, 497-522.

APPENDIX A: Simulation-Based Methodology

A.1 IAWQ ASM1 (Henze *et al.*, 1987) Composite Variables

A.1.1 COD and Suspended Solids Composite Variables

The COD and suspended solids composite variables involve both the state variables of the IAWQ ASM1 (Henze *et al.*, 1987) and stoichiometric fractions. Since all the state variables are in units of g COD m^{-3}, the COD composite variables are simply a sum of the state variables. The soluble COD (*SCOD*) is a sum of the S_I and S_S, while the particulate COD (*XCOD*) is a sum of X_S, X_{BH}, X_{BA}, X_P and X_I. The *SCOD* and *XCOD* make up the total COD. (Hydromantis, 1996).

The suspended solids composite variable is calculated from *XCOD* by dividing the XCOD:VSS ratio (*icv*), which changes the units of *XCOD* to g VSS m^{-3}, resulting in the composite volatile suspended solids (*VSS*). To calculate the suspended solids composite variable (*X*), the *VSS* is divided by the VSS:TSS (total suspended solids) ratio (*ivt*) (Hydromantis, 1996). The COD and suspended solids composite variables and their relationship to the state variables are shown in Figure A.1.

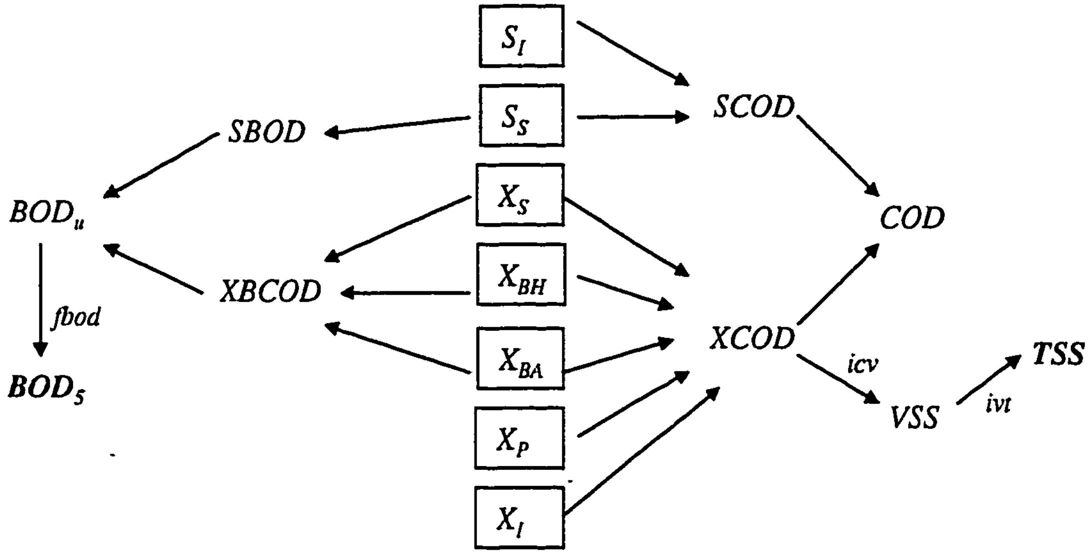

SBCOD = soluble biodegradable COD
XBCOD = particulate biodegradable COD
fbod = BOD_5/BOD_{20}

Figure A.1: COD and suspended solids composite variables and their relationship to the state variables

A.1.2 Nitrogen Composite Variables

The soluble (*STKN*) is the sum of S_{NH} and S_{ND}. *TKN* is the sum of *STKN* and X_{ND}. The total nitrogen is the sum of *TKN* and S_{NO}. Note that inorganic nitrogen is not considered (Hydromantis, 1996). The nitrogen composite variables are shown in Figure A.2.

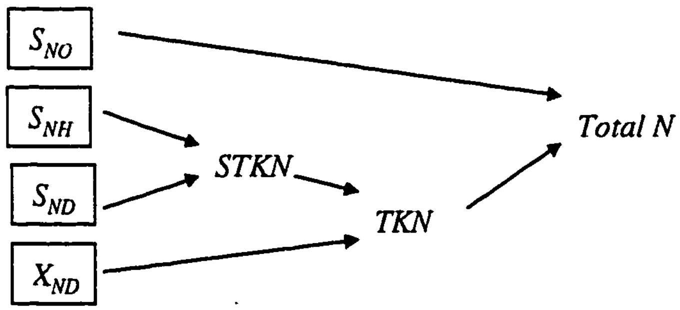

Figure A.2: Nitrogen composite variables and their relationship to the state variables

A.2 Constant Influent

Average values for the flow rate, soluble concentration particulate concentrations of the dynamic influent data were used as estimates for the constant influent data. They are listed as follows:

Influent flow rate:

$$\overline{Q} = 20{,}000\frac{m^3}{d}$$

Influent soluble concentrations:

$$\overline{S}_S = 80\frac{g}{m^3}$$

$$\overline{S}_{ND} = 8\frac{g}{m^3}$$

$$\overline{S}_{NH} = 35\frac{g}{m^3}$$

$$\overline{S}_I = 30\frac{g}{m^3}$$

Influent particulate concentrations:

$$\overline{pCOD} = \overline{SS}\cdot\frac{COD}{SS} = 200\cdot 1.33 = 266\frac{g}{m^3}$$

$$f_{\overline{X}_I} = 0.1 + 0.15\cdot\frac{\left(\overline{Q} - Q_{\min}\right)}{\left(Q_{\max} - \overline{Q}_{\min}\right)} = 0.1 + 0.15\cdot\frac{20000 - 10000}{30000 - 10000} = 0.175$$

$$\therefore \overline{X}_I = 0.175\cdot\overline{pCOD} = 46.55\frac{g}{m^3}$$

$$\overline{X}_{BH} = 0.1\cdot 266 = 26.6\frac{g}{m^3}$$

$$f_{\overline{X}_S} = 0.725 = 1 - 0.175 - 0.1$$

$$\therefore \overline{X}_S = 192.85\frac{g}{m^3}$$

$$\overline{X}_{ND} = 10\frac{g}{m^3}$$

A.3 Initial values for state variables

A.3.1 Carbon removal system with nitrification

Initial conditions for the operation of the aeration tanks are presented in Table A.1. Initial conditions for the settler are presented in Table A.2

Table A.1: Initial values for the state variables in the three aeration tanks

		Tank 1	*Tank 2*	*Tank 3*
S_I	(g COD m^{-3})	30	30	30
S_S	(g COD m^{-3})	1.70284	0.834966	0.652598
X_I	(g COD m^{-3})	1453.27	1453.26	1453.26
X_S	(g COD m^{-3})	83.437	56.042	43.2142
X_{BH}	(g COD m^{-3})	3034.28	3034.66	3024.89
X_{BA}	(g COD m^{-3})	221.524	222.043	221.824
X_U	(g COD m^{-3})	739.052	743.042	747.022
S_{NO}	(g COD m^{-3})	34.8752	38.9222	40.0165
S_{NH}	(g COD m^{-3})	3.35264	0.288316	0.0825584
S_{ND}	(g COD m^{-3})	1.1771	0.690476	0.557398
X_{ND}	(g COD m^{-3})	5.17189	4.03687	3.34499
K_La	(d^{-1})	323.578	120.071	68.3828

Table A.2: Initial values for the settler state variables

State Variable	Concentration (g COD m^{-3})
S_I	30
S_s	0.652598
S_{NO}	40.0165
S_{NH}	0.0825585
S_{ND}	0.55739
Suspended solids:	
Layer 1	30.853

State Variable	Concentration (g COD m^{-3})
Layer 2	58.8579
Layer 3	148.276
Layer 4	745.798
Layer 5	745.798
Layer 6	745.798
Layer 7	3627.16
Layer 8	5429.49
Layer 9	6682.3
Layer 10	8111.59

A.3.2 Carbon and nitrogen removal system

Initial conditions for the operation of the aeration tanks are presented in Table A.3. Initial conditions for the settler are presented in Table A.4.

Table A.3: Initial values for the state variables in the aeration tanks

		Tank 1	*Tank 2*	*Tank 3*
S_I	(g COD m^{-3})	30	30	30
S_S	(g COD m^{-3})	1.53354	1.18937	1.00779
X_I	(g COD m^{-3})	1342.51	1342.51	1342.5
X_S	(g COD m^{-3})	85.4197	67.1563	58.9304
X_{BH}	(g COD m^{-3})	2441.88	2448.22	2445.65
X_{BA}	(g COD m^{-3})	195.452	196.478	196.792
X_U	(g COD m^{-3})	758.074	759.394	761.15
S_{NO}	(g COD m^{-3})	11.204	16.1114	17.8849
S_{NH}	(g COD m^{-3})	6.8989	2.16854	0.516989
S_{ND}	(g COD m^{-3})	0.908818	0.871439	0.788404
X_{ND}	(g COD m^{-3})	5.83949	4.74999	4.34178
K_La	(d^{-1})	0.0	241.011	104.89

Table A.4:Initial values for the settler state variables

State Variable	Concentration (g COD m^{-3})
S_I	30
S_s	1.00779
S_{NO}	17.8849
S_{NH}	0.51699
Suspended solids:	
Layer 1	29.4078
Layer 2	55.8011
Layer 3	136.944
Layer 4	652.445
Layer 5	652.445
Layer 6	652.445
Layer 7	652.445
Layer 8	1492.55
Layer 9	4843.41
Layer 10	7089.9

A.4 Initial Design of the ASP

The initial stages of designing a standard activated sludge plant involved assuming values for:

- the average influent flow,
- influent biodegradable COD concentration,
- number of aeration tanks,
- total hydraulic retention time in all three aeration tanks,
- mean cell residence time or sludge age,
- MLSS concentration,
- recycle ratio,
- overflow rate, surface area and depth of the settler.

The following discussion outlines the general, initial design of the C-removal, C-removal and nitrification, and C- and N-removal systems.

A.4.1 Carbon removal system

The average influent flow and hydraulic retention time were used to estimate the volumes of the three aeration tanks as follows:

BOD_∞	=	bCOD (biodegradable COD)
	=	300 g m^{-3}
Q_{avg}	=	average flow
	=	20,000 m^3 d^{-1}
hydraulic retention time in the three CSTRs	=	8 h

Total volume of the 3 tanks:

V_{tot}	=	hydraulic retention time in the three CSTRs × Q_{avg}
	=	8 h / 24 × 20000 m^3 d^{-1}
	=	6500 m^3

The biomass loading rate was calculated based on the assumption that the MLSS concentration is 4 kg MLSS m^{-3}:

biomass loading rate = $(bCOD \times Q_{avg}) / (X \times V_{tot})$

= $(300\ g\ COD\ m^{-3} \times 20000\ m^3\ d^{-1}) / (4\ kg\ MLSS\ m^{-3} \times 6500\ m^3 \times 1000)$

= 0.231 kg COD/kg MLSS.d

From the biomass loading rate, the volumetric loading rate is calculated as follows:

volumetric loading rate = biomass loading rate × X

= $0.923\ kg\ COD\ m^{-3}\ d^{-1}$

Values for the biomass and volumetric loading rates show that the design of the carbon removal plant is reasonable.

The DO concentration in each of the three aeration tanks is maintained at 2 g m^{-3} with digital PI controllers.

The settler was designed to operate with an overflow velocity of 1 m h^{-1}, therefore it has a surface area of 800 m^2. An average depth of 3 m and a recycle ratio of 1 were chosen. This results in a hydraulic retention time of 1.6 hours. The feed point is taken at 1.95 m from the bottom of the settler.

To avoid nitrification the mean cell residence time was limited to 4 days. As a result, the mass of sludge wasted per day is:

mass of sludge wasted per day = $X_w \times Q_w$

= $V \times X / SRT$

= $(V_{tot} \times X_{tot} + h \times A \times (X_{r,9} + X_{r,10}))/SRT$

= $(6500 \times 4000 + 0.3 \times 800 \times (5000 + 10000))/4$

= 7,400,000 g d^{-1}

= 7400 kg d^{-1}

where

h = height of 1 layer in the settler (10 layers in total)

A = surface area of the settler

$X_{r,n}$ = sludge concentration in layer n of the settler, only the sludge in the 2 lower layers was considered (estimated concentrations)

X_w = $X_{r,10}$

= sludge concentration in the underflow of the settler

= 10000 g m^{-3}

Therefore, the sludge wastage rate is:

$Q_w = 740 \text{ m}^3 \text{ d}^{-1}$

A.4.2 Carbon removal system with nitrification

To obtain complete nitrification the mean cell residence time was estimated to be 15 days. As a result, the mass of sludge wasted per day for this system is:

$$
\begin{aligned}
\textit{daily mass of sludge wasted} &= X_w \times Q_w \\
&= (V_{tot} \times X_{tot} + h \times A \times (X_{r,9} + X_{r,10}))/SRT \\
&= (6500 \times 4000 + 0.3 \times 800 \times (5000 + 10000))/15 \\
&= 1{,}973{,}333 \text{ g d}^{-1} \\
&= 1973 \text{ kg d}^{-1}
\end{aligned}
$$

where

X_w = 10000 g m^{-3}

Therefore, the rate of sludge wasting is:

Q_w = $197 \text{ m}^3 \text{ d}^{-1}$

A.4.3 Carbon and nitrogen removal system

In this design, the first tank is anoxic and used for denitrification. The remaining two tanks are modeled for carbon removal and nitrification. There are two recycle streams: 1) solids from the settler are recycled to the first tank, and 2) an internal recycle of the nitrate-rich mixed liquor from the third tank to the first tank. The DO concentrations in the last two tanks are maintained at 2 g m^{-3} with PI controllers.

BOD_∞	= bCOD
	= 300 g m^{-3}
Q_{avg}	= 20,000 m^3 d^{-1}
hydraulic retention time in the CSTRs	= 12 h

Total volume of the 3 tanks:

V_{tot}	= hydraulic retention time in the CSTRs × Q_{avg}
	= 12 h / 24 × 20000 m^3 d^{-1}
	= 10000 m^3

Again, the biomass loading rate is based on a MLSS value of 4 kg m^{-3}:

biomass loading rate	$= (bCOD \times Q_{avg}) / (X \times V_{tot})$
	= (300 g COD m^{-3} × 20000 m^3 d^{-1}) / (4 kg MLSS m^{-3} × 10000 m^3 × 1000)
	= 0.150 kg COD/kg MLSS.d

The resulting volumetric loading is then calculated as follows:

volumetric loading rate	= biomass loading rate × X
	= 0.6 kg COD $^{m-3}$ d^{-1}

The total mean cell residence time was set to 15 days, therefore the mass of sludge wasted per day is:

mass of sludge wasted	$= X_w \times Q_w$
	= (10000×4000+0.3×800×(5000+10000))/15

$= 2{,}906{,}667 \text{ g d}^{-1}$

$= 2907 \text{ kg d}^{-1}$

where,

$X_w \quad = \quad 10000 \text{ g m}^{-3}$

The resulting wastage rate is:

$Q_w \quad = \quad 291 \text{ m}^3 \text{ d}^{-1}$

The design of the settler is identical to that of the carbon removal plant.

A.5 Final designs for the activated sludge systems

A.5.1 Carbon removal system with nitrification

Nitrification was nearly complete with a sludge age of 15 days. Q_w was changed to 250 m3 d^{-1} because $X_w = 6500$ g COD m^{-3}.

First approximation of the initial values for the state variables used in the operation of the aeration tanks and the second settler are presented in Tables A.5 and A.6, respectively.

Table A.5: Approximate initial values for the state variables

State Variable		*Tank 1*	*Tank 2*	*Tank 3*
S_I	(g COD m^{-3})	30	30	30
S_s	(g COD m^{-3})	10	5	2
X_I	(g COD m^{-3})	1400	1400	1400
X_s	(g COD m^{-3})	100	80	40
X_{BH}	(g COD m^{-3})	2900	2900	2900
X_{BA}	(g COD m^{-3})	200	200	200
S_{NO}	(g COD m^{-3})	30	33	33
S_{NH}	(g COD m^{-3})	5	0	0
S_{ND}	(g COD m^{-3})	0	0	0
X_{ND}	(g COD m^{-3})	0	0	0
K_La	(d^{-1})	230	150	90

Table A.6: Approximate initial values of the state variables in the settler

State Variable	Concentration (g COD m^{-3})
S_I	30
S_s	1
S_{NO}	33
S_{NH}	0
S_{ND}	0
Suspended solids:	
Layer 1	20
Layer 2	100
Layer 3	200
Layer 4	900
Layer 5	900
Layer 6	900
Layer 7	900
Layer 8	2000
Layer 9	4000
Layer 10	6500

The DO-controllers maintained the DO concentration in each of the three compartments at 2 g m^{-3} with the following values for the PI control parameters:

Compartments 1 and 2:	K_c	=	30
	T_I	=	0.05 d
Compartment 3:	K_c	=	20
	T_I	=	0.05 d

A.5.2 Carbon and nitrogen removal system

The total volume was reduced to 8000 m^3 to maintain a reasonable sludge concentration in the system. Additionally, Q_w was reduced to 270 m^3 d^{-1}.

First approximation of the initial values for the state variables used for the aeration tanks and the secondary settler are presented in Tables A.7 and A.8, respectively.

Table A.7: Approximate initial values for state variables

State Variable		*Tank 1*	*Tank 2*	*Tank 3*
S_I	(g COD m^{-3})	30	30	30
S_s	(g COD m^{-3})	10	5	2
X_I	(g COD m^{-3})	1800	1800	1800
X_s	(g COD m^{-3})	250	230	210
X_{BH}	(g COD m^{-3})	3000	3000	3000
X_{BA}	(g COD m^{-3})	200	200	200
S_{NO}	(g COD m^{-3})	10	12	12
S_{NH}	(g COD m^{-3})	9	2	0
S_{ND}	(g COD m^{-3})	0	0	0
X_{ND}	(g COD m^{-3})	0	0	0
K_La	(d^{-1})	0	250	100

Table A.8: Approximate initial values of the state variables in the settler

State Variable	Concentration (g COD m^{-3})
S_I	30
S_s	1
S_{NO}	12
S_{NH}	0
S_{ND}	0
Suspended solids:	
Layer 1	20
Layer 2	100
Layer 3	200
Layer 4	900
Layer 5	900
Layer 6	900
Layer 7	900
Layer 8	900
Layer 9	900
Layer 10	5000

The DO-controllers maintained the DO concentration in the second and third compartments at 2 g m^{-3} with the following values for the PI control parameters:

Compartment 2:	K_c	=	30
	T_I	=	0.05 d
Compartment 3:	K_c	=	20
	T_I	=	0.05 d

APPENDIX B: GPS-X Macros

B.1 Macro for the On-Off Respiration Controller

```
!******************************************************************
!PUT HERE USER DEFINED MACROS
!This section is for definitions, it will be executed
!only during loading of the program

!This macro calculates settling parameters based on SVI and
CLARIF
macro settlingcorrelation(o)
      vmax&o=bound(50.0,2000.0,cc1+cc2*svi&o   +cc3*svi&o**2)
      rhin&o=bound(1.e-5,1.e-2,cc4+cc5*svi&o   +cc6*svi&o**2)
      rflo&o=bound(1.e-5,1.e-2,cc7+cc8*clarif&o+cc9*clarif&o**2)
macro end
!******************************************************************
macro userinitialsection
!INITIAL SECTION
!Macros called here will be executed in the initial section
!Don't put macro definitions here

schedule wason .at. wasstart/24.0
schedule wasoff .at. wasend/24.0

macro end
!******************************************************************
macro userderivativesection
!DERIVATIVE SECTION
!Macros called here will be executed in the derivative section
!Don't put macro definitions here

!This belongs to the on-off controller
```

```
hilimour=oursetpoint
lolimour=oursetpoint-0.01
procedural
 if (qwas.le.minflow.and.oldqwas.gt.minflow) then
     wastime=t*24.0-iwastime
 endif
 oldqwas=qwas
end

!calculate fine on effluent quality as a measure of control
performance

chodeff = sseff+sieff+xseff+xieff+xbheff+xbaeff !COD in effluent
bod5eff = 0.65*(sseff+xseff+(1-0.08)*(xbheff+xbaeff)) !BOD5 in
effluent
solids = (1/1.33)*(xseff+xieff+xbheff+xbaeff) !suspended solids
in effluent
n = snheff+sndeff+xndeff+snoeff !nitrogen in effluent
p = 5 !phosphorous in effluent
norganic = (qconww*1000/180)*(0.35*solids/500+0.45*&
(2*bod5eff+chodeff)/1350)*(0.4+0.6*(365/225))
nnutrients = (qconww*365/10000)*(n+p)
finee77 = ((25)*(1*norganic+1*nnutrients))/365 !effluent quality
fine ECU/d
finebef77 = ((1000)*(1*norganic+1*nnutrients))/365 !fine in BEF/d
finena77 = ((45.45)*(1*norganic+1*nnutrients))/365 !fine in
cdn$/d
klatot = klat1+klat2+klat3 !/d
airflow = ((klatot/24)+0.11)/0.0018 !m3/h
mairflow = 1.225*airflow !kg/h
oxyflow = 0.2*mairflow !kg/h
oxypower = oxyflow/aireff !kw
befcost = 3 !cost of electricity in Belgium BEF/kwh
cdncost = 0.08 !cost of electricity in Can $/kwh
aircostbef = oxypower*24*befcost !BEF/d
```

```
aircostna = oxypower*24*cdncost !cdn$/d
costtotalbef = finebef77 + aircostbef !BEF/d
costtotalna = finena77 + aircostna !cdn$/d
sourt1 = 1.33*ourt1/(xbht1+xbat1) !g O2/h/g MLSS
sourt2 = 1.33*ourt2/(xbht2+xbat2) !g O2/h/g MLSS
sourt3 = 1.33*ourt3/(xbht3+xbat3) !g O2/h/g MLSS
iseo = integ((ourt3-setpourt3)**2,0.0)
iaeo = integ(abs(ourt3-setpourt3), 0.0)
!ises = integ((sourt3-setpsourt3)**2,0.0)
!iaes = integ(abs(sourt3-setpsourt3), 0.0)

macro end

!*****************************************************************
macro userdynamicsection
!DYNAMIC AND DISCRETE SECTIONS
!Macros called here will be executed in the dynamic section.
!(discretes plus code to be executed every communication
interval)
!Don't put macro definitions here

discrete wason
 ctrlour=.true.
 iwastime=t*24.0
 schedule wason .at. t+1.0
end

discrete wasoff
 ctrlour=.false.
 qconwas=0.0
 schedule wasoff .at. t+1.0
end

macro end
!*****************************************************************
```

```
macro userterminalsection
!TERMINAL SECTION
!Macros called here will be executed in the terminal section
!Don't put macro definitions here

macro end
!***************************************************************
```

B.2 Macro for the Respiration Rate Control Strategy with the Sludge Wastage Rate (Stephenson *et al.*, 1981)

```
!*****************************************************************
!PUT HERE USER DEFINED MACROS
!This section is for definitions, it will be executed
!only during loading of the program

!This macro calculates settling parameters based on SVI and
CLARIF
macro settlingcorrelation(o)
      vmax&o=bound(50.0,2000.0,cc1+cc2*svi&o   +cc3*svi&o**2)
      rhin&o=bound(1.e-5,1.e-2,cc4+cc5*svi&o   +cc6*svi&o**2)
      rflo&o=bound(1.e-5,1.e-2,cc7+cc8*clarif&o+cc9*clarif&o**2)
macro end
!*****************************************************************
macro userinitialsection
!INITIAL SECTION
!Macros called here will be executed in the initial section
!Don't put macro definitions here

macro end
!*****************************************************************
macro userderivativesection
!DERIVATIVE SECTION
!Macros called here will be executed in the derivative section
!Don't put macro definitions here

!calculate fine on effluent quality as a measure of control
performance

chodeff = sseff+sieff+xseff+xieff+xbheff+xbaeff !COD in effluent
```

```
bod5eff = 0.65*(sseff+xseff+(1-0.08)*(xbheff+xbaeff)) !BOD5 in
effluent
solids = (1/1.33)*(xseff+xieff+xbheff+xbaeff) !suspended solids
in effluent
n = snheff+sndeff+xndeff+snoeff !nitrogen in effluent
p = 5 !phosphorous in effluent
norganic = (qconww*1000/180)*(0.35*solids/500+0.45*&
(2*bod5eff+chodeff)/1350)*(0.4+0.6*(365/225))
nnutrients = (qconww*365/10000)*(n+p)
finee77 = ((25)*(1*norganic+1*nnutrients))/365 !effluent quality
fine ECU/d
finebef77 = ((1000)*(1*norganic+1*nnutrients))/365 !fine in BEF/d
finena77 = ((45.45)*(1*norganic+1*nnutrients))/365 !fine in
cdn$/d
klatot = klat1+klat2+klat3 !/d
airflow = ((klatot/24)+0.11)/0.0018 !m3/h
mairflow = 1.225*airflow !kg/h
oxyflow = 0.2*mairflow !kg/h
oxypower = oxyflow/aireff !kw
befcost = 3 !cost of electricity in Belgium BEF/kwh
cdncost = 0.08 !cost of electricity in Can $/kwh
aircostbef = oxypower*24*befcost !BEF/d
aircostna = oxypower*24*cdncost !cdn$/d
costtotalbef = finebef77 + aircostbef !BEF/d
costtotalna = finena77 + aircostna !cdn$/d
sourt1 = 1.33*ourt1/(xbht1+xbat1) !g O2/h/g MLSS
sourt2 = 1.33*ourt2/(xbht2+xbat2) !g O2/h/g MLSS
sourt3 = 1.33*ourt3/(xbht3+xbat3) !g O2/h/g MLSS
iseo = integ((ourt3-setpourt3)**2,0.0)
iaeo = integ(abs(ourt3-setpourt3), 0.0)
!ises = integ((sourt3-setpsourt3)**2,0.0)
!iaes = integ(abs(sourt3-setpsourt3), 0.0)
powercostt1 = powert1*24*eprice !$/d
powercostt2 = powert2*24*eprice !$/d
powercostt3 = powert3*24*eprice !$/d
```

```
totalpowercost = powercosttl+powercostt2+powercostt3 !$/d

macro end

!****************************************************************
macro userdynamicsection
!DYNAMIC AND DISCRETE SECTIONS
!Macros called here will be executed in the dynamic section.
!(discretes plus code to be executed every communication interval)
!Don't put macro definitions here

macro end
!************************************************
macro userterminalsection
!TERMINAL SECTION
!Macros called here will be executed in the terminal section
!Don't put macro definitions here

macro end
!************************************************
```

B.3 Macros for the Specific Respiration Rate Control Strategy with Step Feeding (Stephenson *et al.*, 1981)

B.3.1 Macro for the 2-Tank PI Controller

```
!*******************************************************************
!PUT HERE USER DEFINED MACROS
!This section is for definitions, it will be executed
!only during loading of the program

!This macro calculates settling parameters based on SVI and
CLARIF
macro settlingcorrelation(o)
      vmax&o=bound(50.0,2000.0,cc1+cc2*svi&o   +cc3*svi&o**2)
      rhin&o=bound(1.e-5,1.e-2,cc4+cc5*svi&o   +cc6*svi&o**2)
      rflo&o=bound(1.e-5,1.e-2,cc7+cc8*clarif&o+cc9*clarif&o**2)
macro end
!*******************************************************************
macro userinitialsection
!INITIAL SECTION
!Macros called here will be executed in the initial section
!Don't put macro definitions here

macro end
!*******************************************************************
macro userderivativesection
!DERIVATIVE SECTION
!Macros called here will be executed in the derivative section
!Don't put macro definitions here

! Calculate split fraction based on desired flow to tank 3
if (ctrlsourt3 .eq. .false.) then
      frinftoq23 = 0.0
      if (split23 .eq. 1) then
```

```
            frinftoq23 = bound(0.0, 1.0, flowtotank3/qinf)
        endif
else
        flowtk3 = flowtotank3
        frinftoq23 = bound(0.0, 1.0, flowtk3/qinf)
endif

!calculate fine on effluent quality as a measure of control
performance

chodeff = sseff+sieff+xseff+xieff+xbheff+xbaeff !COD in effluent
bod5eff = 0.65*(sseff+xseff+(1-0.08)*(xbheff+xbaeff)) !BOD5 in
effluent
solids = (1/1.33)*(xseff+xieff+xbheff+xbaeff) !suspended solids
in effluent
n = snheff+sndeff+xndeff+snoeff !nitrogen in effluent
p = 5 !phosphorous in effluent
norganic = (qconww*1000/180)*(0.35*solids/500+0.45*&
(2*bod5eff+chodeff)/1350)*(0.4+0.6*(365/225))
nnutrients = (qconww*365/10000)*(n+p)
finee77 = ((25)*(1*norganic+1*nnutrients))/365 !effluent quality
fine ECU/d
finebef77 = ((1000)*(1*norganic+1*nnutrients))/365 !fine in BEF/d
finena77 = ((45.45)*(1*norganic+1*nnutrients))/365 !fine in
cdn$/d
klatot = klat1+klat2+klat3 !/d
airflow = ((klatot/24)+0.11)/0.0018 !m3/h
mairflow = 1.225*airflow !kg/h
oxyflow = 0.2*mairflow !kg/h
oxypower = oxyflow/aireff !kw
befcost = 3 !cost of electricity in Belgium BEF/kwh
cdncost = 0.08 !cost of electricity in Can $/kwh
aircostbef = oxypower*24*befcost !BEF/d
aircostna = oxypower*24*cdncost !cdn$/d
costtotalbef = finebef77 + aircostbef !BEF/d
```

```
costtotalna = finena77 + aircostna !cdn$/d
sourt1 = 1.33*ourt1/(xbht1+xbat1) !g O2/h/g MLSS
sourt2 = 1.33*ourt2/(xbht2+xbat2) !g O2/h/g MLSS
sourt3 = 1.33*ourt3/(xbht3+xbat3) !g O2/h/g MLSS
iseo = integ((ourt3-setpourt3)**2,0.0)
iaeo = integ(abs(ourt3-setpourt3), 0.0)
ises = integ((sourt3-setpsourt3)**2,0.0)
iaes = integ(abs(sourt3-setpsourt3), 0.0)
powercostt1 = powert1*24*eprice !$/d
powercostt2 = powert2*24*eprice !$/d
powercostt3 = powert3*24*eprice !$/d
totalpowercost = powercostt1+powercostt2+powercostt3 !$/d
macro end

!*****************************************************************
macro userdynamicsection
!DYNAMIC AND DISCRETE SECTIONS
!Macros called here will be executed in the dynamic section.
!(discretes plus code to be executed every communication
interval)
!Don't put macro definitions here

macro end
!*****************************************************************
macro userterminalsection
!TERMINAL SECTION
!Macros called here will be executed in the terminal section
!Don't put macro definitions here

macro end
!*****************************************************************
```

B.3.2 Macro for the Split Range Controller

```
!*****************************************************************
!PUT HERE USER DEFINED MACROS
!This section is for definitions, it will be executed
!only during loading of the program

!This macro calculates settling parameters based on SVI and
CLARIF
macro settlingcorrelation(o)
      vmax&o=bound(50.0,2000.0,cc1+cc2*svi&o   +cc3*svi&o**2)
      rhin&o=bound(1.e-5,1.e-2,cc4+cc5*svi&o   +cc6*svi&o**2)
      rflo&o=bound(1.e-5,1.e-2,cc7+cc8*clarif&o+cc9*clarif&o**2)
macro end
!*****************************************************************
macro userinitialsection
!INITIAL SECTION
!Macros called here will be executed in the initial section
!Don't put macro definitions here

macro end
!*****************************************************************
macro userderivativesection
!DERIVATIVE SECTION
!Macros called here will be executed in the derivative section
!Don't put macro definitions here

! Calculate split fraction based on desired flow to tank 3
if (ctrlsourt23 .eq. .false. .and. ctrlsourt3 .eq. .false.) then
      frinftotk23 = 0.0
      frtk23totk3 = 0.0
      if (split23 .eq. 1) then
            frinftotk23 = bound(0.0, 1.0, flowtotank23/qinf)
```

```
            frtk23totk3          =          bound(0.0,          1.0,
flowtotank3/(frinftotk23*qinf))
        endif
else
!When the split fraction to tank 3 (i.e. frinftotk23) is less
than 0.50,
!controller sourt23 is turned on automatic (i.e. set to true).
During
!this time, the influent is fed to only tanks 1 and 3.
        ctrlsourt23= .true.
        ctrlsourt3 = .false.
        flowtk23 = flowtotank23
        frinftotk23 = bound(0.0, 1.0, flowtk23/qinf)
!When the split fraction to tank 3 exceeds 0.50, the influent is
fed to
!tanks 1, 2, and 3.
        if (frinftotk23 .ge. maxsplit23) then
            ctrlsourt23 = .false.
            ctrlsourt3 = .true.
            flowtotankmax3 = qtk23
            flowtk3 = flowtotank3
            if (qinf .le. minflow) then
            qtk23 = minflow
            else
            qtk23 = frinftotk23*qinf
            endif
            frtk23totk3 = bound(0.0, 1.0, flowtk3/qtk23)
        else
!stop flow to tank 2 and feed to tanks 1 and 3 and re-initialize
value
!of flowtotank3.
            frtk23totk3 = 1.0
            flowtk3 = initflowtotank3
        endif
endif
```

```
!calculate fine on effluent quality as a measure of control
performance

chodeff = sseff+sieff+xseff+xieff+xbheff+xbaeff !COD in effluent
bod5eff = 0.65*(sseff+xseff+(1-0.08)*(xbheff+xbaeff)) !BOD5 in
effluent
solids = (1/1.33)*(xseff+xieff+xbheff+xbaeff) !suspended solids
in effluent
n = snheff+sndeff+xndeff+snoeff !nitrogen in effluent
p = 5 !phosphorous in effluent
norganic = (qconww*1000/180)*(0.35*solids/500+0.45*&
(2*bod5eff+chodeff)/1350)*(0.4+0.6*(365/225))
nnutrients = (qconww*365/10000)*(n+p)
finee77 = ((25)*(1*norganic+1*nnutrients))/365 !effluent quality
fine ECU/d
finebef77 = ((1000)*(1*norganic+1*nnutrients))/365 !fine in BEF/d
finena77 = ((45.45)*(1*norganic+1*nnutrients))/365 !fine in
cdn$/d
klatot = klat1+klat2+klat3 !/d
airflow = ((klatot/24)+0.11)/0.0018 !m3/h
mairflow = 1.225*airflow !kg/h
oxyflow = 0.2*mairflow !kg/h
oxypower = oxyflow/aireff !kw
befcost = 3 !cost of electricity in Belgium BEF/kwh
cdncost = 0.08 !cost of electricity in Can $/kwh
aircostbef = oxypower*24*befcost !BEF/d
aircostna = oxypower*24*cdncost !cdn$/d
costtotalbef = finebef77 + aircostbef !BEF/d
costtotalna = finena77 + aircostna !cdn$/d
sourt1 = 1.33*ourt1/(xbht1+xbat1) !g O2/h/g MLSS
sourt2 = 1.33*ourt2/(xbht2+xbat2) !g O2/h/g MLSS
sourt3 = 1.33*ourt3/(xbht3+xbat3) !g O2/h/g MLSS
sourt23 = 1.33*ourt3/(xbht3+xbat3) !g O2/h/g MLSS
iseo = integ((ourt3-setpourt3)**2,0.0)
```

```
iaeo = integ(abs(ourt3-setpourt3), 0.0)
ises = integ((sourt3-setpsourt3)**2,0.0)
iaes = integ(abs(sourt3-setpsourt3), 0.0)
powercosttl = powertl*24*eprice !$/d
powercostt2 = powert2*24*eprice !$/d
powercostt3 = powert3*24*eprice !$/d
totalpowercost = powercosttl+powercostt2+powercostt3 !$/d


macro end

!***************************************************************
macro userdynamicsection
!DYNAMIC AND DISCRETE SECTIONS
!Macros called here will be executed in the dynamic section.
!(discretes plus code to be executed every communication
interval)
!Don't put macro definitions here

macro end
!***************************************************************
macro userterminalsection
!TERMINAL SECTION
!Macros called here will be executed in the terminal section
!Don't put macro definitions here

macro end
!***************************************************************
```

B.4 Macro for Respiration Rate Activity Control Strategy (Sekine, 1988)

```
!***************************************************************
!PUT HERE USER DEFINED MACROS
!This section is for definitions, it will be executed
!only during loading of the program

!This macro calculates settling parameters based on SVI and
CLARIF
macro settlingcorrelation(o)
      vmax&o=bound(50.0,2000.0,cc1+cc2*svi&o   +cc3*svi&o**2)
      rhin&o=bound(1.e-5,1.e-2,cc4+cc5*svi&o   +cc6*svi&o**2)
      rflo&o=bound(1.e-5,1.e-2,cc7+cc8*clarif&o+cc9*clarif&o**2)
macro end
!***************************************************************
macro userinitialsection
!INITIAL SECTION
!Macros called here will be executed in the initial section
!Don't put macro definitions here

macro end
!***************************************************************
macro userderivativesection
!DERIVATIVE SECTION
!Macros called here will be executed in the derivative section
!Don't put macro definitions here

!calculate fine on effluent quality as a measure of control
performance

chodeff = sseff+sieff+xseff+xieff+xbheff+xbaeff !COD in effluent
bod5eff = 0.65*(sseff+xseff+(1-0.08)*(xbheff+xbaeff)) !BOD5 in
effluent
```

```
solids = (1/1.33)*(xseff+xieff+xbheff+xbaeff) !suspended solids
in effluent
n = snheff+sndeff+xndeff+snoeff !nitrogen in effluent
p = 5 !phosphorous in effluent
norganic = (qconww*1000/180)*(0.35*solids/500+0.45*&
(2*bod5eff+chodeff)/1350)*(0.4+0.6*(365/225))
nnutrients = (qconww*365/10000)*(n+p)
finee77 = ((25)*(1*norganic+1*nnutrients))/365 !effluent quality
fine ECU/d
finebef77 = ((1000)*(1*norganic+1*nnutrients))/365 !fine in BEF/d
finena77 = ((45.45)*(1*norganic+1*nnutrients))/365 !fine in
cdn$/d
klatot = klat1+klat2+klat3 !/d
airflow = ((klatot/24)+0.11)/0.0018 !m3/h
mairflow =  1.225*airflow !kg/h
oxyflow = 0.2*mairflow !kg/h
oxypower = oxyflow/aireff !kw
befcost = 3 !cost of electricity in Belgium BEF/kwh
cdncost = 0.08 !cost of electricity in Can $/kwh
aircostbef = oxypower*24*befcost !BEF/d
aircostna = oxypower*24*cdncost !cdn$/d
costtotalbef = finebef77 + aircostbef !BEF/d
costtotalna = finena77 + aircostna !cdn$/d
sourt1 = 1.33*ourt1/(xbht1+xbat2) !g O2/h/g MLSS
sourt2 = 1.33*ourt2/(xbht2+xbat2) !g O2/h/g MLSS
sourt3 = 1.33*ourt3/(xbht3+xbat3) !g O2/h/g MLSS
!iseo = integ((ourt3-setpourt3)**2,0.0)
!iaeo = integ(abs(ourt3-setpourt3), 0.0)
!ises = integ((sourt3-setpsourt3)**2,0.0)
!iaes = integ(abs(sourt3-setpsourt3), 0.0)
seour = 1.33*ourresp/(xbhresp+xbaresp) !g O2/h/g MLSS
rractivity = seour/(sourt3+padbyz)
iserr = integ((rractivity-setprractivity)**2,0.0)
iaerr = integ(abs(rractivity-setprractivity), 0.0)
powercostt1 = powert1*24*eprice !$/d
```

```
powercostt2 = powert2*24*eprice !$/d
powercostt3 = powert3*24*eprice !$/d
totalpowercost = powercostt1+powercostt2+powercostt3 !$/d

!Reset DO set point in tank 3 when the rractivity controller is
off
if (ctrlrractivity .eq. .false.) then
     setpsot3 = 2.0
endif

macro end

!*************************************************************
macro userdynamicsection
!DYNAMIC AND DISCRETE SECTIONS
!Macros called here will be executed in the dynamic section.
!(discretes plus code to be executed every communication
interval)
!Don't put macro definitions here

macro end
!*************************************************************
macro userterminalsection
!TERMINAL SECTION
!Macros called here will be executed in the terminal section
!Don't put macro definitions here

macro end
!*************************************************************
```